Implantable Arterial Blood Pressure Sensor

A Thesis

Submitted to the Faculty

of

Drexel University

by

Marek Swoboda

in partial fulfillment of the

requirements for the degree

of

Doctor of Philosophy

December 2004

Dedications

To my parents

Acknowledgements

The author is deeply indebted to Dr. Ryszard M. Lec and Dr. Jeffrey I. Joseph for their technical guidance and scientific advice during the research phase of this work and in the preparation of the manuscript.

Acknowledgement is also extended to the members of the examining committee for their constructive criticism and valuable suggestions: Dr. Fred Allen, Dr. Peter Lewin, and Dr. Marc Torjman.

The author expresses his appreciation to the School of Biomedical Engineering, Science and Health Systems, Drexel University for financial support of the author during the period of this study.

Table of Contents

LIST OF TABLES…….. ix

LIST OF FIGURES...……..x

ABSTRACT..……...xv

1. INTRODUCTION...……..1

2. BACKGROUND……...4

2.1. Metrology of arterial blood pressure……..5

2.1.1. General principles of blood pressure measurements……...9

2.1.2. Existing methods…….10

2.1.3. Principles and challenges of arterial tonometry…….. 18

2.2. Conclusions…….....20

3. IMPLANTABLE TONOMETRY: FUNDAMENTAL PROBLEMS AND CHALLENGES ……22

3.1. Proposed tonometer arrangement……...23

3.2. Technological and biomedical challenges……. 25

3.2.1. Sensor related problems…….. 26

3.2.1.1. Influence of the visco-elastic properties of the arterial wall on a dynamic response of the arterial tonometer…….....26

3.2.1.2. Influence of the artery - tonometer geometry on the vessel response…….....27

3.2.1.3. Influence of the transducer stiffness on the sensor linearity.. 27

3.2.2. Artery related problems……...28

3.3. Thesis problem statement……...28

3.3.1. Theoretical modeling……...29

3.3.2. Design principles…….....30

3.3.3. Testing methodology……...30

3.4. Conclusions……..... 31

4. THEORETICAL MODELLING.…… 32

4.1. Introduction……..... 32

4.1.1. Biological component - arterial wall……... 34

4.1.2. Arterial wall structure……..39

4.1.3. Mechanical properties of the arterial wall……... 42

4.2. Methods of analysis of the measurement process and arterial wall tonometer interaction……...47

4.2.1. Transfer function…… 48

4.2.2. Lumped parameter model……52

4.2.3. Finite element model……... 56

4.3. Sensor head transfer function…….....60

4.3.1. Results and discussion…….....63

4.4. Lumped parameter model of the implantable arterial tonometer……... 64

4.4.1. Lumped parameter model of the arterial wall under applanation…....65

4.4.2. Complete sensing path model……..71

4.4.3. Results of lumped parameter model simulation…….. 73

4.4.4. Discussion……... 86

4.5. Finite element approach…… 87

4.5.1. Results…… 94

4.5.2. Finite element modeling results analysis and discussion…… 96

4.6. Conclusions…….....102

5. TONOMETER DESIGN….……..…….....106

5.1. Transducer……..107

5.1.1. Scientific basis of piezoelectric force sensor…….. 107

5.2. Piezoelectric transducer design……..111

5.3. Bench-top model design…….....113

5.3.1. Mechanical design of the bench-top system……114

5.3.2. Artery - tonometer coupling mechanism…….....115

5.3.3. Bench-top measurement system……..116

5.3.4. Tonometer signal conditioning system……119

5.3.5. Tonometer signal analysis……...119

5.3.6. Fabrication process used……. 120

5.4. Hand-held prototype design……... 120

5.4.1. Mechanical design of the hand-held prototype……... 120

5.4.2. Artery - tonometer coupling mechanism…….....122

5.4.3. Applanation mechanism of the hand-held prototype…….. 123

5.4.4. Measurement system of the hand-held prototype……124

5.4.5. Signal conditioning and signal analysis…….. 125

5.4.6. Fabrication technology used……126

5.5. Implantable prototype design…….....126

5.5.1. Mechanical design of the implantable prototype……..... 127

5.5.2. Artery - tonometer coupling mechanism…….....129

5.5.3. Applanation mechanism of the implantable prototype……129

5.5.4. Measurement system of the implantable prototype……...……..130

5.5.5. Signal conditioning and signal analysis…….. 130

5.5.6. Fabrication technology used……130

6. TONOMETER TESTING...…….……...……..132

6.1. Static response experiments……... 133

6.1.1. Experiment description……133

6.1.2. Results……. 136

6.1.3. Discussion……... 138

6.2. Tonometer dynamic response……..... 139

6.2.1. Experiment description……140

6.2.2. Results……. 142

6.2.3. Discussion……... 147

6.2.4. Recommendation for future work……... 148

6.3. Pilot in vivo experiments…….. 149

6.3.1. Short term experiments……... 150

6.3.1.1.Experiment description……..…….. 151

6.3.1.2. Results ……..……... 152

6.3.2. Pilot long-term experiments…… 155

6.3.2.1. Experiment description…….....156

6.3.2.2. Pilot results……... 157

6.3.3. Discussion……... 163

6.3.4. Recommendation for future work……..... 167

7. SUMMARY ……168

8. CONCLUSIONS……171

9. FUTURE WORK ……..173

10. LIST OF REFERENCES……...177

APPENDIX A Tonometer prototypes design…….....187

APPENDIX B Lumped parameter simulation results…….……192

APPENDIX C Finite element modeling model description…….……. 202

APPENDIX D Lumped parameter simulation code……...……220

APPENDIX E Signal analysis …….……...…...224

VITA……..……...226

List of Tables

2.1. Comparison of existing blood pressure methods……17

4.1. Typical diameters and wall thickness for main types of arteries……35

4.2. Arterial blood pressure waveform harmonics and their modulus……...74

5.1. Piezoelectric force sensor operating range……. 110

List of figures

2.1. Generic arterial blood pressure cycle in time domain……6

2.2. Arterial blood pressure in frequency domain (Spectrum)……..9

3.1. Example of possible positioning of the implantable tonometer……23

3.2. Implantable tonometer applanation arrangement cross-section view ……. 24

4.1. Segment of the artery with cylindrical coordinate system……... 37

4.2. Example of possible positioning of the implantable tonometer……... 39

4.3. Segment of a muscular artery…….. 40

4.4. Arterial wall cross section…… 42

4.5. Generic relationship between stress and strain in the arterial wall tissue…… 44

4.6. Cross-section of the implantable tonometer…… 50

4.7. Conceptual model of the tonometer sensing path…… 50

4.8. Arterial wall under applanation……... 53

4.9. Conceptual model of arterial tonometry…….. 55

4.10. Stress in flatten artery……. 56

4.11. Preliminary studies showing buckling phenomena…… 58

4.12. Contact pressure on the flat portion of artery…… 59

4.13. Generic tonometer sensor head…….. 60

4.14. Sensor head model……. 61

4.15. Sensor head simplified model…… 62

4.16. Sensor head transfer function……. 64

4.17. Spring-dashpot model of the arterial wall under applanation…… 66

4.18. Force acting on the transducer as a function of displacement and velocity…….. 68

4.19. Force acting on the transducer as a function of displacement; velocity=0…… 69

4.20. Force acting on the transducer as a function of velocity; displacement=const….. 70

4.21. Family of force functions vs. displacement for three different velocities……. 70

4.22. Complete sensing path spring-dashpot representation……... 71

4.23. Complete, simplified sensing path spring-dashpot representation…… 72

4.24. Frequency content of the arterial wall response (input frequency 1 Hz)……... 75

4.25. Time response of the arterial wall and the input signal (first harmonic)……... 75

4.26. Frequency content of the arterial wall response (input frequency 2 Hz)……... 76

4.27. Time response of the arterial wall and the input signal (second harmonic)…….. 76

4.28. Frequency content of the arterial wall response (input frequency 3 Hz)……... 77

4.29. Time response of the arterial wall and the input signal (third harmonic)…….. 77

4.30. Frequency response of the wall-transducer system for $E_{tr} = 10^6$ dyne/cm^2…….... 78

4.31. Time response of the wall-transducer system for $E_{tr}=10^6$ dyne/cm^2……. 79

3.32. Frequency response of the wall-transducer system for $E_{tr} = 10^7$ dyne/cm^2…… 79

4.33. Time response of the wall-transducer system for $E_{tr}=10^7$ dyne/cm^2…….. 80

4.34. Frequency response of the wall-transducer system for $E_{tr}=10^8$ dyne/cm^2……. 80

4.35. Time response of the wall-transducer system for $E_{tr} = 10^8$ dyne/cm^2…… 81

4.36. Frequency response of the wall-transducer system for Etr = 10^9 dyne/cm^2,
input frequency 2H…….. 82

4.37. Time response of the wall-transducer system for $E_{tr} = 10^9$ dyne/cm^2,
input frequency 2Hz…….82

4.38. Frequency response of the wall-transducer system for $E_{tr}=10^{10}$ dyne/cm^2,
input frequency 3Hz…….83

4.39. Time response of the wall-transducer system for $E_{tr} = 10^{10}$ dyne/cm^2,
input frequency 3Hz…….83

4.40. Frequency response of the wall-transducer system for $E_{tr}=10^{10}$ dyne/cm^2, input frequency 4Hz……84

4.41. Time response of the wall-transducer system for $E_{tr}=10^{10}$ dyne/cm^2, input frequency 4Hz……..84

4.42. Frequency response of the wall-transducer system for $E_{tr}=10^{10}$ dyne/cm^2, input frequency 5Hz…… 85

4.43. Time response of the wall-transducer system for $E_{tr}=10^{10}$ dyne/cm^2, input frequency 5Hz…….85

4.44. Amplitude A_n as a function of harmonic number…… 86

4.45. “A” value as a function of harmonic number…… 87

4.46. General view of the artery deformed by applanation……. 89

4.47. Side view (Panel A) and front view Panel (B) of the simulated arterial segment.. 92

4.48. FEM 3-D simulation results: S (von Mises)…….. 95

4.49. FEM 3-D simulation results: S, Pressure……... 95

4.50. FEM 3-D simulation results: Contact Pressure…….. 96

4.51. Contact pressure profile……. 97

4.52. Contact pressure map in systole……. 99

4.53. Contact pressure patterns of measured in 4 points……. 100

4.54. Comparison between contact pressure and arterial pressure……. 101

4.55. Strain in the arterial wall tissue…….. 102

5.1. Piezoelectric PZT-5 transducer used in bench-top and implantable tonometer designs……. 113

5.2. Piezoelectric Tonometer Testing Platform-Schematic…… 115

5.3. General view of the Piezoelectric Tonometer Testing Platform-Photograph…….. 115

5.4. Block diagram-laboratory setup- bench top “mock circulatory system……... 116

5.5. Electronic Measurement System……. 118

5.6. Hand held tonometer…… 121

5.7. Hand held tonometer tip……... 122

5.8. Detailed view of the tip of the hand-held tonometer with adjustable applanation level……. 124

5.9. Arterial Tonometer for Long-term Implantation-general view……... 128

5.10. Disassembled tonometer…….…… 128

5.11. Front view. Miniature tonometer for chronic implantation……. 128

5.12. Tonometer half-view…….. 128

6.1. Bench-top setup schematics for static and dynamic tests…… 134

6.2. Pressure/piezoelectric tonometer phase shift relationship……... 137

6.3. Comparison of the reference signal and tonometer active mode signal…….. 138

6.4. Relationship between applanation level and the tonometer active mode signal… 138

6.5. Comparison of the pressure sensor signal and the tonometer signal……... 143

6.6. Comparison of the tonometer signal with the reference pressure signal in frequency domain……143

6.7. A comparison of the tonometer signal (blue line) and the reference pressure signal (red line) for the frequency 60 bpm……145

6.8. Comparison of the tonometer signal (blue line) and the reference pressure signal (red line) for the frequency 80bpm……. 146

6.9. Amplitude of the spectrum of the signal shown in figure 6.8…….. 146

6.10. Acute animal experiment……... 151

6. 11. Tonometer and reference signal comparison…… 153

6.12. Passive mode tonometer output in recorded in the acute animal experiment…… 154

6.13. Implantable tonometer capable of working in a living organism…….. 156

6.14. Implantation of the implantable prototype……. 157

6.15. Animal study data…….. 158

6.16. An ultrasound visualization of the implanted tonometer and abdominal aorta… 158

6.17. Photograph of the explanted tonometer……. 160

6.18. Four regions chosen for histological analysis…… 161

6.19. Three positions in which the histological measurements were taken..…… 162

6.20. Thickness of the tunica media measured on the abdominal aorta……. 162

6.21. Thickness of the tunica media measured on the abdominal aorta of 20 kilogram dog……..163

6.22. Maximal strain calculated by finite element analysis…… 165

6.23. Relative changes in media thickness…….. 166

Abstract

Implantable Arterial Blood Pressure Sensor

Marek Swoboda

Ryszard M. Lec, Ph.D, Jeffrey I Joseph, D.O.

Although blood pressure measurements are well developed, the existing technology in the field of Arterial Blood Pressure (ABP) measurements is not sufficient in terms of long-term ABP waveform assessment. To overcome existing limitations this dissertation proposes, models, designs and tests a new technique of ABP measurements: implantable arterial tonometry.

The scope of this dissertation is to study how the geometry of the tonometer and its mechanical properties influence sensor output and stress/strain distribution inside the arterial wall. Two models of tonometer, analytical and numerical, are developed. The relationship between the tonometer response and its effective stiffness is calculated using a lumped parameter model. The contact pressure between the artery and the tonometer as well as the arterial wall stress/strain distribution is studied using a Finite Element numerical model.

Based on the theoretical results three prototypes are developed. The piezoelectric dual mode transducer is designed to measure the tonometer-arterial wall contact pressure. The series of in-vitro and in-vivo experiments test the static and dynamic responses of the tonometer.

The results indicate the tonometer's effective stiffness necessary to achieve less than 1% error in the dynamic response of the sensor. The geometry of the tonometer's measurement area is found, which results in less than 1% of error in quasi-static response

of the sensor. In effort to find potential tissue remodeling areas, the internal arterial wall stress/strain distribution generated by the tonometer is found.

The experimental results complement the numerical analysis. The static and dynamic characteristics of the prototype tonometer obtained in-vitro and in-vivo are presented. The explanted tunica media remodeling effect is compared with FE analysis results.

The presented work states and solves basic problems of implantable arterial tonometry. In addition it provides the in-vitro and in-vivo examination of the theoretical results. The thesis develops tools of modeling, designs, and testing procedures for future researchers willing to develop implantable tonometers.

The thesis concludes with a novel design of the implantable tonometer.

1. INTRODUCTION

Blood pressure assessment is probably the single most important medical measurement. Arterial blood pressure is historically the first estimator of blood perfusion and still is the easiest parameter to measure. Therefore, it is a convenient indicator of a patient's health as well as a crucial vital sign. Due to its diagnostic value it is measured in physicians' offices, operating rooms as well as in intensive care units.

The importance of blood pressure measurements lies in the fact that it is strongly associated, through the variable impedance of human organs, with physiology of human organism, and virtually all physiological processes are reflected in blood pressure signals either arterial or venous.

Moreover, some features of the arterial blood pressure such as mean arterial pressure and systolic and diastolic pressure are epidemiologically linked to numerous circulatory system diseases such as heart attack, stroke, heart valve malfunction and arteriosclerosis, as well as to problems with kidney diseases and diabetes (Natarajan, 2003).

The significance of blood pressure measurements can be soundly stressed by epidemiological data. In the United States, 56 million patients suffer from arterial hypertension. They require long-term vigilance and treatment, including constant arterial blood pressure monitoring. Many patients suffer from multiple organ damage due to untreated hypertension. Insufficient diagnostic technology development is partially responsible for this situation, because the current technology does not allow constant, real-time monitoring of those patients. And due to various technical problems, such as large mean errors, it provides inaccurate diagnostic information.

All those facts place the blood pressure measurements at the very core of medical diagnostic and monitoring techniques.

Although one of the first physiological measurements was performed just to measure arterial blood pressure (by Steven Hales in 1733), the biomedical engineering still struggles to develop accurate, reliable and inexpensive blood pressure measurement techniques, transducers and sensors. In this battle for better blood pressure assessment, dozens of concepts are being developed to improve sensor - human body interface (biocompatibility), accuracy, safety and reliability.

At the same time, medical sciences in general and particularly cardiology are developing new methods of blood pressure waveform analysis such as sphygmocardiography. Old-fashioned methods evaluating only mean parameters are currently being challenged by new approaches utilizing the whole spectrum of the blood pressure signal. (Nichols, 1998).

This situation generates new requirements for measurement techniques and inspires the biomedical sensor community to develop new generations of waveform-capable devices and methods.

Advances in the field of implantable devices open completely new opportunities for more accurate, permanent and real-time blood pressure measurements. In the last half of the 20th century, numerous technologies were developed and introduced to the market such as implantable pacemakers, defibrillators, neuro-muscular stimulators and new classes of biomechanical prosthesis (e.g. skeletal prosthesis), vascular grafts and heart assist devices. Those developments in the field of biocompatibility and implantation surgery put new tools in the hands of biomedical engineers working on novel arterial

blood pressure measurements methods. The growing confidence in implantable devices can shift the point of gravity from noninvasive, less accurate diagnostic devices toward miniature, high fidelity implantable sensors.

In addition, the newest trends in medicine tend to employ close loop feedback systems (e.g. in drug delivery devices, pacemakers, implantable defibrillators, etc.) that require real-time reading of the control signal. Therefore, future anti-hypertension drug delivery systems most likely will be based on real-time arterial blood pressure measurements. The same is true for heart assist devices.

All those facts call for long-term, real-time "waveform-capable" methods. Arguably the best solution to all those problems will be the miniature implantable blood pressure sensor capable of constant measuring of the real-time blood pressure waveform. Thus, the author's strong belief is that the future of blood pressure measurements lies in the merger of arterial tonometry and an implantable device that is an implantable arterial tonometer.

Arterial tonometry preserves the arterial wall, and if it is applied directly to the artery, it exhibits superb accuracy (Nichols, 1998). This kind of device has the potential to provide high accuracy and real-time measurements with low biocompatibility risks.

In the author's opinion, the risks from insufficient diagnostics and early prophylactics in the field of hypertension could be significantly higher than potential risks of implantation of the miniature arterial tonometer.

The author's motivation for the presented study was to develop the basis for a long-term, real-time, implantable blood pressure monitoring device, which in the author's opinion will be the workhorse of the 21st century cardiologist.

2. BACKGROUND

Although the importance of the pulse was understood even to the ancient philosophers and physicians such as Galen (130-200 AD), they were not able to acquire it by any quantitative means. Through the several following centuries, blood pressure measurements were impossible due to the lack of sufficient technology and physiological knowledge among the scientists and physicians.

Over the 17th and 18th centuries, advances and discoveries in physics by Newton, Bernoulli and Pascal slowly opened new venues for hydrodynamics development and provided the first glimpse into the human circulation.

The first experiments showing feasibility of blood pressure measurements were performed by Hales (1677-1761). He was also the first one to apply modern physics to the circulatory system, proposing the concept of peripheral resistance and arterial compliance.

Despite Hales' efforts, the lack of mathematical tools, such as statistical analysis and dynamic systems theory, decelerated the understanding of epidemiological and physiological significance of the arterial blood pressure.

The 19th and 20th century developments in mathematics found the base for modern statistical and signal analysis, providing powerful tools to correlate arterial blood pressure signal features with various physiological and medical conditions. All those advances helped build the foundation for modern measurement and diagnostic methods utilizing the arterial blood pressure with its static and dynamic features.

Currently, the modern arterial blood pressure measurements employ a variety of technologies, theories and devices to acquire the parameters of the human pulse.

(Chatzandroulis, 2000), (Druzhinin, 1999), (Haruka, 1994), (Hashemi, 1994), (Hierold, 1999), (Im, 1995), (Kemmotsu, 1991), (Martin, 2000), (O'Rourke, 2003), (Yamakoshi, 1980), (DeLlias,1982),(Taylor, 1973), (Siebenhofer, 1999), (Webster, 1999), (Stein, 1971), (Zhao, 2000)

To understand the richness of information and importance that is carried by the blood pressure signal as well as the complex nature of blood pressure assessment, one has to understand its metrological fundamentals.

2.1. Metrology of arterial blood pressure

The arterial blood pressure signal originates in the left ventricle and propagates through the systemic arteries, changing its static and dynamic parameters. The position of the heart is considered to be the reference point (Burton, 1968) in which the static component (hydrostatic pressure) is assumed to be zero. Blood pressure parameters vary from subject to subject and undergo changes according to the physiological state as well as a wide range of diseases (Marque, 1999). The variability is so large that a detailed description is impossible in this short introduction. Some interesting data are presented in (Nichols, 1998), (Drzewiecki, 1998), (Toyoshima, 1996), (Gardner, 1981), (O'Rourke, 1996), (Gedders, 1970) and (Kelly, 1989). Nevertheless, some average numbers measured on the healthy population can be given. The arterial blood pressure amplitude for a healthy person, measured in the aorta, varies from 40 to 80 mmHg; which corresponds to 120 to 140mmHg at the maximum of the pulse waveform, the so-called systolic pressure, and to 80 to 90 mmHg at the minimum, the so-called diastolic pressure. The frequency of the signal varies from 40 to 200 beats per minute (Togawa, 1999). Thus, the period is in the range from 1.5s to 0.3s. The average period for a resting healthy

subject is about 0.85s. The generic shape of the typical signal, recorded in a main artery, is depicted in figure 2.1. The first rising portion of the pulse has an average dP(t)/dt around 200 mmHg/s, and the falling part dP(t)/dt is around 130 mmHg/s, where P(t) is the blood pressure in time domain. The typical range of amplitudes does not cover the pressure values that can be generated by a hydrostatic pressure. Body position can significantly shift the blood pressure in the aorta arch by as much as 40 mmHg in a standing position, or even 80 mmHg in a reversed position, with head down (Burton, 1968). Also, body movements or exercise such as running can add to the amplitude by 60 mmHg (Nichols, 1998). Aging also increases the average systemic pressure, shifting it by about 1 mmHg per year and slightly increasing the peak-to-peak amplitude of the pulse (Kelly, 1989), (Nichols, 1998).

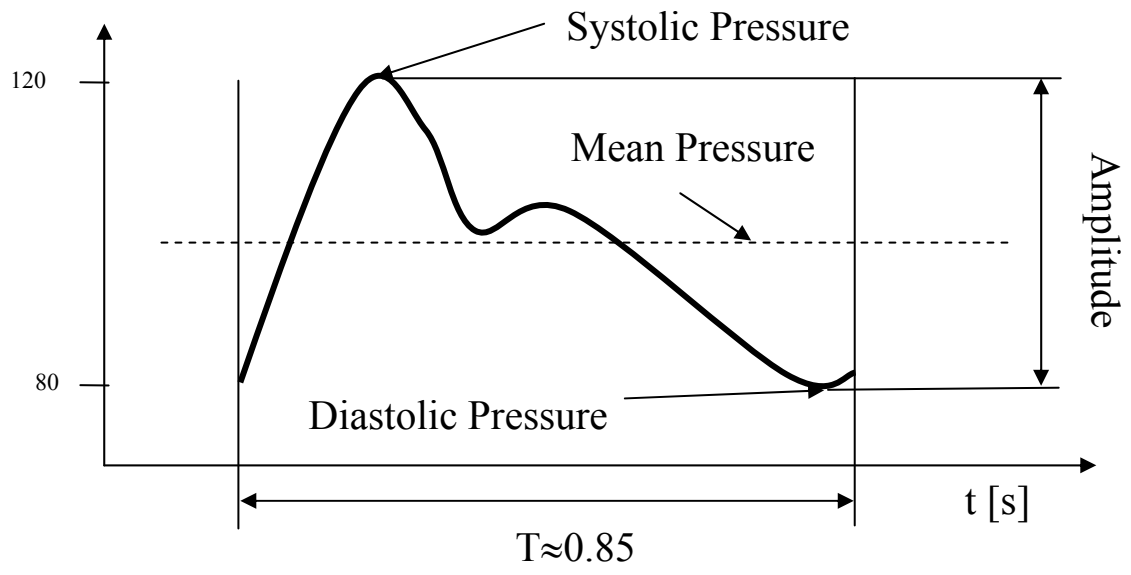

Figure 2.1. Generic arterial blood pressure cycle in time domain

Many authors treat the blood pressure signal as a periodic one and analyze it by using the Fourier transform:

$$F(\omega) = \frac{1}{2\pi} \int_{-\infty}^{\infty} BP(t) \exp(-j\omega t) dt \quad \text{(Formula 2.1)}$$

Where: F(ω) is a Fourier transform, BP(t) is blood pressure function in time domain, j is an imaginary number, and ω is angular frequency.

This approach offers a very convenient set of tools allowing analysis of the signal for specific frequencies – harmonics, by using only two numbers: amplitude of the harmonic and its phase. If the system is assumed to be linear and periodic, the Fourier analysis can provide the complete description of the system dynamics.

The fundamental period is often assumed to be the heart cycle or the multiplication of it. Many workers use the Fourier methodology, such as spectrum analysis, to express the blood signal pressure features (Nichols, 1998), (Drzewiecki, 1998), (Togawa, 1999) and (Bronzino, 1995). Typical blood pressure spectral content is shown in figure 2.2.

In fact, blood pressure is not a pure periodic signal. The long-term extensive studies on Heart Rate Variability (HRV) (Bronzino, 1995) showed the short- and long-term fluctuations in the HR fundamental frequency. Also, the spectral content of the blood pressure signal undergoes changes due to physiological responses of the cardiovascular system. In addition, many types of artifacts are involved, introducing stochastic or rather chaotic components (Vikram, 2004).

The situation is made worse with the technical limitations to the digital signal analysis such as a finite period of collecting data, and a finite period of sampling

(sampling frequency) data or quantization effect (Bronzino, 1995). In a real experiment, the "ideal" continuous formula (2.1) has to be supplemented by a discrete one:

$$F(k) = \frac{1}{N}\sum_{n}^{N-1} BP(n)\exp(-j\frac{2\pi nk}{N}) \quad \text{(Formula 2.2)}$$

Where: F(k) is a Fourier transform, BP(n) is blood pressure function in a discrete time domain, j is an imaginary number, k is an angular frequency, n is the number of sample, and N is the total number of samples.

Thus, the conversion from time domain to frequency domain utilizing the formula (2.2) will introduce an error due to sampling and an energy leakage. The energy leakage is related to the finite size of the analyzing window- $N\Delta t$ where N is number of samples and $1/\Delta t$ is sampling frequency (Roth, 1981). Because the analyzing time window (time limitation, Roth, 1981) has a finite size, by definition it cannot cover all low frequencies. Also, the analyzing window can generate some high frequency artifacts by unmatched signal levels at the ends of the window. The sampling rate limits the frequency range to be analyzed unless the Nyquist criterion is met: $1/\Delta t > 2\ f_{max}$. Where $1/\Delta t$ is sampling frequency and f_{max} is the maximum frequency present in the signal spectrum.

The nature of the blood pressure signal and the tools utilized for its frequency analysis introduce an inherent error. In this thesis, to avoid the narrow and biased frequency analysis approach as the only solution, the blood pressure signals obtained by the tonometer and the reference transducer are analyzed using three different methods: time domain comparison, frequency domain comparison and correlation strength method (Sato, 1993).

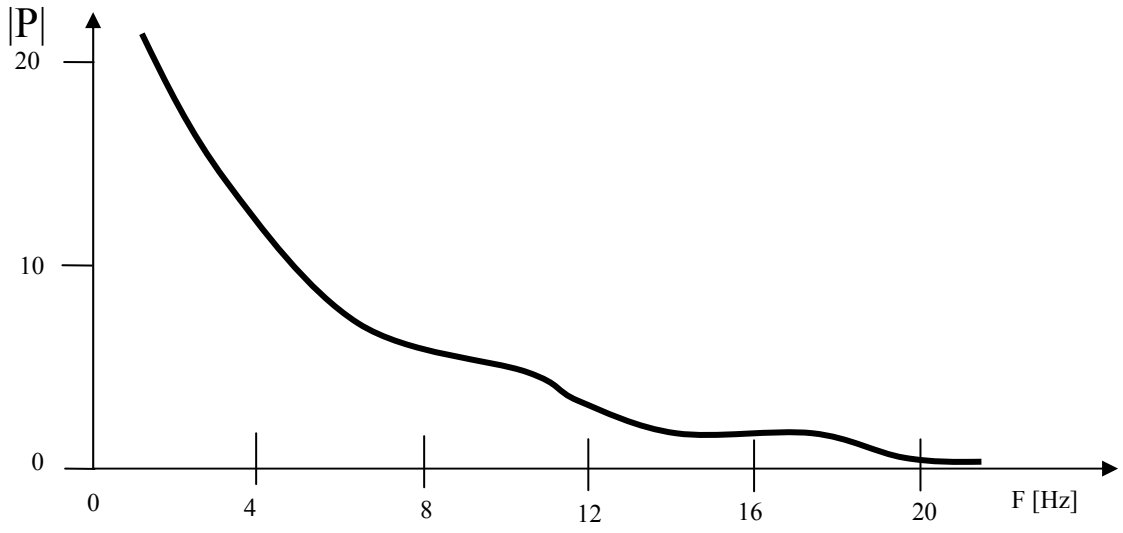

Source: McDonald's Blood Flow in Arteries, W Nichols, MF O'Rourke

Figure 2.2. **Arterial blood pressure in frequency domain (Spectrum)**
In the arterial measurements pressure pulse contains from 6 to 20 harmonics.

2.1.1. General principles of blood pressure measurements

The arterial blood pressure transducer has to meet some specific requirements. They can be divided into static and dynamic. Static requirements are accuracy, linearity and sensitivity. Dynamic requirements are frequency range and dynamic response (e.g. transfer function).

If one assumes that the heart rate can be up to 200 beats per minute, then the required frequency for the blood pressure transducer is from 20 to maximum 66 Hz (Togawa, 1999).

Typical frequency responses of the existing measurement systems are from 7 (Swan-Ganz catheter) to 28 Hz measured for 5F, 100 cm catheter length with dumping coefficients ranging from 0.33 to 0.15 (measured for 8F, 80 cm plus catheter length) (Nichols, 1998).

The pressure range is from -50 to 300 mmHg with overpressure from 5,000 to 10,000 mmHg (Togawa, 1999).

The U.S. standards are very generous and require offset ≤5 mmHg with a standard deviation of 8 mmHg (White, 1993).

2.1.2. Existing methods

Currently, arterial blood pressure measurements can be divided into six groups of techniques:

1. Invasive methods (the human tissue is penetrated in order to feed the blood pressure signal to the measuring device);
2. Noninvasive methods (the measurement does not require any tissue damage);
3. Direct techniques (the sensor measures actual pressure);
4. Indirect techniques (the sensor measures some other parameter related to pressure and the blood pressure is calculated from this parameter);
5. Mean parameters measurements (measures parameters such as systolic, diastolic, mean pressure); and
6. Waveform measurements (records the whole waveform-spectrum of blood pressure).

Korotkoff method

The leading method used in clinical medicine is a noninvasive, indirect, mean parameter measurement called Korotkoff method. This method, developed by a Russian army physician in 1905, is capable of measuring systolic and diastolic pressure using an occlusive cuff with a pressure gauge and a stethoscope.

The method is based on the fact that when pulsatile blood flow passes through the partially occluded artery (typically the brachial artery but a more recent method is applied to the temporal artery (Shenoy, et al, 1993)), it generates cyclic sounds that can be heard via stethoscope. The sounds cannot be heard when blood flows freely or if it is completely stopped. The sound changes its intensity and spectrum according to the level of occlusion; therefore some distinctive sound features can provide information on blood pressure inside the artery.

By occluding the artery with the pneumatic cuff, which allows precise pressure control inside the cuff, one can correlate the occurrence of sounds with the pressure inside the cuff and determine the arterial pressure.

Initially the cuff is pressurized above the systolic pressure. Then the pressure in the cuff is lowered with a rate of 2 to 3 mmHg/s. Pressure in the cuff determines the level of artery occlusion. When pressure in the cuff is higher than the systolic pressure in the artery, the artery is fully occluded (no sound). When pressure in the cuff is lower than the systolic but higher than the diastolic one, the artery is partially occluded (periodic sound appears). And when pressure in the cuff is lower than the diastolic pressure, the artery is not occluded (disappearing sound or no sound).

Some fine adjustment can be made to the method, especially close to the diastolic pressure zone. For example, for seasoned professionals the muffled sound just before sound disappearance is considered to be an indicator of the diastolic pressure.

The Korotkoff method measures indirectly two mean parameters of the arterial blood signal: the systolic and diastolic pressure. Because the Korotkoff sounds are generated repeatedly by the working heart muscle, they have the same period as the

heart beat. The correlation of the sounds with the cuff pressure carries an error dependent on the heart rate and the rate of pressure change in the cuff. The higher the heart rate and the slower the change of pressure in the cuff, the smaller the error. Also, it is very important to notice that this method is not able to measure the systolic pressure of the single heart cycle, but instead it measures the value between two subsequent heart cycles. The systolic values and diastolic values are measured in different heart cycles. The method is not able to record any changes in systolic and diastolic pressure from beat to beat.

The error of the method is estimated to be 5 to 20 mmHg for systolic pressure (usually an underestimation) and 12 to 20 for the diastolic pressure (overestimation), (Bronzino, 1995). The pressure range of this technique is theoretically unlimited, but manometers measuring pressure in the cuff work up to 300 mmHg.

Oscillometry

It is also a noninvasive, indirect, mean parameter technique. Historically oscillometry is an older method than the method of Korotkoff. Some basic principles were established in 1885 by French physiologist Marey. The method was not well understood, thus it was not very popular until now. Recently, due to advances in electronics and theoretical physiology, it gained popularity, especially in automated devices. About 10 years ago, the oscillometric technology was introduced into the home blood pressure market (e.g. Omron®, Samsung, Seinex, Minilife, etc.), driving out the Korotkoff method.

The principle of operation is as follows: the subject's arm is placed in the pressurized pneumatic arm cuff. The cuff is equipped with a pressure transducer.

Initial pressure is set above the estimated systolic pressure, then it is lowered with a rate around 10mmHg/s. Arterial blood pressure pulsation generates pulsation in the cuff. The recorded cuff pressure is high-pass-filtered above 1 Hz (Bronzino, 1995) or 0.5 Hz (Drzewiecki, 1998). The maximum pulsations in the cuff correspond to the mean arterial pressure (Posey, 1969), (Ramsey 1979). The systolic pressure and the diastolic pressure are calculated as a fixed ratio of mean pressure (Geddes, 1983), (Drzewiecki, 1998).

$$O_s/O_m = 0.55; \quad O_d/O_m = 0.85 \qquad \text{(Formula 2.3)}$$

A variation of this method - derivative oscillometry - is being developed. It is able to measure systolic and diastolic pressure directly from the cuff pulsations, but to date the method has not been adopted due to lack of experimental data from a subject population with a wide range of blood pressure (Bronzino, 1995). The mean error of this method for systolic pressure is 9% and 6% for diastolic pressure. The pressure range is theoretically unlimited but automated devices offer the range from 0 to 300 mmHg (Bronzino, 1995).

Oscillometry carries all the disadvantages of the Korotkoff method, but it is very convenient and reliable in automated applications.

Continuous vascular unloading

This interesting method was proposed by Penaz in 1973. Penaz noticed that if pressure in the occlusive cuff is continuously altered to equal the arterial pressure, the artery will be in the constant state of vascular unloading (the arterial wall stress will

be zero). This state can be detected by a large volume pulse. Penaz employed mechanical feedback to continuously adjust the pressure in the cuff. The vascular volume was measured using photoplethysmography. When feedback is applied such that the vascular volume is kept constant, the cuff pressure is assumed to be equal to the arterial pressure.

The technique is commercially available as the FINAPRES®. The main drawback of this method is that it employs pressure in finger arteries (a peripheral vascular location), which is different than the aortic pressure and is prone to artifacts generated by: transducer location in relation to aortic valve (hydrostatic error); pressure waveform reflection (which is related to vascular flow resistance); changes in skin temperature; and vasoactive drugs, anesthetics, etc.

Intraarterial methods

This group of techniques is direct, invasive and measures mean parameters as well as the waveform. The measuring sensor is immersed in liquid and directly measures liquid or blood pressure.

Some transducers are placed inside the vessel, (e.g. FISO Technologies interferometric fiber optic in-vivo pressure transducer; U.S. Patents 5,392,117 and 5,202,939) but usually the transducer is connected to the blood stream via catheter. The catheter is filled with saline, and saline transfers the intraarterial blood pressure to the transducer. Typically the transducer or the catheter is placed in the radial artery. The modern pressure transducers utilized in this type of measurement are built using MEMS technology and work based on the piezoresistive strain gauge (e.g. Deltran®

transducer of Utah Medical Products®, Baxter, Cobe, etc.). The typical operation range for this type of transducer is -50 to 300 mmHg.

Sensitivity 5 μV/V/mmHg ± 1%. The hysteresis is relatively small: ±0.1 mmHg over 0 to 10 mmHg; typical error due to non-linearity: ±1.5 mmHg over 0 to 300 mmHg.

This method requires frequent flushing of the catheter in order to avoid protein cup formation on the tip of it, and it also requires calibration to compensate for the sensor drift. Although most of existing types are temperature compensated, the stability is not very high. Devices with transducers placed outside the body and connected via the catheter have to be analyzed as a dynamic system consisting of several subsystems with their own inertia and elasticity. Thus the Transfer Function of the system changes with, for example, the length of the catheter, its compliance and viscosity of the saline, which is related to temperature (Togawa, 1999). Also, catheter measurements are prone to motion artifacts such as vibration of the saline-filled tubing and change of the transducer position (hydrostatic error).

The mean error of the transducer alone in this class of devices is around ±3 % and it would be the error of the whole method if the transducer is placed directly inside the artery. The mean error of the whole catheter method in clinical practice is difficult to judge due to numerous human-related errors.

Most devices are disposable but some of them, especially those used in research labs, are reusable.

Swan-Ganz method

The variation of direct method is the pressure measurement utilized in the Swan-Ganz catheter. The Swan Ganz method is one of the most invasive techniques because the introduction of the catheter takes place in relatively large vessels (jugular, subclavian or femoral vein) and subsequently the tip of the catheter is placed in the subject's heart. The Swan-Ganz catheter is equipped with a blood pressure sensor, but it is used to measure pulmonary artery pressure and pulmonary capillary wedge pressure instead of arterial. This method shares technological solutions and basic features with the intraarterial methods, but it is used for blood pressure assessment outside the systemic tree. Thus the requirements for the operating pressure range are lower, typically one order or magnitude less, and consequently the accuracy requirements are higher.

Arterial Tonometry

Tonometry was initially developed to measure intraocular pressure. Eventually, Pressman and Newgard (Pressman,1963) adopted this method to arterial measurements. Tonometry is a noninvasive, indirect, mean parameter and waveform measurement technique.

Arterial tonometry is applied to the superficial arteries (e.g. radial). The device is placed above the artery and then gently compresses the skin and the vessel. The tonometer measures the contact pressure between the skin and the tonometer. The contact pressure directly under the tonometer is assumed to be arterial pressure. The justification for this assumption is developed based on an applanation principle. The applanation (flattening of the artery) generates the geometry in which the arterial wall

and other tissue stress is parallel to pressure sensor surface while the arterial pressure acts perpendicularly to the sensor surface. It eliminates the arterial wall tension component in the contact pressure. Under these conditions the contact pressure is equal to the arterial blood pressure.

Although there are commercially available devices such as Colin or Millar, the method is still under scrutiny. Researchers and medical professionals do not agree in terms of method accuracy and stability (Siegel, 1994), (de Jong, 1995), (Sato, 1993), (Weiss, 1996), (Steiner, 2003), (Zorn, 1997). Very often the tonometer has to be frequently calibrated with some auxiliary method such as oscillometry or the method of Korotkoff. The Colin tonometer for instance, has a built-in oscillometric calibrating device.

The commercially available devices are cumbersome and complicated in use, which is the main obstacle in winning with the intraarterial counterparts.

The state of the art is summarized in the table below. Herein, the six groups of methods and their basic features are presented.

Table 2.1 Comparison of existing blood pressure methods

Method type / Method name	Invasive	Noninvasive	Direct	Indirect	Mean parameter	Waveform measurement	Real time long term	High Accuracy
Korotkoff		X		X	X			
Oscillatory		X		X	X			
Vascular unloading		X		X	X	X	X	
Intraarterial	X		X		X	X		X
Swan-Ganz	X		X		X	X		
Tonometry		X		X	X	X		

From the presented description, one can see that all existing blood pressure measurements carry two fundamental drawbacks: they cannot be used for permanent, real-time arterial blood pressure monitoring, (FINAPRES® offers this capability but the pressure obtained by this method is not considered to be the arterial pressure) and they do not offer high accuracy (except the intraarterial method with a sensor placed inside the artery, but this method, on the other hand, cannot be applied for a long term).

To date, the standard techniques available for patients are: non-invasive, indirect, mean parameters methods (Korotkoff and oscillatory), which offer the lowest accuracy and are not able to measure blood pressure waveform; and "waveform capable" intraarterial methods, which are invasive and cannot be applied for a long period of time although they present a higher accuracy.

Two methods that could be good candidates for permanent real-time monitoring (FINAPRES® and tonometry) face serious problems; FINAPRES® measures the unreliable peripheral blood pressure, and tonometry uses bulky devices and shows problems with stability and calibration.

2.1.3. Principles and challenges of arterial tonometry

Tonometry has several distinctive features, placing this technique ahead of other existing solutions. It is a noninvasive, waveform-capable arterial blood pressure measurement method. The tonometer if properly applied can perform precise measurements despite the fact that the blood pressure signal is collected through the arterial wall and several layers of tissue such as connective or adipose. The tonometer stays outside the artery lumen and, unlike the intraarterial methods, the sensor is not

subjected to albumin or thrombus accumulation and theoretically can hold its fidelity for a prolonged period of time.

The typical arterial tonometer measures the contact pressure between the sensor and the skin. Under the special conditions (Drzewiecki, 1979) when the artery and surrounding tissue are flattened by the rigid surface of the sensor, the contact pressure in the center of the applanation region is assumed to be equal to the arterial pressure. The applanation is achieved by compression of the superficial artery between the tonometer and an underlying bone or a large muscle. The applanation has to be kept constant during the measurement, thus the sensor-artery arrangement has to be stable. Therefore not all arteries are suitable for this kind of measurement. Typical measurement sites for tonometry are radial, brachial and sometimes carotid arteries.

According to authors (Drzewicki, Pressman, Nichols, O'Rourke), to obtain an accurate signal the measurement has to be performed in the center of the applanation region. Since the arterial tonometry is usually applied without knowing the exact target artery location and size, some additional techniques have to be employed to collect contact pressure from the proper area. The commercially available devices offer some automated features to position the tonometer and hold it during the measurement. Sometimes an actuator is used to flatten the artery (Colin). In addition, the measurement is performed by an array of sensors placed across the artery. The sensor with the largest amplitude is assumed to be in the center of the applanation area. Also, some devices offer special wrist holders that help to expose the radial artery.

All those techniques try to compensate for the fact that the tonometer is not positioned directly in the center of the artery; but unfortunately they generate the bulk of

additional complicated devices, which diminishes the initial advantages offered by the tonometry.

Also, because all existing methods employ the arteries in the limbs, it is virtually impossible to eliminate motion artifacts while the subject is moving. Motion artifacts are generated by the muscles, body parts and skin movements. Also, body movements change the position of the tonometer in respect to the artery.

2.2. Conclusions

No existing technique offers high accuracy, real-time, long-term measurements and waveform recording. Despite tremendous advances in biomedical engineering, no method can collect real-time blood pressure waveform over months or years to detect long-term trends.

In addition, no long-term measurement method can be used to work in close loop feedback systems where the blood pressure is the control parameter. Thus the arterial blood pressure cannot be utilized in real-time biomedical control systems.
These facts are even more disturbing if one takes under consideration the recent developments in medical devices, especially in areas in which arterial blood pressure plays the key role. For example, recently developed prostheses such as Novacor, AbioCor and Baylor Left Ventricle Assist Devices call for the real-time arterial blood pressure waveform measurements.

Furthermore, the last decades of the 20th century brought new diagnostic methods such as sphygmocardiograhy, which utilize the blood pressure waveform rather than its mean parameters.

New implantable defibrillators can be enriched by the capability of real-time blood pressure measurement to ensure that the mechanical function of the heart has been restored. Numerous existing and emerging applications can benefit from real-time, long-term blood pressure waveform recording. Unfortunately, existing technology does not offer this capability.

In the author's opinion, the ideal solution to the described problem is to develop the implantable arterial tonometer, which will merge the advantages of tonometry with the benefits of the implantable device.

3. IMPLANTABLE TONOMETRY: FUNDAMENTAL PROBLEMS AND CHALLANGES

The implantable arterial tonometer, unlike the traditional one, is placed directly on the vessel, surrounds it and flattens the arterial wall generating proper applanation conditions.

Because the sensor is placed directly on the artery, it performs the measurements through the arterial wall tissue only.

Since the arterial blood pressure is transferred from the arterial lumen via arterial wall tissue to the sensor-arterial wall interface where it generates the contact pressure, the arterial wall mechanical properties are critical for the accurate blood pressure signal assessment.

Deep understanding of the tonometry biomechanical structure, including vessel wall interaction with the tonometer and its dynamic properties, can provide the biomedical engineers and researchers with a tool to evaluate the implantable tonometer advantages and limitations as well as its measurement characteristics under particular working conditions.

Another difference between the traditional tonometer and the implantable one is that the implantable device compresses the artery for a long period of time. It is a well known and documented fact that long-lasting stress/strain triggers remodeling processes on the living tissue, such as smooth muscle cells present in the arterial wall (Kim, 1999), (Kanda, 1992). Long-term implantation of the rigid structure, such as arterial tonometer, around the artery generates a specific field of mechanical stress distributed within the volume of the arterial wall tissue. This stress may initiate remodeling of the arterial wall

tissue. To date, nobody has studied this stress distribution due to the fact that tonometry was considered a short-term, noninvasive and ambulatory measurement only. Some researches have implanted tonometers (Mackey, 1968), but they have not studied how the device influences stress in the arterial tissue.

3.1. Proposed tonometer arrangement

After careful review of the anatomy and implantation procedures, the medical team led by Dr. Joseph and the author have chosen the implantation site for the arterial tonometer on an intrathoracic artery, as shown in figure 3.1. The controller of the device would be placed in the location similar to a pacemaker's, utilizing well-known implantation procedures and accompanying technology.

The proposed design of the implantable tonometer is also schematically depicted in figures 3.1 and 3.2.

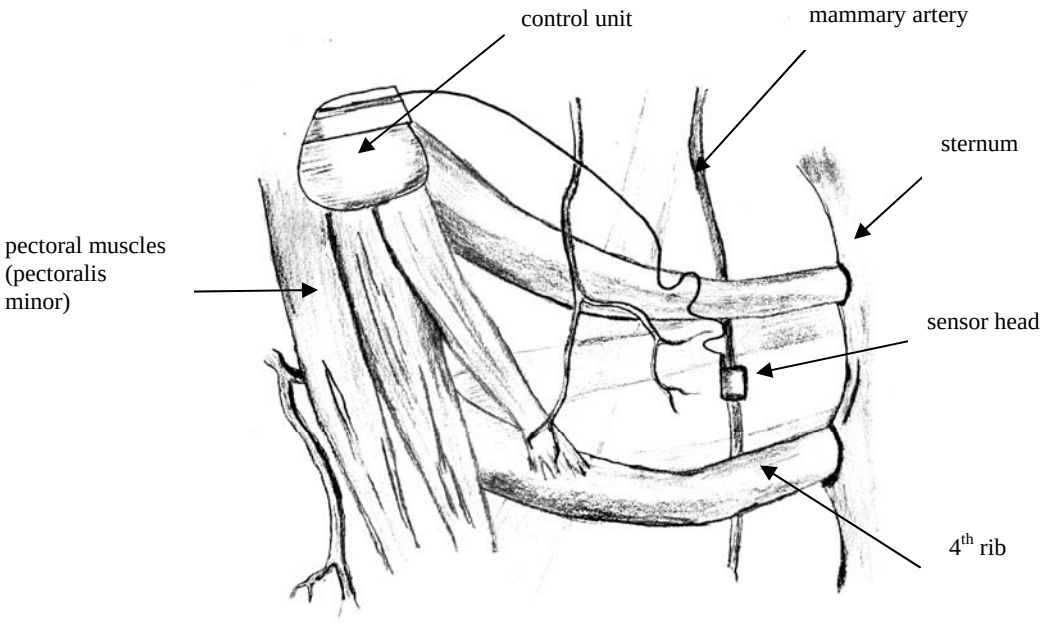

Figure 3.1. **Example of possible positioning of the implantable tonometer**: inside the rib cage on the internal thoracic artery, between 3rd and 4th rib.

The location for the tonometer has been chosen, taking into account safety of the subject and proximity of the aortic valve (minimization of the hydrostatic error). As a general rule, the sensor head of the device has to be placed on the artery, which can be damaged without any consequences for the subject. From a number of small arteries the mammary artery has been chosen. (More comprehensive analysis of the tonometer head implantation site is given in chapter 4.1.1. Biological component - arterial wall.)

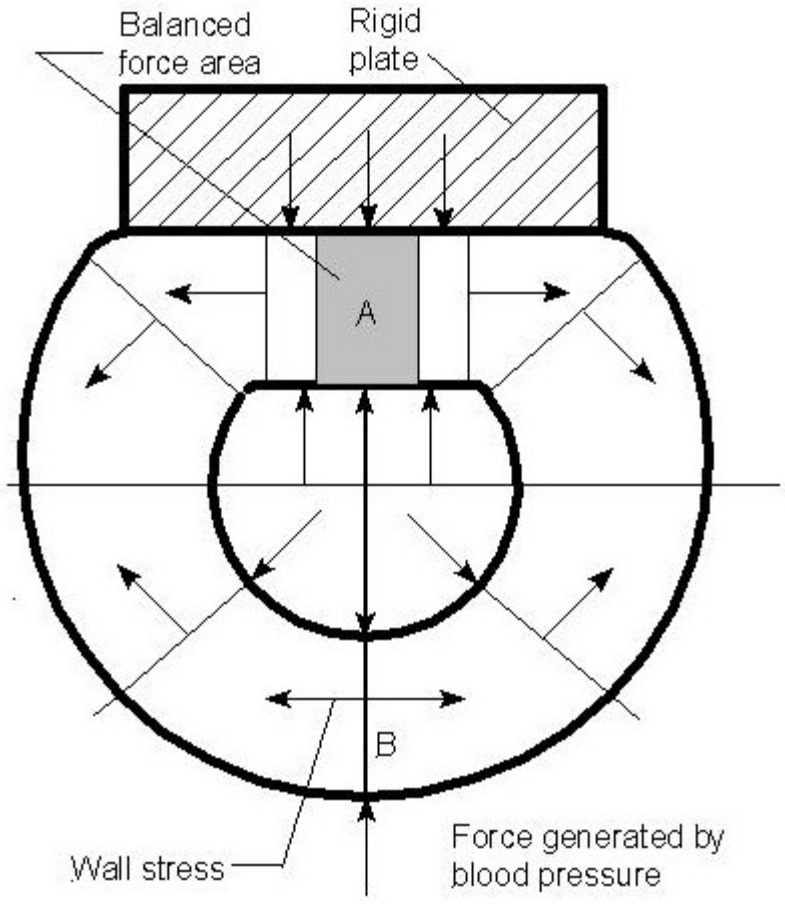

Figure 3.2. **The implantable tonometer applanation arrangement cross-section view**. Force distribution in artery cross-section.

The proposed sensing device consists of a U-shape support structure and flat sensing head. The applanation is generated on one side of the artery.

The schematic stress distribution inside the arterial wall is shown in figure 3.2. According to traditional applanation theory in region A (balanced force area), the internal wall stresses are perpendicular to stress generated by the intravascular blood pressure, thus they do not contribute to the contact pressure between the tonometer and the arterial wall. The U-shape support structure preserves the natural circular shape of the arterial wall in which the arterial wall stress contributes to the contact pressure (see region B).

3.2 Technological and biomedical challenges

The concept of an implantable arterial tonometer generates a series of problems unknown to the traditional tonometry. In the traditional approach, the tonometer compresses the artery only for a short period of time, while the implantable device compresses the vessel permanently. Also, the proposed implantable tonometer (figure 3.2) surrounds the artery, thus the applanation geometry is different than in the noninvasive case.

The applanation theory has to be revised, and the contact pressure between the tonometer and the arterial wall has to be calculated in order to determine how accurately the contact pressure reflects the arterial blood pressure signal.

The implantable device compresses the artery for months or even years, thus the potential risks have to be identified and tools to overcome them have to be provided. In an effort to do so, the internal arterial wall stress/strain has to be determined, allowing future stress-remodeling relationship studies.

Also, the proper sensor has to be designed to eliminate potential metrological problems such as nonlinearity.

The described-above situation generates two groups of problems: those related to the sensor and those related to the arterial wall tissue.

3.2.1. Sensor related problems

Because the implantable tonometer does not measure blood pressure directly, but instead measures pressure generated between the tonometer and the flattened arterial wall (so-called contact pressure), the phenomena occurring during pressure transmission from the arterial lumen to the tonometer are of critical importance. These groups of phenomena have to be studied in theory and experiment to determine vital parameters of the measuring process as well as design criteria for the future clinical devices.

Because the main purpose of this work is to study an arterial wall-tonometer structure as a dynamic system, the majority of the theoretical and the experimental studies have to lead to dynamic characteristics of the sensor.

3.2.1.1. Influence of the visco-elastic properties of the arterial wall on a dynamic response of the arterial tonometer

The arterial blood pressure transmission from the arterial lumen to the measuring transducer occurs in two steps: transmission from the blood volume to the visco-elastic, multi-layer structure of the vessel wall (consisting of tunica intima, tunica media and tunica adventitia), and subsequent transmission from the outer layer of the arterial wall to the transducer’s surface. Only by understanding the phenomena accompanying the pressure transmission through the visco-elastic structure can one properly determine the contact pressure distribution on the interface between the tonometer and the arterial wall.

The relationship between the arterial pressure signal and the contact pressure is the backbone of the whole tonometer measurement process and, importantly, this relationship includes both spatial and time-related effects.

3.2.1.2. Influence of the artery-tonometer geometry on the sensor response

The preliminary experiments have suggested that for vessels with thick walls (wall thickness to outer diameter ratio ≥ 0.1), the internal wall stress distribution generated by the applanation forces may affect the contact pressure (pressure between the arterial wall and the tonometer). Preliminary measurements have shown that contact pressure amplitude varies with applanation level. Thus, the influence of the applanation geometry, specifically applanation level, on the sensor response has to be studied and discussed.

3.2.1.3. Influence of the transducer stiffness on the sensor linearity

The arterial tonometer sensor head has to demonstrate high mechanical compliance in order to be a linear system (Mackey 1968), (Pressman, 1963). As shown in early works of Pressman, low compliance results in nonlinear effects. The implantable tonometer works in a different environment and geometry than the non-invasive device, thus the question of sensor stiffness has to be reformulated according to the sensor arrangement and mechanical properties of the biomechanical interface (arterial wall tissue). The study of tonometer response as a function of sensor stiffness can benefit future researchers by providing them with design criteria and a tool for error calculation.

3.2.2. Artery related problems

There is a need to describe the mechanical phenomena that occur in the volume of the arterial wall tissue surrounded by the tonometer. The implantable tonometer apparently changes the natural curvature of the vessel (figure 4.2). The vessel responds by adjusting itself and modifying natural strains. The internal tissue in the center of the flat region is stretched more than the free artery counterpart, while the internal tissue in the corners of the U-shaped structure undergoes high compression. The region at the bottom of the U-shaped structure undergoes moderate changes compared to those found in the free artery (normal). Knowing that strain is responsible for tissue remodeling (Rachev, 1997), (Kim, 1999), (Kanda, 1992), one can expect some tissue reaction inside the tonometer.

This study has to address the issue by building the mechanical finite element model in order to determine how the tonometer's geometry influences the stress/strain distribution inside the arterial wall tissue. This information is instrumental for future biocompatibility studies, giving a tool in the form of a stress/strain distribution map.

3.3. Thesis problem statement

The thesis identifies the key problem areas regarding implantable tonometer and addresses those problems by providing:

1. Theoretical description of the device's static and dynamic response;
2. Simulation of how the tonometer affects the arterial wall stress/strain map;
3. Sensor design criteria; and
4. Testing in-vivo and in-vitro procedures and signal analysis methods.

Solutions presented in the thesis lead to the fully operational device.

In addition, this thesis is meant to develop the theoretical (simulation), design (design criteria) and testing (in-vitro and in-vivo procedures) tools that will help future researchers in the designing process of the implantable arterial tonometer.

3.3.1. Theoretical modeling

The theoretical modeling of the phenomena occurring during the measurement process and applanation can help to explain the processes of the arterial blood pressure measurement.

In order to understand the tonometer sensor head behavior, the mathematical description of the sensor head transfer function is analyzed – which is the relationship between the input signal (pressure acting on the sensor head) and the sensor response. The transfer function links the design parameters and material parameters of the sensor head with the dynamic properties of the sensor. This simulation explains the link between various technological parameters of the hardware.

In order to understand important aspects of the sensor working on the living tissue, the dynamic response of the arterial wall-sensor head system is studied. The crucial question is how the sensor mechanical compliance influences the sensor linearity and how low the compliance has to be to meet the assumed accuracy requirements.

To verify the applanation theory for the implantable tonometer, the contact pressure map is calculated and analyzed.

The finite element analysis is developed to simulate semi-static behavior of the artery inside the tonometer.

For future biocompatibility studies, the stress/strain distribution map inside the arterial wall is simulated. Such a map will help to explain problems related to unnatural wall stress generated by the tonometer.

3.3.2. Design principles

Utilizing the results from the theoretical models, the design criteria are proposed. The desired tonometer geometry is determined in terms of:

1. Proper sensing area dimensions;
2. Sensing area position; and
3. Tonometer applanation level.

Also, the transducer type and design are proposed to meet linearity and accuracy requirements.

The measurement and signal analysis systems are built to meet transducer requirements.

3.3.3. Testing methodology

To verify modeling and design principles, the set of static and dynamic tests is performed. The relationship between the applanation level and the contact pressure is measured. The linearity of the static response is tested. Also, the dynamic response to the hydraulic signal is measured. The frequency domain analysis follows.

Some pilot in-vivo tests are performed to gain basic knowledge about sensor behavior inside the body and on the living tissue.

The long-term animal experiment is conducted to study the arterial wall remodeling.

3.4 Conclusions

The problems presented in the problem statement and their solutions draw the path from the implantable tonometer concept to the working prototype. Answers to those problems allow us to build a fully functional implantable tonometer.

Modeling provides us with quantitative requirements in terms of sensor geometry and technological parameters and reexamines the applanation theory for the proposed sensor arrangement.

Design is a physical realization of the theoretical results of modeling. Laboratory testing verifies both modeling and design assumptions.

Although the set of problems discussed in the thesis does not exhaust the subject, it establishes a foundation for the implantable tonometry and produces knowledge of how to build a fully functional device.

4. THEORETICAL MODELING

The tonometer designing process requires a set of designing criteria, which can be derived from the theoretical and experimental analysis of the sensor.

In vivo and in vitro experimental testing of the mechanical interaction between the artery and the tonometer, as well as analysis of the physical processes occurring inside the sensor head, is complex and time consuming. Therefore, the theoretical and mathematical description can speed up the analysis process without necessity of building costly and complicated laboratory systems. Theoretical modeling of the tonometer measurement process, based on the mathematical description, can provide valuable information useful from the designer and user points of view.

The implantable tonometer, unlike the noninvasive one, is intended to stay in human body for years. Thus, the influence of the tonometer on the arterial tissue has to be tested. Although the full biocompatibility study cannot be based solely on the theoretical simulation, the biomechanical component can be analyzed using numerical simulation. In other words, the stress and strain distribution generated on the arterial wall by the tonometer can be modeled and analyzed using theoretical and numerical models.

4.1. Introduction

In general, accuracy of the blood pressure measurements is determined by several factors, depending on sensor features as well as spectral content of the input signal. The convenient way of determining the general measurement system performance is a dynamic test. This kind of test can be performed using various methods like step function response or transfer function measurement. Regardless of the method, the dynamic

response of the blood pressure measurement system describes its accuracy (Togawa, 1999).

The dynamic response tells if the measurement system is capable of performing the particular type of measurements intended by a designer. For example, it is a known fact that the natural frequency of the system f_o has to be higher than the frequency of the measured signal. Also, the amplitude and the phase characteristics of the signal should be flat in the working range of frequencies (Togawa, 1999). The same criteria apply to the implantable tonometer.

Three layers of tissuem constitute the arterial wall: tunica intima, tunica media and tunica adventitia. They form the visco-elastic barrier between the pressure signal and the transducer (Bergel, 1961), (Dobrin, 1978) (Dobrin, 1984), (Fung, 1996), (Hansen, 1993). Thus the blood pressure signal undergoes distortion while propagating through this barrier (Westerhof, 1970) (Zhao, 1998). Moreover, inherent stresses to the arterial wall affect the arterial blood pressure being transferred from the vessel lumen to the transducer as well (Drzewiecki, 1979). Both, visco-elastic properties of the arterial wall and internal stresses are dynamic entities and are subject to change over time (Chamiot-Clerk, 1998), (Cheng, 2002), (Bank, 1995), (Joannides, 1997), (Ahlgren, 2001). Thus, without the mathematical description, relating biomechanical properties of the arterial wall and electro-mechanical properties of the transducer to the input and output signals, one cannot precisely predict the tonometer's response and, as a result, properly interpret the tonometer's readings.

The general solution to this problem, if the system is assumed to be linear, is found in the form of a transfer function between the input and the output signals.

$$G_{ij} = \frac{S_i(s)}{BP_j(s)} \qquad (4.1)$$

where G_{ij} is the transfer function; S_i i-th output parameter; BP_j- j-th input parameter.

4.1.1. Biological component-arterial wall

The tonometer is a device that works on the arterial wall. The measurand (arterial blood pressure) is separated from the sensor by the biological structure-living tissue. This structure is not uniform and varies its biomechanical features depending on an individual, health and location (Zhao, 2002), (Latham, 1985), (Lacolley, 2001).

Also, it is known that some arteries are prone to artifacts such as motion artifacts (e.g. those located in limbs) and hydrostatic error (locations above or below the heart). In addition, the anatomy of arteries varies, reflecting their physiological functions. Some of these anatomical features make the artery useless for implantation (e.g. the artery supplies blood to the large organ, and accidental damage of this artery by the tonometer can be dangerous for the subject).

This short overview offers a brief description of arterial features with emphasis on the potential usefulness for tonometer implantation. The overview is concluded by the target artery of choice. The choice of the implantation site determines the biomechanical parameters used in the numerical modeling.

The typical sizes of arteries are shown in the table below (Bronzino, 1995).

Table 4.1. **Typical diameters and wall thickness for main types of arteries**. Numbers are for a 68.7 kg individual with total blood volume 5.2 l.

blood vessel type	internal diameter range [mm]	wall thickness [mm]
aorta	10-30	2-3
main branches	5-2.25	2
large arteries	4-5	1
medium arteries	2.5-4	0.75
small arteries	1-2.5	0.5
arterioles	.0025-.01	002-.003

In general the arterial radius to wall thickness ratio varies from 0.06 to 0.16 (Nichols, 1998).

Typically, the arteries are divided into three groups: elastic arteries, muscular arteries and arterioles. This division takes into consideration major anatomical and functional characteristics:

- **Elastic Arteries (location: aorta, iliac arteries, pulmonary trunk)**

These arteries carry all blood flow or its major part. Typically the tunica media of elastic arteries consists of 40-70 layers of elastic fibers, alternating layers of circular oriented smooth muscle cells; tunica adventitia is thin. Elastic arteries, due to their high mechanical compliance, work as a “shock absorber,” which absorbs and accumulates the energy of the left ventricle contraction. Low concentration of muscle cells make them

good candidates for tonometry (constant visco-elastic parameters of the wall tissue) but they supply a majority of blood flow to the organs, thus they may be medically unacceptable as the implantation site. Also, the absolute radial pulsation of the artery, which is arterial radius change in response to the arterial blood pressure waveform (Darling, 1972), (Iversen, 1995), (Raines, 1973), (Yamakoshi, 1980) requires large applanation to obtain stable measurement conditions. Examples of radial pulsation are presented below (Nichols, 1998).

Human (40-50 yrs) ascending aorta under pressure 124/80 mmHg, radial pulsation: ±3.3 %, vessel OD: 16.4 mm

Human (male av. 47 yrs) descending aorta under pressure 132/77 mmHg, radial pulsation: ± 3.9 %, vessel OD: 10.9 mm

Human (19-35 yrs) abdominal aorta under pressure 116/64 mmHg, radial pulsation: ± 4.6%, vessel OD: 8.1 mm

The arterial pulsation is caused by the fact that the alteration in the internal blood pressure has to be compensated by the circumferential stress of the arterial wall. The increase in blood pressure generates an increase in circumferential stress, which leads to the strain adjustment according to Hook's law. The higher the mechanical compliance of the arterial wall tissue, the higher the strain response (Mekkaoui, 2001). The relationship between the vessel geometry and the transmural pressure is governed by equation (4.2) (Fung, 1984), (Ozkaya, 1991). The equation describes the equilibrium between blood pressure and circumferential stress. It points to the direct link between the circumferential stress and the transmural pressure.

$$T = h\sigma_{\vartheta} = p_i r_i - p_0 r_0 \qquad (4.2.)$$

where: σ_{ϑ}- circumferential stress, θ - angle; p_o – outer pressure; p_i – inner blood pressure; r_i- inner vessel radius; r_i- outer vessel radius; h - wall thickness

Counterintuitively, the equation 4.2. is valid even for non-homogenous, anisotropic materials such as arterial wall tissue.

The variables and coordinate system are shown in figure 4.1.

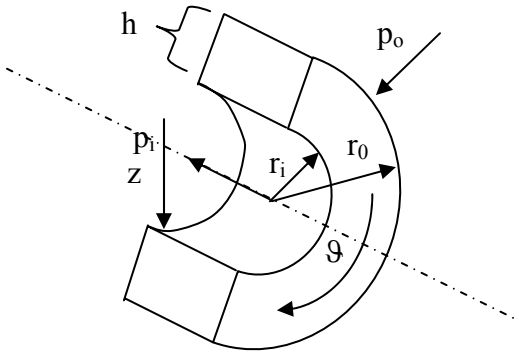

Figure. 4.1. Segment of the artery with cylindrical coordinate system

The bigger the arterial pulsation the more difficult applanation is - the artery has to be compressed more in order to provide a stable flat region. The big radial pulsation eliminates elastic arteries as potential candidates for tonometer implantation.

- **Muscular Arteries (location: most arteries arising off the aorta)**

Their size range is 0.1mm to 2.5 mm OD; relatively thick tunica media, mostly containing smooth muscle cells. The number of smooth muscle cell layers varies from 4 (small arteries) to 40 (large arteries); tunica intima is thinner than in elastic arteries. The function of muscular arteries is distribution of blood flow to various parts of the body. An

interesting feature is presented by one particular artery of this type: the mammary artery, also called the internal thoracic artery (mentioned in chapter 3). It is easily accessible, using a small surgical procedure and even if damaged presents little risk to the subject. It is also remarkably resistant to cholesterol buildup. These particular features were utilized by heart surgeons in the coronary disease treatment before the bypass technique was introduced by Favaloro and Ellis. Early surgical attempts tried to treat coronary heart disease by the direct implantation of the internal mammary artery into the myocardium; they were made by Vineberg and Miller in 1951. Their procedure is well documented and studied, assuring that the mammary artery can be safely used for the implantation procedure. In addition, the mammary artery lies in direct proximity of the aortic valve, which reduces the potential hydrostatic error, and the rib cage protects the device against motion artifacts.

- **Arterioles (location: smallest arteries branching from the muscular arteries)**

Their diameter is less than 0.1mm. Arterioles consist of 2-3 layers of smooth muscle cell; their function is blood pressure and flow regulation by changing the resistive component of local organ impedance. Because of the small diameter and high resistivity/pressure variations, these arteries they are not considered as being useful for tonometer implantation.

The conclusion of the presented overview is that the potential tonometer implantation should be around the muscular artery, close to the aortic valve, preferably inside the rib cage. Those criteria are met by the intrathoracic muscular artery-mammary artery. This target muscular artery is 1-5 mm OD (Nichols, 1998) and has the wall thickness around 10% of the overall arterial outer diameter (OD).

The proposed implantable tonometer concept utilizing the intrathoracic artery is presented in figure 4.2.

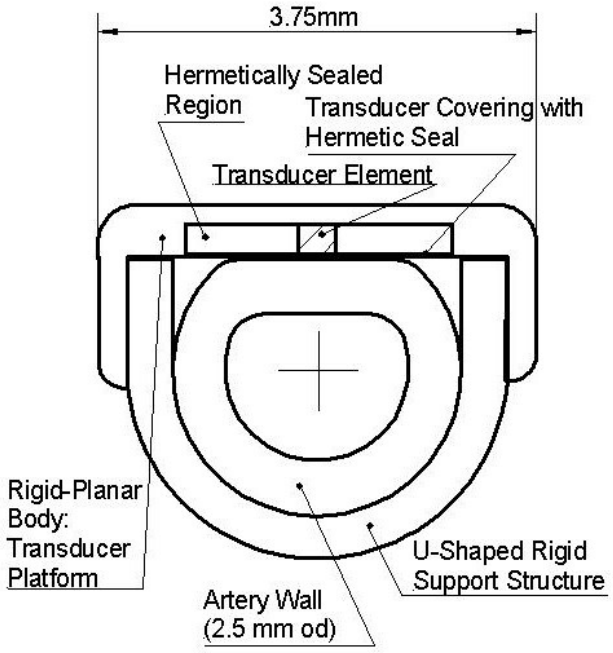

Figure 4.2 **Example of possible positioning of the implantable tonometer** on the mammary artery.

4.1.2. Arterial wall structure

Different types of arteries differ significantly between themselves. The arterial geometry such as arterial OD and the wall thickness depends on the artery type. Also, thickness of the arterial wall internal layers depends on the artery type. On the other hand, some features are common for all arteries. The layer structure is an example of such a feature.

The typical arterial wall segment is shown in figure 4.3. The arterial wall consists of three layers: adventitia, media and intima (Daly, 2002). The demarcation line between tunica media and tunica intima is an internal elastic lamina made of fenestrated

membrane of elastin lined on the intimal side by a coarse fibrous network. The outer elastic lamina demarcates the tunica adventitia.

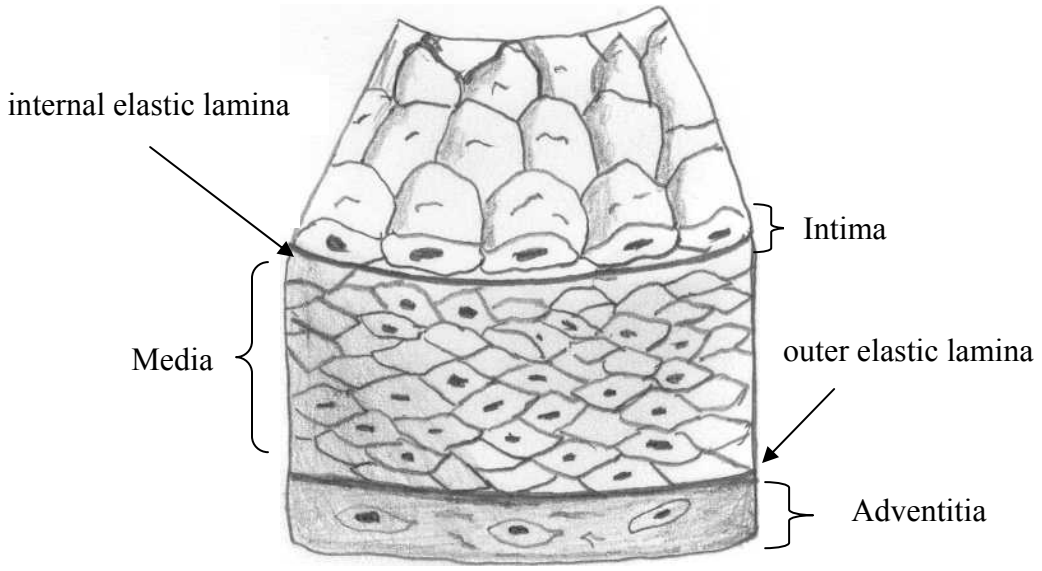

Figure 4.3**. Segment of a muscular artery**. An internal structure of the arterial wall is clearly visible: tunica intima, tunica media and tunica adventitia.

Arterial wall tissue consists mainly of collagen and elastin fibers, which surround smooth muscle cells.

Three arterial wall layers have a significantly different structure and composition (see figures 4.3 and 4.4).

Tunica adventitia is mostly fibrous (mostly collagen and small quantities of elastin) and anchored in surrounding connective tissue. The adventitia and media usually are penetrated by the mesh of smaller arteries (vasa vasorum) that supply blood to the smooth muscle cells. Tunica adventitia is mostly made of fibers. Its outer border is sometimes not well defined, and transition between adventitia and surrounding connective tissue is gradual.

Tunica media is a major determinant of the arterial wall mechanical properties. It is made of collagen and elastin fibers and smooth muscle cells. For example, the fiber composition in the upper part of the aorta is ~70% elastin and ~30 % collagen. Below the diaphragm the composition changes to 40% elastin and 60% collagen, which makes media stiffer. The elastin and collagen fibers form layers running circularly or in a tight helix. Between those layers lay smooth muscle cells. The smooth muscle cells make the media an active mechanical element, which is governed by biochemical elements (e.g. hormones) as well as sympathetic and parasympathetic nervous systems. Smooth muscle cells form a spiral structure, mostly parallel to the elastin, around the lumen, while elastin and collagen form a three dimensional network. Under the physiological pressure, all elements (elastin, collagen and smooth muscle cells) form well-defined layers.

Tunica intima consists mainly of endothelial cells and is a barrier between blood and the arterial wall. Endothelial cells of tunica intima are flat cells, and their shape and pattern depends strongly on shear stresses generated by the blood flow. Tunica intima contributes little to the overall mechanical properties of the arterial wall, although mechanical stress and strain (e.g. applied by the shear stress generated by the blood stream) strongly affect cellular structure and function.

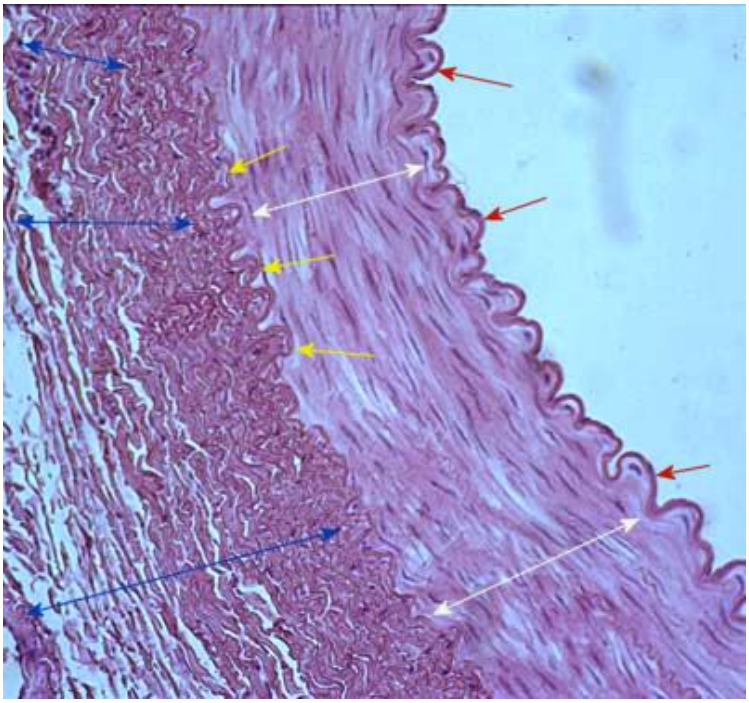

Figure 4.4. **The arterial wall cross section.** Three layers of tissue are shown: red arrow – tunica intima; white arrow – tunica media; yellow arrow – external elastic membrane; blue arrow – tunica adventitia.

4.1.3. Mechanical properties of the arterial wall

The arterial wall visco-elastic properties are described by various authors in different way, using a whole spectrum of models and visco-elastic parameters (Drzewiecki, 1998), (Nichols, 1998), (Learoyd, 1966), (Armentano, 1966). A complicated structure of the arterial wall (e.g. collagen and elastin networks and their connection to the smooth muscle cells) (Fung, 1984), (Osol, 1995) is responsible for such a situation. The strong variability of parameters, such as composition of collagen and elastin and smooth muscle cells concentration along the arterial tree (Nichols, 1998), or among different age groups (Armentano, 1966), as well as between species (Cox, 1978), makes the task even more difficult.

Because of that, mechanical properties of any target artery cannot be expressed as a set of constants. All arterial wall parameters vary with age, subject physiological status, disease, etc. (Wong, 1993) Some parameters vary in short periods (e.g. smooth muscle cell tension) (Hayoz, 1993), while some change over a long period of time and represent specific drift of mechanical properties (e.g. collagen-elastin composition or calcification of tissue) (Armentano, 1966).

Thus, in this paper the mechanical properties are treated as parameters characterized by their range and an average value. The values, which are used in simulations and calculations, are defined based on the literature and, if it is possible, the whole range of physiological values is used. The literature usually presents numbers or range of values: statistical median for population or the center value of the known physiological range. It is necessary to note that those numbers are difficult to validate since many of them are given without information about how they were obtained (in vivo, ex vivo, in situ, etc.) and about the population from which the sample was drawn. Also, some arteries attract more attention from the scientific community due to the fact that they are closely related to popular diseases or treatment (e.g. aorta, coronary arteries, and carotid arteries). In contrast, some vessels are barely described in the physiological literature.

Elastic modulus

Generally speaking, the arterial wall is not a Hookean material. The elastic modulus cannot be defined as a set of constants (Nichols, 1998), (Fung, 1995). Due to the fact that lower stress engages mostly elastin fibers (higher mechanical compliance) and higher stress starts to recruits gradually more collagen fibers (lower mechanical

compliance), the stress-strain relationship for the arterial wall tissue is far from linear (see figure 4.5). The additional stress can be introduced by the activated smooth muscle cells. The smooth muscle cells shift the stress-strain relationship curve as shown in figure 4.5. (Nichols, 1998).

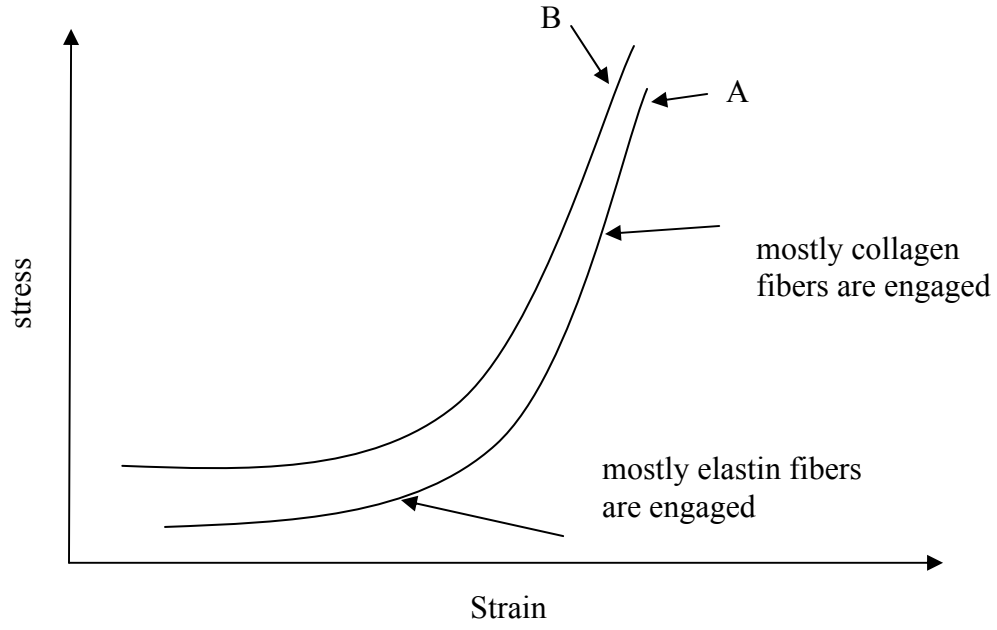

Figure 4.5. **The generic relationship between stress and strain in the arterial wall tissue**. Curve A corresponds to relaxed smooth muscle cells, curve B to activated smooth muscle cells. Based on (Nichols, 1998).

Nevertheless, many authors provide some specific numbers for Young's modulus assuming that under particular conditions the arterial wall is a Hookean and isotropic material. As a commonly accepted practice, the living arteries under physiological load (i.e. blood pressure pulse) are treated as the Hookean isotropic material governed by the Hook's equation.

$$\begin{bmatrix}\sigma_{xx}\\ \sigma_{yy}\\ \sigma_{zz}\\ \sigma_{xy}\\ \sigma_{xz}\\ \sigma_{yz}\end{bmatrix} = \frac{E}{(1-2\nu)(1+\nu)} \times \begin{bmatrix} 1-\nu & \nu & \nu & 0 & 0 & 0 \\ \nu & 1-\nu & \nu & 0 & 0 & 0 \\ \nu & \nu & 1-\nu & 0 & 0 & 0 \\ 0 & 0 & 0 & \frac{1-2\nu}{2} & 0 & 0 \\ 0 & 0 & 0 & 0 & \frac{1-2\nu}{2} & 0 \\ 0 & 0 & 0 & 0 & 0 & \frac{1-2\nu}{2} \end{bmatrix} \begin{bmatrix}\varepsilon_{xx}\\ \varepsilon_{yy}\\ \varepsilon_{zz}\\ \varepsilon_{xy}\\ \varepsilon_{xz}\\ \varepsilon_{yz}\end{bmatrix} \quad (4.3)$$

Or in short form

$$[\sigma] = [D][\varepsilon] \quad (4.4)$$

Thus, only two parameters are commonly used to characterize the static mechanical properties of the arterial wall: Young's modulus E and Poisson's Ratio ν. According to Nichols and others, the Young's modulus in systemic arteries working under physiological conditions is from 2.0 to 8.0 x 10^6 dyne/cm^2 (Nichols, 1998); Poisson's ratio ~0.5 (incompressible material; in this case the material property matrix D in equation 4.4 becomes singular). In addition, sometimes the bulk elastic modulus is given 2.2 x 10^{10} dyne/cm^2 (Nichols, 1998), 4.4 x 10^9 dyne/cm^2 (Carew, 1968).

Bulk modulus is very often overlooked, but in some cases its importance is undeniable. In tonometric measurements the majority of the blood pressure energy is transferred to the sensor by the perpendicular to the arterial wall compression of the tissue, therefore, the bulk (compressional) modulus plays an important role. Utilization of a low compliance transducer even increases bulk modulus importance. Bulk modulus of the artery was calculated by McDonald in 1975 (Nichols, 1998) and is 2.2 x 10^9 N/m^2, which is close to bulk modulus of water equal to 2.05 x 10^9 N/m^2. McDonald's calculations were based on the assumption that the arterial wall contains 70% water (Nichols, 1998). Carew et al. measured arterial wall compressibility (Carew, 1968) and

obtained average arterial wall bulk modulus 4.2 x 10^8 N/m^2. Assuming the arterial wall is being compressed by physiological transmural pressure of 120 mmHg, 15 996 Pa - systolic value for a healthy individual, the change in artery wall thickness (for McDonald's value of bulk modulus) will be equal to 7.3x10^{-6} fraction of the wall's original volume. Assuming arterial wall thickness of 1 mm (large arteries see table 2.1) and only radial changes, the overall compression of the arterial wall will be 7.3 x10^{-9} m. For traditional transducers like Mackay's tonometer (Mackay, 1964), where the device was working with the sensing mechanism displacement close to 0.15 mm, one can say that artery wall thickness changes were negligible (the difference between transducer deflection and wall thickness compression is 5 orders of magnitude-wall thickness compression is roughly 10^5 times smaller than the transducer deflection). On the other hand, the Young's modulus of PZT, used as a transducer in design presented in this work, is 4.4 x 10^{10} N/m^2 (Mad City Labs Nanopositioning Products Catalog). Thus using a PZT type of transducer, one can expect that arterial wall compression will be comparable to transducer displacement (actually, arterial wall compression will be 20 times larger than transducers displacement!). This "inversion" of stiffness ratio introduces new issues, which, to our knowledge, have not been addressed in any tonometry study.

Dumping factor

The static description of the artery is not enough to describe the mechanical response of the artery to the dynamic stimulus such as blood pressure pulse. The elastic real modulus has to be substituted with a complex elastic modulus, capable of describing energy dissipation in the arterial wall tissue. The complex modulus also describes frequency dependent behavior. The arterial structure by nature dissipates energy by

being a viscous material. Numerous authors refer to the mechanical properties of the arterial tissue as visco-elastic. The visco-elastic properties have been described by various models such as Maxwell, Voigt or St Venant (Nichols, 1998), (Drzewiecki, 1998), (Fung, 1984) or their combinations. Some authors also add contractility of the SMC, creating new models such as Hill's model (Fung, 1984), (Drzewiecki, 1998). The value of the viscous component of visco-elastic modulus of the tissue depends on the applied model. In the Voigt model chosen for this thesis the visco-elastic modulus is:

$$E' = E + j\mu\omega \quad (4.5)$$

where E is the real part of the modulus (Young's modulus) μ is viscosity and ω is frequency. The viscosity for such model is ~1.2 x 10^6 dyne/cm^2 (Nichols, 1998).

In real tissue the viscosity is highly frequency dependent and decreases with frequency (in arterial tissue ωμ grows only to 2 Hz and then stays constant with increasing frequency (Nichols, 1998)).

4.2. Methods of analysis of the measurement process and arterial wall tonometer interaction.

A broad range of problems involved in the implantable tonometer measurement process requires a variety of modeling and analysis techniques.

The measurand conversion from the intralumenal pressure to the tonometer response will be simulated using a concept of mechanical system transfer function. This technique will answer the question of how the biomechanical system converts applied pressure to the transducer element displacement. The result is the tonometer's transfer function in frequency domain.

The linearity and error of the implantable tonometer is studied using the lumped parameter model, where the input and output signals are compared in time and frequency domain. The model takes into account typical biomechanical parameters of the muscular artery (i.e. Young's modulus, and viscosity) coupled with the tonometer sensor head equipped with a piezoelectric transducer. This analysis compares typical physiological input – blood pressure waveform recorded in the human aorta – with the tonometer's output. The model helps to understand the inherent nonlinear behavior of the tonometer working on the arterial wall and allows studying optimal configuration to minimize the nonlinear response.

The simulations are performed for the range of transducer's Young's moduli. The outcome of this analysis determines the range for the tonometer's Young's modulus in which the measurements are linear and fall into an assumed accuracy range.

The detailed biomechanical interface and arterial wall phenomena are modeled by a Finite Element Method (FEM). This method models the contact pressure distribution on the interface between the tonometer and the artery as well as the stress and strain map inside the arterial wall. The simulation is four-dimensional (3 dimensions plus time) and reveals a complex nature of the interface phenomena. The contact pressure map is presented and analyzed as well as stress-strain inside the arterial wall to determine how the applanation changes the natural arterial wall stress-strain distribution.

4.2.1. Transfer function

One of the goals of tonometer modeling is to build a mathematical description of the measurement process, i.e. a set of equations describing how the arterial blood pressure signal is transmitted from the artery lumen to the output voltage signal. The

numerical solution to this set of equations will provide the designer with crucial information about the system response to different working conditions, such as different elastic modulus of the arterial wall and viscosity (E_{wall} and η) and different mechanical compliance of the transducer (which transfers to different elastic modulus of the whole transducer-E_{Tr}).

Since the implantable tonometer presented in figure 4.6. is intended to reproduce precisely the shape of the waveform (which is equivalent to a spectrum in frequency domain), the main focus of this work is to gain understanding of dynamic processes occurring in the tonometer-arterial wall biomechanical system. The measuring process takes several steps and starts from the blood pressure waveform (called a BP(t) signal or an input signal) and ends on the output voltage signal, see figure 4.7. Each of the measurement steps introduces a specific disturbance in time and frequency domains. In order to reconstruct properly the parameters of the blood pressure input signal from the output voltage, it is practical to know the transfer function of the entire sensing path. Although, the concept of transfer function is applicable only to linear time-invariant systems, and tonometry, as will be shown in this chapter, faces serious non-linearity, especially during the signal transfer through the arterial wall. Moreover, it is a time varying system due to aging and activity of the smooth muscle cells: vasoconstriction and vasodilatation (Drzewiecki, 1998). The author shows that the linearization is possible for some specific conditions, such as small transducer displacement, low frequency, and stable inherent wall stresses. The transfer function concept allows making the design process more efficient and demanding less-complicated calculations in early stages of the sensor development.

The generic tonometer structure is depicted in figure 4.6.

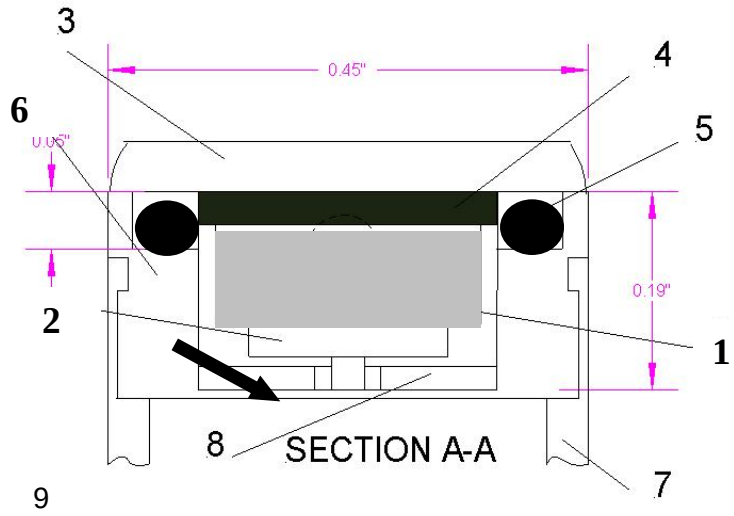

Figure 4.6. Cross-section of the implantable tonometer. (1) force transducer, (2) pin, (3)and (6) stainless steel housing, (4) Rubber layer generating prestress, (5) O-ring, (7) U-shape supporting structure, (8) stainless steel washer, (9) arterial wall. An arrow ↓ indicates a thin wall of a stainless steel housing.

This structure, in terms of signal transfer from the measurand to the output signal, can be represented in form of the diagram shown in figure 4.7.

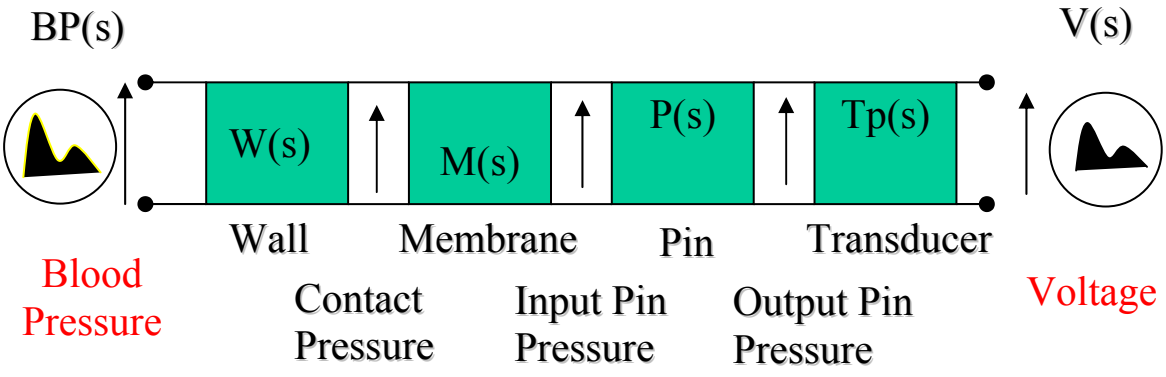

Figure 4.7. Conceptual model of the tonometer's sensing path. ↑ represents signals, and blocks represent transfer functions of each functional element of the tonometer.

Green blocks represent the transfer functions of the physical object while the arrows represent signals being generated.

The corresponding transfer function equations (in s domain) for the sensing path are:

$$BP(s)W(s)M(s)P(s)Tp(s) = V(s) \tag{4.6}$$

$$G(s) = \frac{V(s)}{BP(s)} = W(s)M(s)P(s)Tp(s) \tag{4.7}$$

where: BP(s) is a blood pressure signal, W(s) is wall transfer function, P(s) is the pin transfer function, Tp(s) is transducer transfer function, V(s) is voltage output, G(s), overall tonometer transfer function (see chapter 4.3).

Blood pressure transfer through the arterial wall

In order to simulate the blood pressure signal transfer through the arterial wall a lumped parameter, mechanical model is built. This part of the measurement process is represented in figure 4.7. by the block W(s). It is a first step of the measurement process. The input BP(s) signal-blood pressure is transferred to CP(s) - contact pressure between the arterial wall and the tonometer's head. To obtain W(s) transfer function, one has to express the conversion from blood pressure to contact pressure BP(s) ->CP(s) as a linear process. The necessary assumptions for linearization are made as well as justification for the linearization process is discussed.

Contact pressure to the input pin pressure conversion – membrane contribution

There are many types of membranes that can be used in the tonometer design. The membrane behavior can be studied as a separate problem. The membrane is usually designed to introduce minimal or no disturbance between the forward and backward pressures. It is usually achieved by very large mechanical compliance and small mass. Since this work is not to study the technicalities of various types of membranes, the

membrane is assumed to be an ideal membrane with no influence on the tonometer performance. The generality of the study will be preserved even if the membrane will not be ideal due to the fact that mechanical properties of the membrane can be incorporated in transducer properties and expressed in effective mechanical parameters of the sensor head that are introduced into analysis.

Propagation through the pin and transducer's response

The pin between the transducer and the membrane is considered to be a simple pressure divider. Although the mass of the pin introduces inertia that contributes to the phase shift between the input and output signal and the resonant frequency of the system, it is easier, without losing accuracy, to include this mass into the sensor head effective mass.

4.2.2. Lumped parameter model

The general layout of the two-dimensional tonometer-arterial wall biomechanical system is shown in figure 4.8. For clarity's sake, the membrane and the pin are omitted due to the fact that their contribution is included into effective sensor head parameters. Let us consider the physical situation on the two-dimensional representation of the interface between the tonometer and the arterial wall. The applanation is achieved by compressing the arterial wall by the rigid structure (RS), and the force sensor (FS) is positioned in the middle of the rigid structure. The g is a gap between the force sensor and the rigid structure. Blood pressure compresses the arterial wall, deflecting the force sensor by distance x. Since every force sensor undergoes a deflection during the measurement process, the situation in figure 4.8. shows a general configuration during the measurement process. Assuming that the border conditions do not allow the arterial

wall any motion parallel to the rigid structure (in Y direction), the arterial wall has to be stretched in order to transfer blood pressure to the force sensor (FS).

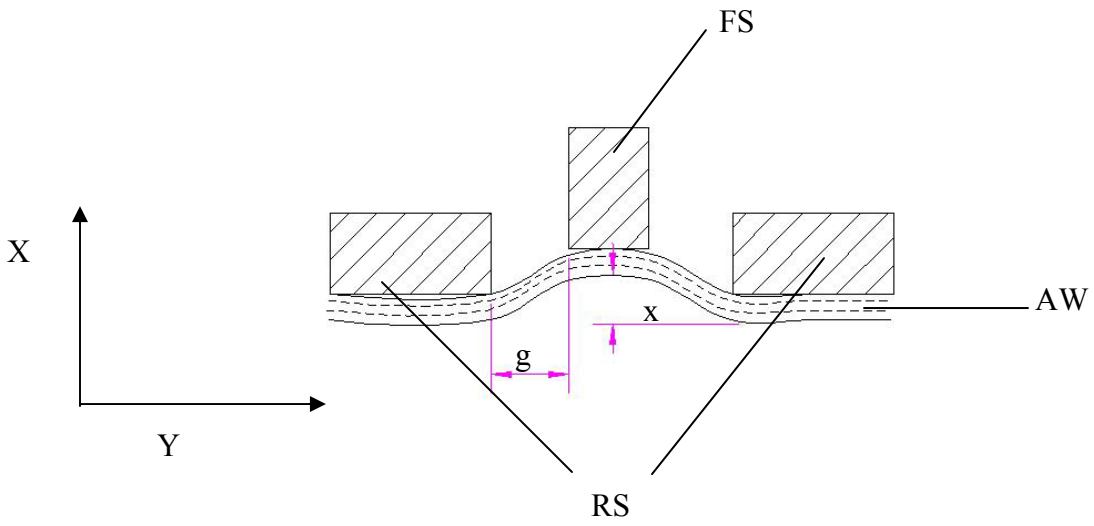

Figure 4.8. **Arterial wall under applanation.** The gap between the force transducer and the rigid body g and the amplitude of deflection x are shown. AW represents arterial wall, RS rigid structure of the sensor head and FS represents force sensor transducer.

Both transfer function as well as the dynamic response of the system depicted in figure 4.8 can be obtained by simulating the arterial wall – tonometer system using a lumped parameter mechanical model (see figure 4.9).

This model is established on a spring-dashpot concept. The spring-dashpot system addresses the problem of dynamic response of the tonometer working on the visco-elastic arterial wall. The model contributes to the general understanding of the measuring process and helps with building the tonometer's sensing path.

The system is built of spring-dashpot linear elements that represent elastic and viscous properties of the living tissue and the tonometer. The spring is responsible for

simulating a Young's modulus (potential energy accumulation) and dashpot represents dumping properties (energy dissipation). For reasons discussed later, the spring dashpot configuration for each physical entity is built as a parallel one.

This configuration of elements is called Voigt model and its response to the mechanical stress is described by the equation (Nichols, 1998):

$$\frac{\Delta L}{L} = \frac{T}{E}\left(1 - e^{Et/\mu}\right) \quad (4.8)$$

Where T is stress, L length of the Voigt element, ΔL change in length, E elastic modulus, μ - viscosity, t- time.

In the model shown in figure 4.9. the Voigt elements simulate longitudinal and perpendicular to the acting force properties of the arterial wall and the longitudinal (compressional) properties of the transducer. The force F is generated by the blood pressure pulse BP(t).

In panel 1A the undisturbed tonometer - arterial wall system is depicted (no pressure applied). The transducer is not compressed and the arterial wall stays undisturbed. In panel 1B the blood pressure generates force F>0 and compresses the arterial tissue, stretches it and consequently compresses the transducer. The springs represent longitudinal and perpendicular elastic modules and the dashpots longitudinal and perpendicular viscous behavior.

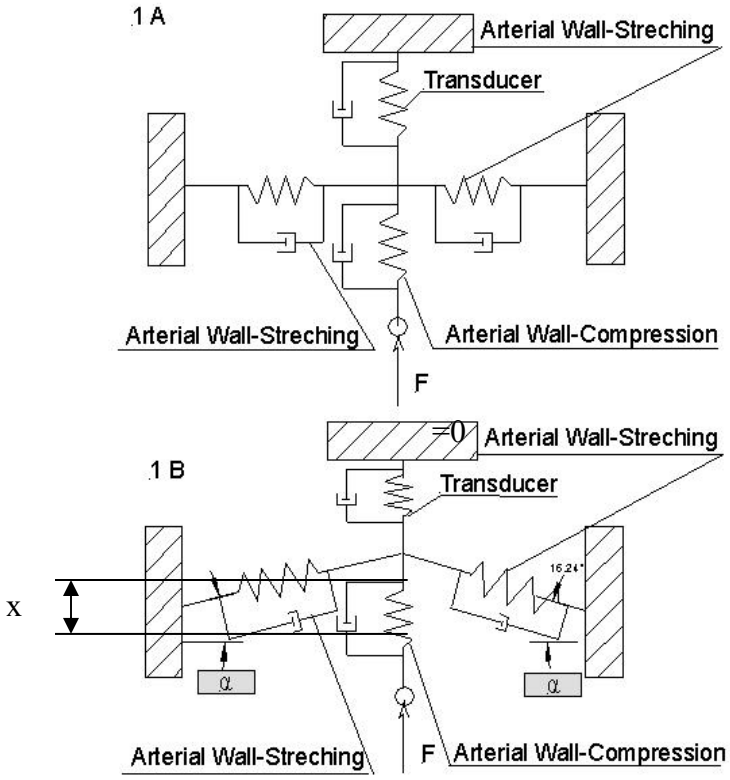

Figure 4.9. Conceptual model of arterial tonometry. Panel A shows applanation without blood pressure applied (F=0). Panel B shows transducer deflected by the force generated by the blood pressure Voigt element representing transducer is compressed. Forces generated by arterial wall stretching introduce nonlinearity in transducer's reading due to angle α between stretched arterial wall and the force F generated by the blood pressure.

In this model the F is BP_j input parameter and the displacement x is S_i output parameter (see equation 4.1). Although, the spring dashpot subsystems are linear, the overall system represents strong non-linear properties due to arterial wall stretching that acts under certain angle α determined by F.

The results of this analysis are presented and discussed with a strong emphasis on their design implications.

4.2.3. Finite element model

Because the in-vivo and in-situ analysis of the biomechanical phenomena taking place during the tonometric measurement process, particularly those within the volume of the arterial wall, is difficult and in some instances virtually impossible, the numerical analysis, such as finite element modeling approach, seems to be of great help in gaining the basic understanding of this part of the tonometry sensing mechanisms.

To model the complicated behavior of the tonometer-arterial wall interface (contact pressure) and the stress inside the arterial wall (see figure 4.10) the finite element model is proposed.

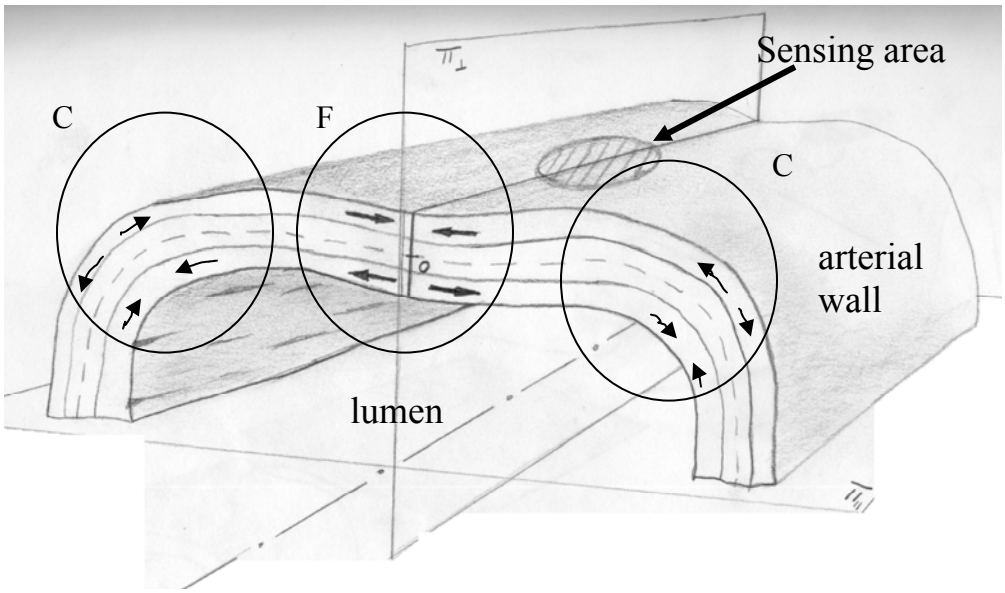

Figure 4.10. Stress in flattened artery. In central region of flattened wall (region F), external layers are compressed and internal stretched. In corners of U-shaped structures (region C), stress distribution is opposite. Circular dashed region shows the position of tonometer's sensing area.

The model reproduces applanation geometry: the artery is encircled by the tonometer. The tonometer consists of the U-shaped support structure and the sensor head. The artery

inside the tonometer is represented by a mash of elastic elements. The model is subjected to the loads simulating arterial pulse pressure and the load generated by artery compression during applanation. First the applanation load is applied and then the pulse is built as a series of static loads. The output is stored as a complete map of stress and strain recorded in the model's nodes. This map is subsequently used for further analysis.

Stress and strain

In general, the non-linear relationship between the circumferential stress and strain is observed in real arterial tissue (see figure 4.5). This relationship and, for the linear approximation, the equilibrium equation 4.2 determine the mechanical behavior of the free artery. In contrast, if the artery is flattened by the tonometer, the natural circumferential stress is disturbed and an additional stress is introduced. The situation is shown in figure 4.10 where the flattened portion of the artery is depicted. Considering the central part of the flattened artery (F region in figure 4.10), the superficial layer is compressed, as indicated by arrows, and the deep layer is stretched. The tissue in the corners of the tonometer support structure region (C regions in figure 4.10) undergoes reversed stress distribution. The additional stress can modify the flattened artery geometry by introducing unbalanced forces, buckling the artery toward the lumen. The preliminary studies, using the silicon mock arteries, have suggested this kind of behavior (see figure 4.11.).

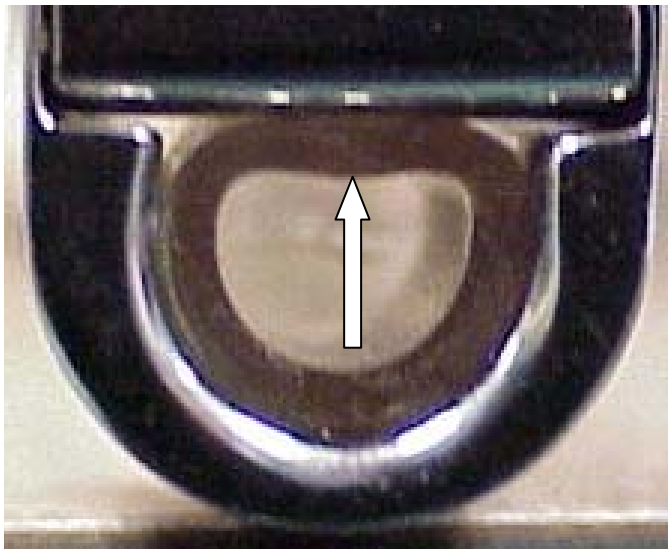

Figure 4.11. Preliminary studies showing buckling phenomena occurring in the center of the applanation region.

As a result, applanation does not generate a flat region in which the stresses are perpendicular to the arterial blood pressure, as would be expected based on the classic tonometry theory. Instead, the arterial wall generates a complicated pattern of stress/ strain distribution.

Therefore, to understand the true nature of this phenomena, the numerical simulation is conducted, and the stress/strain map recorded in model nodes is stored for further analysis.

Tonometer- artery interface (contact pressure)

The buckling effect affects not only the stress inside the arterial wall but also affects the contact pressure. The contact pressure is a direct input for the tonometer sensor head, therefore, the understanding of the contact pressure nature and its relation to the blood pressure is critical to the overall measurement process. The finite element model, built by the author for this study, maps the stress distribution and calculates the

contact pressure, thus the blood pressure signal can be related to the contact pressure (see figure 4.12.).

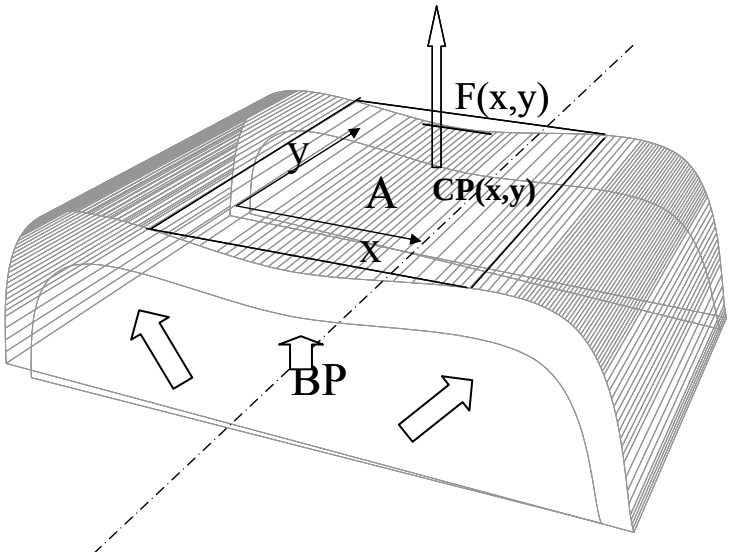

Figure 4.12. Contact pressure on the flat portion of artery. The wall produces force F(x, y) per area A, which is contact pressure CP. To calculate this pressure the FEM simulation and integration over the area A needs to be performed.

The pilot experiments have shown that the contact pressure acting on the sensing element is not uniform and varies along x and y axes (figure 4.11 shows the front view of the mock tonometer and artery, the buckling indicates a decrease in contact pressure in the center of the sensing area). In general, force F acting on the transducer is expected to be a function of: x , y as well as time :

$$F(t) = A\int_x \int_y CP(x, y, t)dxdy; \qquad (4.9)$$

Where:

$$CP(x, y, t) = CP[BP(t), x, y]; \quad (4.10)$$

where A is a contact area between the tonometer and the arterial wall, CP contact pressure, BP blood pressure signal.

Therefore the relationship between BP(t) and F(t) – the actual tonometer input signal – demonstrates a much more complicated nature than that predicted by the traditional theory.

4.3. Sensor head transfer function

The target design of the sensor head is shown in figure 4.13. It consists of: membrane (M), pin (P), piezoelectric transducer (Tr) and elastic support (ES). All these elements are considered to be linear time invariant systems (in terms of transferring mechanical stress). Thus, they can be represented by a spring dashpot linear system (see figure 4.14).

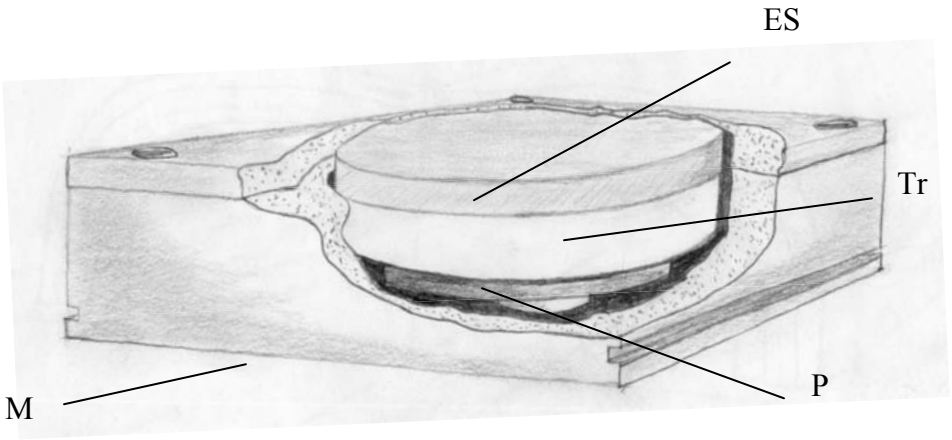

Figure 4.13**. Generic tonometer sensor head**. It consists of membrane, pin, force transducer and elastic support.

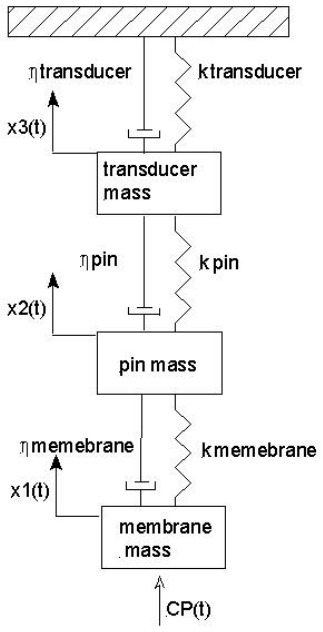

Figure 4.14. **Sensor head model**. A spring-dashpot representation of three major components of the sensor head.

Let us consider the transducer as a system consisting of only one mass, a dashpot and a spring element. This simplification is justified because of the fact that the sensor head consist of the several linear subsystems, thus one can describe the series of linear systems as a cumulative, mass, elasticity and dumping factors. None of them represents the actual physical values. But instead, they are calculated using parameters of elements shown in figure 4.14. The equivalent simplified "spring-dashpot" model is shown in figure 4.15.

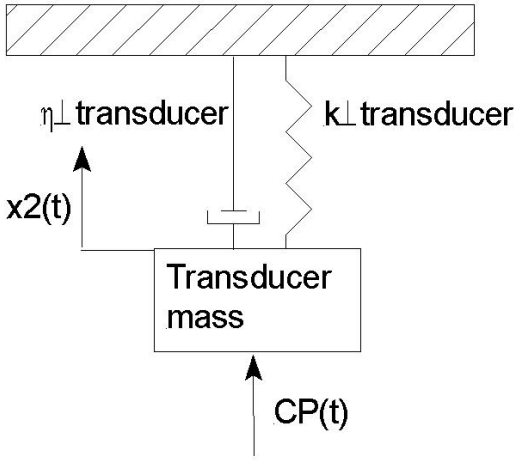

Figure 4.15. **Sensor head simplified model**. A spring-dashpot representation.

In this case the sensor head representation is much simpler than the system containing the arterial wall (figure 4.9) and does not include nonlinear factors since the acting force is parallel to the spring-dashpot system. Corresponding equations are:

$$M_{Tr}\frac{d^2x(t)}{dt^2} = -k_{Tr}x(t) - \eta_{Tr}\frac{dx(t)}{dt} + CP(t); \qquad (4.11)$$

$$\frac{dx(t)}{dt} = v(t); \qquad (4.12)$$

Where M_{Tr} is transducer mass, x transducer displacement, k_{Tr} transducer elasticity, η_{Tr} transducer viscosity, CP contact pressure, v(t) velocity of the transducer displacement.

With the simplified sensor head representation, one can easily calculate the transfer function. The transfer function between the force and the effective mass displacement (force sensor deflection) x(t) is given by:

$$\frac{X(s)}{CP(s)} = \frac{1}{Ms^2 + \eta s + k_{Tr}} \qquad (4.13)$$

where M, η, and k are respectively: effective mass, effective viscosity, and effective elasticity.

Effective parameters were calculated for PZT transducer's mass = .05 g, pin mass= 0.01, membrane mass = 0.001g, PZT η = 6 dyne/cm^2, Stainless steel η= 1 dyne/cm^2, rubber η= 7 dyne/cm^2, PZT k= 4.4x10^{11}dyne/cm^2, Stainless steel k= 19.5 x 10^{11}dyne/cm^2, rubber k=0.23 x 10^{11}dyne/cm^2.

Summarizing, the sensor head can be represented as a linear system because it consists of several linear subsystems arranged in a series, thus the equivalent system can be derived and subsequently the transfer function of it can be calculated. The sensor head mechanical model is shown in figure 4.14. (consisting of the 3 independent elements: membrane, pin and force transducer). It is subsequently converted to the equivalent one shown in 4.15, which consists only of the spring, dashpot, mass elements representing effective values.

4.3.1. Results and discussion

The relationship between the force generated by the contact pressure and the sensor displacement in terms of sensor head transfer function is presented in figure 4.16. The magnitude of s_{21} parameter is almost constant and phase also changes by 5x10^{-6} degrees in a frequency range from zero to 20 rad/s (~6.36 Hz). For blood pressure measurement, this type of change is negligible (order of 10^{-10} in magnitude and 10^{-6} in phase). Mechanically the sensor head can be considered as an element that does not introduce any change to the input signal.

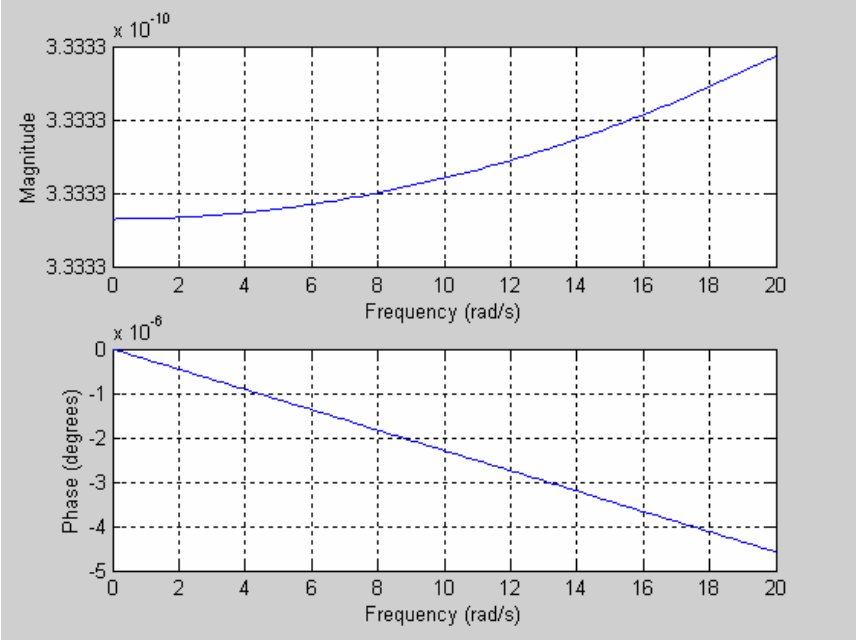

Figure 4.16. **Sensor head transfer function**. Magnitude and Phase plots.

4.4. Lumped parameter model of the implantable arterial tonometer

The lumped parameter model presented in this chapter simulates the dynamic properties of the arterial wall under applanation, sensor head, and the overall system (sensor head coupled with the arterial wall). Initially, the analysis of the arterial wall is performed to show nonlinear behavior of this part of the measurement system, and then the whole process is reconstructed to find out how the nonlinearity can be minimized by changing sensor head mechanical compliance. The analysis is performed with the typical input signal recorded in the human aorta. The aortic pressure is decomposed into harmonics and the first five of them are used in calculations. The remaining higher harmonics are omitted for clarity's sake and due to the fact that they carry only a minute amount of signal energy and their contribution to the measurement process is negligible.

4.4.1. Lumped parameter model of the arterial wall under applanation

The model shown in figure 4.17 represents basic features of the arterial wall biomechanical system. The spring represents the elastic modulus of the arterial wall while the dashpot simulates wall tissue viscosity. The mass of the arterial wall is simulated by the effective mass concentrated in the center of the system, between two Voigt type elements.

Arterial wall properties. The key point in modeling of the wall response is the mechanical properties of the arterial wall tissue. The arterial wall model employed in the dynamic response lumped parameter simulation takes into consideration two fundamental features of the human tissue: elastic modulus and viscosity. Both parameters constitute the complex visco-elasticity:

$$E` = E + \eta \varpi j \qquad (4.14)$$

where E' is a complex viscoelastic modulus consisting of E, the Young's modulus, and ηω is the viscous loss component (Nichols, 1998). The equivalent mechanical model for this type of viscoelasticity is a spring and dashpot arranged in parallel (Armentano, 2001). Because in the presented simulation the tissue undergoes small strains and the input signal consists of low frequency harmonics (0-20 Hz) (O'Rourke, 1996), the model assumes E and η to be constant. This is consistent with other researchers' work (O'Rourke, 1996), (Drzewiecki, 1998), and (Learoyd, 1966). This lumped parameter model does not take into consideration the three-layer structure of the arterial wall and does not include changes in E' due to smooth muscle activity (Drzewiecki, 1998), thus it's more valid for the large vessels such as the aorta, where the smooth muscle concentration in tunica media is lower then for muscular arteries where smooth muscle

cells are higher in number. Nevertheless, this approach allows us to build relatively simple dynamic models and study the dynamic behavior of the biomechanical and mechanical components of the tonometer system.

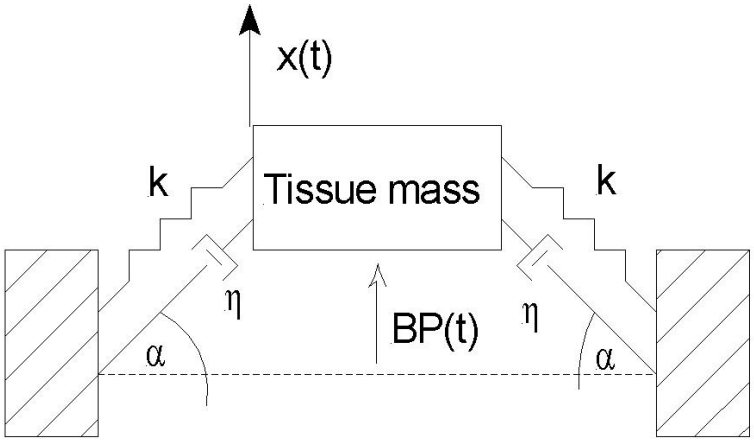

Figure 4.17**. Spring-dashpot model of the arterial wall under applanation** and undergoing deformation due to the arterial blood pressure BP(t). Where k is elastic constant, η viscosity, BP blood pressure, x transducer's displacement.

Presented in figure 4.17, the model shows mechanical arrangement and relations between the input signal (intraluminal arterial blood pressure BP(t)) and the arterial wall displacement x(t).

This model is a simple non-linear oscillator described by the following system of equation:

(4.15)

$$M\frac{d^2x(t)}{dt^2} = -2k\sin(\alpha)(\sqrt{g^2 + x^2(t)} - g) - 2\eta\sin(\alpha)\frac{d(\sqrt{g^2 + x^2(t)} - g)}{dt} + BP(t);$$

(4.16)

$$\frac{dx(t)}{dt} = v(t);$$

Where:

$$\alpha = \arctan\frac{x(t)}{g};$$

(4.17)

$$\frac{d(\sqrt{g^2 + x^2(t)} - g)}{dt} = \frac{x(t)}{\sqrt{g^2 + x^2(t)}}\frac{dx(t)}{dt}$$

(4.18)

The first equation describes forces acting on the mass M. The left side represents inertia, while the right side describes respectively: forces generated by springs, dashpots and the blood pressure input signal. Where: x(t) is the wall displacement (output signal), g is the gap between rigid structure and sensing element, BP(t) blood pressure, v(t) velocity of wall displacement, η wall viscosity, k wall elastic modulus.

Choosing x(t) and v(t) as the state variables and labeling them x_1 and x_2 respectively, one obtains a simple linear system of differential equation describing nonlinear oscillator depicted in figure 4.17.

(4.19

$$\frac{dx_2}{dt} = \frac{-2k}{M}(\sqrt{g^2 + x_1^2} - g)\sin(\arctan\frac{x_1}{g}) - \frac{2\eta}{M}\sin(\arctan\frac{x_1}{g})\frac{x_1}{\sqrt{g^2 + x^2_1}}x_2 + \frac{BP(t)}{M};$$

$$\frac{dx_1}{dt} = x_2;$$

(4.20)

This system is relatively easy to analyze despite the fact that it's nonlinear. The Runge-Kutta method was employed to solve the system.

Arterial wall transfer function for small displacements

For some types of force transducers such as piezoresistive and piezoelectric, the transducer displacement x(t) can be reduced to micrometers or even angstroms (e.g. for piezoelectric transducers), thus, it is reasonable to consider neglecting the contribution of wall longitudinal elasticity on the transducer response.

Let's consider force that acts on the wall while the wall movement is restricted to very small displacements. Mathematical meaning of this assumption is a limit of the following formula:

$$\lim_{x\to 0, v\to 0} F(x,v) = -2k\sin(\alpha)(\sqrt{g^2 + x^2(t)} - g) - 2\eta\sin(\alpha)\frac{d(\sqrt{g^2 + x^2(t)} - g)}{dt} \quad (4.21)$$

The limit is equal to 0. What can be clearly shown on the F(x,v) 3D plot. Force acting on the arterial wall as a function of x and v is shown in figure 4.18.

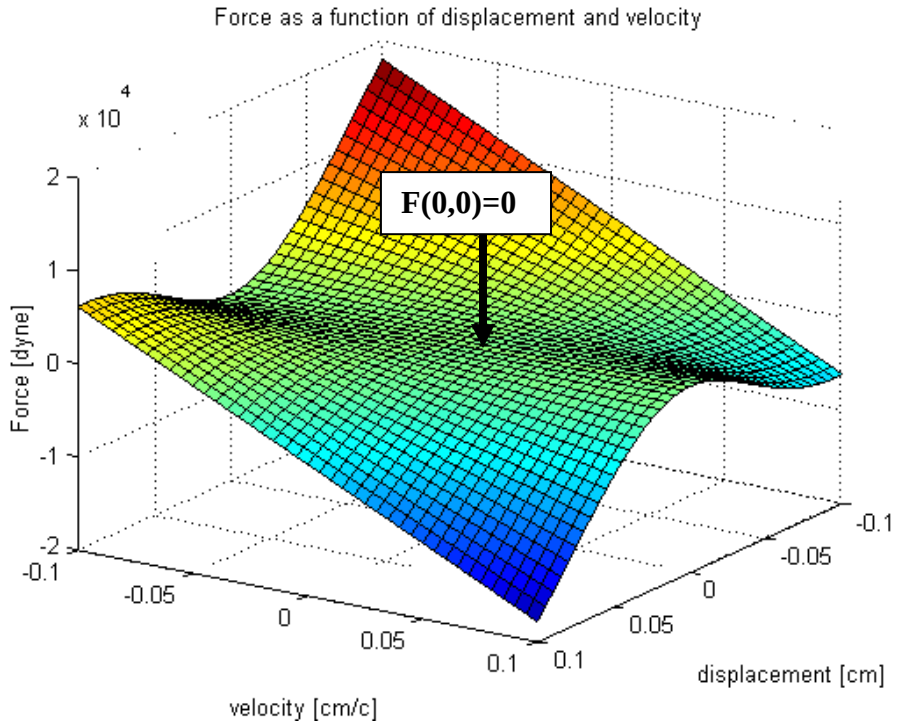

Figure 4.18. Force acting on the arterial wall as a function of displacement and velocity.

Also, on the force vs. displacement (fixed velocity) and force vs. velocity (fixed displacement) graphs (figures 4.19 and 4.20) the force function limit clearly approaches 0 while x and v are approaching 0. Figure 4.21 shows F(x) for three different velocities of the wall. The higher the velocity the higher the gradient dF(x)/dx, but around 0 all functions rapidly approach their limit equal 0. Thus, the longitudinal contribution of the arterial wall can be neglected under the condition that the transducer's displacement and its velocity are negligible. If x and v approach zero, the sensor head lumped model can be constructed consisting only of spring and dashpot connected in parallel and acting in the same direction as force generated by the blood pressure.

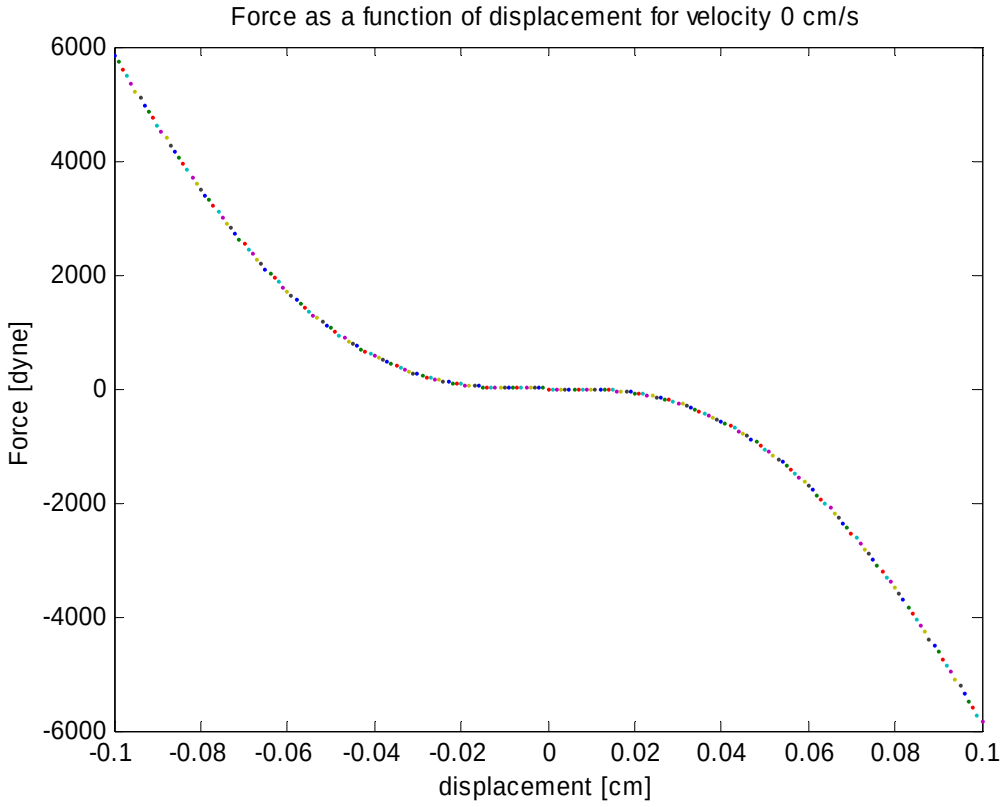

Figure 4.19. Force acting on the transducer as a function of displacement; velocity=0.

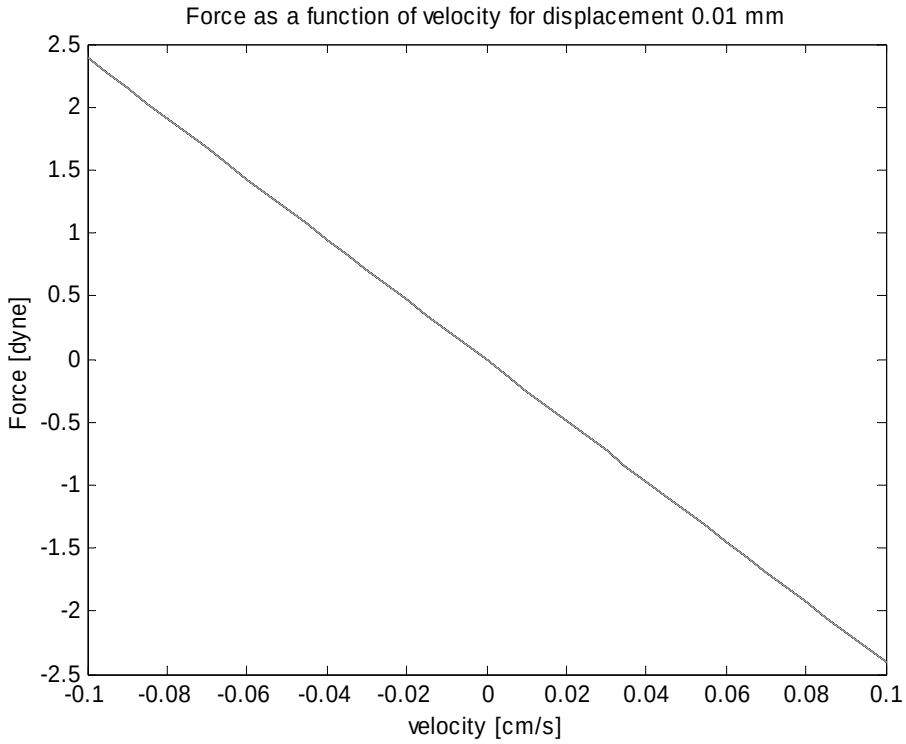

Figure 4.20. Force acting on the transducer as a function of velocity; displacement=const.

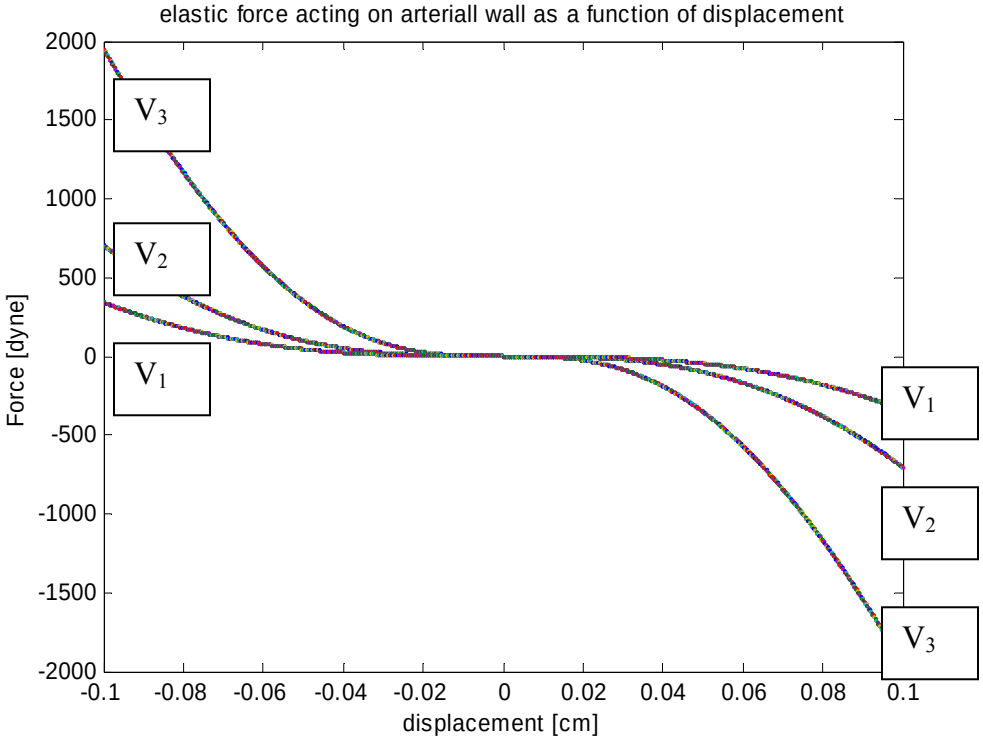

Figure 4.21. **Family of force functions vs. displacement for three different velocities**. $V_3 > V_2 > V_1$

4.4.2. Complete sensing path model

The complete path representation is shown in figure 4.22. The transducer part is shown in its simplified form using effective parameters M, η, and k.

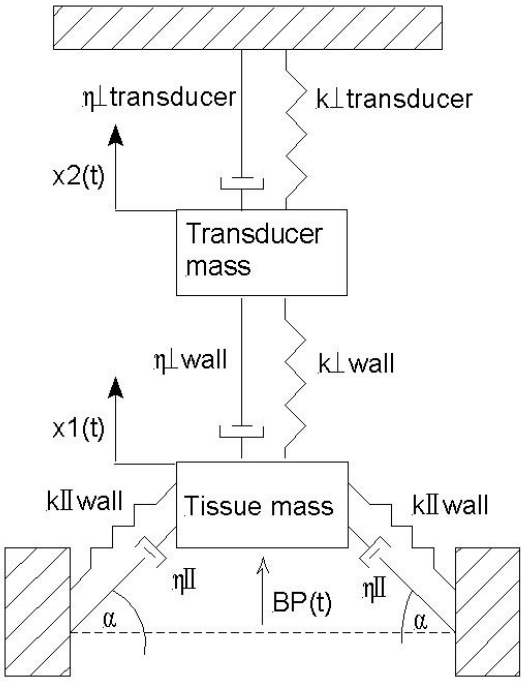

Figure 4.22. The complete sensing path spring-dashpot representation.

Simplifying further, one can reduce the linear components of the system by introducing effective mass for transducer and the arterial wall as well as effective elasticity and viscosity. The resulting model is shown in figure 4.23.

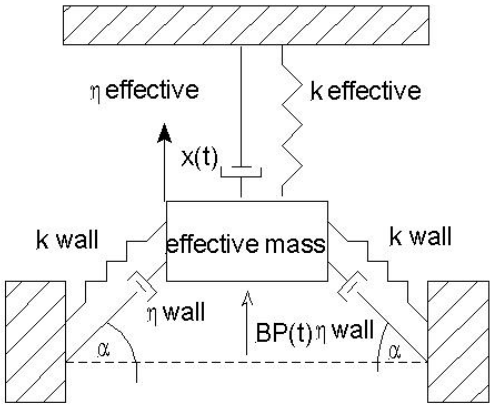

Figure 4.23. The complete, simplified sensing path spring-dashpot representation.

The complete lumped parameter model is described by a set of equations:

$$\frac{dx_2}{dt} = -k_{tr}x_1 - \eta_{tr}x_2 - \frac{2k}{M}(\sqrt{g^2 + x_1^2} - g)\sin(\arctan\frac{x_1}{g})$$
$$-\frac{2\eta}{M}\sin(\arctan\frac{x_1}{g})\frac{x_1}{\sqrt{g^2 + x^2_1}}x_2 + \frac{BP(t)}{M}; \quad (4.22)$$

$$\frac{dx_1}{dt} = x_2; \quad (4.23)$$

Where: x(t) is the wall displacement (output signal), g is the gap between rigid structure and sensing element, BP(t) blood pressure, v(t) velocity of wall displacement, η wall viscosity, k wall elastic modulus, η_{tr} transducer viscosity, k_{tr} transducer elastic modulus, x_2 transducer velocity, x_1 transducer displacement.

This model takes into consideration linear and nonlinear forces acting on the transducer. This model will be used to simulate the system's dynamic behavior. Several simulations are performed to show:

i. Influence of the transducer stiffness Etr on the transducer response.

ii. Transducer response to the first 5 harmonics of the arterial blood pressure signal.

4.4.3. Results of lumped parameter model simulation

The results of the simulation are presented below. Initially the non-linear behavior of the arterial wall under applanation is presented, and then subsequently the whole sensor is simulated.

Simulation of the non-linear arterial wall response

The simulation was run for the typical muscular artery parameters where $k=1000000$ dyne/cm^2; $\eta=1200000$ dyne/cm^2 (Nichols, 1998). And transducer parameters used in 4.3.

The input signal, the arterial blood pressure wave, was simulated by the first 5 subsequent harmonics of the input signal (from 1st to 5th). The amplitudes of harmonics were typical for the BP waveform recorded 45 cm from the aortic arch (approximately the border between the elastic and the muscular arteries), (Nichols, 1998). The frequency of the first harmonic is 1 Hz.

Applied harmonics had the following amplitudes:

Table 4.2. Arterial blood pressure waveform harmonics and their modulus.

Harmonic Number	Modulus [mmHg]
1st	9
2nd	6
3rd	5
4th	1.8
5th	1.8

The arterial wall response to the first five harmonics is presented below. The frequency responses for the first three harmonics are shown in figures 4.24, 4.26 and 4.28 (the complete series of responses is presented in Appendix B). The comparison in time domain between the input signal and the arterial wall response for the first three harmonics is shown in figures 4.25, 4.27 and 4.29 (the complete series of responses is presented in Appendix B).

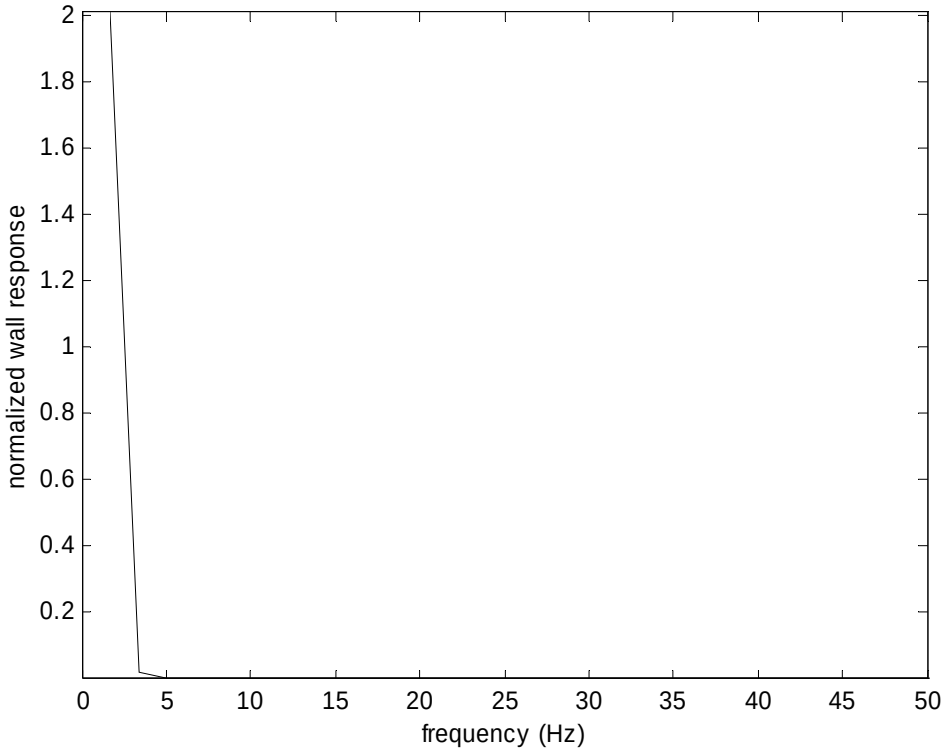

Figure 4.24. **Frequency content of the arterial wall response (input frequency 1 Hz**, amplitude 9 mmHg).

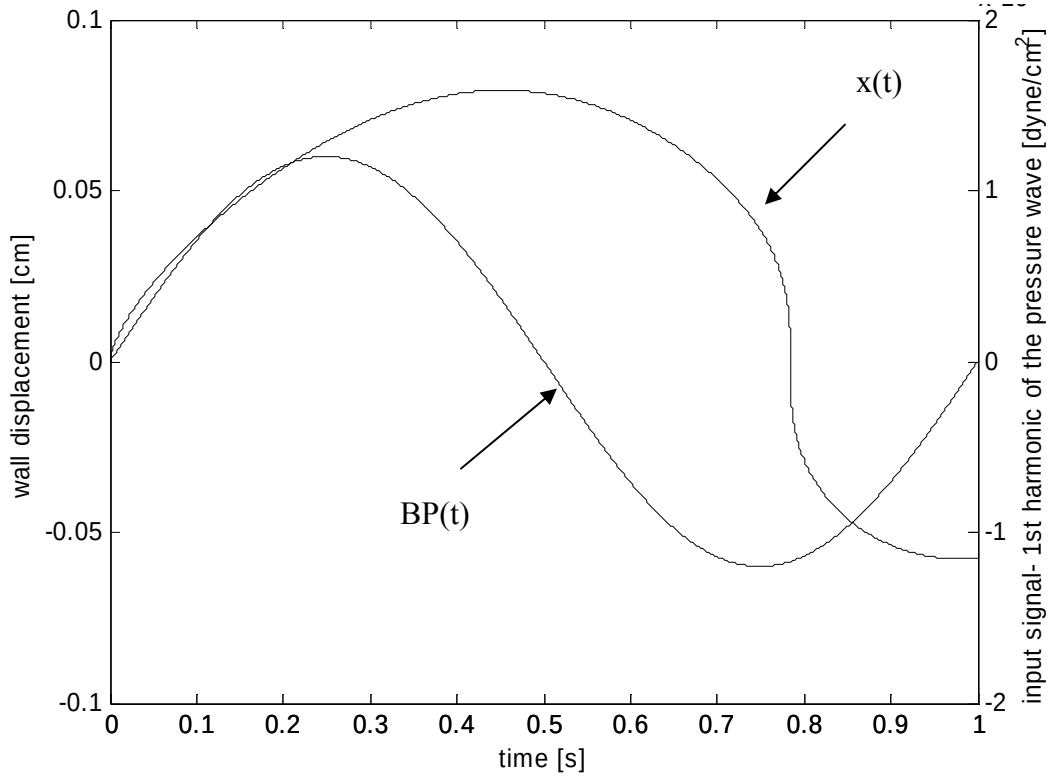

Figure 4.25. Time response of the arterial wall and the input signal (first harmonic).

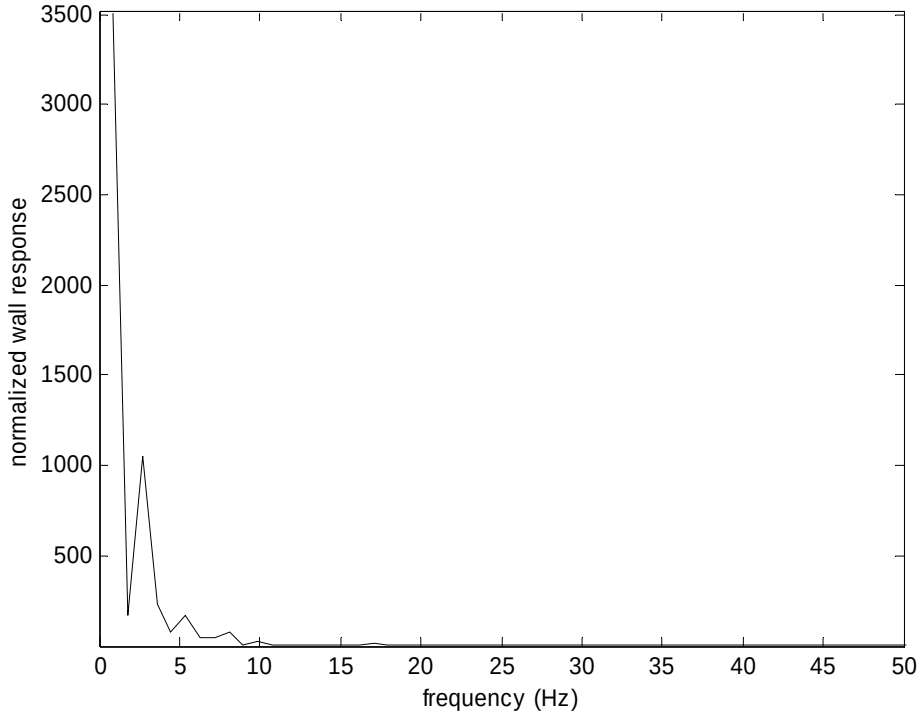

Figure 4.26. **Frequency content of the arterial wall response (input frequency 2 Hz)**, amplitude 6 mmHg).

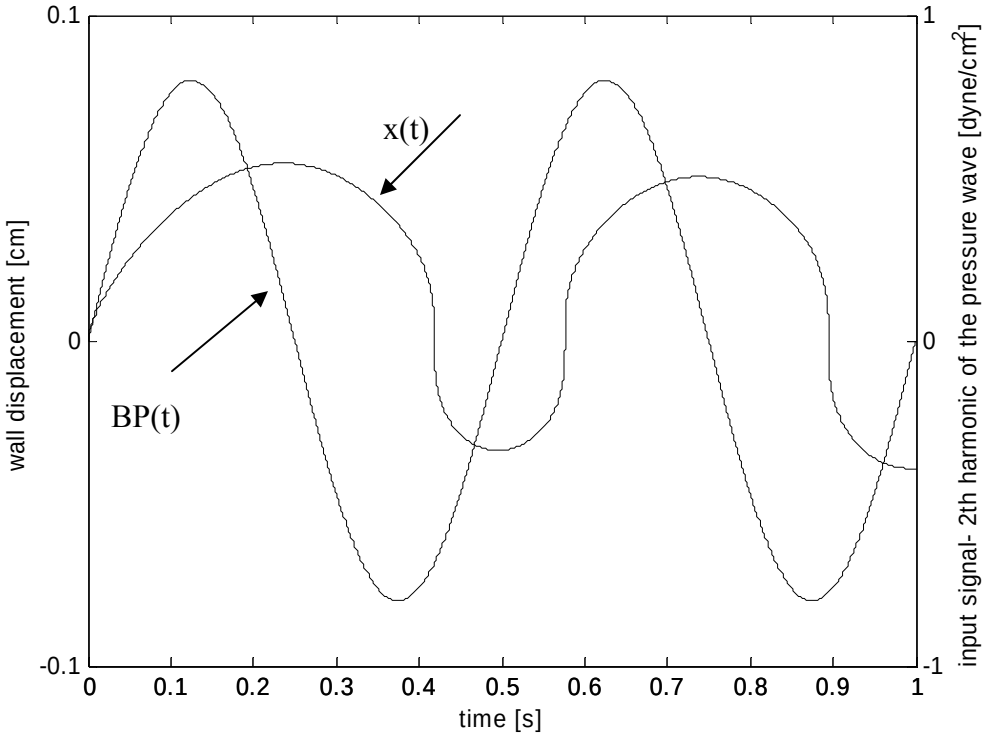

Figure 4.27. Time response of the arterial wall and the input signal (second harmonic).

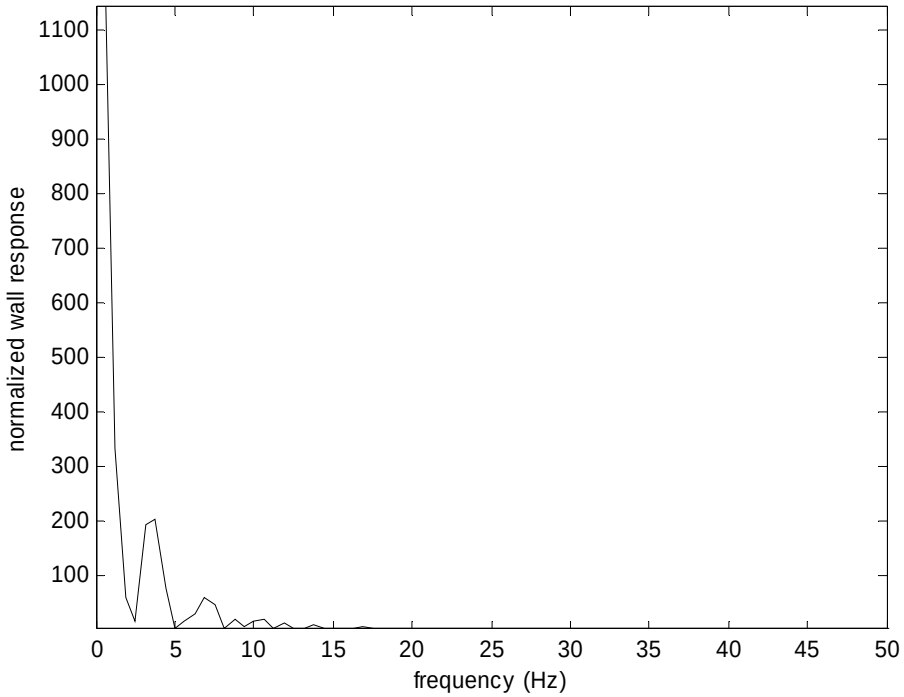

Figure 4.28. **Frequency content of the arterial wall response (input frequency 3 Hz**, amplitude 5 mmHg).

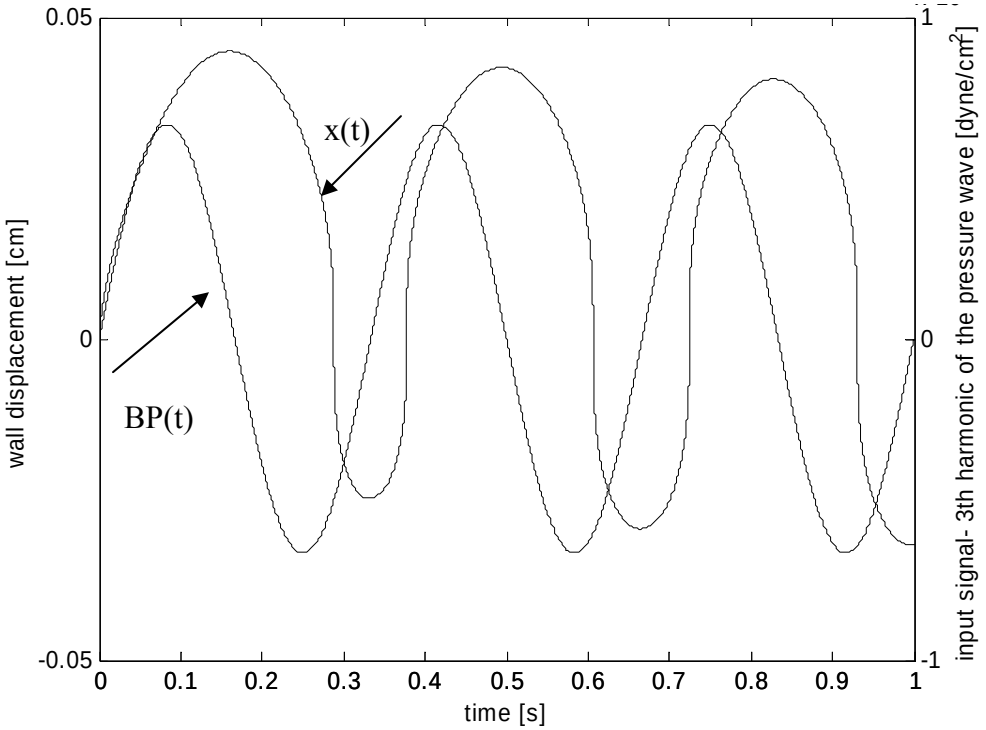

Figure 4.29. Time response of the arterial wall and the input signal (third harmonic).

Artery – tonometer system response

The wall-transducer system depicted in (figure 4.23) was tested. The frequency was fixed at 1 Hz and the transducer elasticity was changed in range from Etr=10^6 to Etr=10^10 dyne/cm^2. The results for Etr=10^6, 10^7, 10^8 dyne/cm^2 are presented below (the whole sequence is presented in Appendix B).

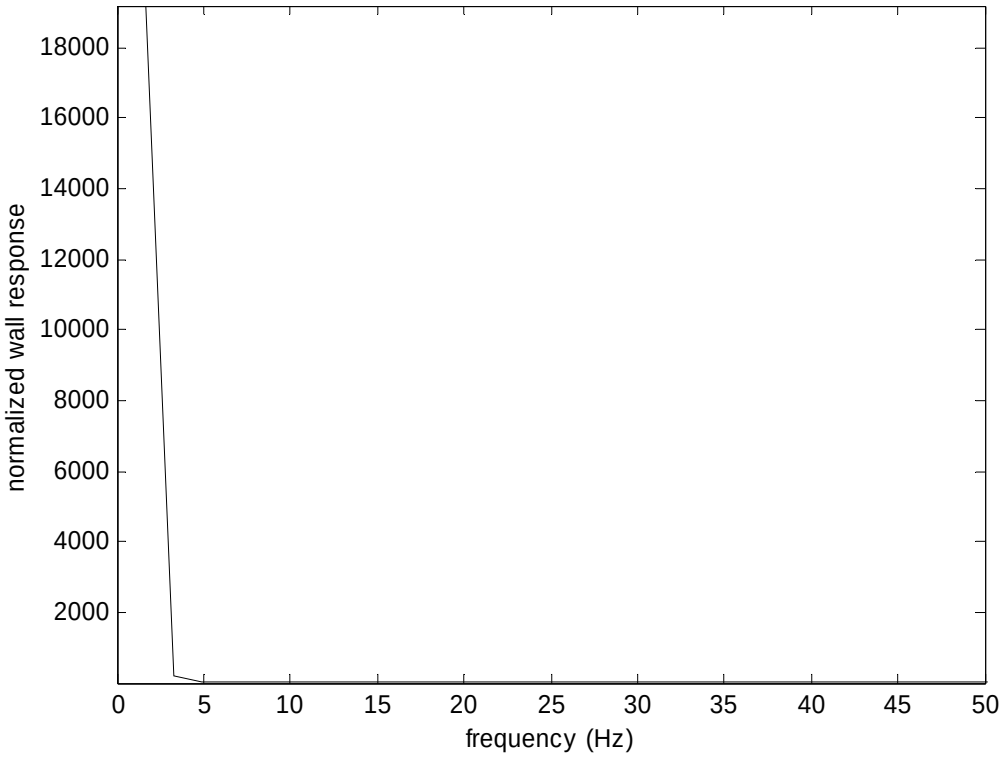

Figure 4.30. Frequency response of the wall-transducer system for Etr = 10^6 dyne/cm^2.

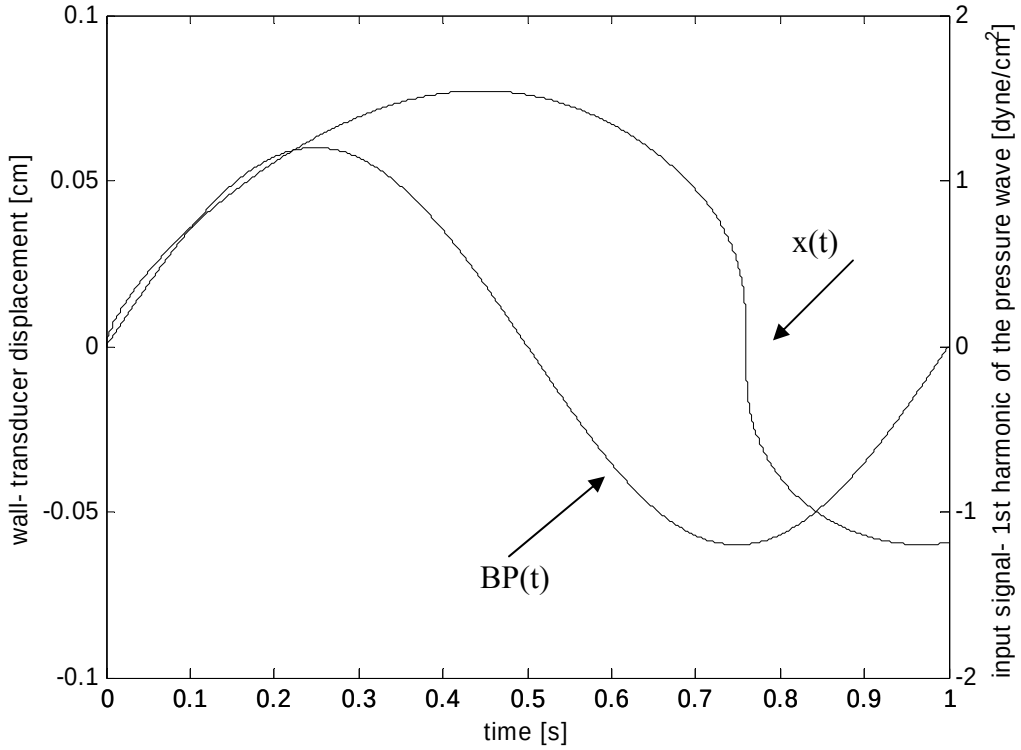

Figure 4.31. Time response of the wall-transducer system for Etr=10^6 dyne/cm^2.

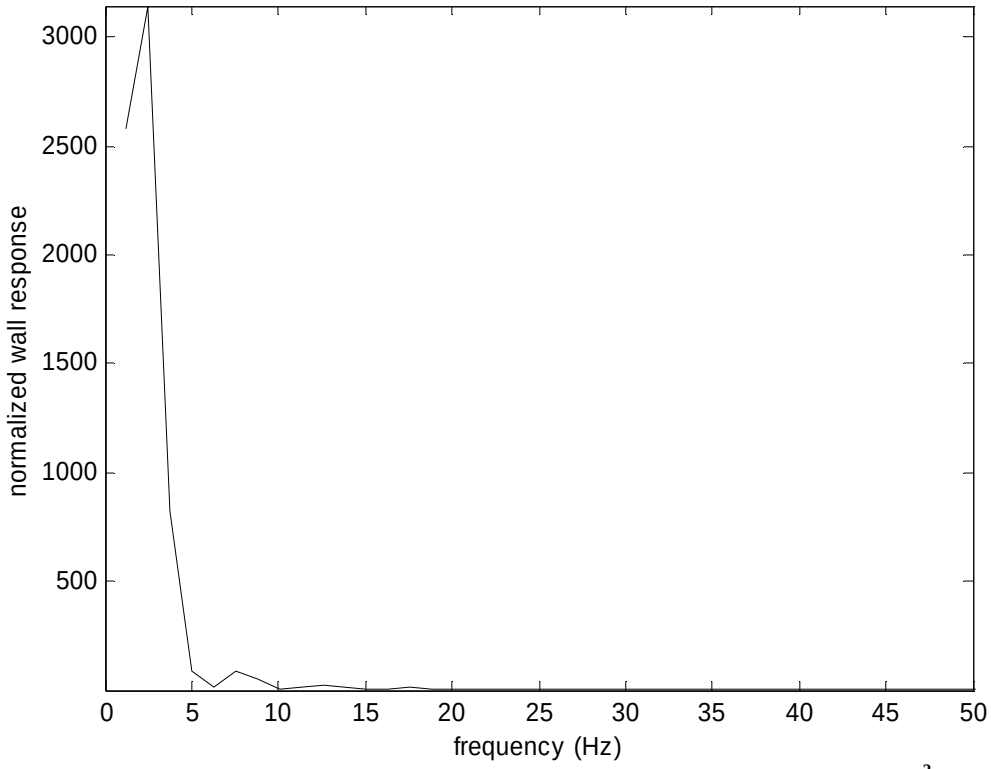

Figure 4.32. **Frequency response of the wall-transducer system for Etr = 10^7 dyne/cm^2.**

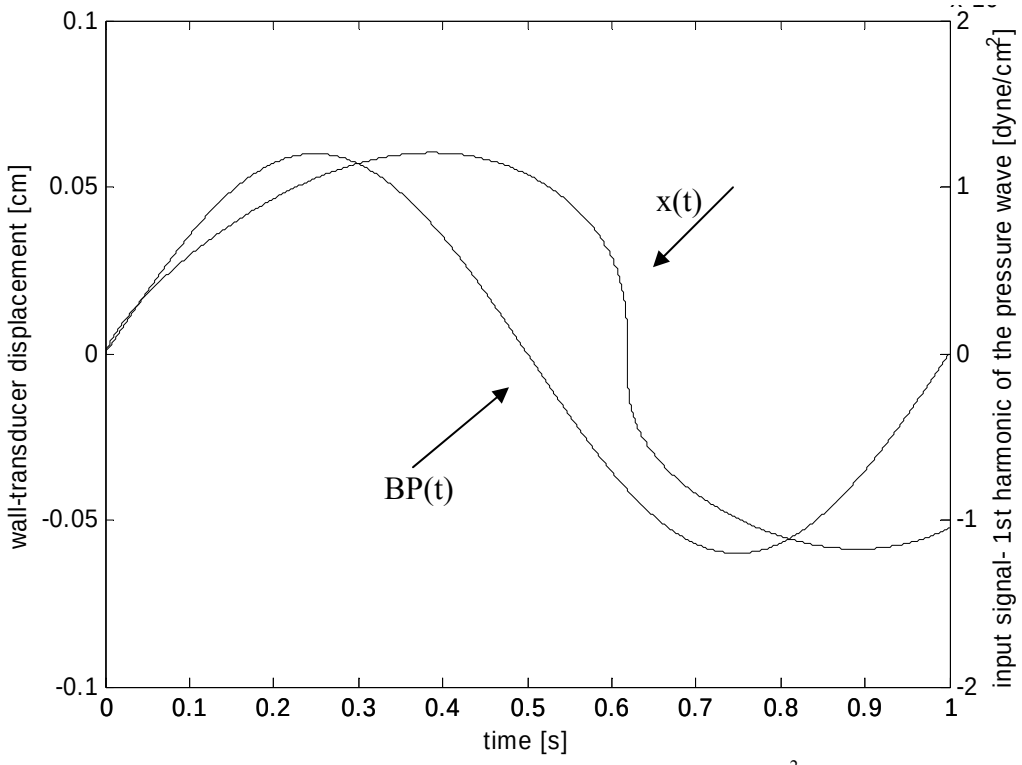

Figure 4.33. Time response of the wall-transducer system for Etr=10^7 dyne/cm^2.

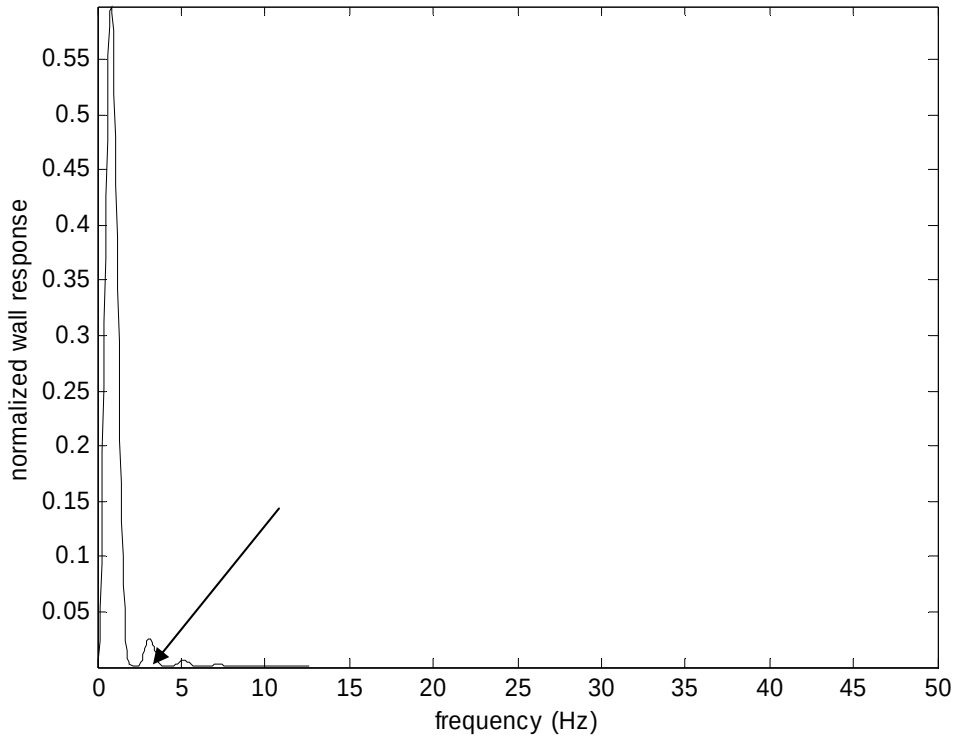

Figure 4.34**.** Frequency response of the wall-transducer system for Etr = 10^8 dyne/cm^2.

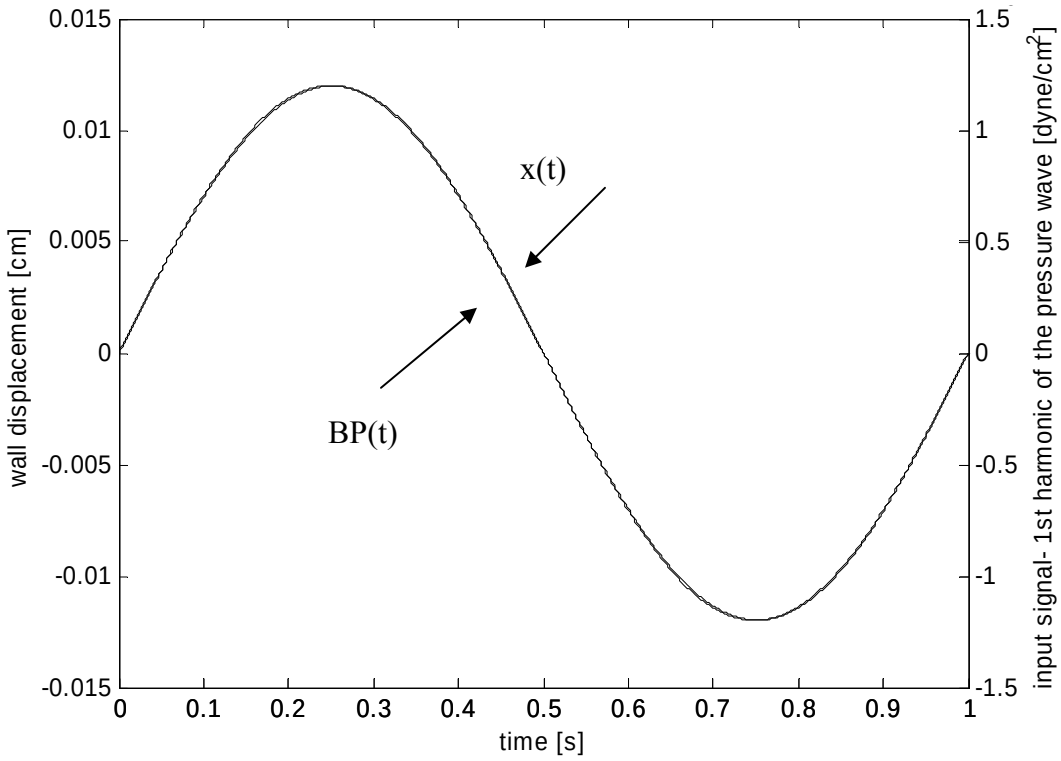

Figure 4.35. Time response of the wall-transducer system for Etr = 10^8 dyne/cm^2.

Then, the input signal frequency was varied from 1 – 5 Hz. The amplitude of applied harmonics was kept on the physiological level (see table 4.2.)(Nichols, 1998) and the transducer stiffness was fixed as E=10^10 dyne/cm^2. The results for input frequencies from 2-5Hz are shown below (figures 4.36-4.43).

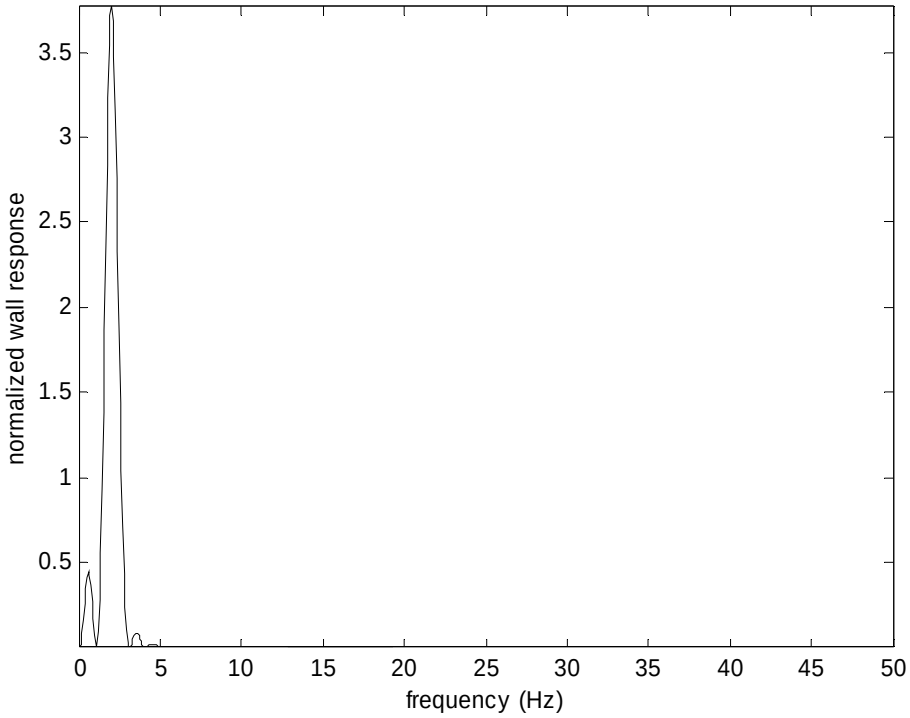

Figure 4.36. Frequency response of the wall-transducer system for Etr = 10^10 dyne/cm^2 , input frequency 2Hz.

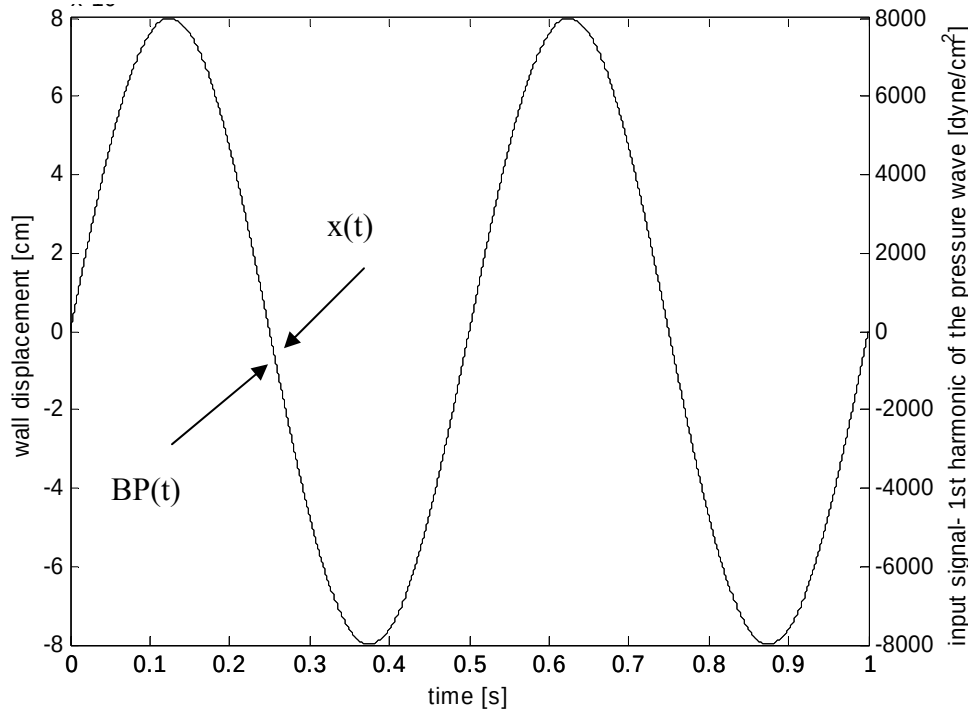

Figure 4.37. Time response of the wall-transducer system for Etr = 10^10 dyne/cm^2, input frequency 2Hz.

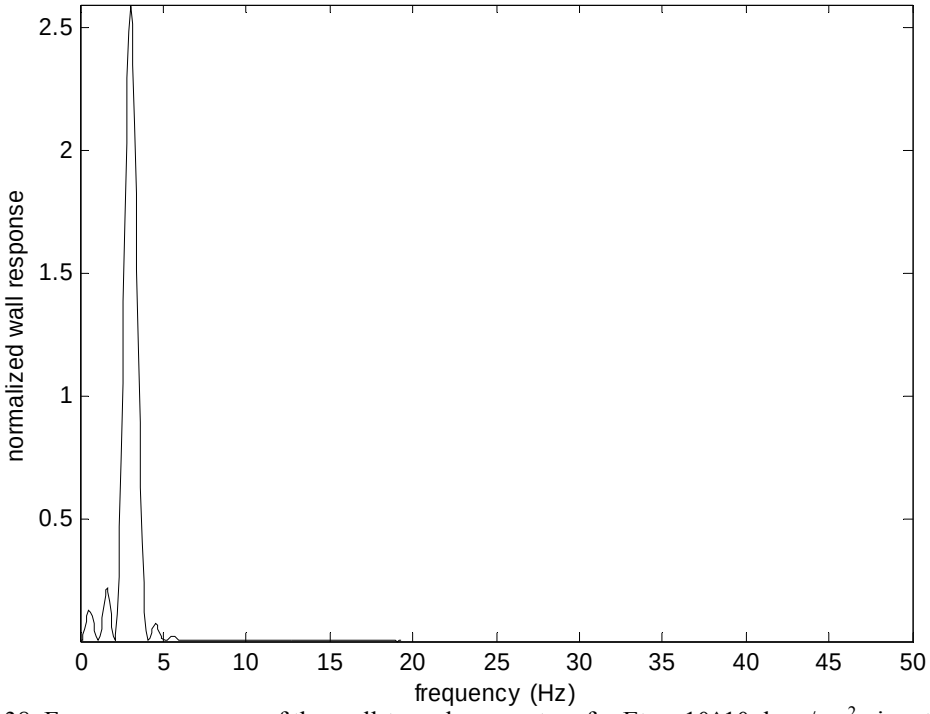

Figure 4.38. Frequency response of the wall-transducer system for Etr = 10^10 dyne/cm^2 , input frequency 3Hz.

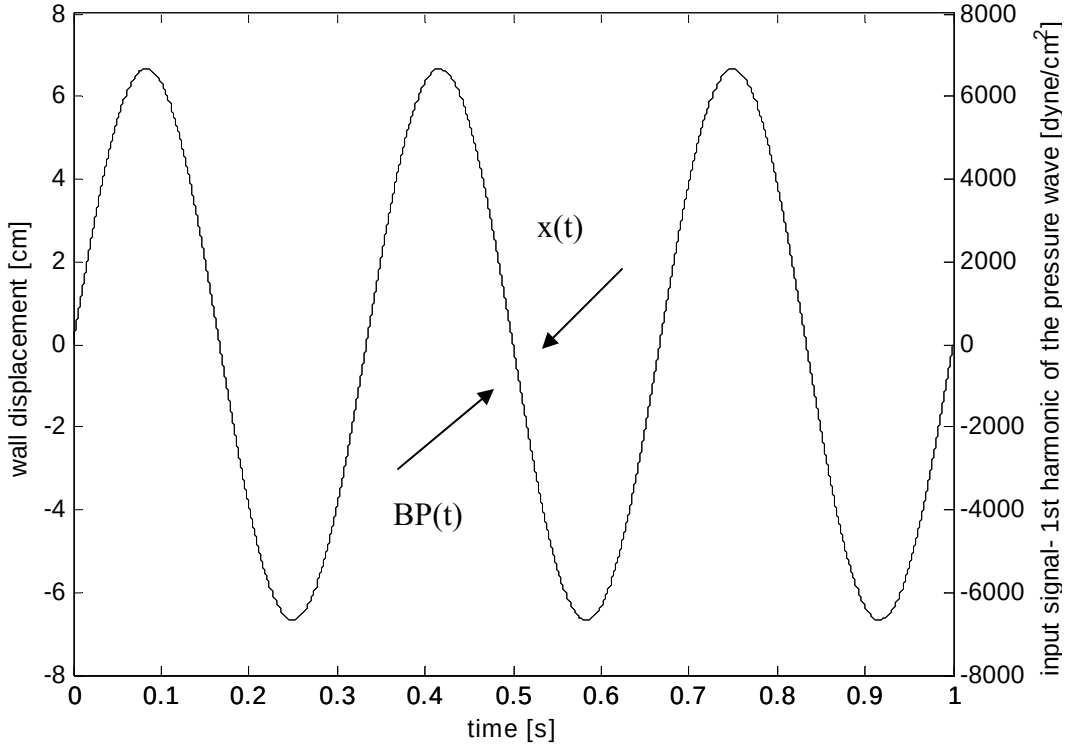

Figure 4.39. Time response of the wall-transducer system for Etr = 10^10 dyne/cm^2 , input frequency 3Hz.

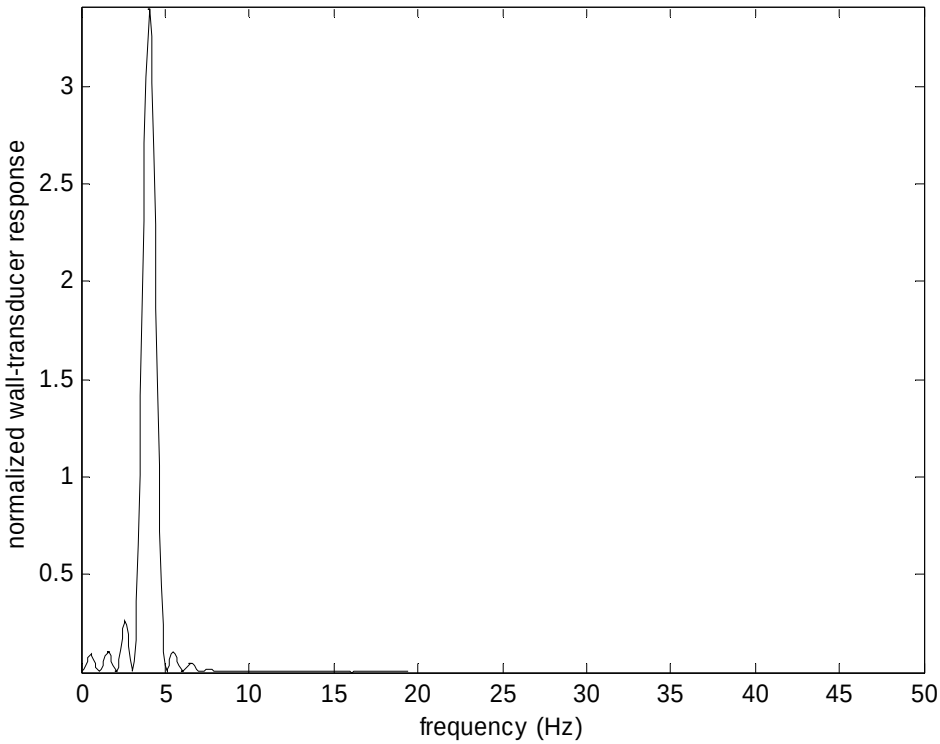

Figure 4.40. Frequency response of the wall-transducer system for Etr = 10^10 dyne/cm^2 , input frequency 4Hz.

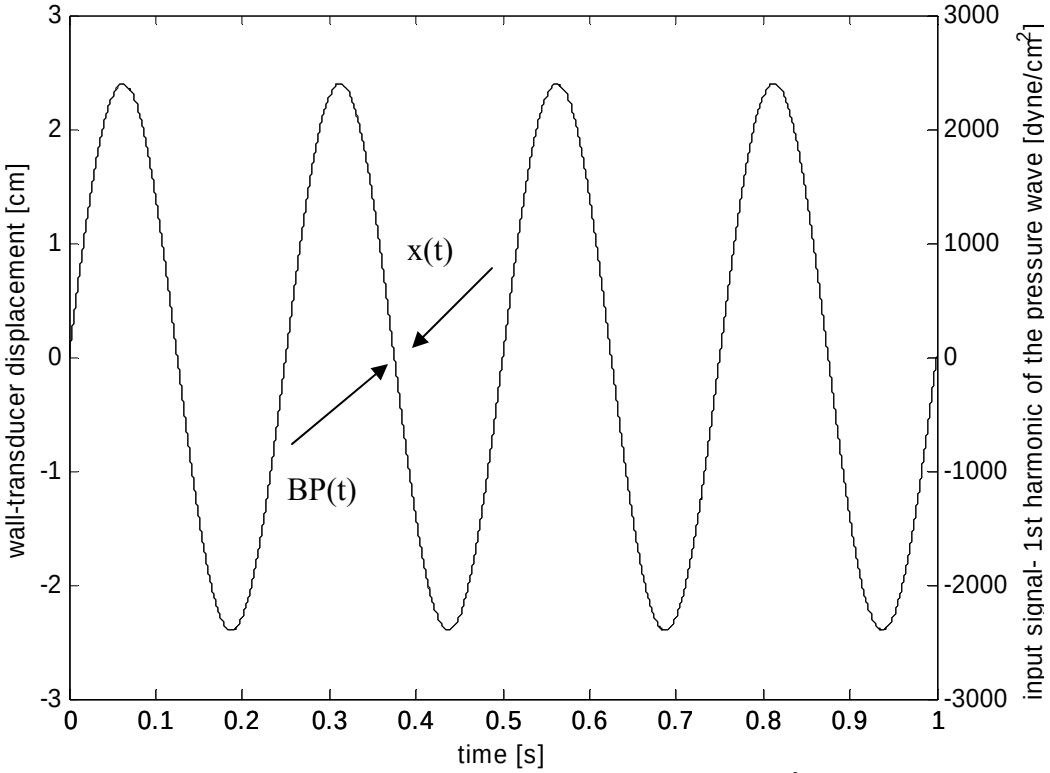

Figure 4.41. Time response of the wall-transducer system for Etr = 10^10 dyne/cm^2 , input frequency 4Hz.

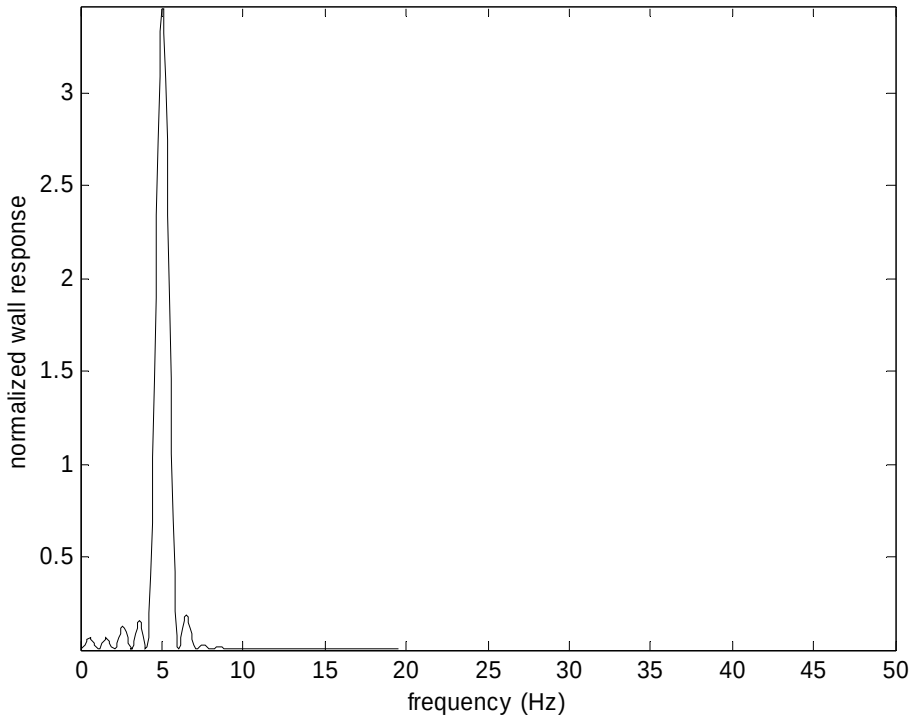

Figure 4.42. Frequency response of the wall-transducer system for Etr = 10^10 dyne/cm^2 , input frequency 5Hz.

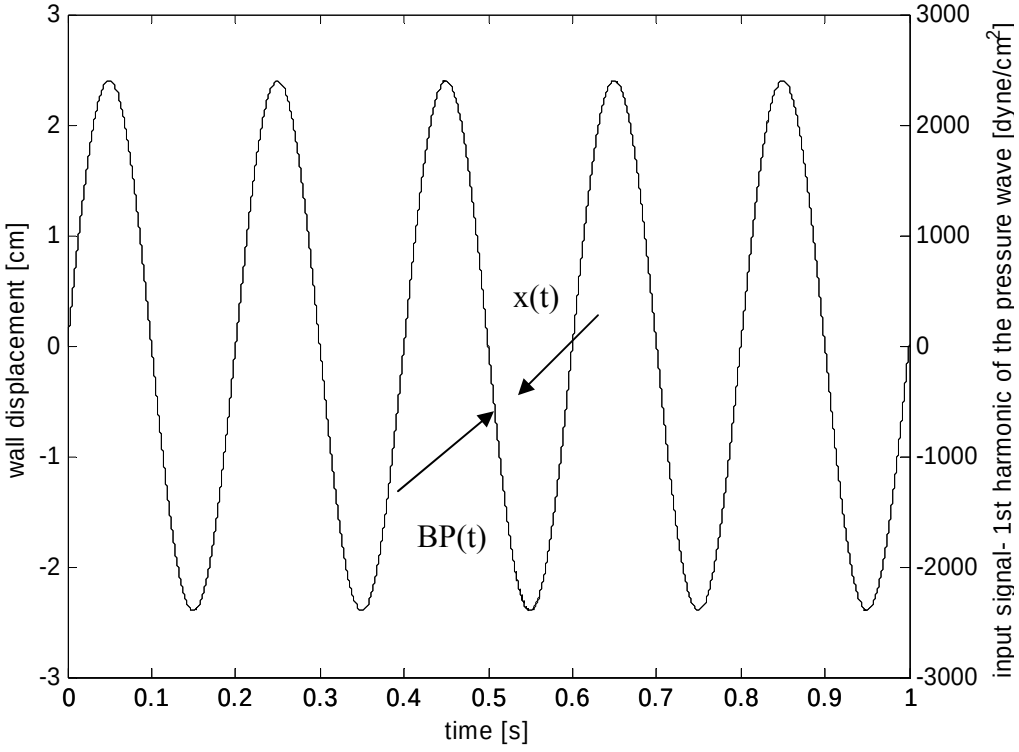

Figure 4.43. Time response of the wall-transducer system for Etr = 10^10 dyne/cm^2 , input frequency 5Hz.

4.4.4. Discussion

Lumped parameter model analysis and discussion

i. The arterial wall under applanation

The spectral content of the wall response was independent from the wall elasticity. The nonlinear response was observed, some additional harmonics were generated in arterial wall response spectrum. The relationship between amplitudes of additional harmonics was found and is described by the equation:

$$A_n = Ae^{cnf}e^{anf-b} \quad (4.24)$$

Where A_n is the amplitude of n-th harmonic, and A, a, b, c are constants, f is frequency of the input signal, and n is a harmonic number. The calculated constants are:

A= 414116; a=0.0734; b=0.6552; c=-1.277.

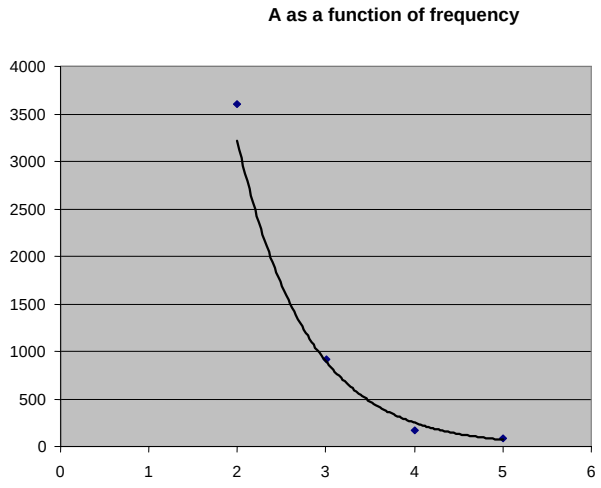

Figure 4.44. Amplitude A_n as a function of harmonic number.

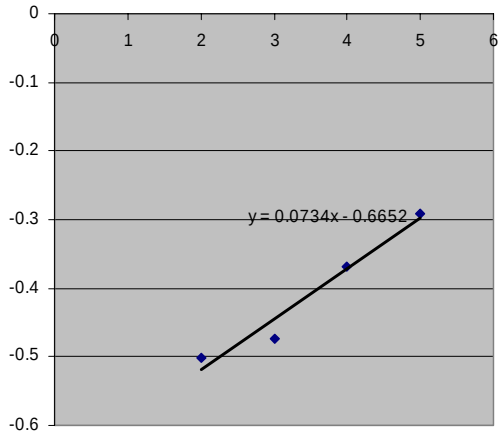

Figure 4.45. "a" value as a function of harmonic number.

ii. The arterial wall – transducer system has been tested for different sensor head stiffness to show how the linearity of the system changes with sensor head stiffness. The simulation shows that a transducer stiffness higher than $E=10^8$ dyne/cm^2 produces a linearity error less than 1% for all input frequencies from 1-5 Hz.

4.5. Finite Element Modeling Approach

Although some of the general features of the dynamic system can be described by the lumped parameter model, some important problems for the designing process, such as contact pressure distribution, influence of the applanation geometry on the contact pressure, and internal wall stress and strain distribution, cannot be addressed by this simplified approach. To attack these problems a detailed mechanical analysis has to be performed.

The arterial wall is not a homogenous or isotropic structure. Also, it is not a Hookean material (Nichols, 1998), (Fung, 1984). Thus, in general the strain is complicated function of stress and its first derivative. Fortunately, under some specific conditions such as small strain and low frequency, a couple of simplifications can be

made. Firstly, if strain is small, the nonlinear behavior can be linearized. Secondly, if strain is small, the non-isotropic behavior can be neglected (Nichols, 1998). This approach is presented by most authors and is proven to be correct in most *in vivo* experiments (Nichols, 1998). In the case being considered in this thesis, the artery is intent to be kept inside the rigid structure, thus the strain will be minimal. This simplifies the stress-strain relationship to the Hookean case:

$$\sigma_{ij} = c_{ijkl} e_{kl} \quad (4.25)$$

where σ_{ij} is stress tensor; c_{ijkl} tensor of elastic constants independent of stress or strain; e_{kl} strain tensor. Furthermore, the c_{ijkl} tensor consists only of two independent variables. Usually the arterial wall mechanical properties are described by the Young's modulus E, and Poisson's ratio ν. (Fung, 1984), (Nichols, 1998).

The FE model represents the object, i.e. arterial wall, under two types of loads: physiological arterial blood pressure pulsation BP(t) and applanation (flattening by the tonometer).

Let's start from the model of the arterial wall under applanation, with no pressure applied, which is kept inside the support structure represented by two elements: U and F (figure 4.46). The model that will be analyzed is restricted to the upper left part of the arterial wall and the tonometer. This simplification is justified by the problem symmetry. The U element represents the portion of the U-shaped structure while the F element represents the applanation flat area of the sensor. The free artery is labeled as A while the label B indicates the artery compressed by the element F and restricted by the element U. The whole artery undergoes a deformation, and each region of the free artery is deformed by the support structure. Transition from the free artery A to the compressed artery B for

two segments of the artery (labeled I and II) is depicted in figure 4.46. Each segment of the arterial wall is bent by the moment of forces L (see detailed view in figure 4.46) and each cross-section is rotated by angle α. This rotation generates elongation or shortening of layers equal δl above or beneath the neutral layer (the layer that does not undergo any strain). Thus the stress-strain relationship applied to the layer is given by the equation 4.26.

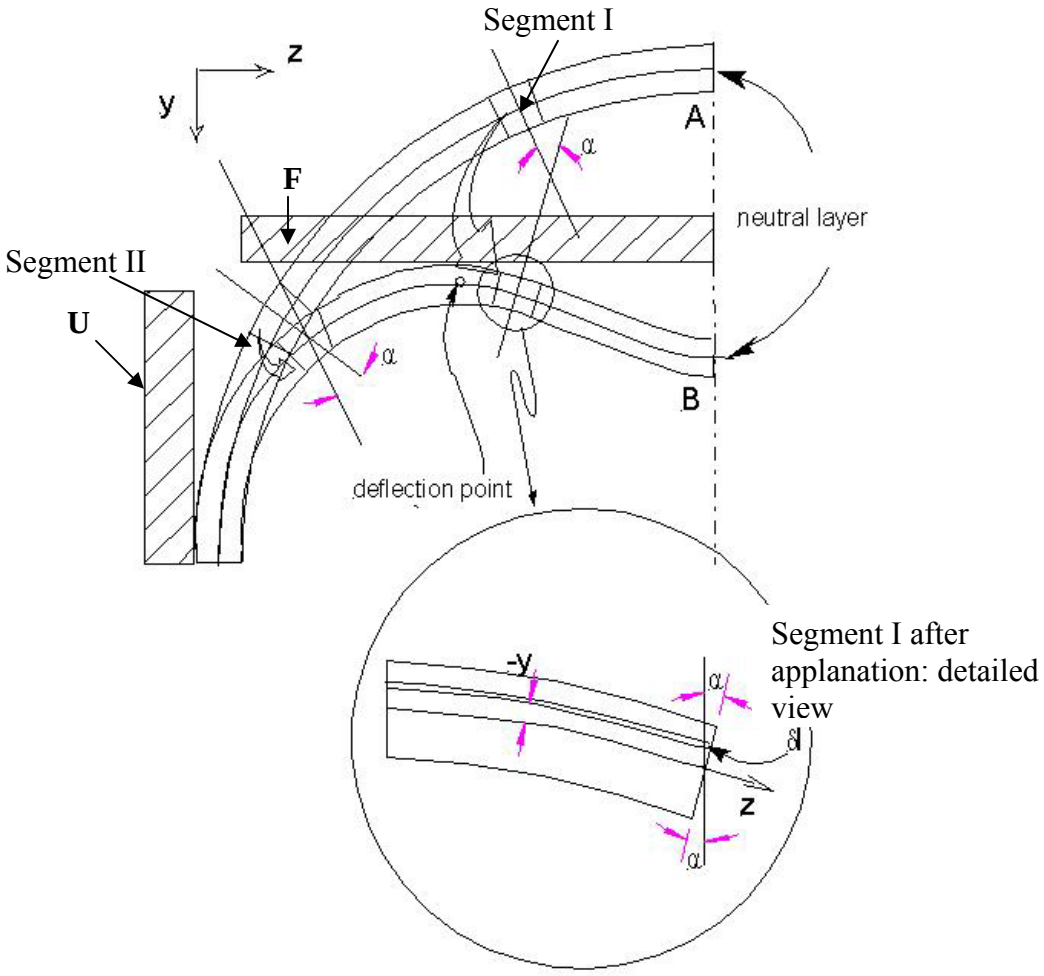

Figure 4.46. **General view of the artery deformed by applanation**. Position A non-deformed artery, position B deformed artery.

$$T_{ZZ} = E\frac{\Delta l}{l} \quad (4.26)$$

Where E is Young's modulus and T_{ZZ} is stress along the z axis, Δl is elongation due to stress, l is length of the segment. Knowing that:

$$\Delta l = -y\alpha \quad (4.27)$$

4.26 and 4.27 leads to

$$T_{ZZ} = \frac{E\alpha}{l} y \quad (4.28)$$

The contribution to the momentum L of the force acting on the infinitesimally thin layer is:

$$dL = -yT_{ZZ} bdy \quad (4.29)$$

Where dy is the layer thickness and b is an assumed wall dimension along the x axis. Thus, integrating from –h/2 to h/2, one obtains:

$$L = \int_{-h/2}^{h/2} y^2 dy = \frac{Edh^3}{12l}\alpha \quad (4.30)$$

and consequently

$$\alpha = \frac{2lL}{bh^3 E} \quad (4.31)$$

The equation 4.31 gives the relationship between the angle α and the bending momentum L. To obtain a displacement u_l of the arterial segment along the y axis, one has to substitute:

$$T_{xx} = T_{yx} = T_{zx} = 0, (4.32)$$

$$T_{xy} = T_{yy} = T_{zy} = 0, (4.33)$$

to the tensor stress-strain relationship (4.32 and 4.33 mean that there is no external force acting on the arterial wall except bending momentum L):

$$T_{xx} = \lambda\tilde{\sigma} + 2\mu s_x (4.34)$$

$$T_{xy} = 2\mu e_{xy} (4.35)$$

$$T_{xz} = 2\mu e_{xz} \quad (4.36)$$

etc. and knowing that E can be expressed using Lame coefficients:

$$E = \frac{\mu(3\lambda + 2\mu)}{\lambda + \mu} \quad (4.37)$$

We obtain:

$$0 = \lambda\tilde{\sigma} + 2\mu s_x \quad (4.38)$$

$$0 = \lambda\tilde{\sigma} + 2\mu s_y \quad (4.39)$$

$$T_{ZZ} = \lambda\tilde{\sigma} + 2\mu s_z \quad (4.40)$$

$$e_{yz} = e_{zx} = e_{xy} = 0 \quad (4.41)$$

By adding first three equations and knowing 4.38 we obtain:

$$(3\lambda + 2\mu)\tilde{\sigma} = \frac{E\alpha}{l} y \quad (4.42)$$

By elimination of the Young's modulus and introducing Poisson's ratio we obtain:

$$\tilde{\sigma} = -\frac{\mu}{\lambda + \mu}\frac{\alpha}{l} y = -\frac{2\eta\mu}{\lambda}\frac{\alpha}{l} y \quad (4.43)$$

Using equations 4.38-4.41:

$$s_x = s_y = -\frac{\lambda}{2\mu} \quad (4.44)$$

$$\tilde{\sigma} = \eta\frac{\alpha}{l} y \quad (4.45)$$

$$s_z = \frac{\lambda + \mu}{\mu}\tilde{\sigma} = -\frac{\alpha}{l} y \quad (4.46)$$

considering the characteristic equation, a the system of partial differential equation can be written in the following form:

$$\frac{\partial u_x}{\partial x} = \frac{\eta\alpha}{l} y, \frac{\partial u_z}{\partial y} + \frac{\partial u_y}{\partial z} = 0 \quad (4.47)$$

$$\frac{\partial u_y}{\partial y} = \frac{\eta\alpha}{l} y, \frac{\partial u_x}{\partial z} + \frac{\partial u_z}{\partial x} = 0 \quad (4.48)$$

$$\frac{\partial u_z}{\partial z} = \frac{\alpha}{l} y, \frac{\partial u_y}{\partial x} + \frac{\partial u_x}{\partial y} = 0 \quad (4.49)$$

Where: u_x displacement along x, u_y displacement along y, u_z displacement along z, η Poisson's ratio.

The solution of these equations generates the geometry of the arterial wall after applanation. Then the pressure inside the artery will be applied changing equations 4.32 and 4.33. Since the internal arterial wall will be loaded with hydrostatic pressure BP=-T thus:

$$T_{x(n)} = T\cos(n,x); T_{y(n)} = T\cos(n,y); T_{z(n)}\cos(n,z) \quad (4.50)$$

The mathematical structure becomes highly complicated and virtually impossible to solve by any analytical means. Here, the finite element method offers substantial advantage. The whole structure can be built as a set of finite elements with particular Young's modulus and Poisson's ratio. The strain-stress relationship for the whole structure is broken into linear relationships of the set of finite volumes.

The disadvantage of this method is that pressure, force strain, etc., become discrete instead of continuous. To minimize this problem, one has to develop a dense computational grid with nodes placed close enough to avoid large discontinuities.

Due to problem symmetry, the model is built for ¼ of the tonometer-artery structure (see figure 4.47). This allowed increasing the number of nodes without increasing the numerical cost of calculations.

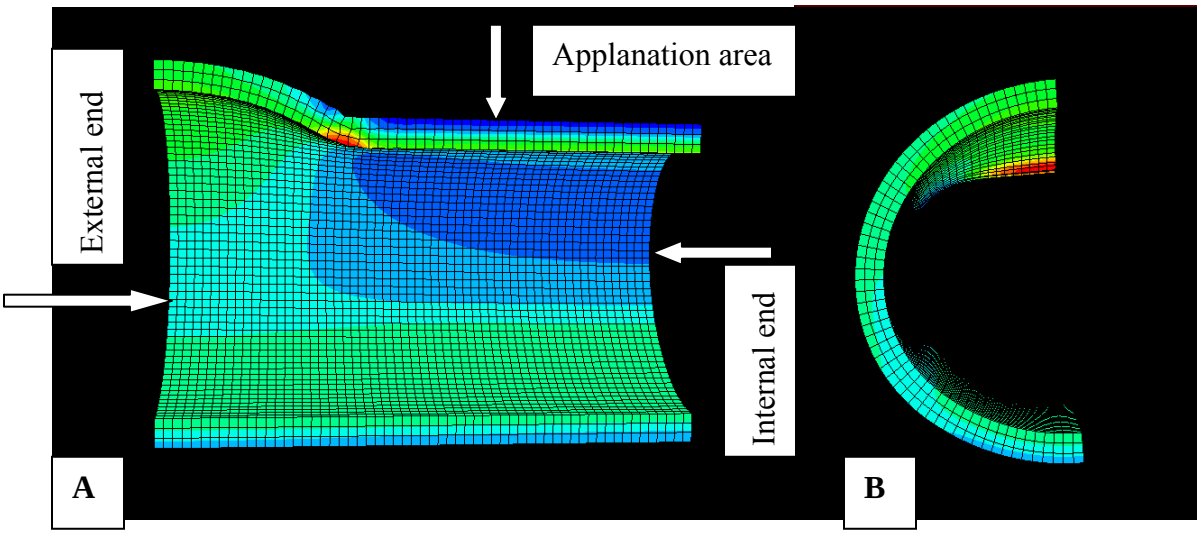

Figure 4.47. **Side view (Panel A) and front view Panel (B) of the simulated arterial segment.** The artery is flattened by the rigid body (applanation area) and pressurized from inside, simulating the working conditions of the natural artery.

Mesh describing arterial biomechanical structure

Since the lumped parameter modeling excluded transducers with macroscopic deformation and in order to simplify the calculation, the tonometer was modeled as a rigid body.

The mesh that the author decided to use in this model is a three-layer mesh with volume elements no bigger than 0.15 x 0.15 x 0.15 mm. It resulted in 43, 200 element model shown in figure 4.47.

Arterial wall tissue - material properties

The simulation is intended as a quasi-static simulation, thus viscosity and inertia of the model have been ignored. In this case the arterial wall tissue was assumed to be elastic material with Young's modulus from $0.4x10^6$ to 10^6 dyne/cm^2 and Poison ratio 0.4999 (Drzewiecki, 1998).

Simulation boundary conditions

The boundary conditions were chosen to meet symmetry requirements of the model as well as some mechanical assumptions:

1) The arterial wall is able to move freely in directions tangent to the tonometer surface.

2) The external end of the artery (outside the tonometer) can move only in XY plane.

3) The internal end can move (inside the tonometer) only in XY plane.

4) The wall can move after contact with tonometer, thus "buckling" effect can be simulated.

Simulation time incrementation

The load was applied in 3 steps: 1) applanation-duration 0.1 s; 2) ramp pressure function-duration 0.1 s; and 3) Arterial pulse-duration 1 s. Steps 1 and 2 were not

subdivided into smaller increments. The time incrementation of the 3rd step was decided based upon the average human aortic blood pressure pulse features (O'Rourke, 1996). The pulse was sampled with frequency 20 Hz. During each 1/20 s period the load was changed from p(n-1) value to p(n) value using the ramp function to obtain close to the natural arterial pulse shape. The whole process consisted of 22 time increments. Due to the numerical calculations, some of the time increments were farther divided into the smaller steps if software recognized the large displacement due to applied loads. The example list of time increment is attached in Appendix C in FEM code.

Arterial blood pressure waveform and arterial applanation as a simulation load

To study the influence of the applanation on the artery apart from the effects caused by the arterial pulse, the author decided to separate the load into 3 steps as mentioned above. The load that was applied on the artery consists of the applanation period (ramp force starting from 0 and reaching 6000 dyne/cm^2), pressurization of the artery to the minimal arterial pressure period (80 mmHg – 103 974 dyne/cm^2), and finally the arterial pressure pulse period (diastolic pressure 80 mmHg, systolic pressure 130 mmHg). The simulation load as a time function is shown in figure 4.54.

In such a configuration the applanation effects and pulse effects can be studied separately.

4.5.1. Results

Simulation of the blood pressure transmission through the arterial wall

The stress distribution (contact pressure) on the tonometer's sensor head is responsible for force generation on the sensing element. The internal wall stresses generated by the BP signal are shown in figures 4.48 and 4.49 (4.48 - average stress (von Mises); and 4.49 - pressure inside the arterial wall) The internal stresses are transferred to

the interface between the tonometer and the arterial wall generating contact pressure (see figure 4.50).

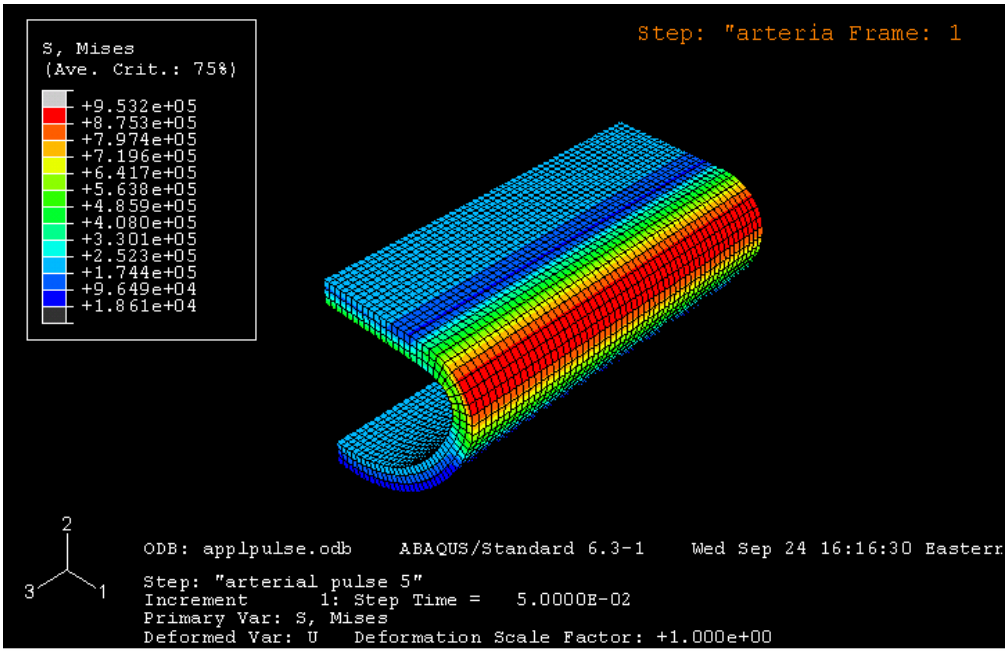

Figure 4.48. **FEM 3-D simulation results: S (von Mises)**. A visualization of the stress distribution on the arterial wall inside the tonometer support structure. Average stresses on the arterial wall inside the tonometer, under applanation and pressurized to the mean arterial pressure.

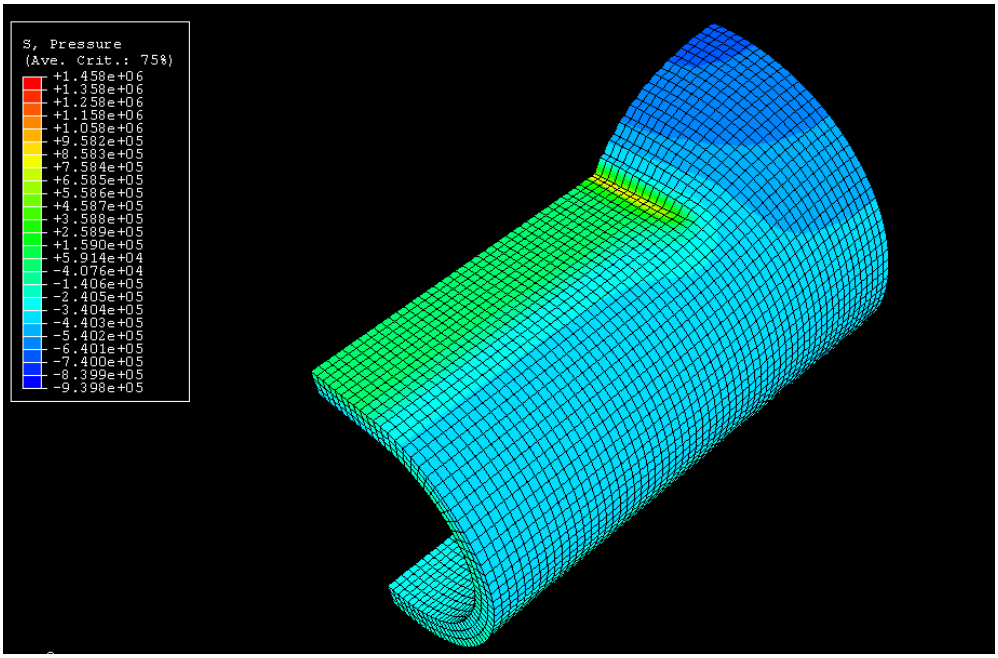

Figure 4.49 **FEM 3-D simulation results: S, Pressure**. Average stresses (pressure) on the arterial wall under applanation and pressurized to the mean arterial pressure.

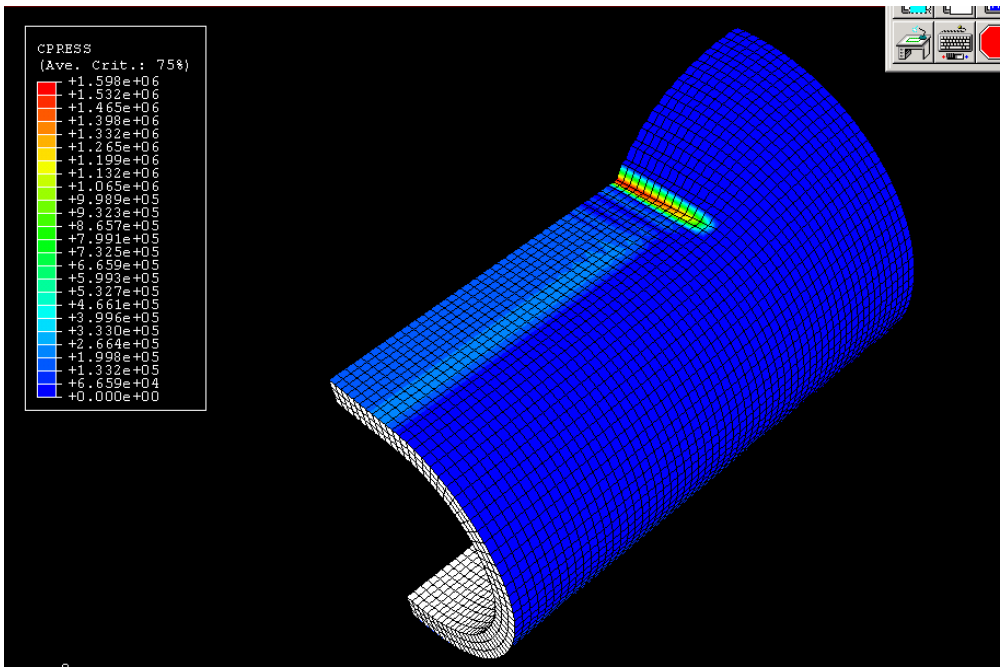

Figure 4.50. **FEM 3-D simulation results: Contact Pressure**. Contact Pressure map is shown between the arterial wall and the transducer. Artery is pressurized to the mean arterial pressure.

4.5.2. Finite element modeling results analysis and discussion

The finite element simulation was designed to show not only the blood pressure signal transmission through the arterial wall (correlation between the blood pressure and the contact pressure analysis) but also the effects caused by applanation. To do so, the applanation of the artery was performed prior to pressurizing the model of the vessel. The applanation period reveals that the contact pressure generated only by applanation depends strongly on position of the rigid structure, in other words it depends on applanation level (see figure 4.51 A and B). Figure 4.51 A is a profile of the contact pressure perpendicular to the vessel axis (from the middle of the sensor head "0" to the edge of the sensor head "1.2"). Figure 4.51 B is a profile of the contact pressure along the vessel axis, in the middle of the sensor head (from the sensor edge "0" toward the center of the sensor head).

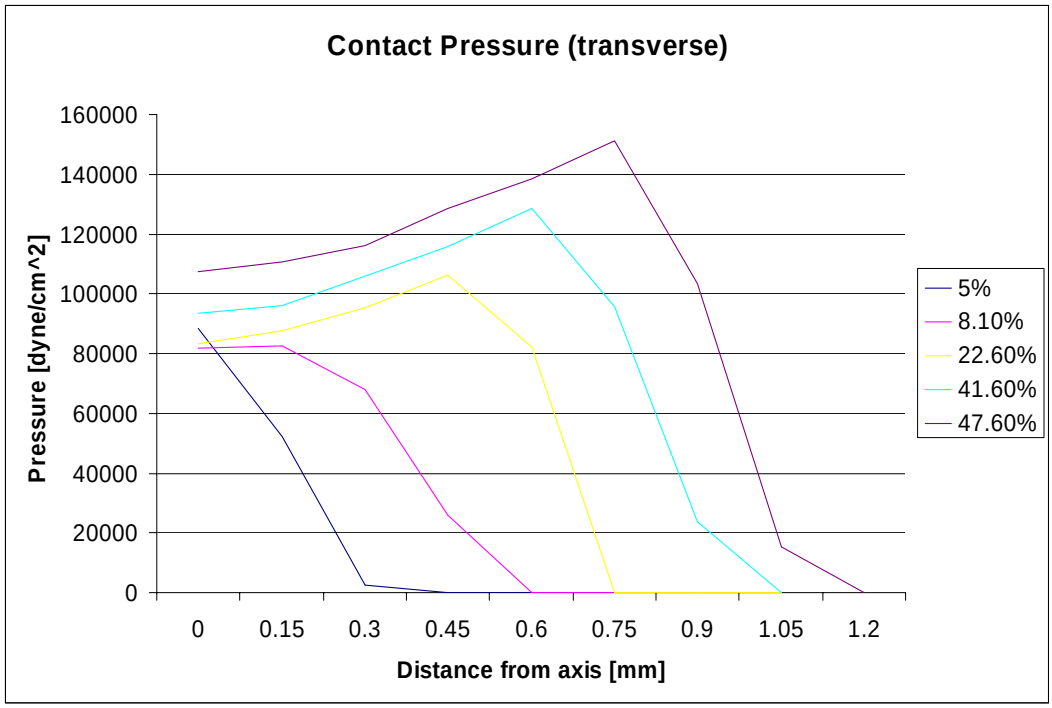

A

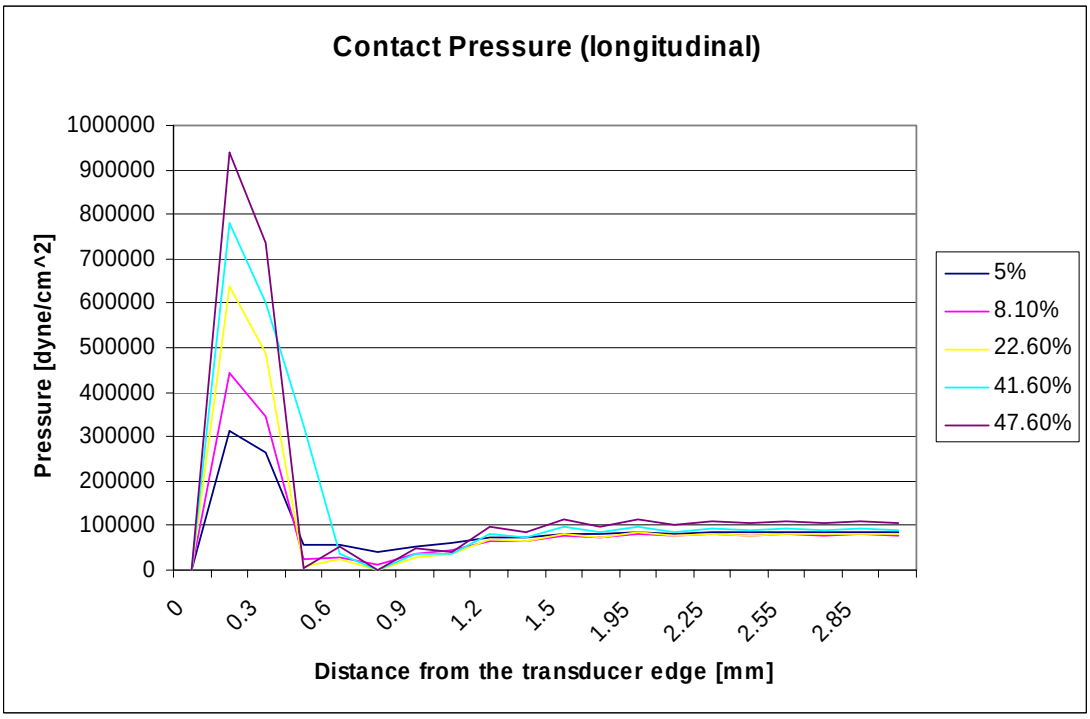

B

Figure 4.51. **Contact pressure profile**. The amplitude is measured in different points along the artery axis (Panel B) and transversally (Panel A) to the artery axis. Contact pressure is measured for different applanation levels expressed in %.

Moreover, despite the fact that the applanation is applied by constant force, the contact pressure response in some places of the flattened area (e.g. center) is nonlinear and even non-monotonic. This means that the contact pressure does not rise with the applanation force in monotonic fashion.

Some aspects of the biomechanical system under analysis change with blood pressure applied to the artery. The pressurized artery starts to adhere to the tonometer surface and the contact pressure becomes a sum of blood pressure and stresses related to applanation. The residual stress generated by applanation is responsible for discrepancies between blood pressure and contact pressure. It is especially apparent close to the transducer edge and far from the vessel axis (figure 4.51 A and B).

The results show that distribution of the contact pressure between the tonometer head and the arterial wall is not homogenous. In figure 4.52, an example map of contact pressure in systole is presented (E_{wall} = 600 000 dyne/cm^2). The maximum of the contact pressure gradient is located directly under the transducer's edge, then sharply drops, undergoes some minor fluctuations and stabilizes approximately 2 mm from the sensor edge. Also, in the direction perpendicular to the vessel axis the contact pressure gradient reaches its maximum on the edges of the applanation region.

The criterion of 1% error is met (for arterial stiffness from E_{wall}= 500 000 to 1 000 000 dyne/cm^2 and applanation level from ~8% to ~22%) in the region starting 2 mm from the senor head edge, measured along the vessel axis and 0.3 from the vessel axis, measured transversally to the axis. Thus, the sensing area should not be closer to the tonometer's front edge than 2 mm and not further from the vessel axis than 0.3 mm. These restrictions guarantee that the contact pressure on the transducer will not change

under physiological conditions, due to the applanation level or arterial stiffness, more than 1% of its value.

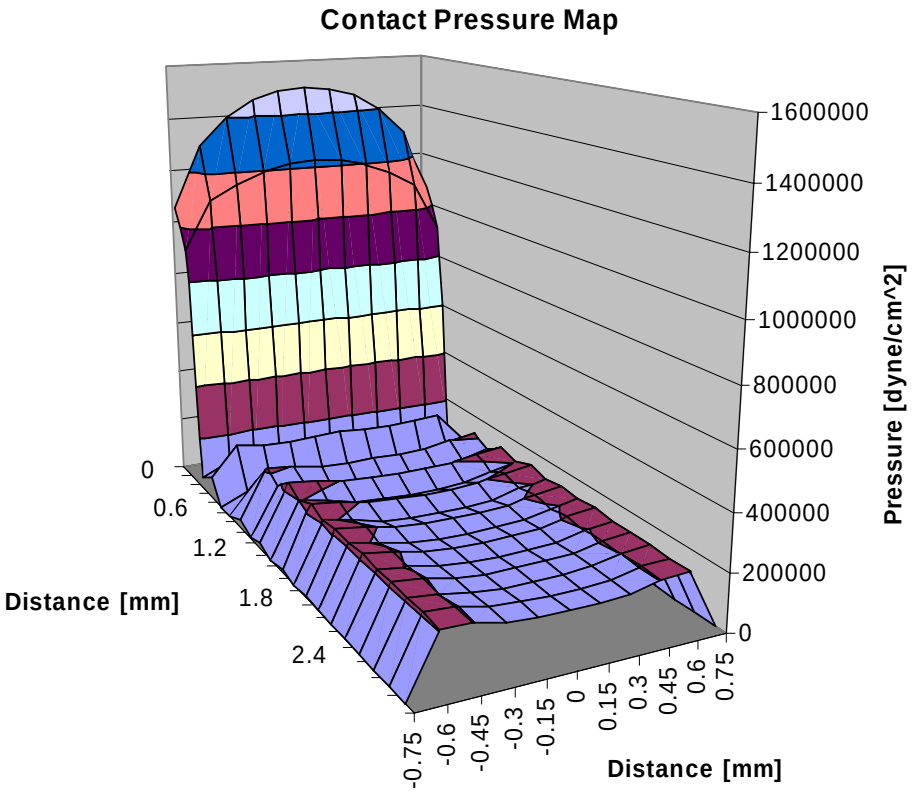

Figure 4.52 Contact pressure map in systole

The presented simulation contradicts the traditional tonometry assumption, that applanation generates some area on the flattened artery, where the contact pressure is constant and proportional to the blood pressure signal. In general, the closer to the arterial wall plane of symmetry the lower the amplitude of the contact pressure (see figures 4.51 and 4.52). What is even more interesting, the contour of the contact pressure does not reflect exactly the contour of the measured blood pressure (figure 4.53). In some areas, especially on the margins of the sensing head, the contact pressure sharply rises

during the systole but drops to zero (loss of the mechanical contact between the arterial wall and the tonometer) at the end of the diastolic period (figure 4.53). This can be explained by the fact that the arterial wall is not fixed to the tonometer and the margins of the applanation area are moving by responding to the arterial pressure changes. This movement results in rapid changes of the contact pressure and even in loss of contact between the arterial wall and the sensor.

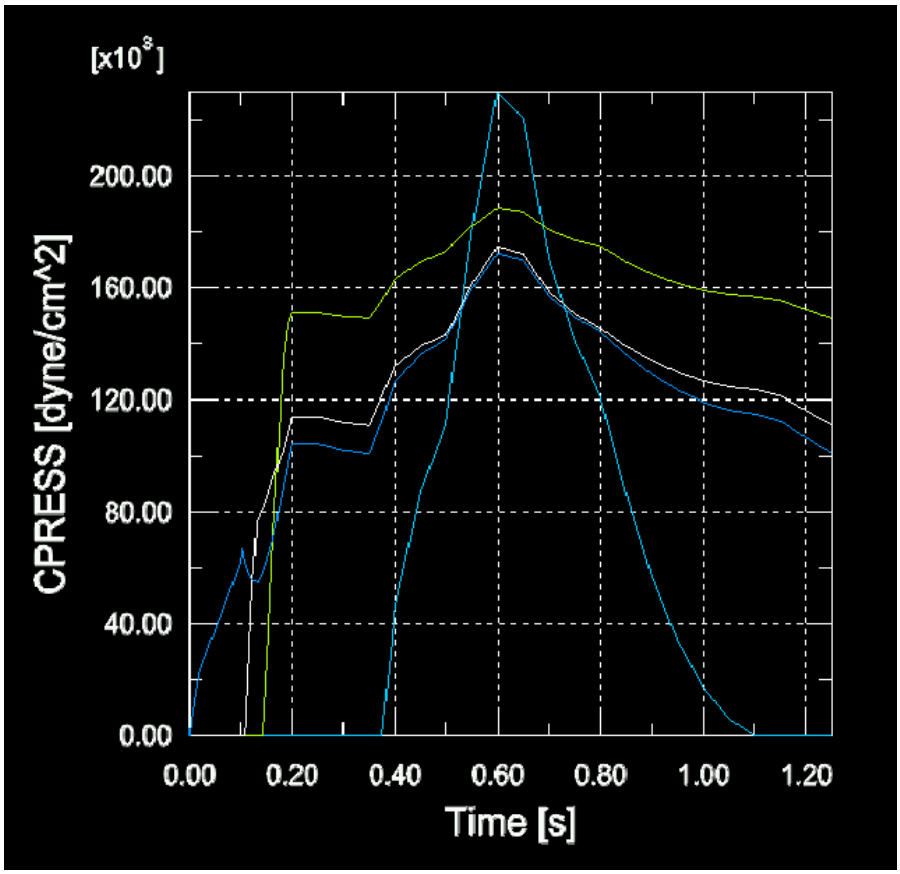

Figure 4.53. **Contact pressure patterns measured in 4 points** on the sensing area. The points lay on the line perpendicular to the vessel axis in the center of the sensor head.

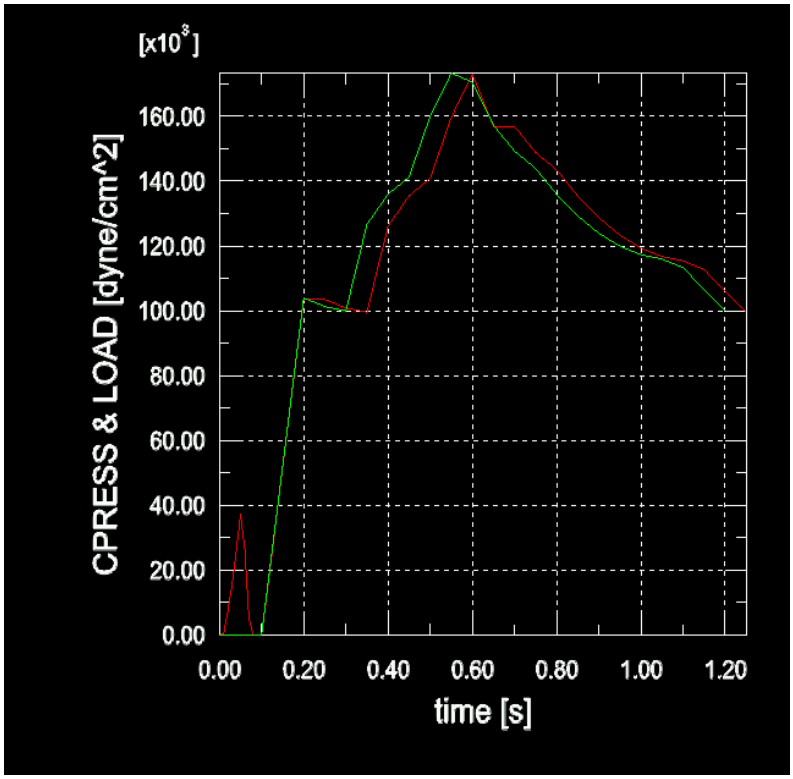

Figure 4.54. **Comparison between contact pressure and arterial pressure**. Conact pressure (red line) was measured in the center of the applanation region. The arterial pressure signal is represented by the green line.

The contact pressure and the arterial blood signal do not share the same contour (signal spectrum) even if measured in an optimal location. In figure 4.54, one can see that with the contact pressure measured in the center of the applanation area (an optimal position for the measurement according to Pressman, Drzewiecki, and O'Rourke), the green line is not in exact agreement with the contact pressure response. Although the amplitude of the blood pressure signal is exactly the same, the contact pressure signal underestimates the pressure signal almost over the whole cardiac cycle.

The simulation also revealed that the tonometer applies unnatural strain inside the arterial wall. The strain measured in a normal artery (Normal), the bottom of the U-shaped support structure (BU), center of the flattened portion (BF) and corners of the U-shaped portion of the artery (BC) is shown in figure 4.55. The flattened area undergoes

the biggest negative strain (compared to the relaxed non-pressurized artery). On the other hand, the corners undergo the highest strain.

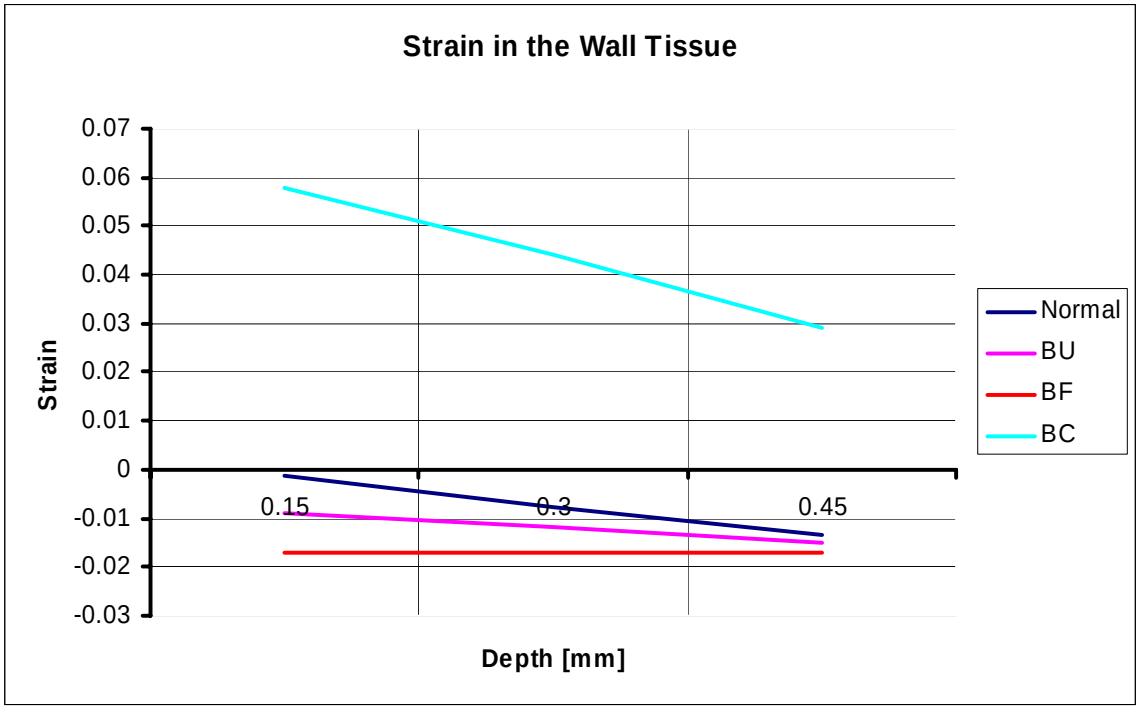

Figure 4.55. Strain in the arterial wall tissue.

This may suggest that the flattened portion and the corners will undergo some kind of physiological reaction as a response to unnatural strain. The regions BF and BC should be a subject of scrutiny in later in-vivo studies.

4.6. Conclusions

Two type of modeling, lumped parameter model and FEM quasi-static, provided results describing the dynamic behavior of the transducer-arterial wall system as well as the spatial distribution of the mechanical variables such as stress and strain. These results indicate the way in which the prototype should be designed (area of integration, level of

applanation and transducer stiffness) as well as show limitations of the tonometer (e.g. pressure gradient on the edges of the sensing area generates a substantial error).

Lumped parameter model.

The overall lumped parameter model analysis leads to some key conclusions.

i. The arterial wall introduces strong non-linearity.

ii. The spectral response of the arterial wall non-linear system does not depend on arterial visco-elastic properties.

iii. The non-linear effects of the tonometric measurements decrease with transducer stiffness.

Let me discuss these conclusions and point out the practical implications.

i. The arterial wall non-linear response was manifest in both time and frequency domains. The input frequency always generated several peaks in harmonic frequencies (usually up to 5th harmonic) and some subtle disturbances in sub-harmonic frequencies. The non-linear response of the arterial wall is a serious issue and may jeopardize the measuring process if the transducer has low mechanical compliance. The model, which was presented in chapter 4.3, shows that even when the applanation meets all requirements listed in (Drzewiecki, 1998), (Nichols, 1998), (Drzewiecki, 1983) but at the same time the mechanical compliance of the transducer is low, the tonometer response is highly nonlinear and virtually useless for the dynamic measurements.

ii. The series of simulation conducted for different transducer elastic modulus shows that linearity of the system increases with increased transducer stiffness. This phenomenon is also important for practical application. The ideal transducer for tonometry should have the infinite stiffness to eliminate the arterial wall non-linear effect. This is a strong indication for a practical design to use the stiffest available transducer, which is a piezoelectric force transducer. The simulations have shown that the transducer's stiffness should be greater than wall stiffness by two orders of magnitude (E_{wall} >10^8 dyne/cm^2) to obtain an error less than 1%.

Finite element model analysis.

The FEM modeling has revealed that:

i. Applanation generates internal arterial wall stress that contributes to the tonometry measurement error.

ii. Contact pressure value generated by applanation depends on position and level of applanation.

iii. In the thick-wall arteries, the traditional assumption that the applanation generates the area with constant contact pressure is not true.

iv. The error of the tonometer undergoes changes during the whole cardiac cycle and depends on the position of the sensing element. Thus the area of integration (size and shape of the pressure collecting pin) determines the final error made by the device.

v. The 1% error requires narrowing the region of integration to the area that lies 2 mm from the tonometer edges and 0.3 from the vessel axis (for 5 mm OD vessel, wall thickness .25 mm).

vi. The tonometer generates stress in the arterial wall volume, which is very different from the natural one (see figure 4.55). Especially in regions BF (flattened arterial wall) and BC (corners of the support structure). Thus it is very likely that the tonometer will trigger remodeling reaction in those locations.

5. ARTERIAL TONOMETER DESIGN

The lumped parameter model along with the finite element analysis has provided very important information about the tonometer measurement process. Some parts of this process, such as the influence of the internal arterial wall stress on the signal amplitude and error as a function of applanation level, demand the carefully experimental studies. Thus, they require the prototype capable of working as an experimental tool.

Because of that, all the prototypes presented below have been designed to be capable of changing applanation level.

The lumped parameter model indicated that the transducer for a tonometer working on a living artery should exhibit low mechanical compliance ($E_{Tr} \geq .10\text{^}8$ dyne/cm^2). This requirement as well as a desire to obtain an easy to analyze, high amplitude, high power signal has resulted in the PZT based transducer, designed to fit all the tonometer prototypes.

Two objectives guided the mechanical design of the prototypes: to minimize the tonometer error due to the contact pressure gradient (shown in figures 4.51 and 4.52), and to design a device capable of obtaining an experimental relationship between the applanation level and the tonometer output amplitude and accuracy.

From a medical point of view, the ideal tonometer must not deform the artery or the deformation should be minimal in order to preserve the natural blood flow conditions and the natural stress distribution within the arterial wall tissue. From the sensor point of view, the level of deformation should be optimal for the measurement, which means a relatively large area of flat arterial wall (as shown in chapter 4, figure 4.51 between 8% and 22% of applanation). These two requirements are contradictory, since the applanation

suitable for blood pressure measurement requires theoretically at least 8% artery compression (figure 4.51). To address those issues and find the optimal range of applanation, the in-vivo and in-vitro applanation studies are necessary.

This chapter presents a technical description of three tonometer prototypes that are a result of theoretical analysis shown in chapter 4. Those prototypes have been used for the mock artery and pilot in-vivo tests. The first bench-top prototype is a basis for the two following designs, which are the refined versions of their predecessor. The last prototype represents the fully functional implantable device that can be used for the long-term measurements in a living organism.

5.1. Transducer

The transducer presented in this chapter is common for all three tonometer designs. On the other hand, it represents the heart of the system, providing a conversion from mechanical stress to the electrical output signal. The transducer type selection process and the transducer design are presented prior to the specific tonometer designs.

5.1.1. Scientific basis of piezoelectric force sensor.

There are several sensing mechanisms that have been historically used for the development of the force/stress transducers (Fraden 1997, Gardner 1994, Doeblin, 1990, Gautschi 2002, Toh 2000, Benes 1995). Currently, technically important force transducers are mostly based on piezoelectric, piezoresistive, optical, and capacitive sensing techniques. All these techniques, except piezoelectric, require a relatively large mechanical deformation of a sensing element in order to achieve high sensitivity and large dynamic range of the measured force. Therefore, a typical design approach utilizes a thin membrane (high “effective” mechanical compliance) as an interface, which

transforms the force into the large deformation, and which is detected by a displacement transducer. As a result, these techniques suffer in the case of the applanation method, where a rigid transducer is required at the contact area between the artery and the tonometer (as shown in chapter 4, in lumped parameter simulations).

In a piezoelectric force transducer, transduction of mechanical quantities (force, displacement) into electrical (voltage, charge or current) and vice-versa takes place within the material via the deformation of the crystal lattice (Kino 1987, Auld 1990, Lec 2001, Luck 1998). This sensing mechanism allows the transducer to detect the deformation in the order of angstroms, thus allows measuring the force with virtually no displacement (which potentially reduces nonlinearity of the tonometer). The PZT transducer does not need a macroscopic deformation (such as bending) in order to measure the force applied to the rigid applanation element. Also, the material-based electromechanical coupling effect leads to two distinct modes of operation of the transducer, in contrast to all other techniques. The first mode, often called a passive mode, refers to a direct generation of an output voltage or electric charge under the acting force. In this case the sensor does not need any external power supply to produce a response, which is of tremendous advantage for implantable sensors. The relation between acting forces (stresses) and responses (the output voltage or charge) can be derived from the constitutive relations for piezoelectric materials. In most cases, the modeling and analysis is carried on for finite size devices, therefore the considered variables are presented in the form of stresses (force over the area), electric fields (voltage over the thickness), and electric induction (charge over the area) (Kino G 1987):

$$T_{ij} = c_{ijkl}S_{kl} - e_{nij}E_n \quad (5.1)$$

$$D_m = e_{mkl} S_{kl} + \varepsilon_{mn} E_n \quad (5.2)$$

Where: T - stress, D is an electric charge, S - deformation, E - electric field,

c - elastic constant, e - piezoelectric coefficient, and ε - dielectric constant.

From these equations one can determine the magnitude of the electric charge (D vector), or the voltage (from E vector) caused by the applied force. These equations are linear, which implicates that, in principle, both static and dynamic forces can be measured. The one (and practically only) approach here is to make the sensing element a finite size with system electrodes placed on its surfaces. Such an element, from an electrical point of view, is a capacitor, and this element under the acting static force will discharge or leak the electric charge. Therefore, this mode of operation can't be used for static pressure measurements. However it exhibits excellent sensitivity, linearity and wide band frequency response (from 0.01 Hz to several MHz) in measurement of dynamic pressures. In Table 5.1 the amplitude sensitivities of the piezoelectric sensing plates of the shape of a thin disk are included. One may notice the strong voltage response of the order of mV for the physiological pressure range.

Table 5.1. **Piezoelectric force sensor operating range** associated with passive and active sensing.

Sensor Material	**Deformation** (m) at 80 mmHg-120 mm Hg	**Voltage** (V) at 80 mmHg-120 mm Hg	**Frequency Shift** (Hz) at 80 mmHg-120 mm Hg
SiO_2 (x-cut)	1.27×10^{-11}-2.04×10^{-11}	5.8×10^{-4}-9.1×10^{-4}	90-145
$LiNbO_3$ (z-cut)	5.02×10^{-11} - 8.03×10^{-11}	2.3×10^{-2}-3.78×10^{-2}	~30
PZT	1.55×10^{-11}-2.48×10^{-11}	0.261-0.416	~20

Typical responses of a passive and active sensor for a physiological force range are given. The presented force sensitivities evidence attractiveness of piezoelectric materials for tonometer applications. It is worth noting that the deformation of the piezoelectric element is negligible (the necessary condition for the applanation and requirement obtained from the lumped parameter model in chapter 4), the amplitude of the voltage and the change in the frequency are large and easy to measure.

The second mode referred as an active mode of operation utilizes nonlinear features of piezoelectric materials under an applied force. The features state that under the force, the material parameters of piezoelectric materials (such as elastic, dielectric and other constants) undergo changes that are linearly proportional to the applied force. The nonlinear constitutive equations can be written in the following form (Gagnepain 1982, Kosinski 1997, Hammond 1998):

$$T_{ij} = \left[c_{ijkl} + \tfrac{1}{2} c^*_{ijklqr}\, S^*_{qr}\right] S_{kl} - \left[e_{nij} + \tfrac{1}{2} e^*_{nijqr}\, S^*_{qr}\right] E_n \quad (5.3)$$

$$D_m = \left[e_{mkl} + \tfrac{1}{2} e^*_{mklqr}\, S^*_{qr}\right] S_{kl} + \left[\varepsilon_{mn} + \tfrac{1}{2} f^*_{mnqr}\, S^*_{qr}\right] E_n \quad (5.4)$$

where the parameters with "*" represent the nonlinear materials constants coupled with the acting force, and S* represents the deformation of the crystal caused by the acting force. The appropriate measuring devices, which accurately and conveniently measure the induced changes in the material due to the acting force, can be engineered in the form of a resonant piezoelectric system or phase detector. Typically, the change in the device resonant frequency Δf_R is measured (Gerber 1985, Hammond 1998):

$$\Delta f_R = F \text{ x } (K\ f_R\ n) /w \qquad (5.5)$$

where F - acting force; K - nonlinear material constant; f_R - resonant frequency of the sensor; w frequency

n - order of the harmonic mode of the sensor and w - size of the sensor.

Although the author decided, in order to simplify the measurement system design, to utilize the phase shift detector. Where the phase shift is given by the formula:

$$\Delta\Phi = F \text{ x } C \quad (5.6)$$

Where $\Delta\Phi$ is a phase shift between the input voltage excitation and output voltage measured on the input and output ports of the transducer. S is applied stress and C is a constant specific to the sensor geometry and piezoelectric properties of the transducer.

5.2. Piezoelectric transducer design

Metrological mechanism

The author has used a PZT-5 transducer to convert stress generated by blood pressure to voltage. The reason for this was a high output voltage in a passive mode of operation (see Table 4.1) and a relatively high power of the output signal, which is easier to condition.

As mentioned before, two different phenomena are utilized as a sensing mechanism: the spectrum of the pressure waveform is reconstructed using a simple piezoelectric effect (Passive Mode). Voltage generated on transducer electrodes is collected by conditioning charge amplifier and sent to the digital oscilloscope and Data Acquisition System (the voltage is proportional to the first time derivative of pressure:

$$V_{out} = K \frac{dP(t)}{dt} \qquad (5.7)$$

Actual pressure P(t) is measured using a different mechanism. Due to the nonlinear properties of the piezoelectric material, stress applied to the PZT structure changes velocity of the electro-acoustic wave propagated in the material. This velocity change can be used to measure applied stress. Not all frequencies are affected in the same way. Some frequencies, depending upon sensor geometry and material properties, are affected more, some less. In these studies we choose, using a network analyzer, the most sensitive to stress frequency (260-320 kHz). In the discussed design, the absolute pressure value P(t) is measured using a phase shift between the applied sinusoidal signal and the signal passing through the transducer (Active Mode).

In the final design, these two modes of operation are combined to measure a complete blood pressure waveform (direct piezoelectric effect to reconstruct shape and peak-to-peak amplitude; and phase shift to calibrate the device to absolute pressure measured within the artery).

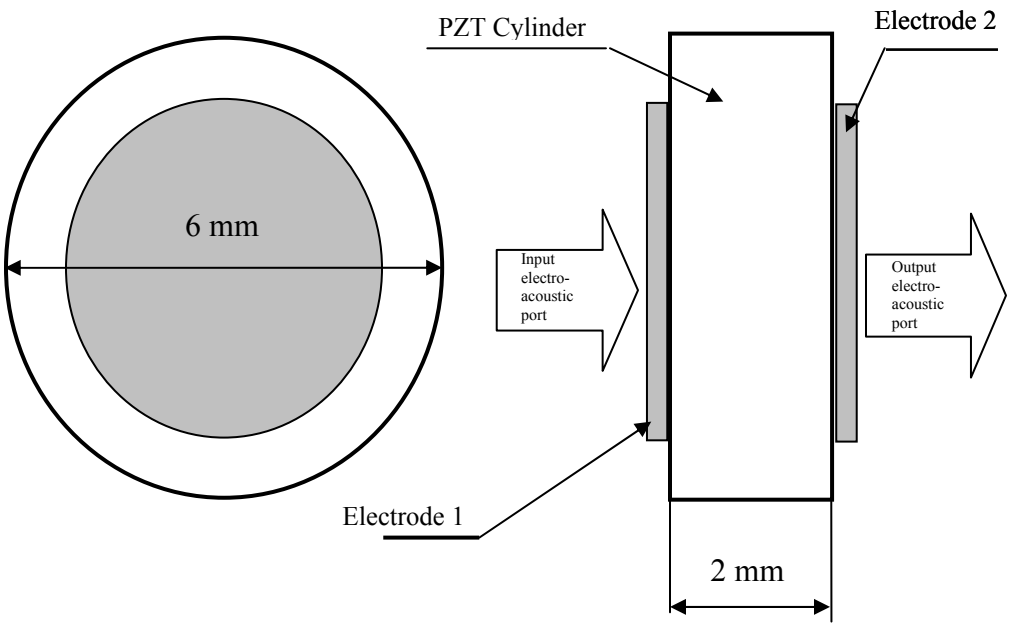

Figure 5.1. **Piezoelectric PZT-5 transducer used in bench-top and implantable tonometer designs**. PZT cylinder is sandwiched between two silver electrodes (electrode 1 and 2). Two sides of the cylinder constitute electro-acoustic input and output ports for the active mode of operation. Stress is applied along the cylinder axis of symmetry, perpendicularly to the electrode surfaces.

5.3. Bench-top model design

The bench-top model was the first to test the piezoelectric tonometer concept. In particular, the device was designed to test the relationship between the applanation level and the amplitude of the output signal. The bench-top model tonometer was integrated with the testing platform shown in figure 5.2 and 5.3. The tonometer prototype was equipped with the precise positioning mechanism to secure the applanation level (micrometer screw) and the precision distance meter (RDP Electronics, probe type GTX2500) as well as an array of sensors to control the temperature, flow and reference pressure signal. The temperature and flow were controlled to secure exactly the same

conditions for the measurement (the temperature changes change the properties of the PZT material, and a different flow rate may generate an unstable noise level).

5.3.1. Mechanical design of the bench-top system

A novel Transducer Testing Platform was constructed, able to precisely control the alignment and degree of applanation of the tonometer in relation to the mock vessel wall.

The tonometer testing platform was designed and constructed to be used with the "mock arterial circulation" (figure 5.2 and figure 5.3). The device incorporated a positioning system to align the transducer's pin with the mock vessel wall and a micrometer to precisely control the degree of applanation. The rigid-planar body contained the PZT transducer and the transducer pin. The length of the transducer pin relative to the surface of the rigid-planar surface could be changed. This testing platform permitted a systematic study of applanation tonometry applied directly to the outside wall of a "mock artery." The tonometer pin was 1 mm in diameter, and the sensing area was far from the edges (7 mm) of the rigid structure, which satisfied the requirements stated in chapter 4 for the applanation area.

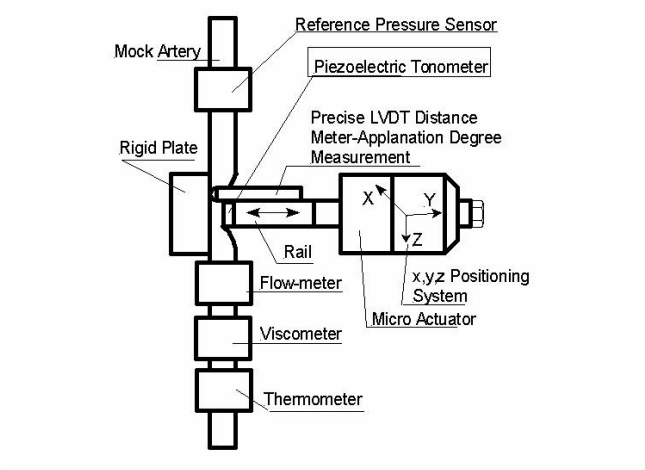

Figure 5.2. The Piezoelectric Tonometer Testing Platform-Schematic.

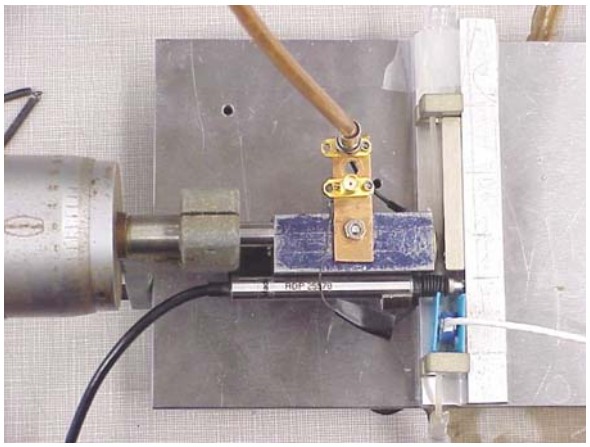

Figure 5.3. A general view of the Piezoelectric Tonometer Testing Platform-Photograph.

5.3.2. Artery–tonometer coupling mechanism

The artery and the PZT transducer are coupled by the rigid plastic pin. The pin is leveled with the rigid surface of the housing. Due to its shape, the pin acts as a force divider distributing the mechanical stress collected by the narrow end and passing it to the transducer surface. The pin is separated from the housing by an air gap and forms a mechanical bridge between an arterial wall and the transducer.

5.3.3. Bench-top measurement system

The measurement system consists of three major groups of devices: the tonometer signal collecting and analyzing devices, the reference signals collecting and analyzing devices and the reference signal generating devices ("mock circulation").

Design and Construction of the Bench-Top "Mock Arterial Circulation"

The very important part of the measurement system was the reference signal generator. Since the tonometer required the input pressure signal close to the physiological one, the special "mock circulation" has been designed and built in order to test the PZT tonometer under pressure, flow and vessel wall conditions that simulate those of a small to medium mammalian artery.

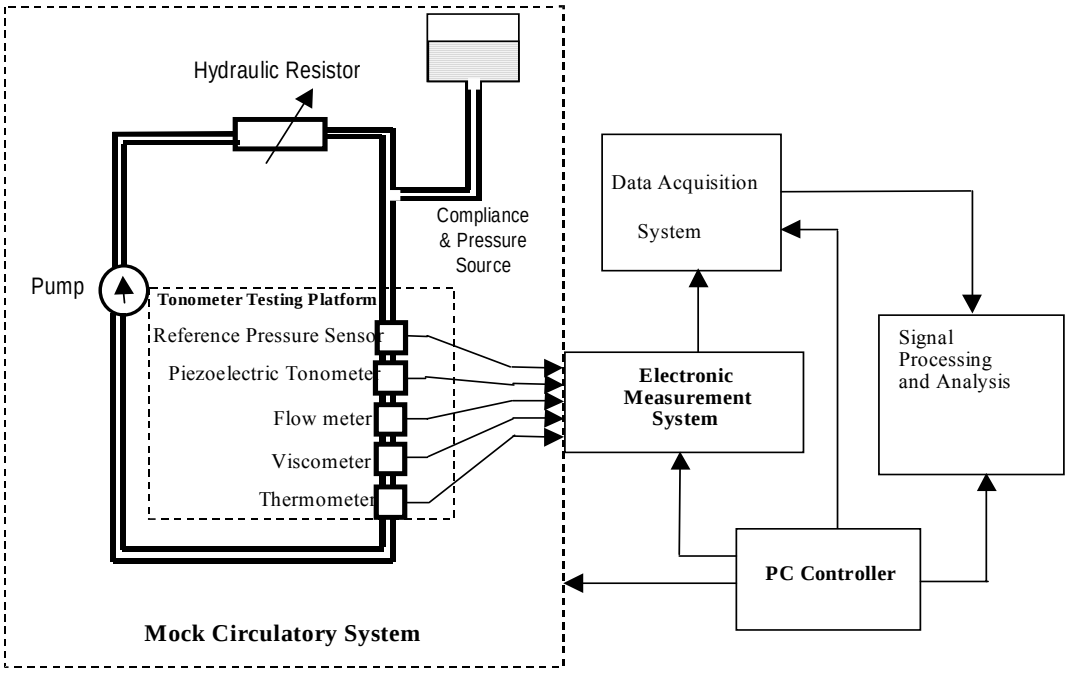

Figure 5.4. Block diagram-laboratory setup of the bench-top "mock circulatory system."

The pulsatile pump and tubing circuit produces the pressure waveforms similar to the blood pressure pulse within a peripheral human artery (adjustable pressure range 40-300 mm Hg, mean flow range 10-200 ml/min, pulse rate 40-200 bpm). The testing system consists of six integrated subsystems: the "Mock Arterial Circulation," the Tonometer Mechanical Testing Platform, the Electronic Measurement System, the Data Acquisition System, the Signal Processing / Analysis System, and the PC-based Experiment Control System (figure 5.5).

The "circulatory system" consisted of a pulsatile pump (Baxter drug infusion pump and later Baxter perfusion pump), tubing, a hydraulic resistor, a static pressure source, and an elasticity compliance chamber. The output signal from the PZT has been compared to the measurements made with the reference sensors placed in-series. The measurements for pressure, flow and temperature have been made using calibrated sensors from commercial venders (Cobe Medical, Inc., Transonic Instruments). Studies have been completed using synthetic tubing (latex rubber, polyethylene, polypropylene) from 1.8 to 5.0 mm outer diameter and 0.02 to 1.2 mm wall thickness.

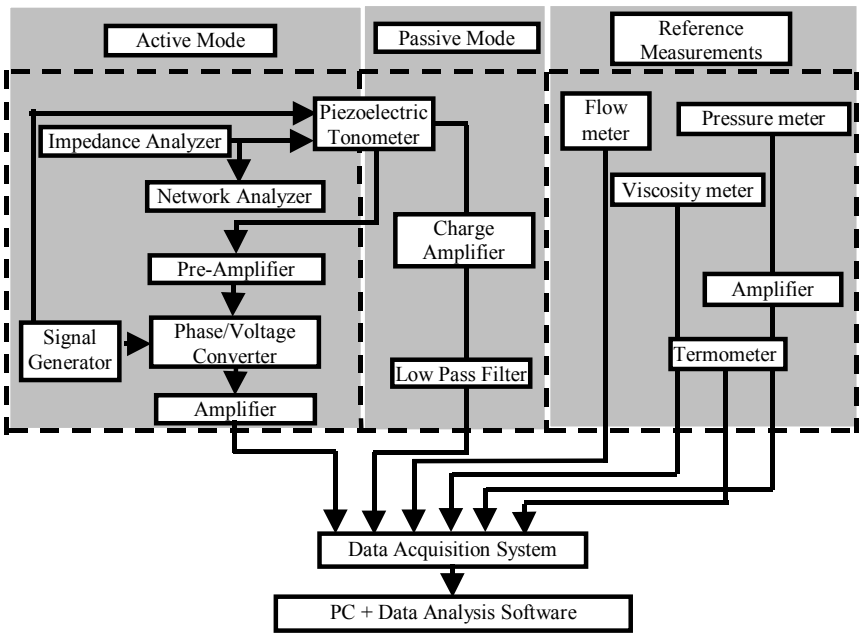

Figure 5.5. The Electronic Measurement System.

The performance of the piezoelectric force sensor and the tonometer sensor heads has been characterized and analyzed using the Electronic Monitoring System. The system for measuring the output signals from the PZT transducer and the reference transducers consisted of three major blocks: 1) Active Mode Block, 2) Passive Mode Block, and 3) Reference Measurements Block. The Active Mode Block was designed to excite the PZT element, and pre-process the output signal using advanced high frequency measurement systems based on a network analyzer and an impedance meter. The Passive Mode Block measured the static/voltage response of the sensor. This block included DC/low frequency, high-input impedance charge amplifier-based detecting systems and filters. The Reference Measurements Block provided driving electronic circuitry for the reference signals (pressure, flow and temperature) and displayed the results.

5.3.4. Tonometer signal conditioning system

The Data Acquisition System collected sensor output signals from all three blocks. Signals were processed and analyzed by the Signal Processing and Analysis Units. Commercial data acquisition and signal and error analysis were used to evaluate PZT transducer performance (Figure 5.5).

The reference signals were collected without conditioning using HP infinium digital oscilloscope.

The tonometer passive mode signal was initially amplified by the charge amplifier and then filtered by the low-pass filter (cut off frequency 40Hz).

The active mode signal was measured by three distinct methods: the network analyzer, the impedance meter, and the phase detector.

The network analyzer and impedance meter outputs were collected directly by the device “on board” data storage capabilities, while the phase detector output was amplified and then sent to the data acquisition system.

5.3.5. Tonometer signal analysis

The signal analysis was performed off line using Excel, LabVIEW and Matlab software. The signal analysis included additional filtering, normalization, digital integration (for the passive mode signal), amplitude calculations, Fourier analysis (for both active and passive modes), and comparison in time and frequency domain. The software performing signal analysis is presented in Appendix E.

5.3.6. Fabrication process used

The fabrication process used in the bench-top prototype includes several technologies:

The PZT cylindrical transducer with silver ports was glued to the pin using epoxy adhesive. The electrodes were soldered to the transducer silver ports. The transducer was positioned inside the housing by fit press technique using an elastic band as a separation between the housing and PZT. The housing was machined out of stainless steel, providing an electromagnetic shield for the PZT disc. All mechanical parts were machined from metal components to secure stable and precise mechanical action.

5.4. Hand-held prototype design

The hand-held tonometer is capable of applanation studies in-vivo. It was necessary to build a hand-held device with a miniature, precise, adjustable applanation mechanism suitable for animal experiments on the small mammalian arteries as well as in laboratory calibration studies. This device bridges the gap between the laboratory setup and a living organism by being able to operate in both environments. The arterial tonometer has been constructed for the short-term arterial pressure waveform measurements, performed on an exposed artery of the anesthetized animal, without implanting the tonometer into the subject body. The arterial tip was designed to stay in the animal organism for a short period of time, while the mechanical applanation mechanics stayed outside the body.

5.4.1. Mechanical design of the hand-held prototype

The prototype mechanics were designed in the form of a pen-like shape with the transducer mounted on the tip of the device (see figure 5.6-7). The contact pressure is

collected by a pin (5.6-6). The desired level of applanation can be achieved by a micrometer screw (5.6-9) driving the applanation mechanism 5.6-10.

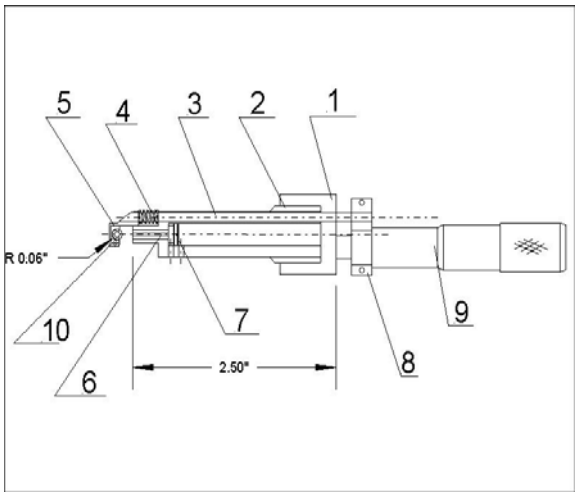

Figure 5.6. **Hand-held tonometer** for short-term testing. 1) rear cup, 2) main body, 3) rod with a hook like support, 4)spring, 5) U-shaped inserts, 6) pin, 7)piezoelectric transducer, 9) micrometer adjusting the applanation level, 10) vessel.

The micrometer screw moves the U-shaped support structure (5.6-5) in relation to the rigid support structure (transducer housing 5.6-3). The U-shaped support structure is equipped with inserts (5.6-5) that hold the artery. The inserts are fabricated with diameters ranging from 2.0 mm to 4.0 mm (0.25 mm increments) to accommodate a wide range of arterial diameters.

This type of design allows for the device to be used with the different arterial diameters. The surgeon can measure the diameter of the artery with a caliper, and the appropriate insert can be chosen to optimize mechanical fixation and minimize vessel lumen compression (figure 5.7). In figure 5.7, a segment of the mock artery is placed

inside the tonometer to show the position of the artery, during the experiment, in respect to the tonometer.

Figure 5.7. **Hand-held tonometer tip**. Silicone tubing is placed in the U-shaped support structure

The detailed design is shown in Appendix A.

5.4.2. Artery-tonometer coupling mechanism

The hand-held prototype coupling mechanism was altered with respect to the bench-top prototype in order to meet hermetic sealing requirements regarding protection of the PZT transducer against moisture. A thin aluminum foil was glued (epoxy adhesive) over the surface of the rigid-planar body to provide a hermetic seal. The foil was glued only to the housing of the transducer, leaving the connection between the pin and the foil free. This technique was intended to minimize the transmission of shear forces to the transducer. Covering the transducer pin with foil (25 micrometer thickness) provided hermetic sealing. Altered that way, the tip of the hand-held device was able to operate in contact with moisture and liquid.

5.4.3. Applanation mechanism of the hand-held prototype

The problem that has to be addressed by implantable devices working in living environment is the lack of any stable support for the vessel. Thus the design has to compensate for this by stabilizing the artery during the measurement process and by providing a constant level of applanation. The traditional external tonometry uses the subject's bones as a platform on which the applanation process can be performed, but if the device is intended for implantation this concept is not practical anymore. In the presented prototype, the artery is encircled by the tonometer and is pushed against the force transducer by a hook-like support structure. The applanation mechanism utilized in this prototype provides a stable position on the artery with respect to the transducer sensing area (rigid pin) by holding the artery between the hook-like support structure and the rigid body with the incorporated piezoelectric senor. The hook-like structure enables the surgeon to insert the artery into the tonometer measurement area and then compress it by tiding the micrometer screw that elevates the hook-like support structure (see figure 5.8.).

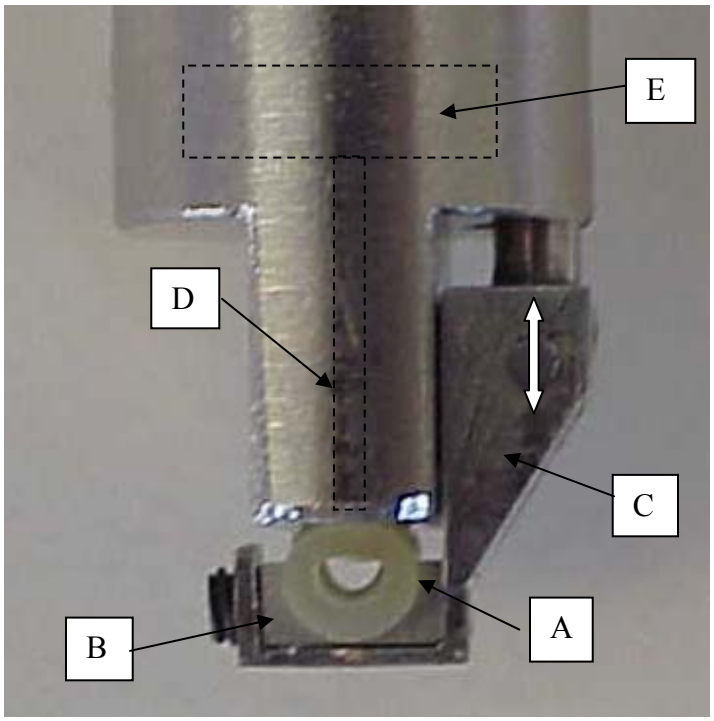

Figure 5.8. **Detailed view of the tip of the hand-held tonometer with adjustable applanation level**. The mock artery (A) is held in the U-shaped artery holder, (B) can be flattened by moving the adjuster (C) up or down. The white arrow indicates directions of movement. Pressure is received by pin (D) and transmitted to the piezoelectric transducer (E) mounted inside the tonometer's housing.

Figure 5.8 shows the tip of the tonometer attached to the mock artery (2A). The U-shaped supporting structure was designed to change its distance from the tonometer's body, providing a wide range of applanation levels. The PZT transducer (2E) was placed inside the tonometer's cigar-shaped body. The blood or liquid pressure signal was collected by a pin (2D) that transferred pressure to the PZT transducer.

5.4.4. Measurement system of the hand-held prototype

Since the same PZT transducer was used in the hand-held prototype as in the bench-top model to convert stress generated by blood pressure to voltage, the measurement setup is similar to the bench-top one. The spectrum of the pressure

waveform is reconstructed using a direct piezoelectric effect (Passive Mode). Voltage generated on the transducer's electrodes is collected by a conditioning charge amplifier and sent to the digital oscilloscope and Data Acquisition System (the voltage is proportional to the first time derivative of pressure.

The actual pressure P(t) is measured using the active mode. Due to nonlinear properties of the piezoelectric material, stress applied to the PZT transducer changes velocity of the electro-acoustic wave propagated in it. To measure applied stress, the phase shift between the signal entering the transducer and coming out of it is measured. In these studies we have chosen, using network analyzer, the frequencies with maximum phase shift. (it means the frequencies for which the phase shift change per 1 Pascal of applied pressure was maximum). In the presented design the absolute pressure value P(t) is measured using the phase shift between the applied sinusoidal signal (1 V_{p-p} amplitude) and the signal passing through the transducer.

In the final design, these two modes of operation will be combined to measure complete blood pressure waveform (direct piezoelectric effect to reconstruct shape and peak-to-peak amplitude; and phase shift to calibrate the device to absolute pressure measured within the artery).

5.4.5. Signal conditioning system and signal analysis

The signal conditioning system compared to the bench-top setup was equipped with additional filtering options (HP infinium signal averaging option (averaging for 4 samples) and a sine filter).

Signal analysis was the same as in the bench-top experiments (see Appendix E).

5.4.6. Fabrication technology used

The fabrication technology utilized in the hand-held prototype enables using the device in contact with living tissue without causing trauma. Thus, the body of the tonometer was fabricated out of stainless steel, edges were smoothly rounded to avoid injury of the arterial wall and minimize the arterial spasm caused by the contact with sharp edges. The aluminum foil was glued using medical grade epoxy adhesive to provide the hermetic sealing of the transducer tip. The cables were shielded with the aluminum foil, and the whole device was covered by the latex protection layer.

The transducer was placed inside the transducer body by using a fit-press technique. The PZT cylinder was separated from the stainless steel housing by the plastic band.

The tonometer pin was glued to the PZT transducer with the epoxy adhesive.

5.5. Implantable prototype design

The third and the final tonometer design presented in this chapter combines the best features of the previously presented devices and meets requirements for an implantable tonometer. Previous experiments proved that the PZT transducer was able to measure the contact pressure through the aluminum foil. With this device the author took the technology one step further and used only one piece of metal to fabricate the housing and the membrane. As a consequence, the author avoided sealing between the membrane and the housing. The device was designed to perform long-term experiments in a living organism.

After first experiments on the femoral artery with the hand-held prototype, the author decided to build the tonometer capable of performing BP real-time measurements on the aorta of a 20-30 kilogram dog or mini pig (less motion artifacts). The choice of the

target artery determined the tonometer size and shape. It was designed to be easily mounted on the artery by adding a tongue-and-groove mechanism connecting the U-shaped support structure to the tonometer senor head.

5.5.1. Mechanical design of the implantable prototype

The implantable tonometer device intended to stay around the artery has to meet some critical requirements:

- The shape has to be compact and as small as possible to avoid excessive compression of surrounding tissue.
- The shape of the tonometer has to minimize bending and twisting of the artery to avoid artery compression leading to blood flow decrease.
- The wires have to be mechanically secure to avoid motion artifacts. The best position is to place some length of the wire along the artery.
- The wire stress has to be mechanically unloaded by leaving some extra length forming a loop close to the tonometer.

Taking into consideration the mentioned-above requirements, a miniature, stainless steel arterial tonometer was designed and constructed. The figures from 5.9 to 5.12 show respectively: general view of the device, view with partially removed support structure,

front view of the device with the mock artery, and the tonometer head cross section.

Figure 5.9. Arterial Tonometer for Long-term Implantation-general view.

Figure 5.10. **Disassembled tonometer** shows the idea of artery fixation between U-shaped and flat structures.

Figure 5.11
Front view. Miniature tonometer for chronic implantation.

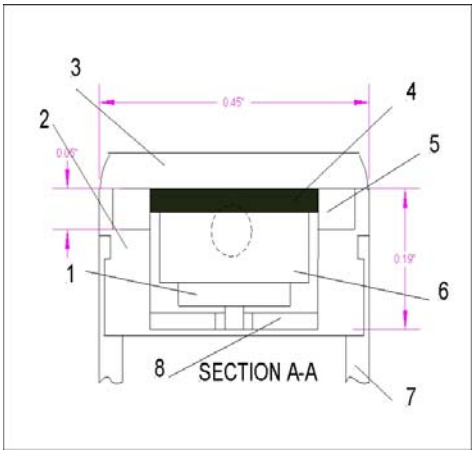

Figure 5.12 Tonometer half-view.

The preliminary experiments were performed to determine whether this stainless steel "wall": 1) provided an effective barrier against the invasion of water vapor, and 2) allowed the vessel wall forces to be transmitted to the transducer pin without loss or distortion of the signal. The tonometer prototype provided a reasonably high signal-to-

noise ratio (10-12) with the accurate measurement of the pulse pressure wave (in comparison to a calibrated pressure transducer).

5.5.2. Artery-tonometer coupling mechanism

The coupling mechanism in this prototype is unique and consists of a thin stainless steel membrane and a rigid plastic pin. The first time, the author decided to use the membrane that was an integral part of the housing. The infinitesimally small deflection of the transducer does not require good flexibility of the contact pressure transmitting membrane. This concept proved successful and reliable. The transducer is coupled to the artery in a slightly different manner than in previous devices. The PZT cylinder is sandwiched between the rubber layer and the rigid pin. The sides of the transducers are free and separated from the housing by the air gap (see figure 5.12). The membrane is supported by the washer, which allows the membrane to deflect only on the small area of 2 mm in diameter and separates the transducer from the peripheral high contact pressure gradients (figure 4.58).

5.5.3 Applanation mechanism of the implantable prototype

The applanation mechanism was simplified in order to meet the implantation requirements. The applanation level and the support for the artery are provided by the geometry of the removable U-shaped support structure (see figures 5.9-5.10). The support structure is attached to the tonometer housing by the tongue-and-groove mechanism. This solution makes it easy to mount the tonometer around the artery and, at the same time, secure a very stable measurement platform after the support structure is fixed.

5.5.4 Measurement system of the implantable prototype

The measurement system of the implantable prototype is analogous to the system used with the hand-held prototype. The only, but very important, difference is that the implantable device is connected to the measurement devices via jack. The jack is mounted on the shield and covered with silicon cable. This cable after the measurements is disconnected from the measurement system, covered with the additional silicone protection and buried under the subject's skin. It stays in the subject's body until the next experiment. This kind of connection decreases the SNR ratio, especially in the Passive Mode.

5.5.5 Signal conditioning system and signal analysis

The signal conditioning system was identical to that used in the hand-held prototype. The Signal Analysis system was built in LabVIEW software (see Apendix E).

5.5.6 Fabrication technology used

The 8.0 mm x 12.0 mm x 8.0 mm sensor head was machined from implant grade stainless steel and finished to a smooth-round contour. Packaging methods were developed to provide a long-term hermetic seal without adversely affecting the transducer's ability to measure the underlying vessel wall forces. A one-piece metal housing was designed with a precisely machined channel for the PZT transducer and pin. In the current preferred design, a 25-micrometer wall of stainless steel separates the transducer pin from the underlying blood vessel wall (see figure 5.12).

The miniature sensor head was machined with gentle curves to avoid tissue trauma and geometry to maintain optimal alignment of the transducer pin with the flattened portion of the arterial wall. An O-ring, compression fitting and three coatings of implant grade silicone were added to the top of the sensor head to minimize the risk of

invading moisture. Transducer wires were placed within a thin, flexible elastic catheter (Hickman Catheter), the lumen of which was subsequently filled with implant-grade silicone (Medtronic Medical). The catheter and strain relief assemble were attached to the rigid-planar body (transducer platform) with a clip and silicone adhesive. U-shaped support structures were machined from implant-grade stainless steel (5.0 mm to 7.0 mm inner diameter - 0.25 mm increments for mini pig abdominal aorta) and finished to a smooth-round contour. The upper arms of the U-shaped structure attach firmly to the rigid-planar body using a tongue-and-groove design (figure 5.10).

6. TONOMETER TESTING

The tonometer prototypes have been tested under varius conditions emulating important aspects of the blood pressure signal and human body environment.
The basic parameters of the sensor have been tested under laboratory coinditions, while the sensor capability of working inside the human body has been tested in animal experiments.

In-vitro experiments

As a result of theoretical modeling, some design criteria have been determined such as mechanical compliance of the transducer, dimensions of the sensing area and the range of applanation level necessary to obtain the output signal with less than a 1% error.

This theoretical outcome has produced requirements for the prototype design. Three prototypes equipped with the low mechanical compliance PZT force transducers have been fabricated for the bench-top and in-vivo experiments. To prove that those prototypes, fabricated upon theoretical calculations and assumptions, meet static and dynamic requirements for measuring arterial blood pressure waveform, a set of tests was designed and performed. The bench-top, static experiments have been prepared to test the tonometer error, linearity and the influence of the applanation level on the tonometer signal.

Also, the dynamic tests on various types of tubing have been performed to test the dynamic response of the tonometer. The dynamic tests concentrated on transitional phases and show a relationship between the input and output signal in time and frequncy domains.

6.1. Static response experiments

The static tests help to explain basic transducer characteristics such as the device's error, sensitivity and linearity and some other features (e.g. linear range of operation). The static response is measured under the assumption that the input signal is applied for an infinitesimally long period of time, which in fact means that the output signal is measured after it is stabilized and the transitional phenomena are ignored.

Also, in this chapter, the influence of the applanation level on the tonometer output was tested. Although it's not strictly speaking a static test, because the pressure signal was applied in a form of a pulse, and the amplitude of the output periodic signal was measured, the author decided to include this kind of study to the static experiments due to the fact that the applanation level was the input parameter, which was changed during the experiment. And the applanation level was applied in long periods of time, where the conditions reached a stable state.

All static tests were performed using the active mode of operation since the passive mode was not capable of measuring the static loads.

6.1.1. Experiment description

In figure 6.1 the experimental setup for the static tests is shown. A hydraulic pump generates the input signal. It is connected to the elastic mock artery. The tonometer, along with the reference pressure transducer, collects the pressure signal.

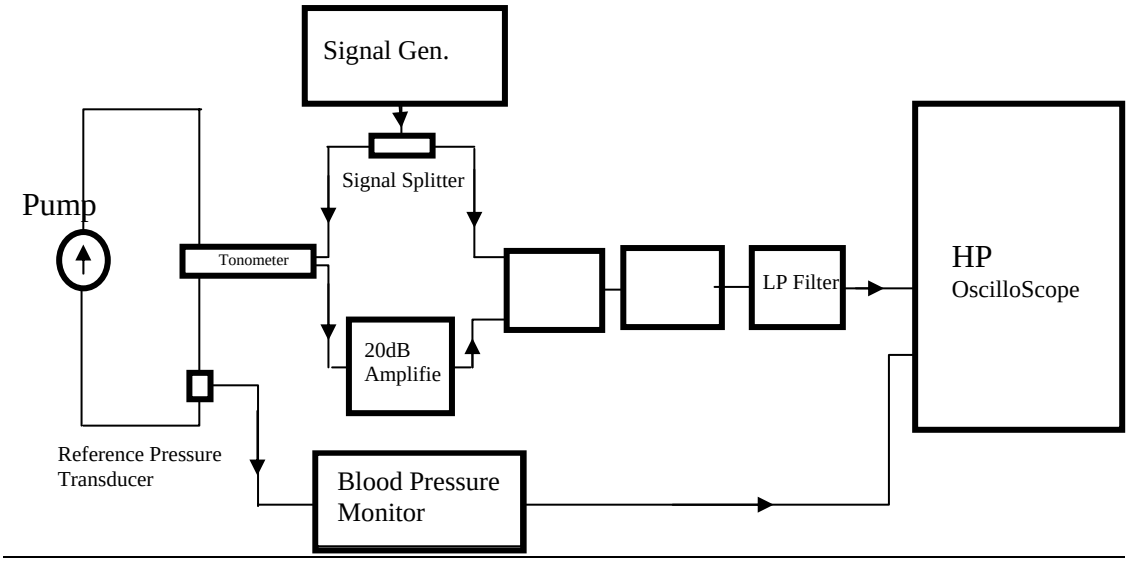

Figure 6.1. Bench-top setup schematics for static and dynamic tests.

The Signal Generator produces a frequency of 321.5 kHz. The signal is split with a power splitter. One part of the signal is sent to the PZT transducer and generates piezoelectric oscillations of the sensor. The second, reference part of the signal is sent to the Phase detector. The signal, which enters the PZT, is transferred through it and changes amplitude and phase due to tension applied to the PZT by the mock artery wall (equation 5.6). To equalize amplitudes of the reference signal and the PZT signal, the 20 dB Power amplifier is used. The Phase Detector detects the difference between reference signal phase and the phase of the signal transmitted through the PZT sensor. The output of the Phase Detector is amplified with a 20 dB power amplifier, and then it enters the Low Pass filter with a cut-off frequency of 40 Hz. Reference pressure measurement is performed with a standard blood pressure monitor (Space Lab 512). Reference pressure signal and tonometer signal are recorded with the digital oscilloscope HP Infinium.

Experiment I. Tonometer linearity tests

The tonometer was tested in a bench-top environment using the setup shown in figure 6.1. The sensor active mode response was tested by applying static pressure to the 5 mm OD mock silicone rubber and PVC arteries (Young modulus from $4x10^6$ to $1.7x10^7$ dyne/cm^2). The applanation level was fixed at 16% (center of the theoretical applanation range). Pressure was applied in a physiological range from 0 to 180 mmHg in steps (30 mmHg each). The phase shift between the 267 kHz sinusoidal input signal applied from the signal generator and the PZT output signal was measured with a HP network analyzer.

Experiment II. Influence of the applanation level on the output signal amplitude

The second experiment was designed to test influence of the applanation level on the tonometer output signal amplitude. The experimental setup schematic is the same as in experiment I (figure 6.1). The tonometer and reference pressure waveforms are recorded (see figure 6.3), and the amplitude of the tonometer signal and the reference pressure is collected.

The experimental setup consists of a Pressure Wave Generator (Volumetric infusion pump FLO-GARD 6200), Hydraulic Circuit, Tonometer Probe, Reference Pressure Monitor, Measurement System, and Data Acquisition System (HP Infinium Digital Scope).

The pulsatile flow was generated in the mock circulation (60 bpm 120/80 mmHg). The applanation level was adjusted using the applanation mechanism of the bench-top prototype. The applanation was changed from 0% (no contact between the artery and the

tonometer) up to complete occlusion of the artery, using the tonometer applanation mechanism. The amplitude of the output signal of the tonometer was recorded every 25 μm.

Two series of experiments were performed. One experiment was performed with the rubber mock artery 5 mm OD, (wall thickness 0.8 mm, Young's modulus $4x10^6$ dyne/cm^2), the second one with the silicone mock artery OD 4.8 mm (0.2 mm Young's modulus $1.7x10^7$ dyne/cm^2).

6.1.2. Results

Static characteristic. The results of Experiment I have shown very high linearity of the signal r^2=0.98 and error less than 3%. The Young's modulus had no observable influence on the static response. The static characteristic obtained for the mock 5 mm OD artery, (wall thickness 0.8 mm, Young's modulus $4x10^6$ dyne/cm^2) is shown in figure 6.2. The Phase shift vs. pressure relationship shows high linearity. However, phase changes are rather small. The overall phase shift corresponding to pressure range from 0 to 180 mmHg is close to 3.5 degrees. The sensitivity of the tonometer working in the active mode is 0.0194 degree /mmHg. The contact pressure at 0 mmHg was detected with the phase shift of 0.033 degree, which is less than 1% of the measured range of physiological pressure. The maximal detected error was measured at 90 mmHg and was 3.3%.

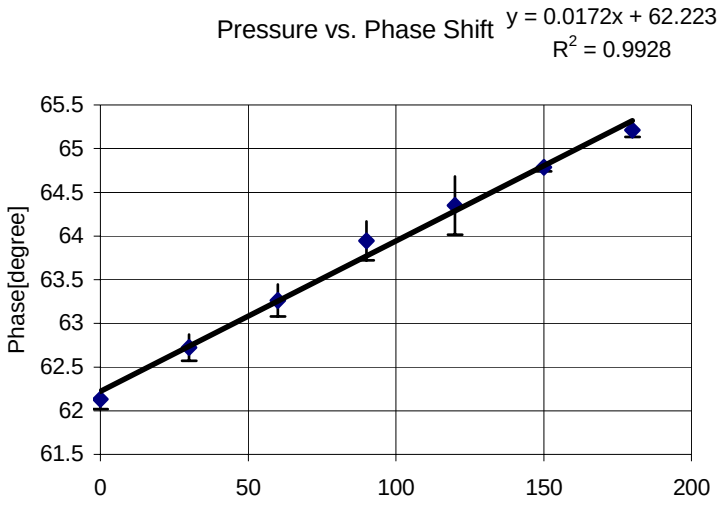

Figure 6.2. Pressure/piezoelectric tonometer phase shift relationship.

Influence of the applanation level. The influence of applanation level on the signal amplitude (tonometer and reference signals are shown in figure 6.3) is shown in figure 6.4. One can notice that an applanation level from 15% to 20% of the mock artery OD keeps amplitude on level from 1 to 2 V (Average ~1.5 V). Beyond this range, amplitude of the signal drops gradually. It indicates that the maximum amplitude the applanation should be kept in a range between 15% to 20% of arterial OD. The theoretical calculation (chapter 4) showed that the range of 1% error lies between 8% and 22% of applanation.

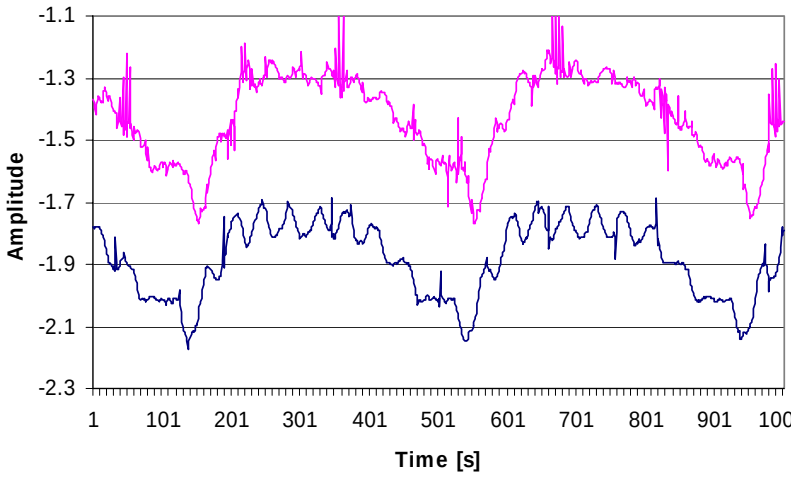

Figure 6.3. **Comparison of the reference signal** (blue line) **and tonometer active mode signal** (purple line) in the applanation influence on the output signal experiment.

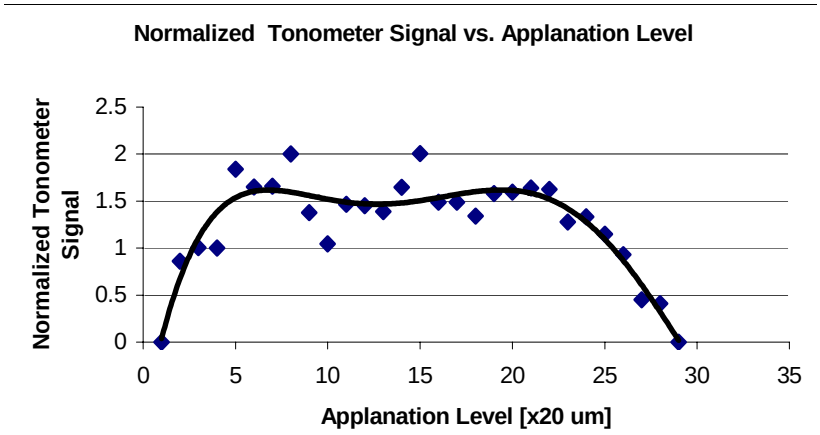

Figure 6.4. **Relationship between applanation level and tonometer active mode signal** amplitude.

6.1.3. Discussion

The static tests have shown that the tonometer designed according to the theoretical calculations exhibits a very linear characteristic in the physiological range of pressures; it has a small maximal error of 3.3%. This is consistent with the literature (Drzewiecki, Nichols, Pressman) and with the theoretical modeling presented in chapter 4.

However, it does not mean that the tonometer signal reflects direct pressure in the tube. The tonometer signal averages the contact pressure as shown in figures 4.51 and 4.52. The contact pressure as was shown in chapter 4 consists of the applanation component and the blood pressure component. In addition, the sensitivity of the active mode is low, which can, in later applications, generate problems with noise. The technical solution to this problem can be to switch from phase detection (equation 5.6) to frequency detection (equation 5.5) using oscillators.

The changes in applanation level can dramatically lead to large errors, due to the contact pressure gradient (see figures 4.51 and 4.52). The influence of the applanation level on the tonometer signal is similar to those calculated by the theoretical model. It revealed the existence of a measuring window that is consistent with the theoretical studies (to small or to large applanation level results in drastic changes in signal amplitude). The relatively stable region in terms of signal amplitudes exists in the range from 15% to 20%. However, it is narrower than what was theoretically predicted. Moreover the stable region is shifted toward higher applanation levels.

6.2. Tonometer dynamic response tests

The dynamic tests compare the input and output signals in time and frequency domains. Contrary to static tests, they provide information about time-related changes in the sensing path. Usually, those time-related changes deal with the dissipation and accumulation of input signal energy in various stages of the transduction process.

In the presented case the energy dissipation occurs due to viscous properties of the mock artery, and accumulation takes place in elastic structures of the arterial wall. Commonly accepted methods of studying dynamic response are time function and spectra

comparisons. The linearity between the input and output signals also can be obtained by eliminating time using the phase plot and than calculating strength of the linear correlation between input and output signals.

The dynamic tests were performed using the setup shown in figure 5.4, allowing simultaneously recording of the passive and active modes along with an array of reference signals. The input and output signals were collected in 10 s periods and than analyzed offline. The time functions, spectra and linear correlation are presented and compared.

The linearity in the dynamic response is calculated from the time functions of the input and output signal. Thus, the linearity calculated in chapter 6.2 is different from the one calculated in 6.1 in the sense that the dynamic linearity includes dynamic phenomena such as phase shift between signals and frequency related dumping.

6.2.1. Experiments description

This experiment was designed to test the tonometer mounted on the hand-held device. The bench-top test provided the author with information about the tonometer characteristics before testing the device on the living subjects. The bench-top stable environment gave the necessary constant conditions that established a baseline to which the characteristics obtained in less stable conditions, such as the living subject, will be compared.

Experiment I (Hand-held prototype).

Pulsatile pressure with the spectrum broader (0-200 Hz) than the regular physiological blood pressure spectrum was applied to the mock circulation. Tests were conducted for the range of pump frequencies simulating various heart rates (50-120 bpm,

with increment 5 bpm). For active and passive mode the samples of 10 s signals were collected using a Data Acquisition System. Mean pressure was changed using the hydraulic resistor.

The pump generates a pulsatile flow in a mock artery. The tonometer was placed on the silicone rubber mock artery (5mm OD, wall thickness 1 mm) in series with the reference pressure transducer (Cobe Medical). Reference and tonometer signals are collected and compared offline. Two modes of operation require two separate measurement setups. The active mode setup consists of: signal generator, phase to voltage converter or network analyzer and Data Acquisition System. The passive mode setup consists of conditioning amplifier (charge and operational amplifier with adjustable input impedance) and Data Acquisition System.

Specific conditions recreated the conditions in the real artery of the anesthetized animal.

The input signal (hydraulic) conditions were as follows: pressure: 90/40 [mmHg]; flow: 220 [ml/min]; Pulse: 120 [bpm] (2 [Hz]); applanation level: 16%.

A tonometer mounted in the mechanical holder was attached to the elastic tubing (∅ 5 mm, wall thickness .8 mm, Young's modulus $1.7x10^7$ dyne/cm^2). Then the tubing was flattened (applanation level 16%).

Two signals were synchronously recorded: pressure sensor signal (from BP monitor analog output) and the tonometer signal (voltage signal from the piezoelectric plate with high input impedance oscilloscope or the phase shift with the phase detector).

Experiment II (Implantable prototype).

A systematic study was completed using the implantable prototypes and mock arterial circulation. Reference pressure was measured with a commercial piezoresistive pressure sensor (Cobe Inc.) and a BP monitoring system designed for human vital sign monitoring in the hospital. The system provided a stable pressure signal, with the ability to control one variable at a time. Flow through the mock artery (5 mm outer diameter, 0.2 mm wall thickness, Young's modulus $4x10^6$ dyne/cm^2) was varied from 200 ml/minute (frequency 40 bpm) to 400 ml/min (frequency 80 bpm). Flow varied in a direct and linear fashion with frequency of the Sarns roller pump, using water and more viscous fluids. Resistance was precisely controlled using a hydraulic resistor, 15 cm distal to the sensor head. The sensor head produced approximately 13% to 16% applanation of the "vessel wall," depending upon the size/wall thickness of the tubing studied. Temperature of the circulating fluid and sensor head was controlled using a water bath (thermistor connected to the vessel wall adjacent to the sensor head). The input and output signals were collected in the same way as in Experiment I, and the analysis was performed using time and spectra comparison, as well as linear correlation.

6.2.2. Results

Experiment I (Hand-held prototype).

The experiments provided two important pieces of information about the relationship between input and output signals.

The time comparison shows the close agreement between pressure and the tonometer output signal. The signals are slightly shifted in time by ~25 ms and the reference signal output lags compared to the tonometer, which is generated by the positioning of the

tonometer, slightly toward the pump. The average error is in the range of ±3%. The linearity is r^2=0.98.

The frequency comparison shows that the spectra are close (less than 1%) up to the 8th harmonic (16 Hz). Above the 8th harmonic the discrepancies become significant (more than 50% of the input signal). The tonometer underestimates the input signal in these frequencies.

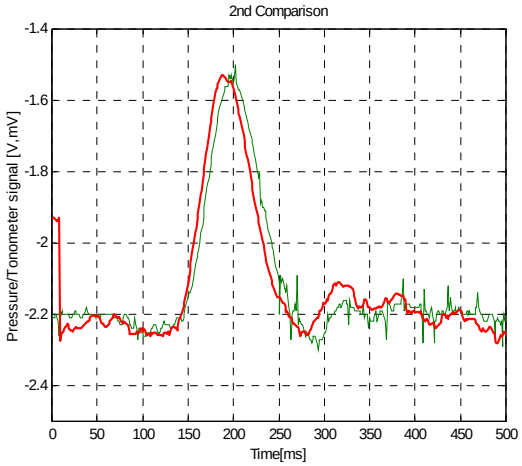

Figure 6.5. **Comparison of the pressure sensor signal and the tonometer signal**. The green line represents reference pressure, the red line represents piezoelectric tonometer signal.

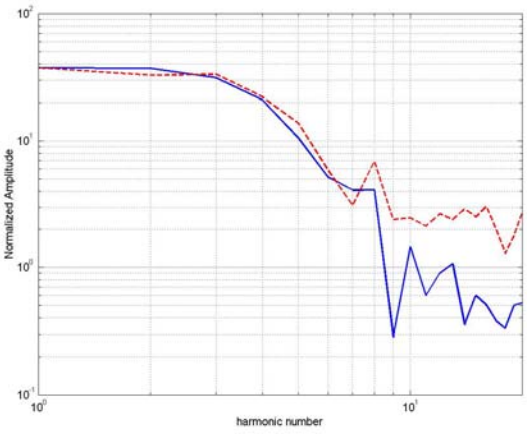

Figure 6.6. **Comparison of the tonometer signal (blue solid line) with the reference pressure signal (red dashed line) in frequency domain**. The amplitudes of both spectra are very similar up to 8th harmonic of the signal, which is up to 16 Hz.

Experiment II (Implantable prototype).

The implantable tonometer prototype was able to measure the pressure waveform with accuracy over a wide range of pressure, flow and temperature. In the first series of experiments, the sensor head was placed around thin-walled PVC tubing.

Initially, pressure was held constant while changing frequency. Tonometer and reference pressure waveforms (recorded over a range of frequencies - 20, 40, 60, 80 bpm) were correlated from r^2=0.77 to 0.94 (see example figure 5.7).

Pressure was varied in the second series of experiments while maintaining constant frequency. Separate data sets were collected at a fixed frequency of 60 and 80 bpm. Tonometer and reference pressure waveforms correlated closely over a wide range of pressures: r^2=0.78 to 0.98 (for pressure pulsations 91/26 to 239/139 mm Hg).

In a third series of experiments, pressure was allowed to vary depending upon frequency of the roller pump. Pressure varied from 25/2 mm Hg (mean 9.6 mm Hg) to 154/54 mm Hg (mean 87 mm Hg) while varying frequency from 20 to 80 bpm. In general, tonometer and reference pressure waveforms correlated closely. Although the signal became increasingly noisy at the lower range of pressure in both the tonometer and reference pressure signals, the tonometer signal was sufficiently high to measure the peak and valley amplitudes, including details of the waveform.

Temperature of the fluid/sensor head was varied in the fourth experiment, while keeping all other variables constant. Pressure waveforms measured with the tonometer and reference method were not grossly affected by changing temperature over a wide range (31.7 Celsius to 40.4 Celsius).

In addition, several experiments were repeated using thick-walled (1,100 micrometer wall thickness, 6.5 mm outside diameter, 4.3 mm internal diameter) and thin-walled (800 micrometer wall thickness, 5.5 mm outside diameter, 3.9 mm internal diameter) silicone rubber tubing. The wall thickness/composition did not have an influence on the contour of the pressure waveform, there was no consistent pattern relating wall thickness to accuracy of the tonometer. The measurements made with the tonometer compared closely with the reference signal.

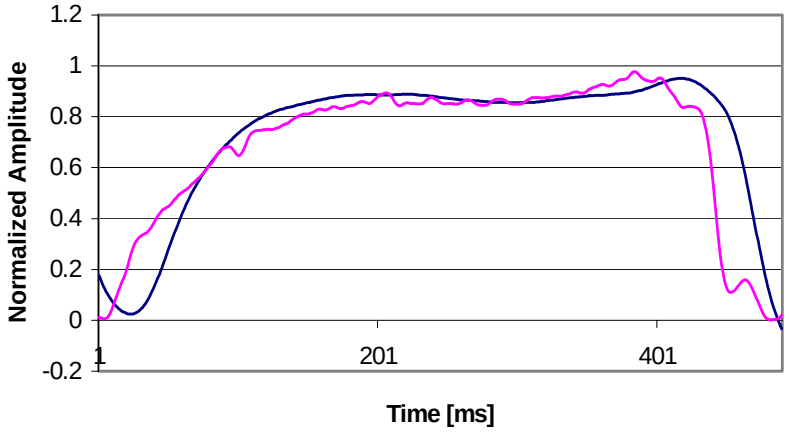

Figure 6.7. **A comparison of the tonometer signal (blue line) and the reference pressure signal (red line) for the frequency 60 bpm,** pressure 90/26 mmHg.

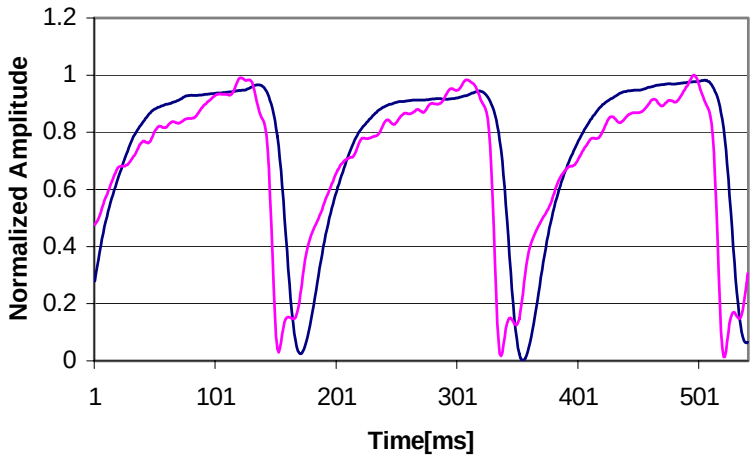

Figure 6.8. **A comparison of the tonometer signal (blue line) and the reference pressure signal (red line) for the frequency 80 bpm**, pressure 150/60 mmHg.

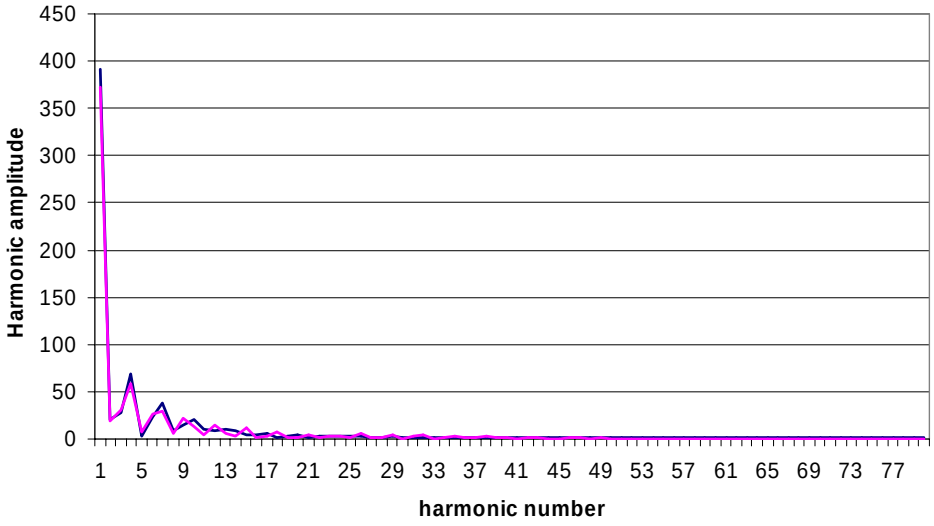

Figure 6.9. The Amplitude of the spectrum of the signal shown in figure 6.8.

6.2.3. Discussion

The main purpose of the dynamic response experiments was to determine how accurately the spectrum of the pressure signal is reproduced by the tonometer.

The systematic applanation studies showed that the arterial tonometer signal is delayed compared to reference signal (see figure 6.5.). The average measured delay time was equal to ~20 ms. The delay was introduced by the signal conditioning system (filtering and phase detection).

The normalized amplitude of the tonometer signal reaches the plateau after 15% of applanation. The plateau exists up to 20% and then the signal decreases up to zero level.

The sensor dynamic range was shown to be slightly insufficient for the blood pressure signal, and an extension of the dynamic range has to be made. To measure blood pressure in real time, the sensor has to carry frequencies up to 20 Hz (for resting adult subject, for higher heart rates even up to 66 Hz, see chapter 2). Figures 6.5 and 6.6 show the comparison of the tonometer signal with the reference blood pressure transducer signal. Two signals are compared in time and frequency domains. Both comparisons show the high quality of the tonometer's signal for low frequencies. However, the tonometer's response above 16 Hz shows some discrepancies.

The studies also show an increase of the error for the low amplitudes of pressure. This confirms the theoretical conclusions that the contact pressure contains the applanation component not related to the blood pressure, which contributes more to the tonometer readings when the blood pressure signal drops.

Conclusions:

1. **Piezoelectric material used, as a passive sensing element, in the tonometer is able to reconstruct a pressure shape without an external energy source (see figures 6.5 and 6.6)**.
2. **Active mode of piezoelectric sensor, in the tonometer, is able to measure an exact value of pressure (see figure 6.2) and can follow dynamic pressure changes (see figure 6.3).**
3. **Piezoelectric tonometer output, in the active mode of operation, is in a linear relationship with applied pressure (see figure 6.2). This feature can be used as a calibration technique for the piezoelectric tonometer working in passive mode or as a sensing mechanism by itself.**
4. **Implantable tonometer may work in passive mode of operation using no energy.**
5. **The combination of passive and active mode of operation may be utilized in the implantable tonometer, resulting in very low power consumption.**
6. **One transducer is capable of working in two modes of operation without changing the sensor configuration.**

6.2.4. Recommendation for future work

The very valuable feature of the piezoelectric force sensor is its ability to work in both active and passive modes. The future work will be focused on developing an

electronic circuitry to enable the tonometer operating in both modes simultaneously. It will give the opportunity to increase the reliability of operation and automatic calibration. The implantable sensor requires low energy consumption. Dual modes of operation could be the best solution for this type of application. The idea of dual modes of operation is as follows:

The sensor works in passive mode of operation collecting pressure path shape. This mode does not require an energy supply for the sensing element. The voltage is generated by mechanical force, which is generated by the blood pressure. The disadvantage of passive mode is that output voltage is proportional to the dP/dt and thus cannot be used for calculating exact value of the blood pressure.

In time intervals the sensor is switched by the electronic circuitry to active mode, where the piezoelectric crystal is vibrated by applied voltage. The phase shift of the output signal is proportional to the pressure, which gives a calibration point for the pressure pattern obtained from the passive mode.

A combination of these two modes gives full information about the shape and amplitude of the blood pressure signal.

6.3 Pilot in-vivo experiments

In the author's opinion, the promising results of the in-vitro tests, presented in chapter 6.2, justified in-vivo experiments. The characteristics obtained in the in-vitro studies provided data that shows high potential of the tonometer prototypes in terms of the static and dynamic accuracy. Thus, the in-vivo approach seems to be a natural consequence leading to the ultimate analysis.

On the other hand, the modeling results, shown in chapter 4, have provided some information such as potential remodeling problems that cannot be verified by using only the mock arteries.

To test the tonometer in the environment that is close to the target one, the series of in-vivo experiments has been designed. To test how the tonometer works on the living arterial wall tissue and how its characteristics differ from the in-vitro application, the acute experiments were designed. To study the tissue response (remodeling), to the long-term applanation, the long-term in-vivo experiments were performed. However, the tonometer signal was also recorded in long-term experiments.

6.3.1 Short-term experiment

The goal of the short-term experiment was to determine the tonometer response to the natural blood pressure pulse measured on the living artery. The in-vivo experiment differs from the in-vitro one not only in terms of the spectrum of the input signal, but also in terms of visco-elastic properties of the vessel. Because of the uniqness of the arterial mechanical properties, without testing the tonometer on the living, visco-elastic artery it is impossible to predict the device's characteristic.

In order to provide the ability to change the applanation level, the hand-held tonometer was used. It offered the opportunity to adjust the level of applanation from 0 to 100%. The target applanation level was initially set to 15% (as a result of modeling and in-vitro experiments), but very soon it became clear that exposed arteries alter their diameter very rapidly with large amplitude of changes. With the hand-held device, the author was able to correct the applanation level in case of unexpected arterial spasm or dilation, keeping the contact between the sensing area of the tonometer and the artery.

Together with the medical team, the author has decided to use a femoral artery. Although it is not a muscular artery and the mechanical properties are slightly different than those of a muscular vessel, the femoral artery offers several adventages for the acute pilot experiment. First, it is easy to access the femoral artery without serious risk to the subject. Second, it is easy to introduce the reference transducer in close proximity to the tonometer placed arround the femoral artery. Third, the size of a 20-pound dog's femoral aretry is close to the human mammary artery.

6.3.1.1. Experiment description

To test the tonometer's performance in-vivo, an acute experiment was conducted. A 20-pound dog was anesthetized and its femoral artery (~3.5 mm OD) exposed.

The cigar-shaped tonometer was implanted short-term around the femoral artery of the anesthetized dog (figure 6.10). A catheter was placed in the lumen of the artery, just distal to the implanted tonometer. The catheter was attached to non-compliant tubing, and a commercial pressure transducer was calibrated to a mercury manometer (Cobe Medical).

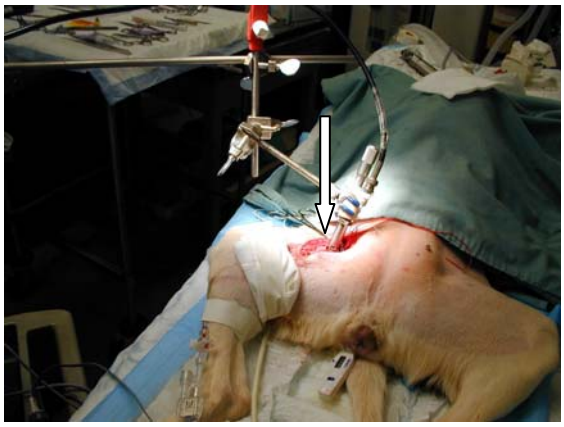

Figure 6.10. **Acute animal experiment**. Animal model – 20-pound dog. An arrow indicates the position of the arterial tonometer.

6.3.1.2 Results

A systematic study was performed to determine the optimal degree of applanation for the pulsatile pressure signal measurements.

The pulse pressure amplitude reached a maximum plateau with increasing amounts of vessel wall applanation. In our studies, a high signal-to-noise ratio could be obtained when the degree of vessel wall applanation exceeded 10%. The pulse pressure amplitude reached a plateau over the range of 10% to 80% applanation. We concluded that the optimal degree of applanation was within the range of 15% to 20% of artery OD. This range provided a high signal-to-noise ratio, maintained a large vessel lumen, and minimized the risk of signal loss due to blood vessel vasoconstriction.

The results were close to those obtained by Drzewiecki, and Kelly, (Drzewiecki 1983, Kelly 1989) for noninvasive tonometers.

The tonometer was able to accurately measure the arterial pressure waveform over the physiological range of blood pressure (from the minimum diastolic 60 mm Hg up to maximum systolic 180 mmHg), heart rate (40 to 120 bpm), and vessel diameter (dilatation ~6 mm OD and constriction ~4 mm OD). Figures 6.11 and 6.12 illustrate an excellent correlation between the pressure waveform measured with the implanted tonometer and the pressure waveform measured with the reference pressure transducer. The correlation coefficient was 0.938 (active mode) and 0.89 (passive mode) and was calculated using the formula:

$$Cov(R,T) = \frac{1}{n}\sum_{i=1}^{n}\left(r_j - \mu_x\right)\left(t_i - \mu_y\right) \quad \textbf{(6.1)}$$

Where R and T are respectively reference and transducer signals. A similar correlation could be demonstrated over a wide range of blood pressure. The passive mode shows a lower correlation with the reference signal, and the reason is electromagnetic noise in frequencies 0-100 Hz that made it difficult to filter it out using standard techniques. Both modes of operation were able to measure the blood pressure signal.

From the medical point of view several observations were made. A strong signal could be obtained after the intravenous infusion of epinephrine (increased contractility and heart rate), neosynephrine (vasoconstriction), nitroglycerine (vasodilation), atropine (increased heart rate), and esmolol (decreased heart rate). The signal was lost when neosynephrine was applied topically to the outside of the arterial wall (within the sensor lumen). The tonometer's transducer was no longer in contact with the vessel wall after profound vasoconstriction.

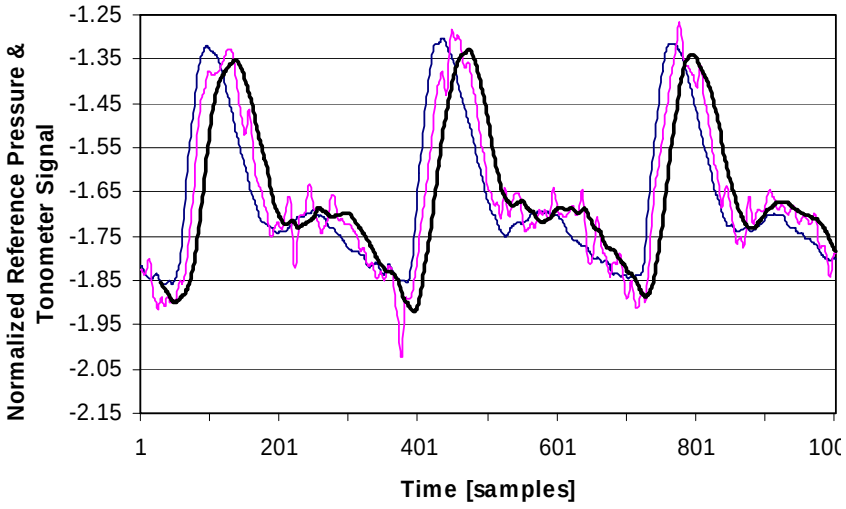

Figure 6.11. Tonometer and reference signal comparison.

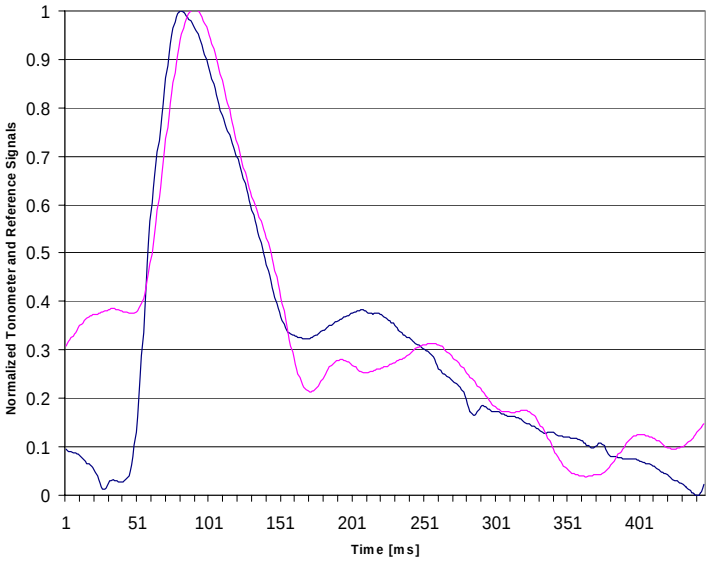

Figure 6.12. Passive mode tonometer output is recorded in the acute animal experiment.

The animal's extremities and body were vigorously manipulated while monitoring the pressure signal. External motion did not produce significant noise in the tonometer output signal. The tonometer housing effectively shielded the transducer pin from forces external to the blood vessel wall. Manual compression of an adjacent artery caused a transient change in the pressure waveform.

Discussion

Acute studies have proof that signal quality was enough to reconstruct a full spectrum of the blood pressure signal. The tonometer active mode signal has good linear correlation with the reference signal: linear correlation (r^2) equal to 0.93 (active mode) and 0.89 (passive mode). The correlation is slightly worse then in-vitro experiments (r^2=0.98). A comparison of the reference signal and tonometer signals is shown in Figures 6.11 and 6.12. Both modes showed to be capable of measuring a spectrum of the

arterial blood signal over the wide range of physiological conditions (various heart rate and vessel smooth muscle tonus).

6.3.2 Pilot long term experiments

It is a well-known and documented fact that the arterial wall tissue remodels under certain mechanical stresses and strains generated by blood flow, blood pressure or external constraints (Kim B, 1999; Kanda K, 1992). The concept of an implantable tonometer assumes that the arterial remodeling that occurs inside the support structure will not be harmful to the subject and will not affect the tonometer's accuracy. Two groups of tests were designed: in-vivo measurements on the living subjects (including tonometer characteristic measurements and ultrasound visualization) and ex-vivo studies (including tissue gross examination and histological studies).

The Null hypothesis regarding remodeling was that the remodeling triggered by the implanted tonometer is statistically insignificant. The author chose media thickness as a testing parameter. The media thickness measured inside the tonometer was compared with the average media thickness measured proximal and distal to the sensor. Thus, the Null hypothesis is formulated as

$$\frac{\mu_p + \mu_d}{2} = \mu \qquad (6.2.)$$

where μ_p is a mean thickness of the intima media measured proximal to the sensor, μ_d is a mean thickness of the intima media measured distal to the sensor, μ is a mean thickness of the intima media measured within the sensor.

Also, the ultrasound visualization was planned to observe the tonometer-arterial wall geometry inside the living subject, as well as any harmful process such as calcification or inflammation.

In terms of tonometer measurement capabilities, the tonometer characterization inside the body was planned.

6.3.2.1 Experiment description

Long-term implantation – *in-vivo* and *ex-vivo* analysis

The implantable tonometer shown in figure 6.13 was implanted around the mini pig's abdominal aorta (~6 mm OD). The identical device was implanted around the 20-kilogram dog's abdominal aorta (~6 mm OD). The tonometer's applanation level was fixed at 16%. Every week, the animals were anesthetized, and an intra arterial reference pressure blood pressure transducer was introduced to the femoral artery. 10 s samples of reference and tonometer signals were recorded. After 3 months, the dog was anesthetized and in-vivo visualization of the abdominal aorta was performed using an intravascular ultrasound catheter, and a video camera connected to the fiber-optic endoscope. The same procedure was performed on the mini pig after 8 months of implantation. Before video recording, the abdominal aorta was flashed with a jet of saline. After the in-vivo visualization, the animals were perfused with formalin to fix arterial tissue, then a segment of the artery with the tonometer was explanted. Ex-vivo histological, microscopic studies were performed.

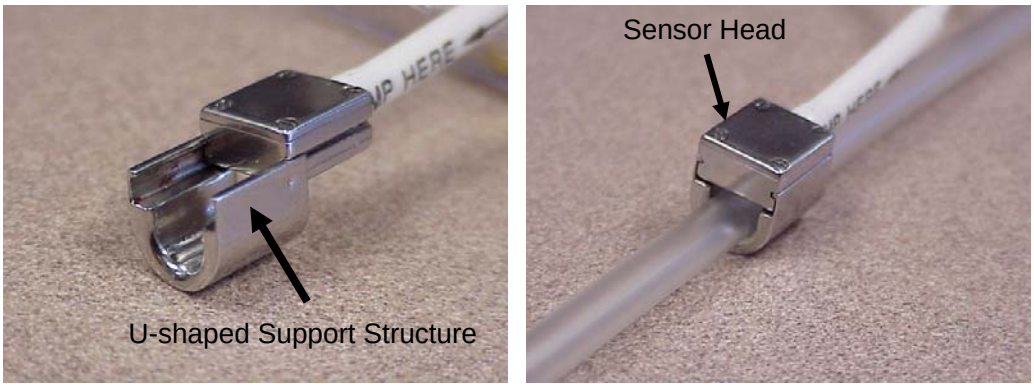

Figure 6.13. The implantable tonometer capable of working in the living organism.

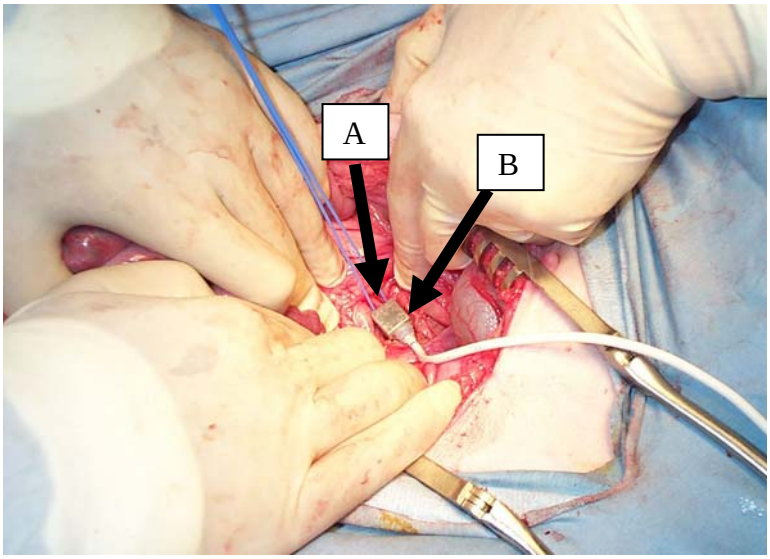

Figure 6.14. **The implantation of the implantable prototype** B around the mini pig abdominal aorta A**.**

6.3.2.2 Pilot results

In-vivo and ex-vivo analysis revealed the basic characteristic of the tonometer working in the living organism along with important tissue reactions to the long-term tonometer implantation.

In-vivo analysis

The in-vivo tonometer characteristic revealed relatively good correlation between the tonometer signal and the reference measurements (.75). The tonometer signal and the reference signal are compared in figure 6.15.

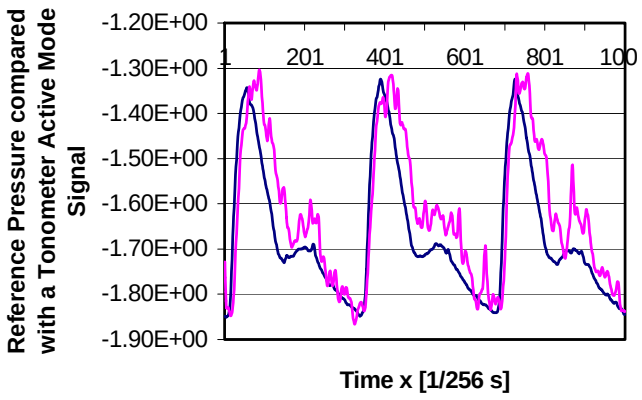

Figure 6.15. **Animal study data**. Reference pressure (blue line) compared with a tonometer signal (magenta line).

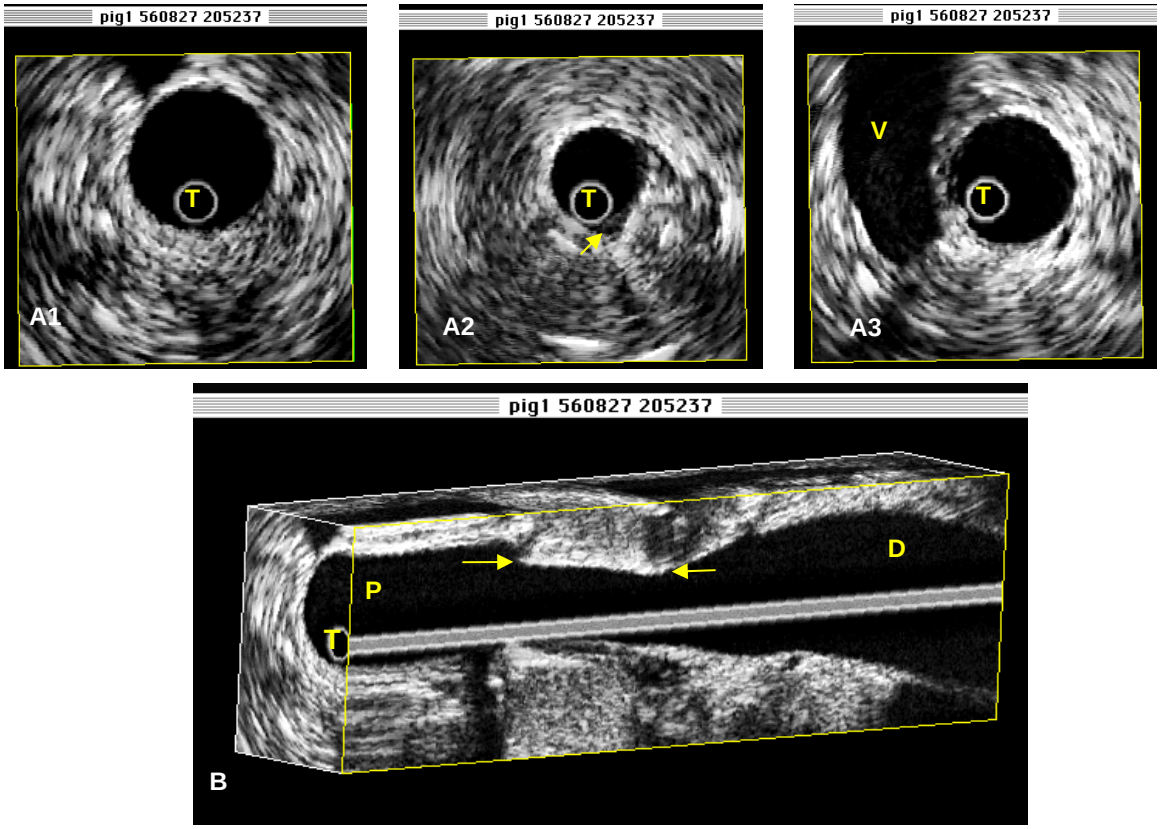

Figure 6.16. **An ultrasound visualization of the implanted tonometer and abdominal aorta** of the mini pig. Cross-section A1 is proximal to sensor, A2 inside the sensor, A3 distal to sensor. With permission of Dr. Ji Bin Liu.

Ultrasound visualization in-vivo revealed that the sensor implanted into the pig was bent by about 6° in respect to vessel axis (see picture 6.16 panel B). The vessel was constricted by the tonometer and underwent post-stenotic dilatation. Proximal (10 mm toward heart) cross-sections of the vessel were circular, with SI (shape index) equal to .95, and healthy. Distal (10 mm beyond sensor) stayed healthy and circular as well (SI=0.98). In corners of the U-shaped structure the ultrasound probe detected some soft structures, which might be inflammation, but further studies didn't confirm that. The applanation area was smooth and flat, which means the sensor met applanation principles in both cases: after 3 and 8 months of implantations. The arterial segment surrounded by the tonometer stayed circular with the exception of that flattened by the sensor rigid body. Differences in its ID (inner diameter) for 10 evenly distributed segment cross-sections were less than 5%.

Ex-vivo analysis

Figure 6.17 shows an explanted tonometer from the mini pig after 8 months, along with a segment of abdominal aorta. The tonometer is encapsulated by a fibrous cap, the cap is connected to the artery, and its length is about 30mm. There are no signs of necrotic tissue or inflammation. Figure 6.17 shows an internal surface of the arterial wall. This picture was taken from the proximal end of the explanted artery segment.

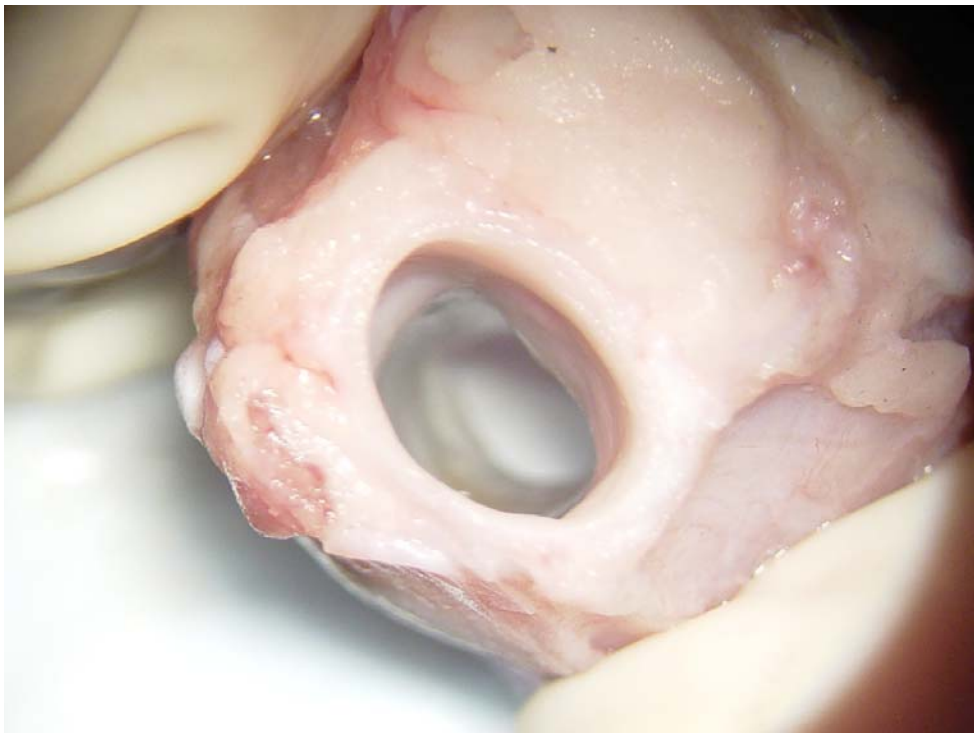

Figure 6.17. **A photograph of the explanted tonometer** after the 8-month experiment. The internal surface of the artery appears healthy and smooth. With permission of Dr. Jeffrey Joseph.

Gross examination of explanted arteries, both in the dog and mini pig, shows no signs of inflammation, necrotic tissue or calcification. Internal wall surfaces – endothelial cells – appeared smooth and clean. The outer surface – tunica adventitia – was also clean and smooth. The artery wall that was inside the tonometer's U-shaped structure was thinned, in both experiments, compared to proximal and distal segments. The actual thinning amount is determined later on histological slides. Thinning can be explained by remodeling due to pressure unloading or unnatural strain. Inside the tonometer, the arterial wall was supported by the metal structure, and circumferential stress was eliminated, thus the artery responded and remodeled by reducing tissue volume. A firm fibrous capsule was formed around the device. The capsule was attached to the vessel wall, securing the tonometer from accidental motion.

The histological analysis revealed some additional facts. The tunica media was measured on histological slides. The slides represent tissue from the locations shown in figures 6.18 and 6.19. In figures 6.20 and 6.21 the average thickness of tunica media is shown in locations A, BF, BU, BC and C. For both animals the media was thicker in region BC and thinner in region BF. Although the opposite reactions took place in the region labeled BU. The dog's media became thinner while the pig's media had thickened.

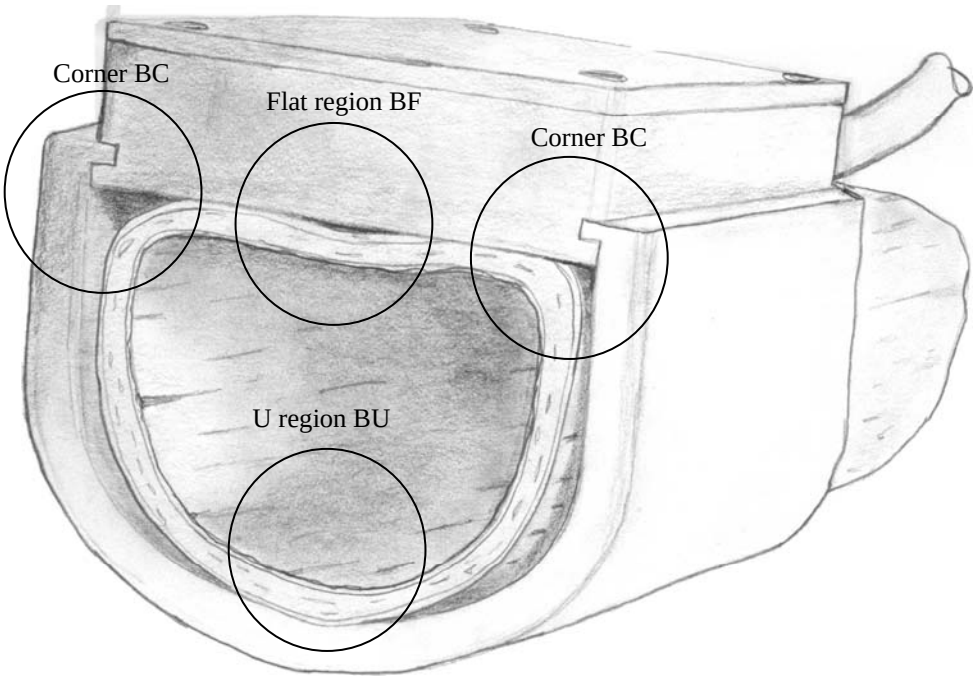

Figure 6.18. Four regions chosen for histological analysis.

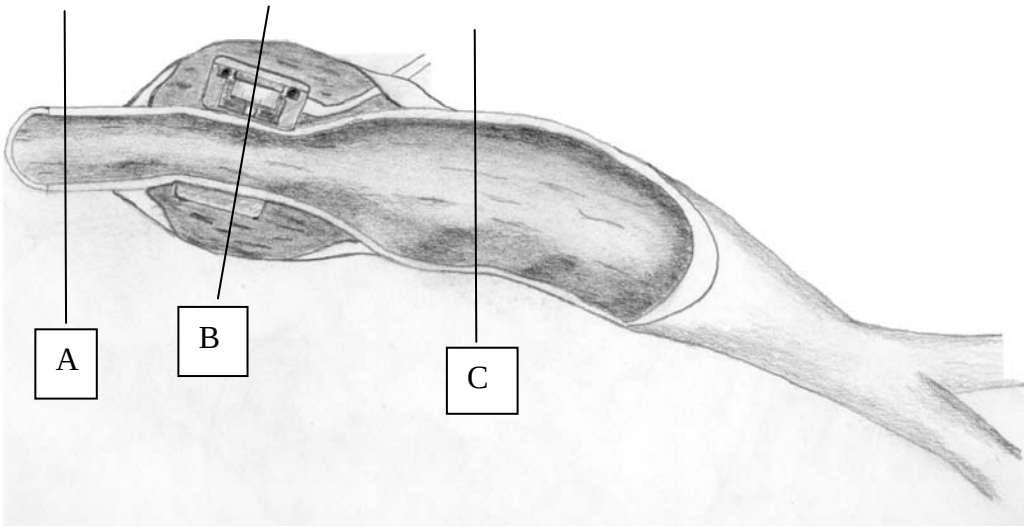

Figure 6.19. **Three positions in which the histological measurements were taken.** Regions A and C are circular, thus in this position no subdivision is needed. In region B, regions BU, BC and BF are specified as shown in figure 6.18.

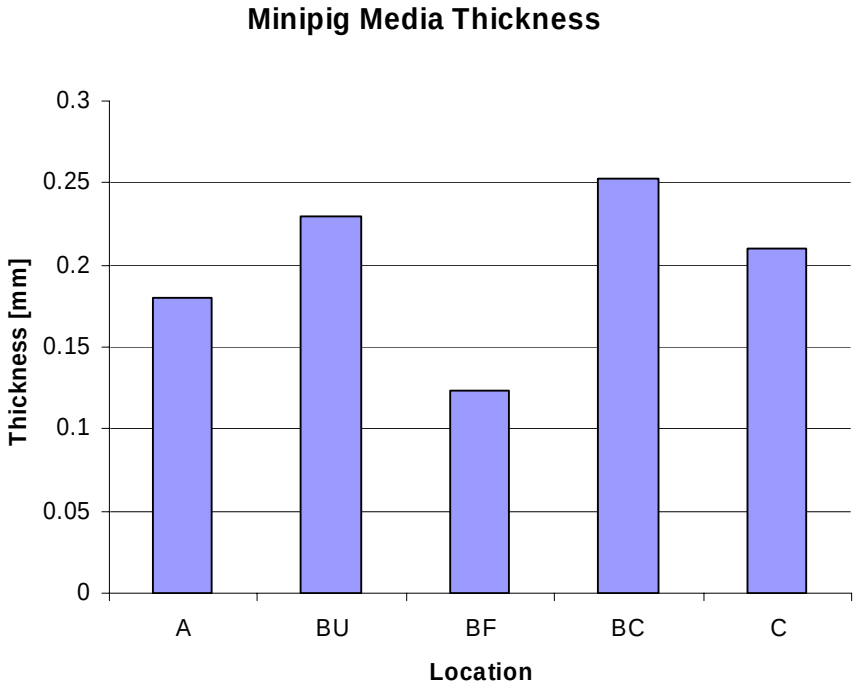

Figure 6.20. **Thickness of the tunica media measured on the abdominal** aorta of the mini pig after 8 months of tonometer implantation. Positions of regions A, BU, BF, BC and C (normal) are shown in figures 6.18 and 6.19.

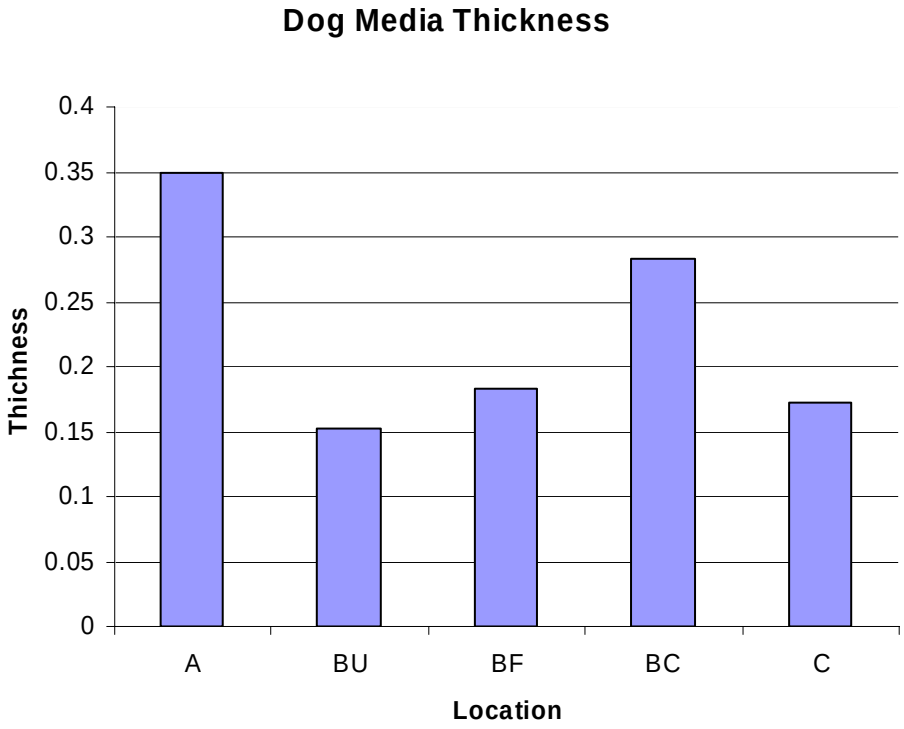

Figure 6.21. **Thickness of the tunica media measured on the abdominal aorta of the 20-kilogram dog** after 3 months of tonometer implantation. Positions of regions A, BU, BF, BC and C (normal) are shown in figure 6.18 and 6.19.

6.3.3 Discussion

Acute Experiments

The tonometer working in the passive mode provided a high quality measurement of dynamic changes of arterial blood pressure. The passive piezoelectric output signals provided accurate information about a spectrum of the arterial blood pressure while the active measured the absolute pressure. The accuracy of the tonometer signal in-vivo was less than that obtained in-vitro. The difference in SNR was from 11% to 15%. This decrease in SNR can be explained by motion artifacts present in the in-vivo environment. The subject was connected to the ventilator, which generated a pressure wave in a low

frequency range (~ 0.2 Hz- breathing frequency) but also vibrations in a higher frequency (hundreds of Hz). The electromagnetic noise in an operating room was also higher (27 mV) than in laboratory settings. The linearity dropped from r^2 = .98 to r^2=.93, which is probably due to mechanical properties of the arterial wall mentioned in chapter 4 on mechanical simulation.

The PZT-based tonometer can be used to measure the arterial blood pressure in-vivo. Accuracy, linearity, and sensitivity of the tonometer fall in the range acceptable for the clinical instruments.

Long-term experiments

The first implanted tonometer failed due to moisture, which entered the sensor head during the first day of implantation. Although, the tonometer was left in the animal's body to proceed with biocompatibility studies. Sealing of the sensor head was improved in the prototype that was implanted into the 20kg dog. Long-term signal studies were limited to 27 days. After this period, the sensor head was also damaged by moisture. However, during 27 days, the sensor signal did not change its amplitude and signal to noise ratio (27 days signal is presented in figure 6.15). Linearity of the signal was r^2=0.75. The signal was strongly disturbed by motion artifacts, though still representative in terms of spectrum content to arterial blood pressure signal.

An interesting hypothesis about wall tissue behavior can be formulated based on the modeling performed in chapter 4. As shown in chapter 4, strain inside the tonometer is much different from the natural one. In the regions labeled as BC (corners of the tonometer support structure), strain is much higher than normal (see figure 6.22). In

locations BU and BF it is lower than normal. It corresponds to the long-term results shown in figure 6.23. Regions with elevated strain responded by thickening, and those with lowered strain respond by thinning. Although, the regions BU respond inconsistently. The reason is unknown to the author.

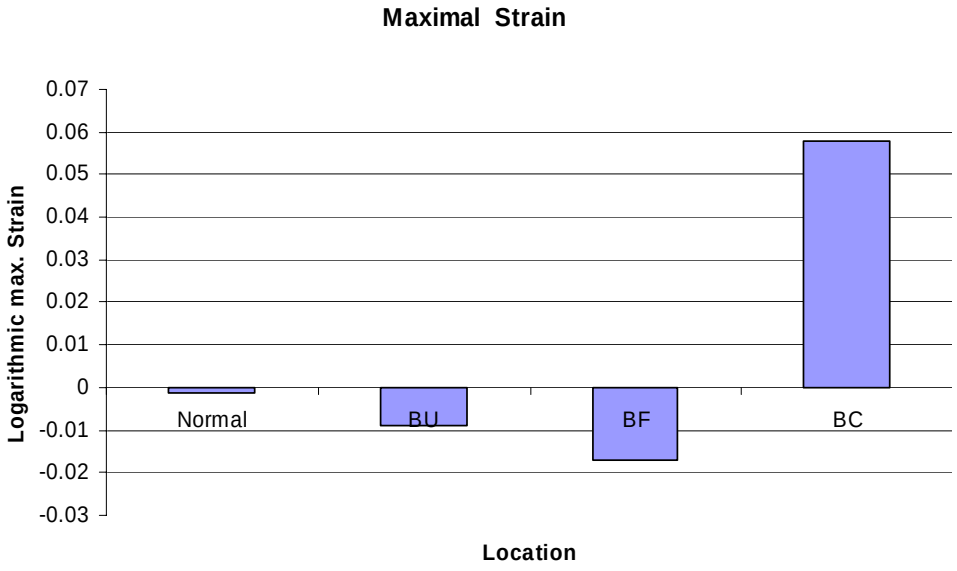

Figure 6.22. **Maximal strain calculated by finite element analysis** in regions BU, BF, BC and in the normal artery.

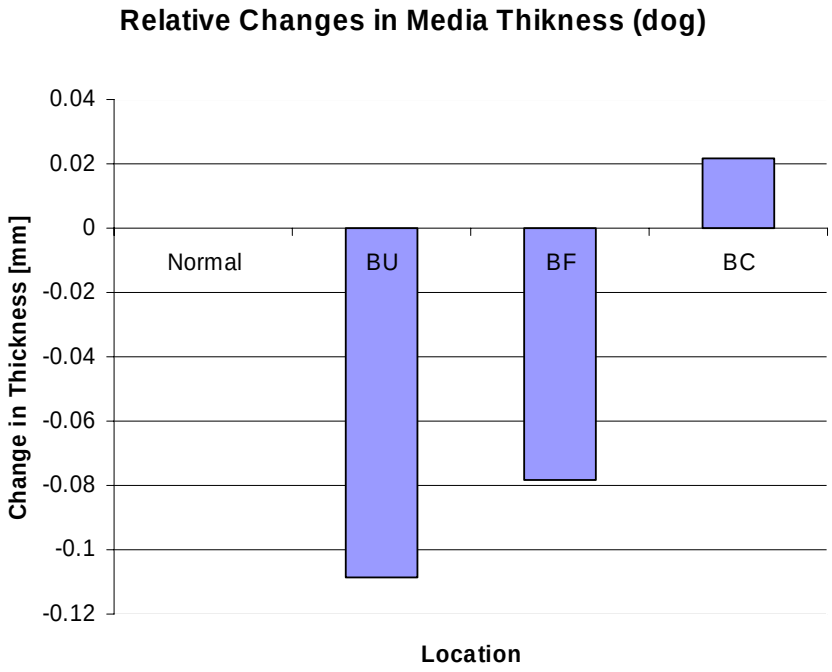

A

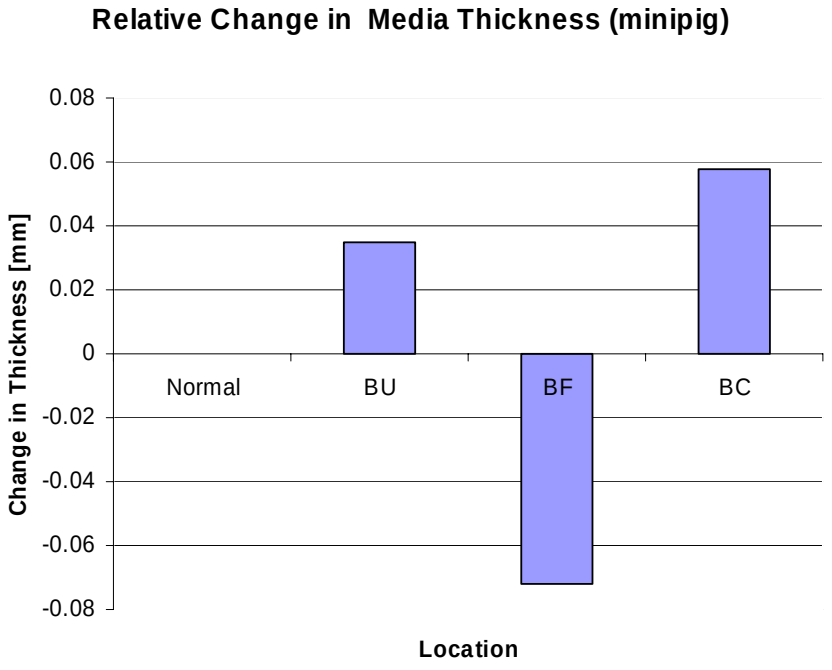

B

Figure 6.23. **Relative changes in media thickness**. A dog; B mini pig.

6.3.4 Recommendation for future work

The implantable tonometer has to be improved in terms of sealing. The tonometer's failure in the long-term experiments was due to moisture. The problem of sealing is a complex one and requires separate studies, most likely based on the existing technology utilized in pacemakers (e.g. compressed high-density epoxy and titanium housing).

The current procedure is very labor extensive and takes 12-14 hours per person per procedure.

The implantation procedure has to be revised to make the procedure less time consuming and less risky for the subjects, which suggests a smaller, local surgical procedure. It will probably require changing the target vessel from the abdominal aorta to a more superficial vessel – femoral or intrathoracic artery.

Future work should focus on the systematic study on a representative sample of living subjects to calculate the accuracy, error and linearity of the tonometer. Since this device is intended to be used in people with cardiovascular problems, there is a need to extend in-vivo studies on diseased animals (hypertension, artero-sclerosis).

7. SUMMARY

This thesis offers an interesting research for the biomedical engineers involved in the implantable blood pressure sensors as well as the implantable sensors in general. It studies several aspects of the blood pressure sensor implanted around the artery, starting from the theoretical models and simulations, through the sensor design and laboratory testing and ending on the in-vivo experiments and analysis.

The modeling is done on two distinctive levels: the dynamic response simulation and the finite element analysis.

The dynamic response simulation studies the lumped parameter models to show how the dynamic input signal, the arterial blood pressure BP(t), is translated to the sensor output. The modeling incorporates the arterial wall visco-elastic properties, the transducer elastic properties and the simplified bio-mechanical structure build of spring-dashpot elements. The simulations are conducted for different arterial wall Young's moduli and different input frequencies of the input signal (the physiological spectrum according to Nichols et al. (1998) is used). The nonlinear response of the system is presented and the linearization for the stiff transducer is proposed. The outcome of this modeling is a requirement for the transducer in terms of mechanical compliance. The maximal compliance acceptable for the implantable tonometer is calculated and is shown that 1% error criteria is met for transducer with Young's modulus two order of magnitude higher than the arterial wall $E_{Tr} \geq 10^8$ dyne/cm^2.

The semi-dynamic studies are performed using the finite element model. The transducer and the vessel segment models are built and assembled together to mimic their mutual position in the implantation site. The vessel elastic properties are set to the range

of physiological values (E_{wall} = 10^5 – 10^10 dyna/cm^2). During the simulation the vessel undergoes deformation due to the transducer geometry (flattening by the transducer sensor head) and subsequently due to the blood pressure pulse that simulates the physiological dynamic blood pressure waveform. The map of the contact pressure between the transducer and the vessel is presented as well as the internal wall stress distribution. Both quantities are a function of the applanation level and blood pressure. The contact pressure gradient on the interface is related to an error that the transducer commits due to the pressure transfer through the elastic barrier of the vessel wall. Assuming the acceptable error on the 1% level, the sensing area for 6 mm OD vessel was determined (2 mm away from sensor edges, in longitudinal direction and not further than 0.3 mm from the transducer axis in direction perpendicular to the vessel axis).

At the same time, the internal wall stress distribution indicates areas where the remodeling of the arterial wall tissue is expected due to the non-natural stress/strain rate. The flattened portion of the artery undergoes large negative strain compared to the natural one (i.e. free artery under physiological pressure). On the other hand, the tissue in corners of the U-shaped structure undergoes large positive strain compared to the free artery. Those observations suggest a large possibility of remodeling in the flattened area and in corners of the support structure.

Both simulations deliver the design criteria such as stiffening of the transducer and the tonometer's geometry requirements. Simulation predicts theoretical accuracy of the transducer. The potential problem areas in terms of tissue remodeling are also identified and discussed.

Based on the simulation results (i.e. the calculated transducer mechanical parameters and tonometer geometry), the series of prototypes is built, and its detailed design is presented and discussed. The mechanical and sensory design aspects are offered with short justifications of applied solutions and fabrication technology.

The fabricated prototypes serve in a series of tests including bench-top, in-vitro and in-vivo procedures. The in-vitro experiments showing the static and dynamic properties of the tonometer are described and the results are presented and discussed. The dynamic properties are tested using close to physiological input signal generated by mock circulation. The in-vitro tests confirm theoretical assumptions based on the numerical simulations.

The in-vivo short- and long-term pilot experiments are described and the results are discussed. The in-vivo experiments test transducer performance in a living organism as well as tissue response-remodeling to the long-term implantation. The input-output data are presented and analyzed along with the intravascular 30 MHz USG high-resolution visualization. Subsequently, the histological analysis of the arterial wall is presented. The results are compared to the modeling data and discussed. The remodeling is confirmed on the pilot sample.

8. CONCLUSIONS

The influence of the implantable tonometer design on the tonometer performance has not ever been studied in a systematic fashion. Thus, there were no indications of how to proceed with the research and design of such a device. The author had to choose the method using his own biomedical engineering intuition and experience.

Fortunately, the implantable tonometer design approach presented in this thesis proved to be efficient and correct. The device designed to the requirements obtained from the theoretical studies worked properly in both in-vitro and in-vivo environments. The data obtained from the prototypes were of clinical quality and revealed the tremendous potential of the implantable tonometer as a clinical tool.

The theoretical modeling showed some limitations in tonometer accuracy and potential danger in long-term tissue reaction. Both predictions were positively confirmed in small series of pilot experiments, although further studies are necessary to obtain statistically significant results. The thesis established the critical problem areas that have to be taken into consideration in any future design.

Beside the fact that the arterial tonometry (non-invasive version of it) is a well-known technique, some new problems came to light as a result of the author's simulation and tests. The applanation theory presented in early work on tonometry (Pressman, Drzewiecki, Nichols, Bronzino) was far insufficient in explaining the time and space dependent features of contact pressure. It also ignored the stress in the volume of the arterial wall, which is of critical value in long-term applications due to the remodeling processes.

The new model presented by the author gives a more detailed way of predicting contact pressure distribution in the applanation area as well as giving the volume stress distribution in the arterial wall tissue.

Besides the theoretical aspect, the presented thesis also has a very strong practical and engineering component. The design challenges discovered by the theoretical modeling were addressed by innovative device design such as a two-mode force transducer, and a highly rigid sensor head. It has resulted in complete prototypes being capable of working in a hostile in-vivo environment and measuring the pressure through the living tissue of the arterial wall.

9. FUTURE WORK

The goal of this thesis is to give future researchers the directions needed to design an implantable blood pressure sensor. Apparently, it is impossible to cover all aspects of the sensor design in one thesis, thus there is a need for future work. The future work will be necessary to pursue some research that has been done in this thesis as well as in other areas untouched by the author. In order to continue the author's efforts, the future work should improve applied modeling techniques, refine the prototype design and test the new design in-vitro and in-vivo.

Modeling

The future modeling should upgrade the models presented by author to the two-layer structure in order to simulate the adventitia behavior. Since the adventitia has different elastic characteristics than the media (because in the adventitia the ratio of collagen to elastin fibers is in favor of collagen ones), on the border between them - interior elastic lamina - the interesting stress behavior is expected. The new model will be a direct extension of the structure presented in chapter 4 by adding an external layer with modified Young's modulus to create a non-homogenous, two-layer vessel.

Also, the influence of the smooth muscle cells on the arterial wall response is very interesting and would be very helpful to add FEM simulations with Young's modulus modified by the SMC contraction. The error introduced by the SMC can be analyzed by simulating contact pressure as a function of the SMC stress.

The dynamic response model (lumped parameter model presented in chapter 4) also can be modified by adding both an adventitia component and a time-varying SMC component.

This can enhance the understanding of the dynamic behavior of the transducer-arterial wall structure.

In some cases, the stress-strain relationship of the arterial wall is strongly nonlinear (it happens when the collagen recruitment begins, see figure 4.5). It is difficult to determine when the artery-tonometer system works in this nonlinear region and how it affects the tonometer's performance. It would be very useful to simulate the tonometer's operation in this region by making the arterial properties nonlinear. Since most modern FEM software accept nonlinear elastic properties (including those used in this thesis program: Abaqus) the problem appears to be relatively easy to solv, having given FEM simulations in Chapter 4 and Appendixes B and C.

Design

Also, the prototypes require further development. The existing issues with losing contact between the tonometer and the artery during the arterial spasm can be avoided by adding an auto-adjusting mechanism, which can compensate for the arterial OD changes by varying the support structure diameter.

The tonometer prototype size also calls for an improvement. The relatively large dimensions of the PZT transducer have resulted in a bulky design. By using a smaller piezoelectric element one can easily scale down the entire design, making possible implantation on smaller arteries in smaller animals. This will reduce future animal research costs by using less expensive subjects.

The telemetry also seems to be of great importance, giving an opportunity to measure blood pressure around the clock in non-anesthetized animals. It will radically

change the amount of data that are being retrieved from the tonometer and will make possible the motion artifacts studies.

In-vitro experiments

As a natural consequence of the new modeling data and the new design, the need for the new bench-top tests will arrive. The new prototypes, such as an adjustable support structure tonometer, have to be tested in terms of static and dynamic characteristics. Also, some new methods can be utilized such as photo-elastometry (physical stress-strain modeling), which will evaluate and calibrate FEM models.

It would also be very interesting if the two-layer vessel is created to evaluate the two-layer structure behavior in terms of static and dynamic responses.

Ex-vivo and in-vivo experiments.

The interesting approach, from the practical point of view, is to test the tonometer on the living, explanted arteries. This kind of test allows increasing the number of short-term measurements without the high cost of animal experiments. Although, the ex-vivo experiments carry some disadvantages, such as luck of the natural SMC tonus, it could be a very valuable intermediate step between the laboratory and the in-vivo experiments. The appropriate vessel for this kind of experiment seems to be a rabbit aorta, since it resembles the thin wall mammary artery that most likely is the target vessel for the implantable tonometer.

In the in-vivo experiments the long-term stability question has to be answered, which includes the studies of stability in term of the error and the dynamic range of the sensor. The further histology studies are required to give the statistically significant answers in terms of arterial wall tissue remodeling in response to applanation. The

changes in SMC concentration and orientation as well as density of the collagen and elastin fibers in critical areas should be investigated.

Finally, the study on the mammary artery has to be performed. First, on the explanted vessel, and then in the living organism. The new implantation procedure has to be prepared and tested.

A very important set of issues is related to the tonometer behavior in hypertensive subjects. It is not only because the hypertensive subjects provide the different range of signal amplitudes but because their arteries most likely will respond differently to the long-term applanation. It is expected that the arteries of the hypertensive subject will remodel in a different fashion than those of the healthy subject.

In the author's opinion, the future work should concentrate on those issues that lead directly to the clinical application. It is the author's belief that an implantable arterial blood pressure sensor opens new venues in cardiology and medical devices in terms of early diagnostic for the former and close loop control for the latter.

10. LIST OF REFERENCES

1. Ahlgren AR, Åstrand H, et al**,** Dynamic behavior of the common femoral artery: age and gender of minor importance, Ultrasound in Medicine & Biology ,Volume 27, Issue 2 , February 2001, pp 181-188

2. Armentano R, Alterations with Age in the Viscoelastic Properties of Human Arterial Walls, Circulation Research, Vol XVII March, 1966

3. Armentano R, Pessana F, Graf S et al. Frequency Dependance of Arterial Wall Young Modulus After De-endothelization, Memorias II Congreso Latinoamericano de Ingeneria Biomedica, Habana, 2001

4. Auld B, Acoustic Fields and Waves in Solids, Krieger Pub Co; 2nd edition 1990

5. Bank AJ, Dresing TJ et al, The contribution of smooth muscle to arterial elastic mechanics in normal human subjects in vivo, American Journal of Hypertension , Volume 8, Issue 4, Part 2 , April 1995, page 63A

6. Benes E. Groschl M, Burger W, Schmidt M, Sensor based on piezoelectric resonator, Sensors and Actuators A 48 , 1995, pp 1-21

7. Bergel DH, The static Elastic Properties of the Arterial Wall, J. Physiol, 1961, 156, pp 445-457

8. Bronzino JD, The Biomedical Engineering Handbook, 1995

9. Burton AC, Physiology and Biophysics of the Circulation, Year Book Medical Publishers Inc, Chicago,1968

10. Carew TE, Vaishnav RN, Patel DJ, Compressibility of the Arterial Wall, Circulation Research, Vol XXIII, July 1968

11. Chamiot-Clerc P, Copie X, Renaud J-F, Safar M and Girerd X' Comparative reactivity and mechanical properties of human isolated internal mammary and radial arteries, Cardiovascular Research Volume 37, Issue 3 , March 1998, pp 811-819

12. Chatzandroulis S, et al. Miniature pressure system with a capacitive sensor and a passive telemetry for use in implantable applications, Journall of Michromechanical Systems, Volume 9, Issue 1, 2000 pp 18-23

13. Cheng Koon-Sung et al, Impaired carotid and femoral viscoelastic properties and elevated intima-media thickness in peripheral vascular disease, Atherosclerosis 164 , 2002, pp 113-120

14. Cox RH, Comparison of carotid artery mechanics in the rat, rabbit, and dog, American Journal of Physiology. 234(3):H280-8, 1978 Mar.

15. Daly C et al, Analysing the 3D Structure of blood Vessel using Confocal Microscopy, The American Microscopy and Analysis, November 2002

16. Darling RC, Raines JK, Brener BJ, Austen WG, Quantitative segmental pulse volume recorder: A clinical tool, Surgery Vol 72, No. 6 , 1972, pp 873-887

17. de Jong, Jan R. MD; Ros, Henk H. PhD; de Lange, Jaap J. PhD, MD Separation of the Oscillometric Calibration from the Arterial Tonometer Signal. Anesthesiology. 82(5):1301, May 1995.

18. De Llinás ES, and Distéfano N**,** Optimal modeling of an arterial system, Mathematical Biosciences Volume 60, Issue 2 , August 1982, pp 177-195

19. Dobrin BD, Mechanical Properties of Arteries, Physilogical Reviews, Vol 58, No2, April 1978

20. Dobrin PB, Canfield TR, Elastase, collagenase, and the biaxial elastic properties of dog carotid artery, Heart Circ. Physiol 16 , 1984, pp H124-H131

21. Doeblin EO, Measurement Systems Application and Design, McGrawHill, Boston, 1990

22. Druzhinin A, Lavitska E, Maryamova I, Medical pressure sensors on the basis of silicon microcrystals and SOI layers, Sensors and Actuators B 58 1999, pp 415-419

23. Drzeweicki GM. Arterial Tonometry. M.S. Thesis. University of Pennsylvania. Philadelphia, PA, 1979

24. Drzewiecki GM, Analysis and Assessment of Cardiovascular Function, 1998

25. Drzewiecki GM, Melbin J, Noordergraaf A. Arterial Tonometry: Review and Analysis. *J Biomech.* 16(2) 1983, pp 141-152,

26. Fraden J, Handbook of Modern Sensors: Physics, Designs, and Applications, AIP Press; 2nd edition, 1997

27. Fung YC Biomechanics Circulation, Springer Verlag, New York, Second Edition, 1996

28. Fung YC, Biomechanics, Mechanical properties of Living Tissue, Springer Verlag, New York, 1984

29. Fung YC, Liu SQ, Determination of the mechanical properties of the different layers of blood vessel in vivo, Proc Natl Acad Sci U S A; 92 (6): March 14, 1995, pp 2169–2173

30. Gagnepain J J, Piezoelectricity, M. E. Sharpe, 1982

31. Gardner J,. An artificial neural emulator for an odour sensor array, Sensors and Actuators B: Chemical Volume 19, Issues 1-3 , April 1994, pp 661-664

32. Gardner RM, Direct Blood Pressure Measurement-Dynamic Response Requirements, Anesthesiology, 54, 1981, pp 227-236

33. Gautschi G. Piezoelectric Sensorics, Springer, Berlin, 2002

34. Gedders LA, The direct and indirect measurements of blood pressure, Chicago 1970, Year Book Medical Publishers, Inc.

35. Geddes LA, Voelz M, Combs C, and Reiner D.. Characterization of the oscillometric method for measuring indirect blood pressure. Ann. Biomed. Eng10, 1983, pp 271-280

36. Gerber E, Precision Frequency Control: Acoustic Resonators and Filters Academic Pr. , 1985

37. Hammond J, Lec RM, A non-contact piezoelectric torque sensor, Proceedings of the 1998 IEEE, 27-29, May 1998, pp 715-723

38. Hansen F et al, Non-invasive measurement of pulsatile vessel diameter change and elastic properties in human arteries: methodological study, Clin Physiol. 1993 Nov;13(6) , pp 631-43.

39. Haruka Okino, Measurement of intraluminal pressure from external pressure with strain transducer, J. APPL. Physiol. 19(3), 1964, pp 546-549,

40. Hashemi A, Katz ML, Carter AP, et al, The Piezoelectric Pulse Sensor Device: A Prospective Evaluation, Ann Vasc Surg 1994; 8, pp 367-371

41. Hayoz D, Tardy J, Rutschmann J et al. Spontaneous diameter oscillations of the radial artery in humans, Am j. Physiol. 264 (Heart Circ. Physiol. 33) , 1993, pp H2080-H2084

42. Hierold C et al. Low power integrated pressure sensor system for medical applications, Sensors and Actuators A: Physical Volume 73, Issue 1-2, 9 March 1999

43. Im J, Lessard CS, A study for the development of a noninvasive continuous blood pressure measuring system by analyzing radial pulse from a wrist IEEE_EMBC and CMBEC, 1995

44. Iversen HK, Madsen P, Matzen S, Secher NH. Arterial diameter during central volume depletion in humans . *Eur J Appl Physiol & Occup Physiol*. 72(1-2), 1995, pp 165-169

45. Joannidès R, Moore N, Bakkali El.H, Schoenmakers-Smits C, de la Guerronière V and Thuillez C: Decrease in arteriolar and medium-size arterial tone during subchronic high water intake in humans; Atherosclerosis Volume 134, Issues 1-2 , October 1997, pp 299-300

46. Kanda K, Matsuda T, Oka T, Two-dimensional orientational response of smooth muscle cells to cyclic stretching, ASAIO Journal, 1992, 38:M382-M385

47. Kelly R, Hayward C, Ganis J, Daley J, Avolio A, O'Rourke M, Noninvasive Registration of the Arterial Pressure Pulse Waveform Using High-Fidelity Applanation Tonometry Journal of Vascular Medicine and Biology Vol.1 No. 3 June 1989

48. Kelly RP, Hayward C, Avolio A, O'Rourke M. Noninvasive Determination of Age-Related Changes in the Human Arterial Pulse. , Circulation 1989;80, pp 1652-1659

49. Kemmotsu O, Ueda M, Otsuka H et al, Blood Pressure Measurement by Arterial Tonometry in Controlled Hypthension, Anesth Analg 1991:73, pp 54-8

50. Kim B, Nikolovski J *et al*, Cyclic mechanical strain regulates the development of engineered smooth muscle tissue, Nature Biotechnology, VOL 17 October 1999, pp 979-983

51. Kino, G.S., Acoustic Waves: devices, imagining, & analog signal processing, 1987, Englewood Cliffs: Prentice-Hall, Inc.

52. Kosinski J, Acceleration sensitivity of surface wave resonators, Ultrasonic and Frequency Control, IEEE Transactions on, Volume: 44, Issue: 6, Nov.1997, pp 1343-1347

53. Lacolley P et al, Mechanical properties and structure of carotid arteries in mice lacking desmin, Cardiovascular Research 51, 2001, pp 178-187

54. Latham RD, Maj M.D, Westerhof N, Regional wave travel and reflections along the human aorta: a study with six simultaneous micromanometric pressure, Circulation 72, No. 6, 1985, pp 1257-1269

55. Learoyd, BM, Taylor MG, Alteration with Age in the Viscoelastic Properties of Human Arterial Walls, Circulation Research, Vol XVIII, March 1966

56. Lec R, Piezoelectric Biosensors Recent Advances and Applications, IEEE International Frequency Control Symposium and PDA Exhibition, 2001

57. Luck R, and. Agba EI; On the design of piezoelectric sensors and actuators, ISA Transactions Volume 37, Issue 1 , 1 March 1998, pp 65-72

58. Mackay RS, Bio-Medical telemetry, Sensing and Transmitting Biological information from Animals to Man, 1968

59. Mackay RS, The application of physical transducers to intracavity pressure measurement, with special reference to tonometry, Med. Electron Biol, Engng, Vol 2, 1964, pp 3-19

60. Marque V, Kieffer P, Atkinson J, Lartaud-Idjouadiene I, Elastic properties and composition of the aortic wall in old sponateously hypertensive rats, Hypertension, Volume 34, Issue 3, September 1999, pp 415-422

61. Martin M, Development of a miniature, implantable fiber-optic pressure senor, ASAIO Journal, Volume 46, Issue 2 March-April 2000, 195

62. Mekkaoui C, Friggi A, Rolland PH, Bodard H, Piquet P, Bartoli JM and Mesana T Simultaneous Measurements of Arterial Diameter and Blood Pressure to Determine the Arterial Compliance, Wall Mechanics and Stresses *In vivo,* European Journal of Vascular and Endovascular Surgery Volume 21, Issue 3 , March 2001, pp 208-213

63. Natarajan S and Nietert PJ; National trends in screening, prevalence, and treatment of cardiovascular risk factors; Preventive Medicine, Volume 36, Issue 4, April 2003, pp 389-397

64. Nichols WW, O'Rourke MF, Mc'Donald's Blood Flow in Arteries, Theoretical, experimental and clinical principles, fourth edition, 1998

65. O'Rourke MF, Accurate measurement of arterial pressure, Journal of Human Hypertension (2003) 17, pp 445-447

66. O'Rourke MF, Gallgher DE, Pulse Wave Analysis, Journal of Hypertension 1996, 14 (suppl 5), pp S147-S157

67. Osol G, Mechanotransduction by vascular smooth muscles, Journal of Vascular Research, Volume 32 Issue 5, September 1995, pp 275-292

68. Ozkaya N, Nordin M, Fundamentals of Biomechanics, Van Norstrand Reinhold, New York, 1991

69. Posey JA, Geddes LA, Williams H, and Moore AG. The meaning of the point of maximumoscillations in cuff pressure in the indirect measurement of blood pressure. Part 1. Cardiovasc.Res. Cent. Bull. 1969, 8, pp 15-25

70. Pressman GL, Newgard PM. A transducer for the continuous external measurement of arterial blood pressure. *IEEE Trans Biomed Elect*. 10, 1963, pp 73-81

71. Rachev A, Theoretical study of the effect of stress-dependent remodeling on arterial geometry under hypertensive conditions, Journal of Biomechanics, Volume 30, Issue 8 , August 1997, pp 819-827

72. Raines K, Jaffrin MY, and Rao S, A noninvasive pressure-pulse recorder: development and rationale, Med. Instrum. 7, Vol. 7, No 4. September-October 1973, pp 245-250

73. Ramsey III M. Noninvasive blood pressure determination of mean arterial pressure. Med. Biol.Engng. Comp1979., 17, pp 11-18,

74. Roth O, Digital Signal Analysis Using Digital Filters and FFT Techniques, Bruel and Kjaer, Naerum Denmark1981

75. Sato T, Nishinaga M, Kawamoto A, Ozawa T, Takatsuji H**,** Accuracy of a continuous blood pressure monitor based on arterial tonometry. Hypertension. 1993 Jun;21(6 Pt 1), pp 866-74

76. Shenoy D, von Maltzahn WW, and Buckley JC.. Noninvasive blood pressure measurement on the temporal artery using the auscultatory method. Ann. Biomed. Eng. 1993. 21, pp 351-360,

77. Siebenhofer A, Kemp CR, Sutton AJ, Williams B, The reproducibility of central aortic blood pressure measurements in healthy subjects using applanation tonometry and sphygmocardiography. Journal of Human Hypertension, 1999, Vol 13, November 9, pp 625-629

78. Siegel LC, Brock-Utne JG, Brodsky JB, Comparison of arterial tonometry with radial artery catheter measurements of blood pressure in anesthetized patients. Anesthesiology. 1994 Sep;81(3), pp 578-84

79. Stein PD, Blick EF, The potential usefulness of the arterial tonometry for the measurement of instantaneous changes in arterial blood pressure J Assoc Adv Med Instrum. 6(4), 1972, pp 272-275,

80. Stein PD, Blick EF. Arterial tonometry for the atraumatic measurement of arterial blood pressure. *J Appl Physiol.* 30(4), 1971, pp 593-596,

81. Steiner LA, Johnston AJ, Salvador R, Czosnyka M , Menon DK, Validation of a tonometric noninvasive arterial blood pressure monitor in the intensive care settings. Anesthesia. 2003 May; 58(5), pp 448-54

82. Taylor MG, Hemodynamics, Ann Rev. Physiol. 35, 1973pp 87-116

83. Togawa T et al, Biomedical Transducers and Instruments, CRC Press1999

84. Toh S, Tay Ch, Rahman M, Al GA As semiconductor sensor for contact pressure measurement, Sensors and Actuators 79, 2000, pp 31-35

85. Toyoshima T, Kuwajima I, Suzuki Y, Aono T, Ozawa T, Circadian Variation in blood pressure in elderly hypertensive patients, Nippon Ronen Igakki Zasshi, Volume 33, Issue 8, 1996

86. Vikram K. Yeragani, R. K. A. Radhakrishna, K. R. Ramakrishnan and S. H. Srinivasan, Measures of LLE of heart rate in different frequency bands: a possible measure of relative vagal and sympathetic activity**,** Nonlinear Analysis: Real, , Available online 15 January 2004

87. Webster J, Measurement, Instrumentation and Sensors, Handbook, CRC Press, 1999

88. Weiss B. M., Spahn D. R., Rahmig H., Rohling R. and Pasch T., Radial artery tonometry: moderately accurate but unpredictable technique of continuous non-invasive arterial pressure measurement, British Journal of Anaesthesia, Vol 76, Issue 3, pp 405-411

89. Westerhof N, Noordergraaf, Arterial viscoelasticity: generalized model. Effect on input impedance and wave travel in the systemic tree, Journal of Biomechanics, Volume 3, Issue 3, May 1970, pp 357-379

90. White WB, Berson AS, Robbins C, et al. National standard for measurement of resting and ambulatory blood pressures with automated sphygmomanometers. Hypertension 1993;21, pp 504-9

91. Wong M, Edelstein J, Wollman J et al, Ultrasonic-Pathological Comparison of the Human Arterial Wall, Verification of Intima-Media Thickness, Arteriosclerosis and Thrombosis 1993: 13, pp 482-486

92. Yamakoshi KI, Shimazu H, Togawa, T, Indirect Measurement of Instantaneous Arterial Blood Pressure in the Human Finger by the Vascular Unloading Technique, IEEE Transactions on Biomedical Engineering, Vol BME-27, No.3 March 1980

93. Zhao S. Z., Ariff B, Long Q, Hughes AD,' Thom S.A, Stanton A V, and Xu X Y; Inter-individual variations in wall shear stress and mechanical stress distributions at the carotid artery bifurcation of healthy humans, Journal of Biomechanics, Volume 35, Issue 10 , October 2002, pp 1367-1377

94. Zhao S. Z., Xu X. Y., Collins M. W., Stanton A. V., Thom S. A. and Hughes A. D.' Numerical analysis of blood-wall interactions in arterial structures, Journal of Biomechanics, Volume 31, Supplement 1 , July 1998, p 18

95. Zhao SZ, Xu XY, Hughes AD; Thom SA, Santon AV et al. Blood flow and vessel mechanics in a physiological realistic model of a human carotid arterial bifurcation, Journal of Biomechnics Volume 33, Issue 8, August 2000, pp 975-984

96. Zorn EA, Wilson MB et al, Validation of an arterial tonometry monitoring using Association for the Advancement of Medical Instrumentation standards, Blood Pres Monit. 1997 Aug: 2(4), pp 185-188

Appendix A Tonometer prototypes design

The tonometer prototype underwent three stages of development:
Bench-top model, hand-held prototype, implantable prototype. All prototypes have utilized the same PZT transducer (shown in Chapter 5).

Bench top prototype

The purpose of the bench top model was to test the feasibility of utilizing two-mode PZT transducer in pressure measurements conducted directly on the elastic tubing.
In addition to PZT transducer placed on the adjustable rail the device consists of positioning system to adjust the level of applanation, the displacement measurement system controlling level of applanation and set of reference transducer to control flow conditions and provide reference data (see figure1)
To provide the mechanical stability and avoid motion artifacts in higher frequency range, such as mechanical vibrations, the system was placed on a massive metal base (figure 2, G). The reference pressure signal was collected using Cobe Medical piezo-resistive pressure transducer. The design is shown in figure 1 while figure 2 shows the actual device with accompanying equipment.

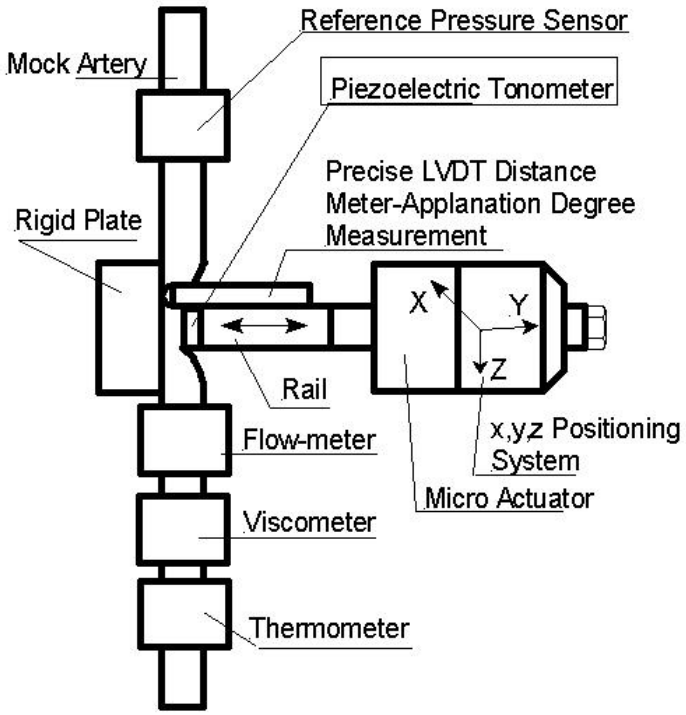

Figure 1. Bench-top model of the arterial tonometer.

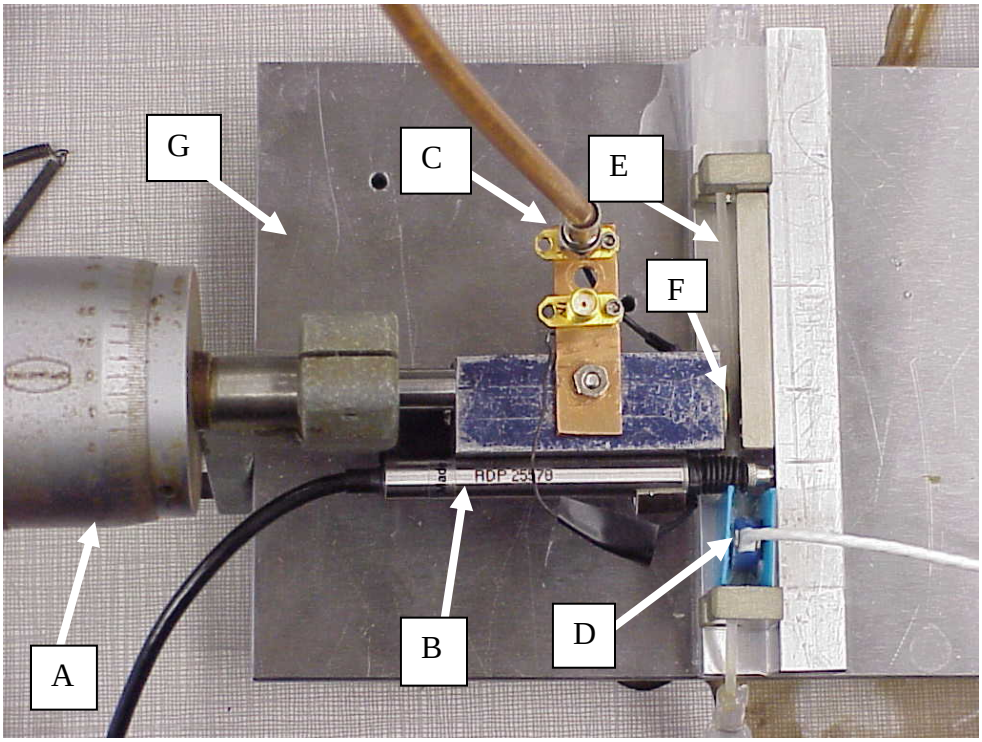

Figure 2. Bench-top model of the arterial tonometer. (A) micrometer screw;(B) LVDT distance meter;(C) output signal connector (D) flow meter (E) mock artery (F) tonometer pin, (G) metal base.

Hand held prototype

The hand-held prototype has been developed to provide transition from the bench-top environment to in-vivo conditions. The device has been designed to be operational under lab and short term in in-vivo conditions. The devices tip was hermetically sealed using aluminum foil and epoxy adhesive.
Under limited surgery conditions (exposed femoral artery) the cigar shape design allows to reach the artery and attach the tonometer transducer to it using hook like mechanism controlled by micrometer (see figure 3). The device works in two modes of operation and the level of applanation is adjustable by the micrometer screw which stays outside the subject's body.

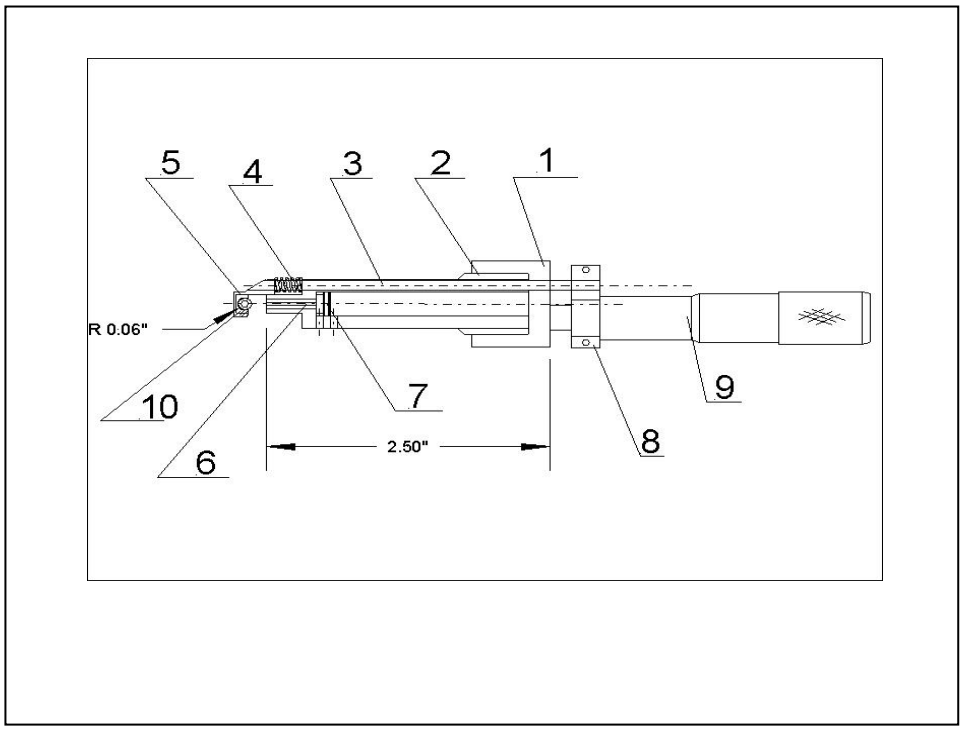

Figure 3. Assembly view of the arterial tonometer for short-term testing.1) rear cup 2) main body 3) rod with a hook like support 4)spring 5) U-shape inserts 6) pin 7)piezoelectric transducer 9) micrometer adjusting the applanation level 10) vessel

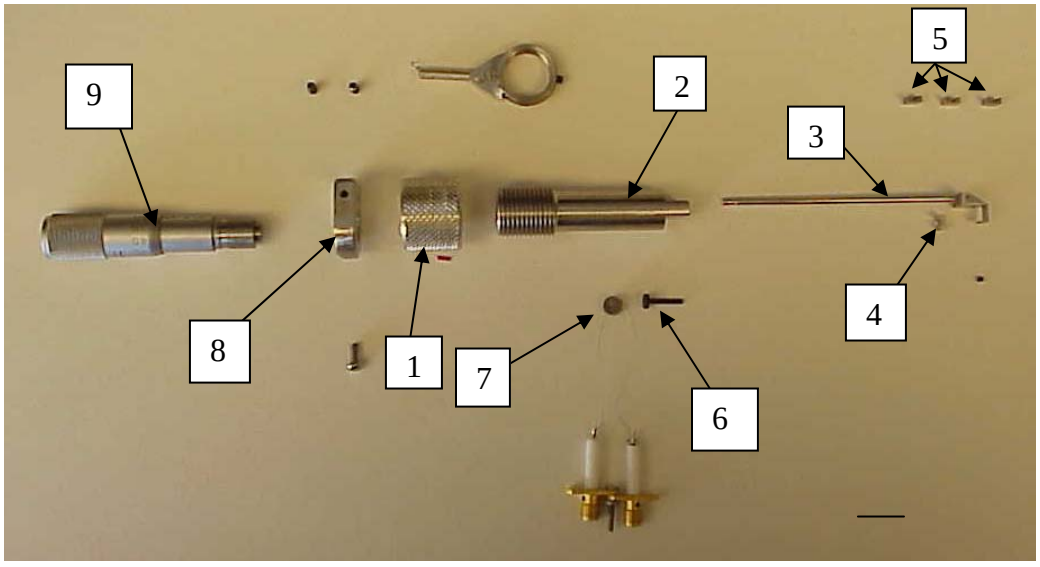

Figure 4. Disassembled arterial tonometer for short-term testing.1) rear cup 2) main body 3) rod with a hook like support 4)spring 5) U-shape inserts 6) pin 7)piezoelectric transducer 9) micrometer adjusting the applanation level

Implantable prototype

The implantable prototype has been developed to test the concept of implantable tonometer in long term in-vivo experiments. The PZT transducer has been completely sealed inside stainless steel housing. The housing bottom wall has been precisely machined to 25 micrometers thick wall. This wall has been attached via a pin to the PZT transducer. The groove-and-tongue mechanism has been utilize to join the tonometer head with a support U shape structure which was responsible for holding and securing the artery. The detailed view of the tonometer sensor head is depicted in figure 5. The actual disassembled device is shown in figure 6.

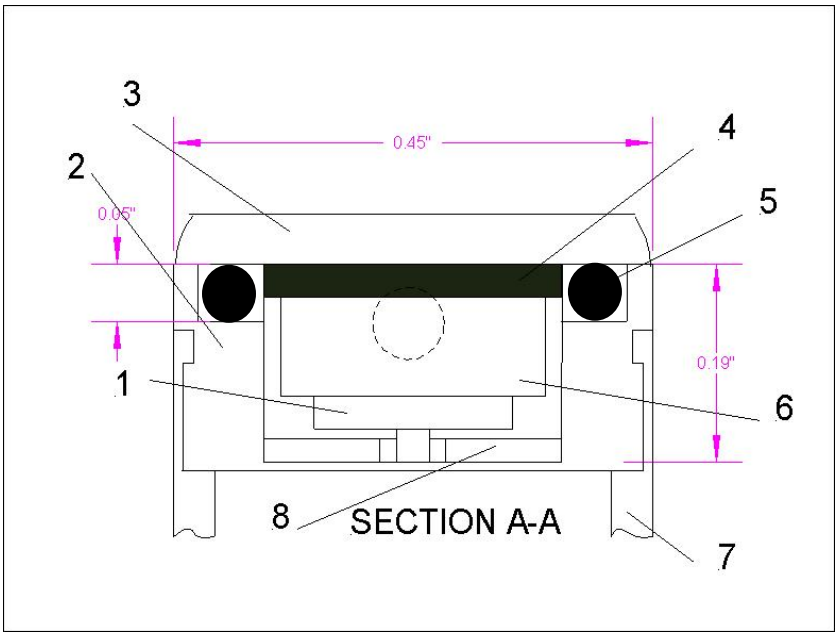

Figure 5. Cross-section of the implantable tonometer. (1) pin (2) stainless steel housing (3) Stainless steel lid (4) Rubber layer generating prestress (5) O-ring(6)PZT transducer (7) U-shape supporting structure

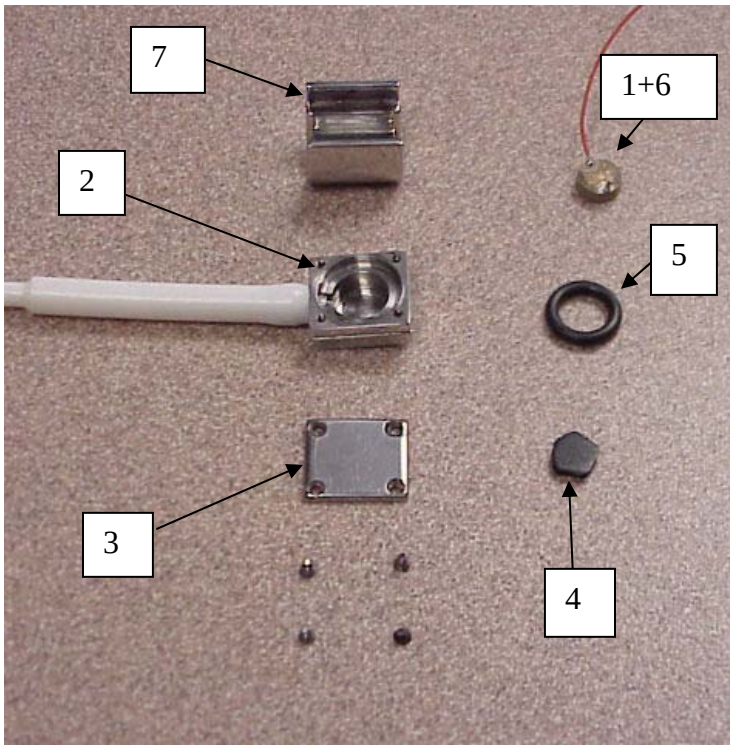

Figure 6 Disassembled implantable tonometer. (1) pin (2) stainless steel housing (3) Stainless steel lid (4) Rubber layer generating prestress (5) O-ring(6)PZT transducer (7) U-shape supporting structure

Appendix B Lumped parameter simulation results

Arterial Wall response for input listed in table 4.2.

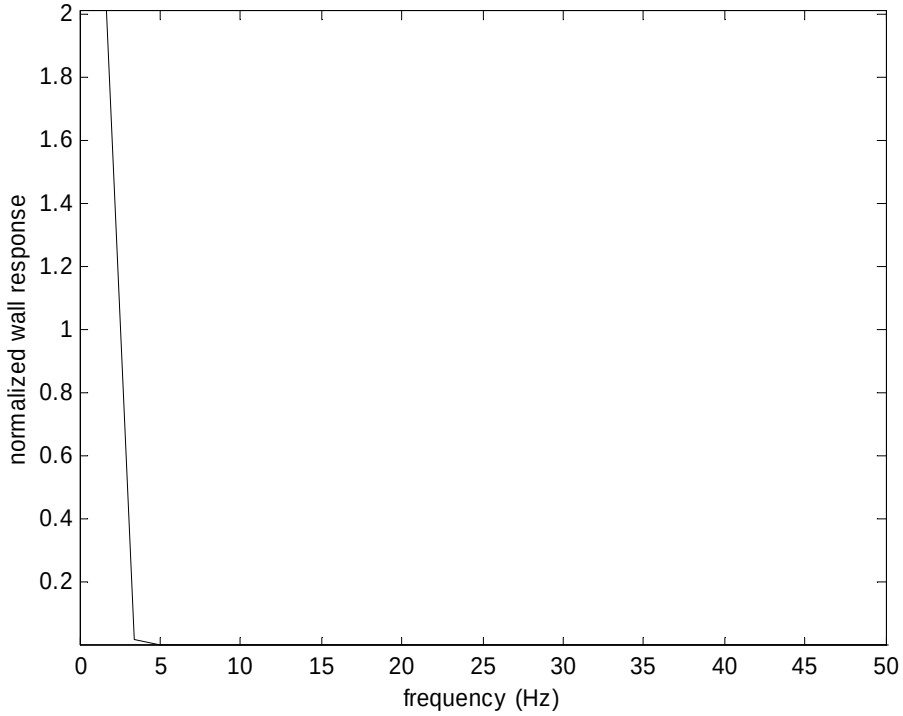

Figure 1. Frequency content of the arterial wall response (Input frequency 1 Hz, Amplitude 9 mmHg)

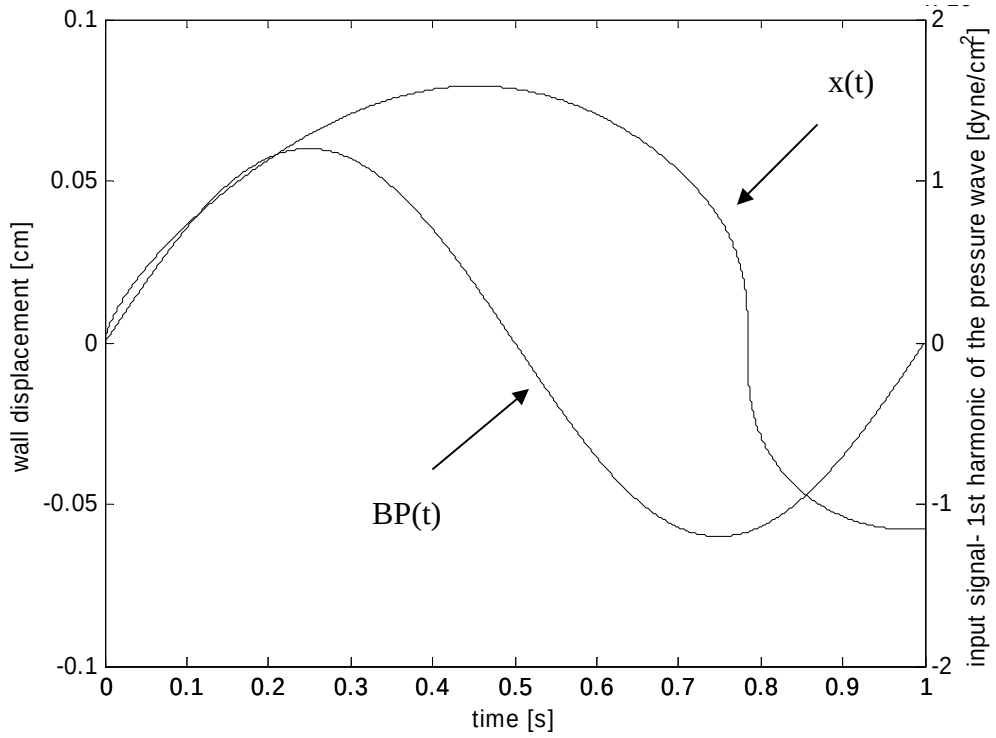

Figure 2. Time response of the arterial wall and the input signal (first harmonic)

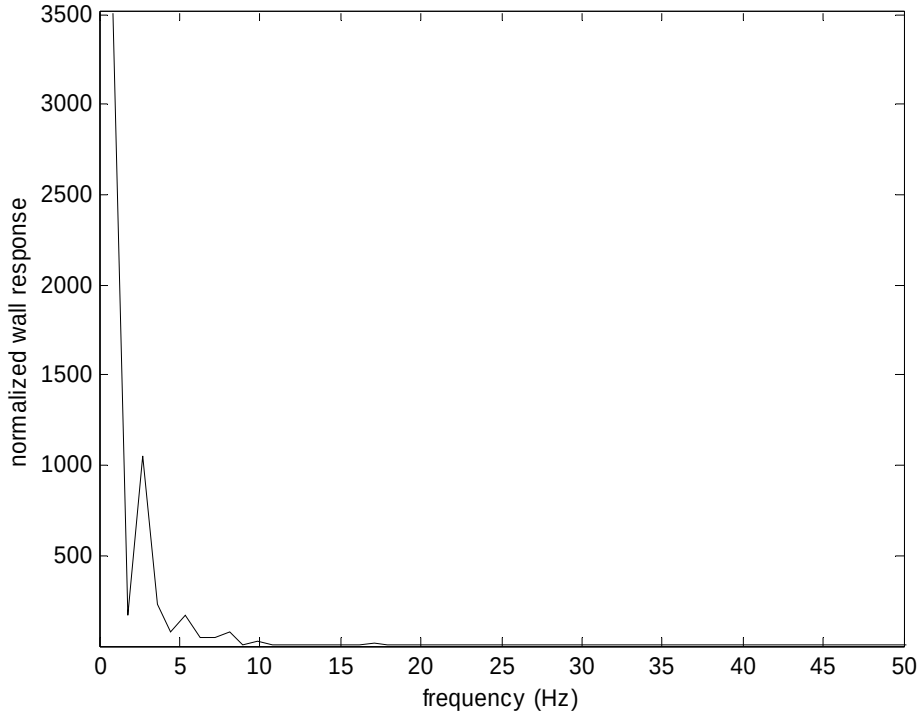

Figure 3. Frequency content of the arterial wall response (Input frequency 2 Hz, Amplitude 6 mmHg)

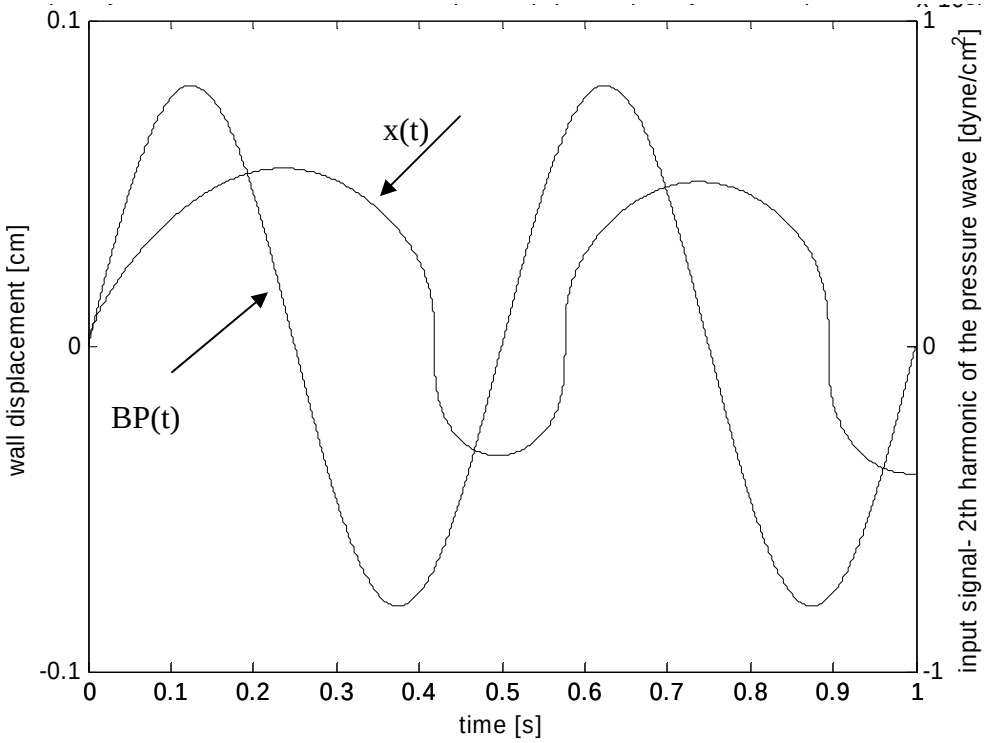

Figure 4. Time response of the arterial wall and the input signal (second harmonic)

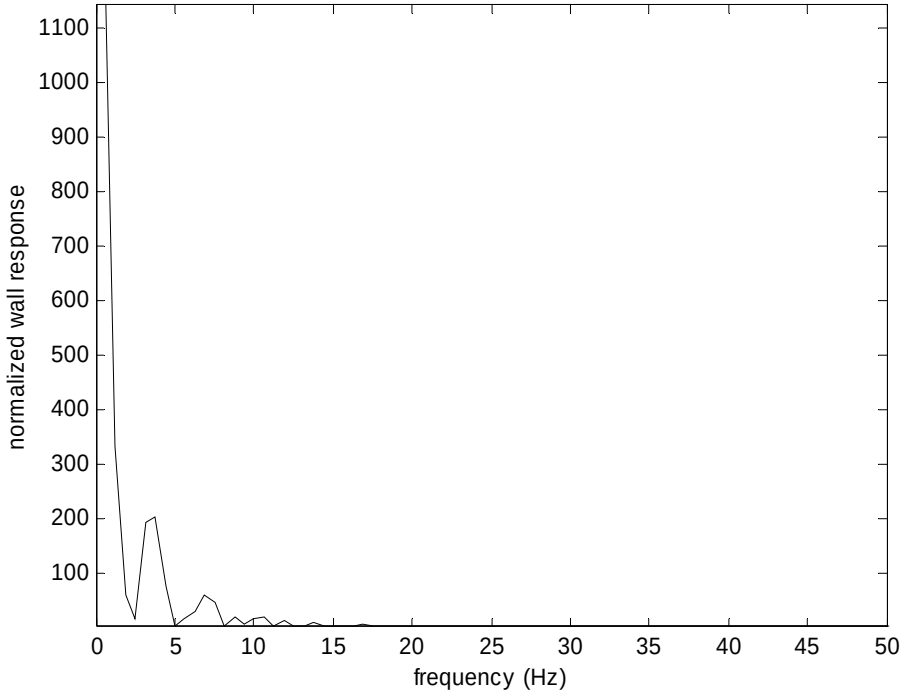

Figure 5. Frequency content of the arterial wall response (Input frequency 3 Hz, Amplitude 5 mmHg)

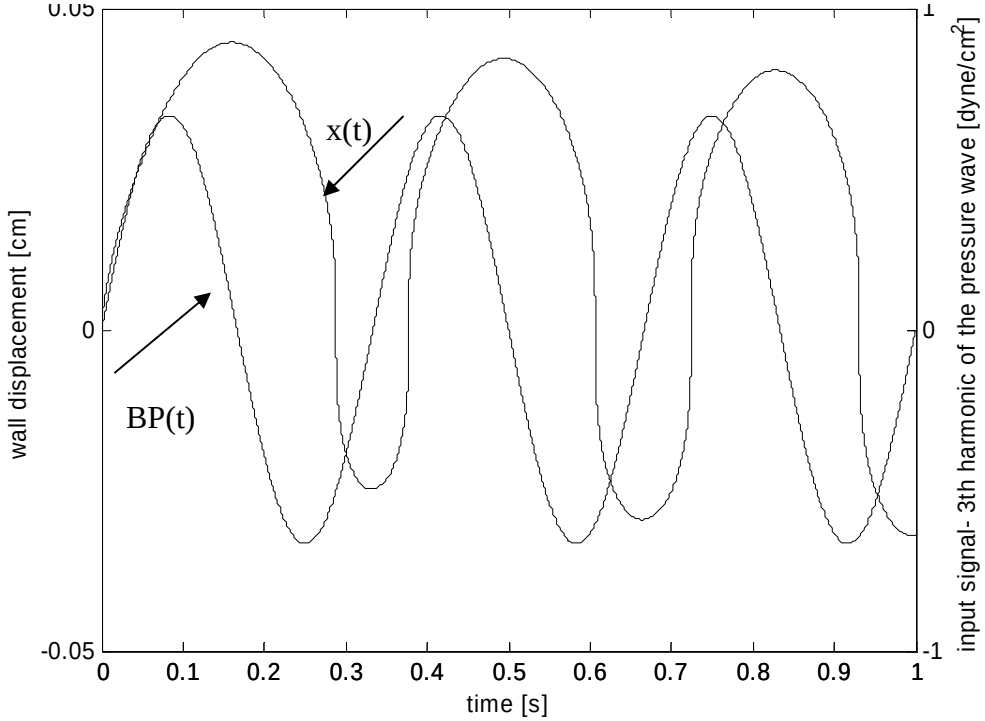

Figure 6. Time response of the arterial wall and the input signal (third harmonic)

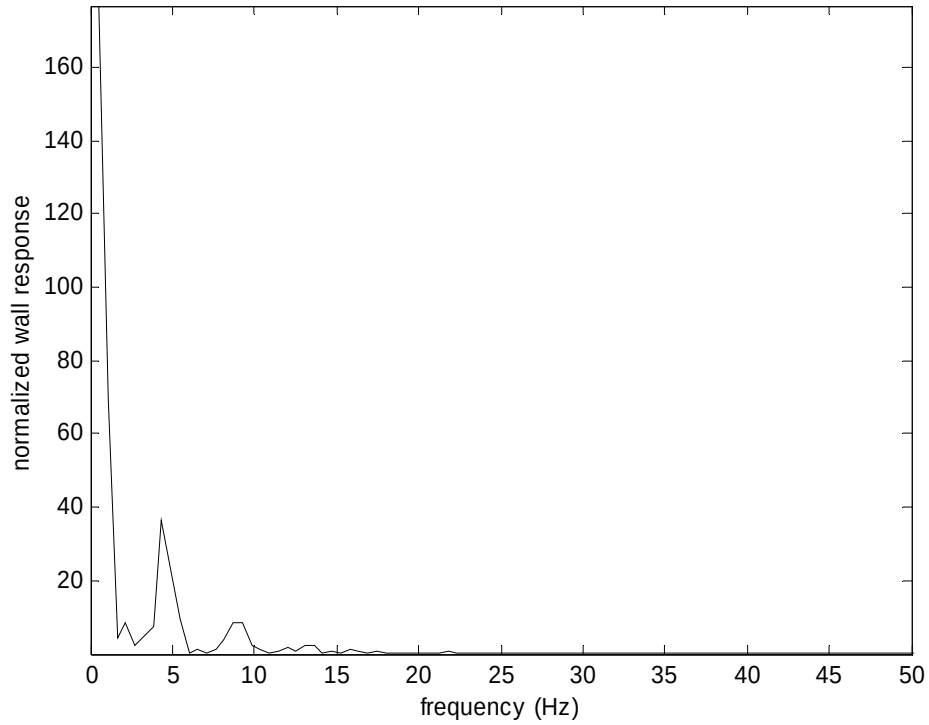

Figure 7. Frequency content of the arterial wall response (Input frequency 4 Hz, Amplitude 5 mmHg)

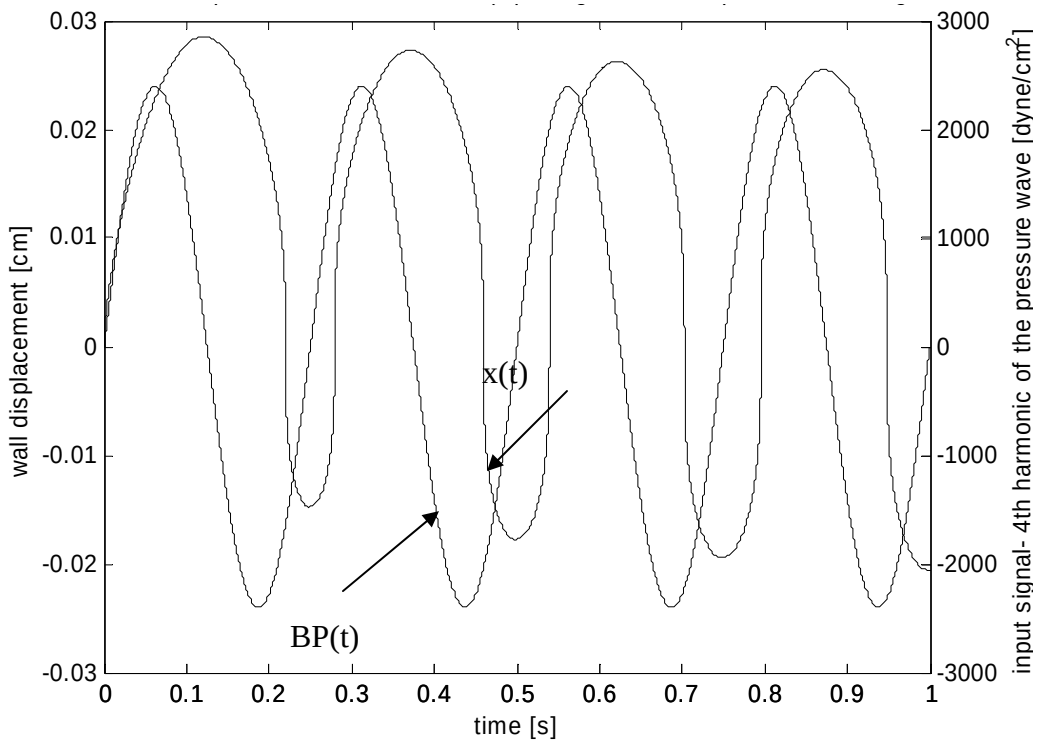

Figure 8. Time response of the arterial wall and the input signal (fourth harmonic)

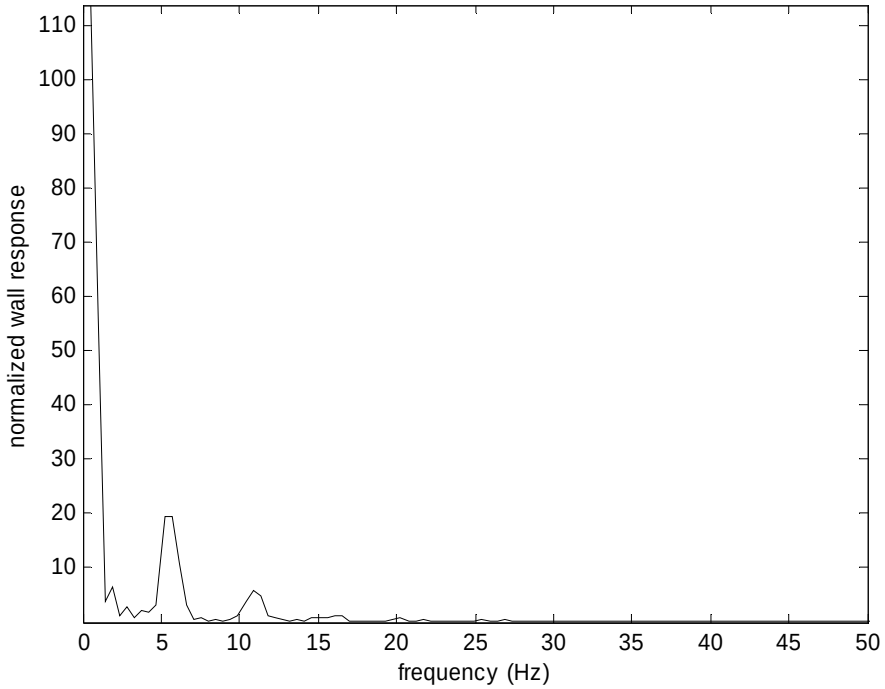

Figure 9. Frequency content of the arterial wall response (Input frequency 5 Hz, Amplitude 1.8 mmHg)

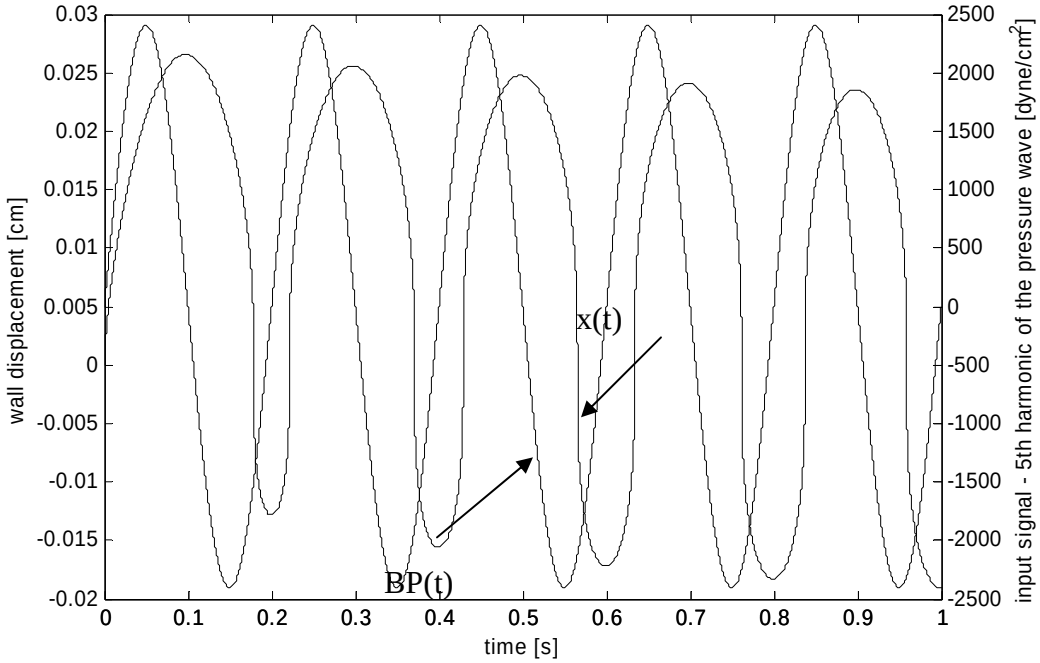

Figure 10. Time response of the arterial wall and the input signal (fifth harmonic)

Artery wall-tonometer system response transducer Young's modulus range: Etr = 10^6 ÷ 10^10 dyne/cm^2 Input signal: 1 Hz (first harmonic from table 4.2)

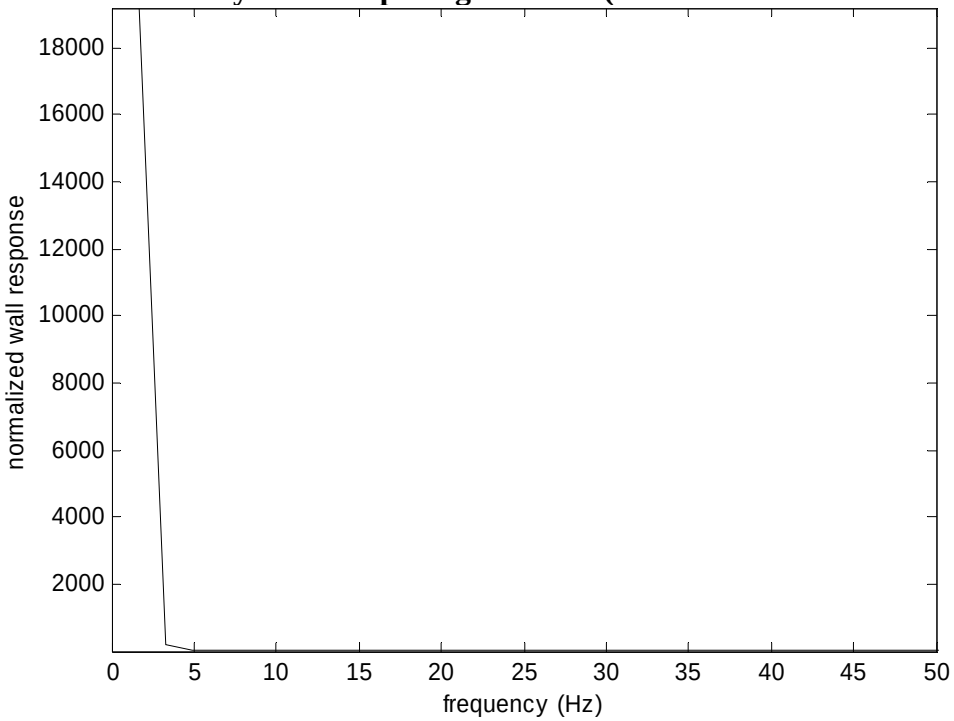

Figure 11. Frequency response of the wall-transducer system for Etr = 10^6

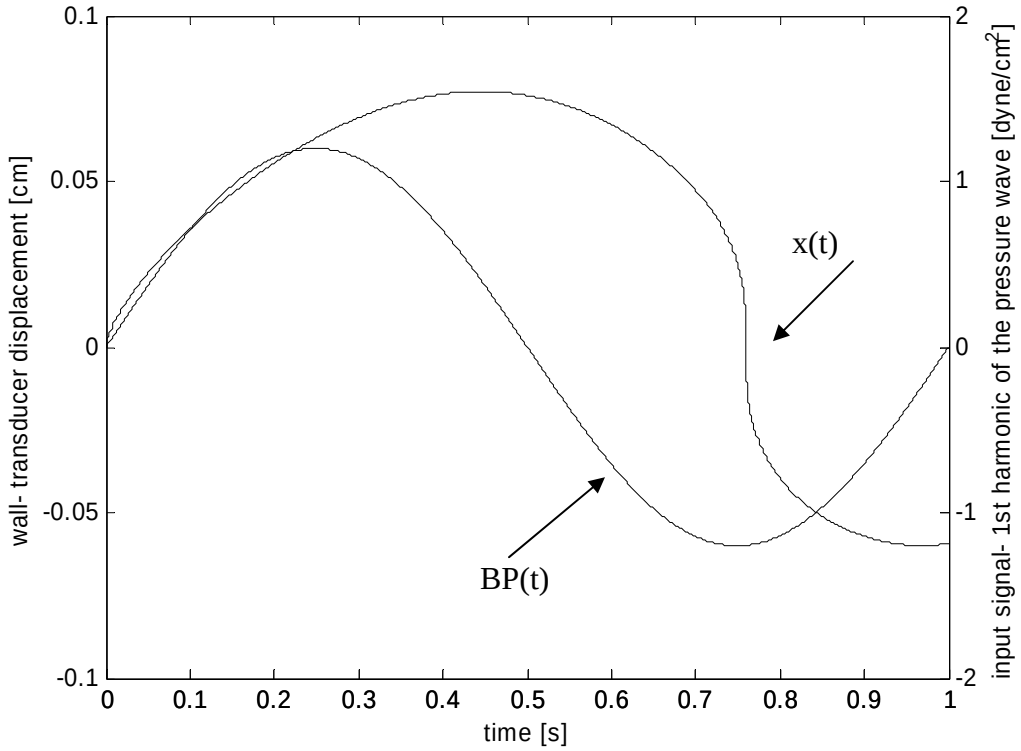

Figure 12. Time response of the wall-transducer system for Etr=10^6

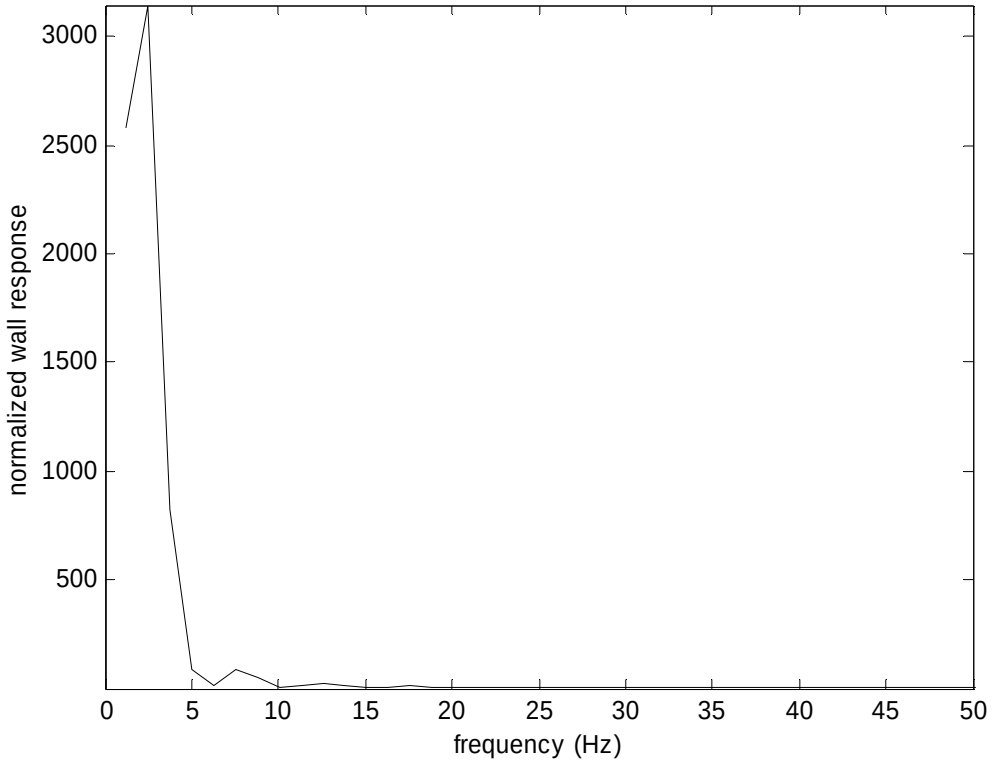

Figure 13. Frequency response of the wall-transducer system for Etr = 10^7

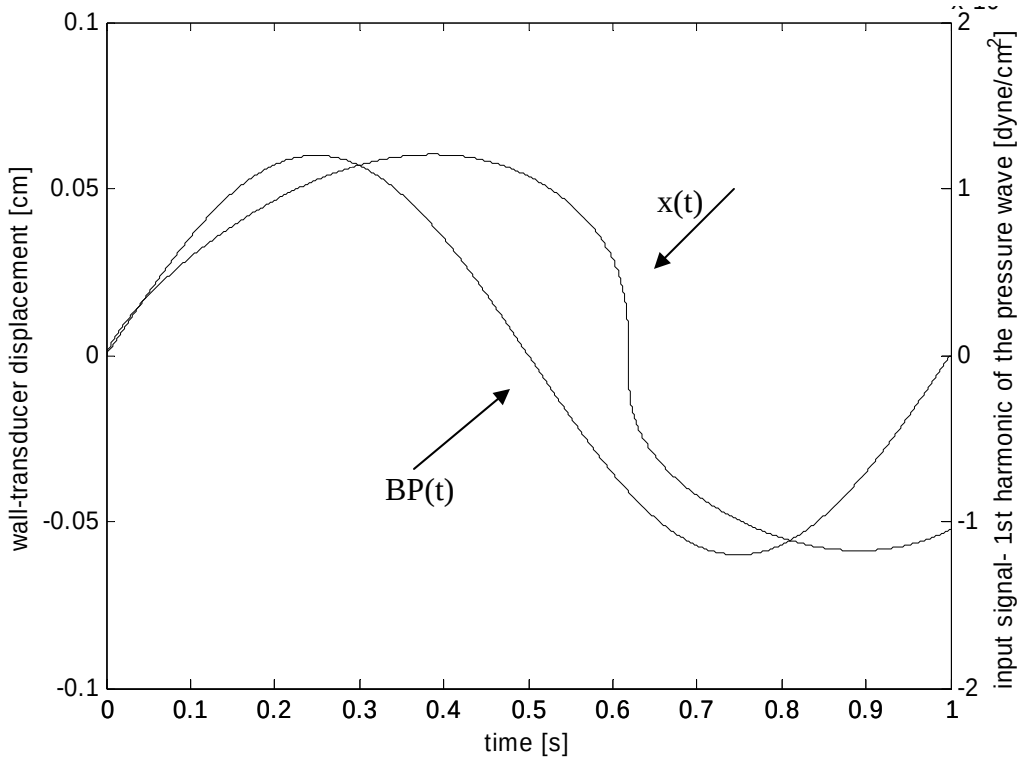

Figure 14. Time response of the wall-transducer system for Etr=10^7

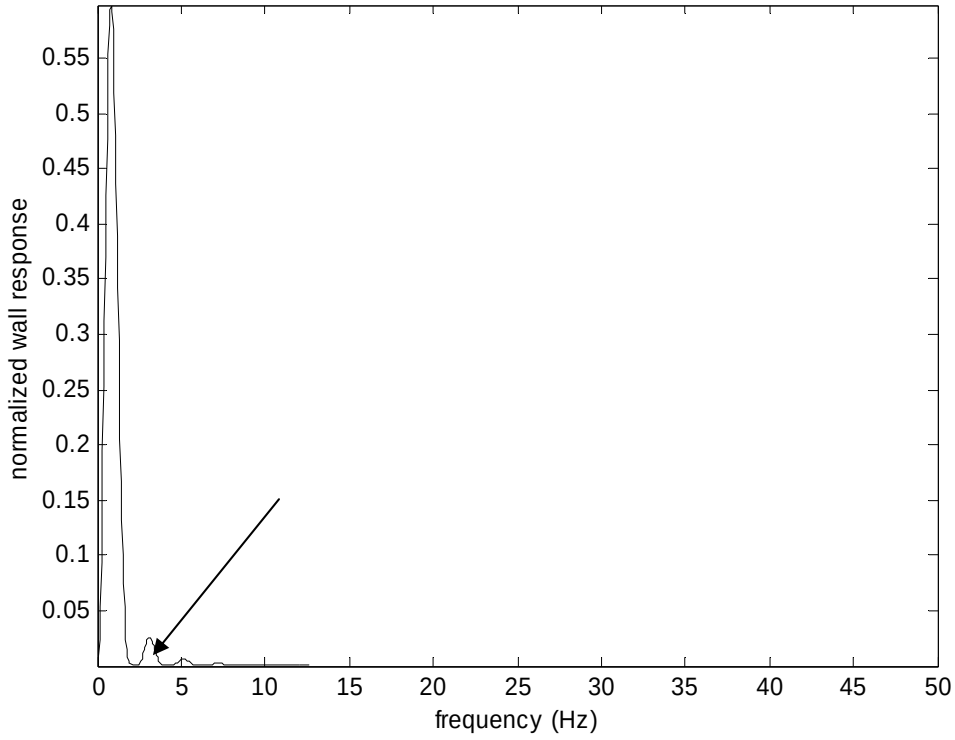

Figure 15. Frequency response of the wall-transducer system for Etr = 10^8

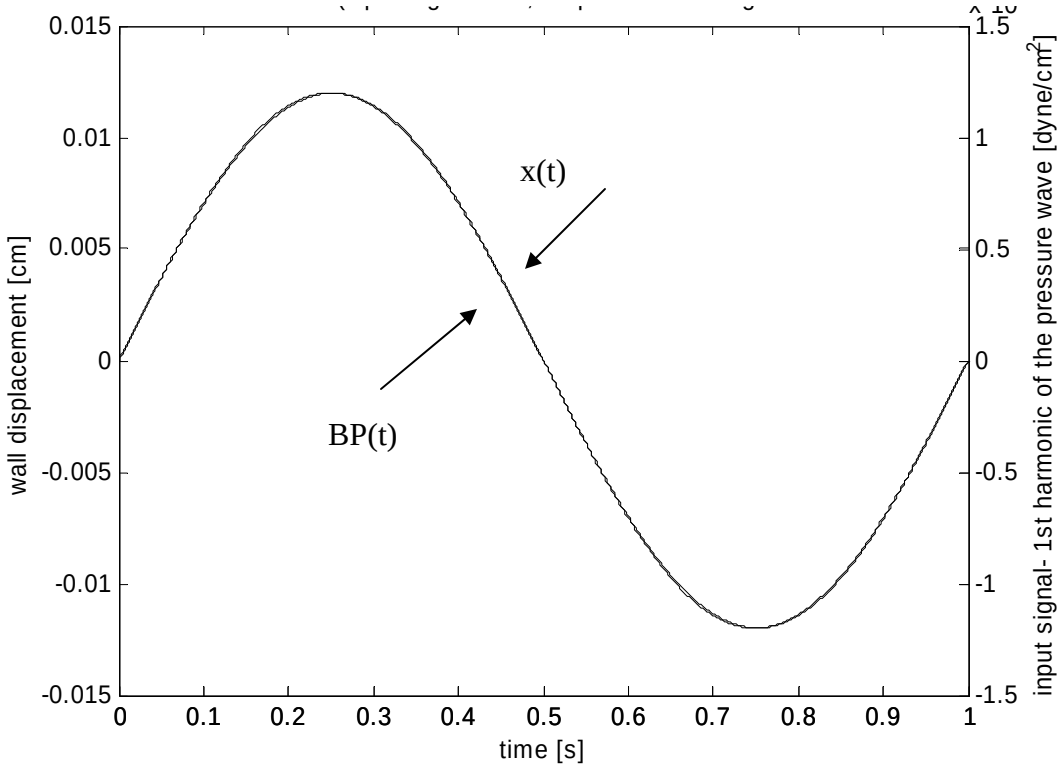

Figure 16. Time response of the wall-transducer system for Etr=10^8

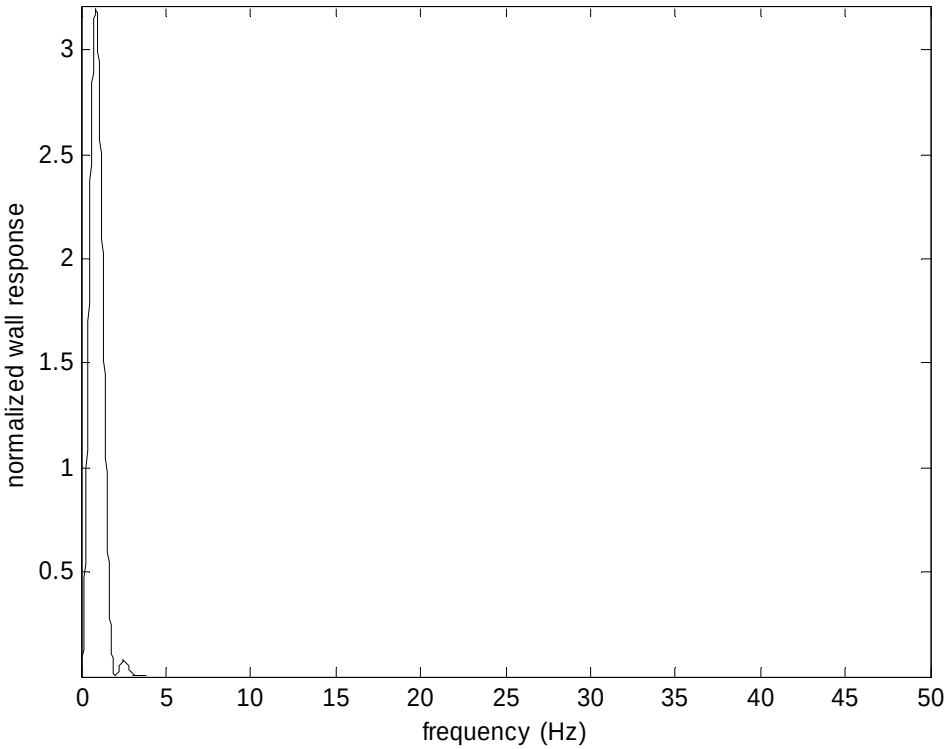

Figure 17. Frequency response of the wall-transducer system for Etr = 10^9

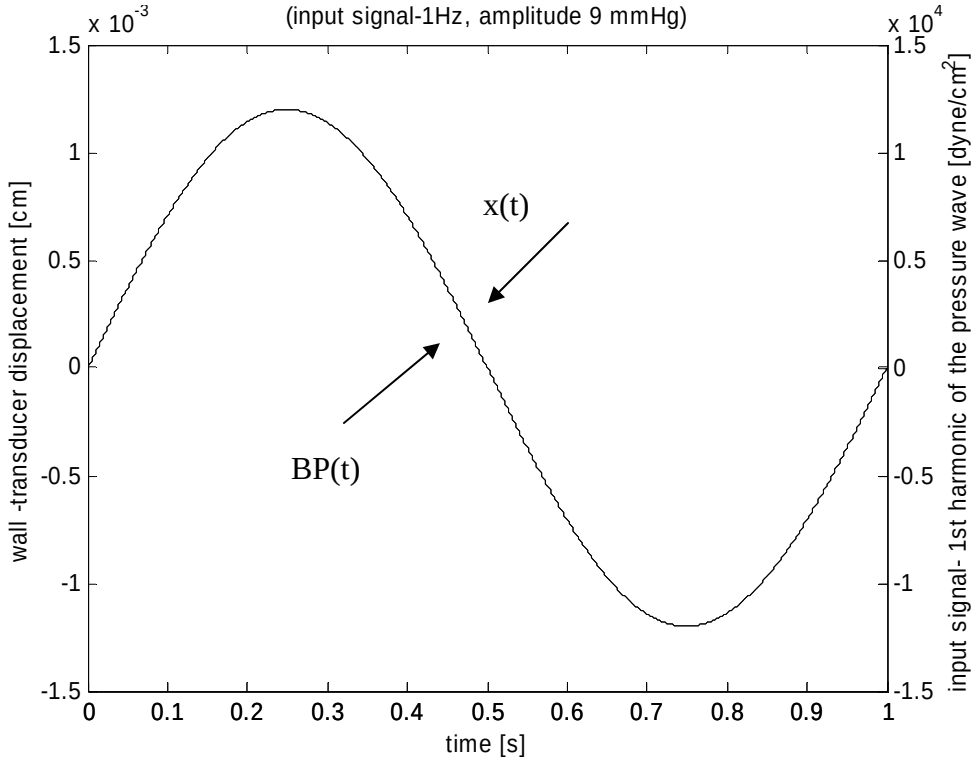

Figure 18. Time response of the wall-transducer system for Etr=10^9

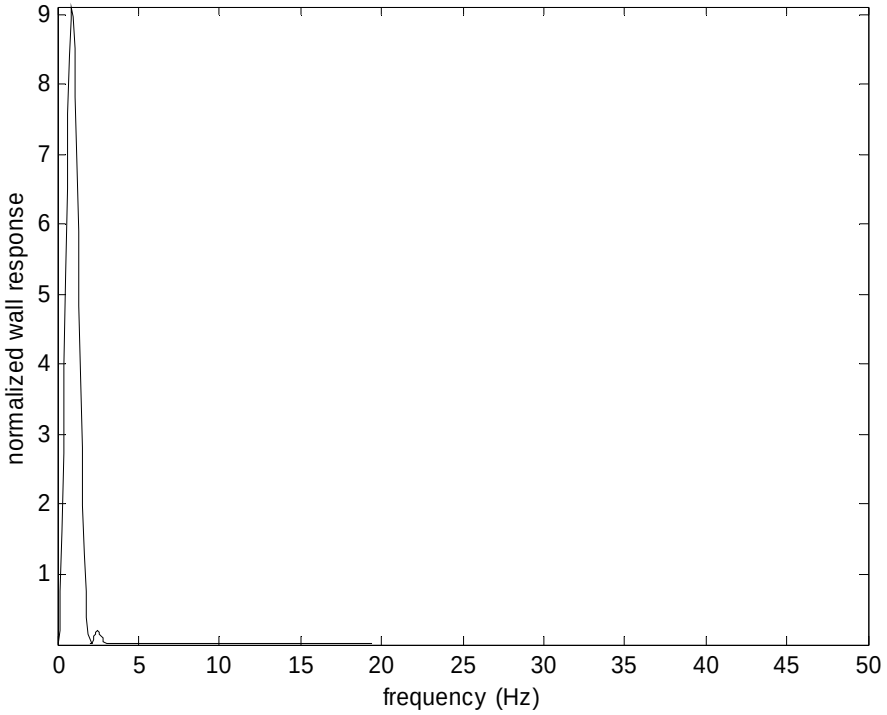

Figure 19. Frequency response of the wall-transducer system for Etr = 10^10

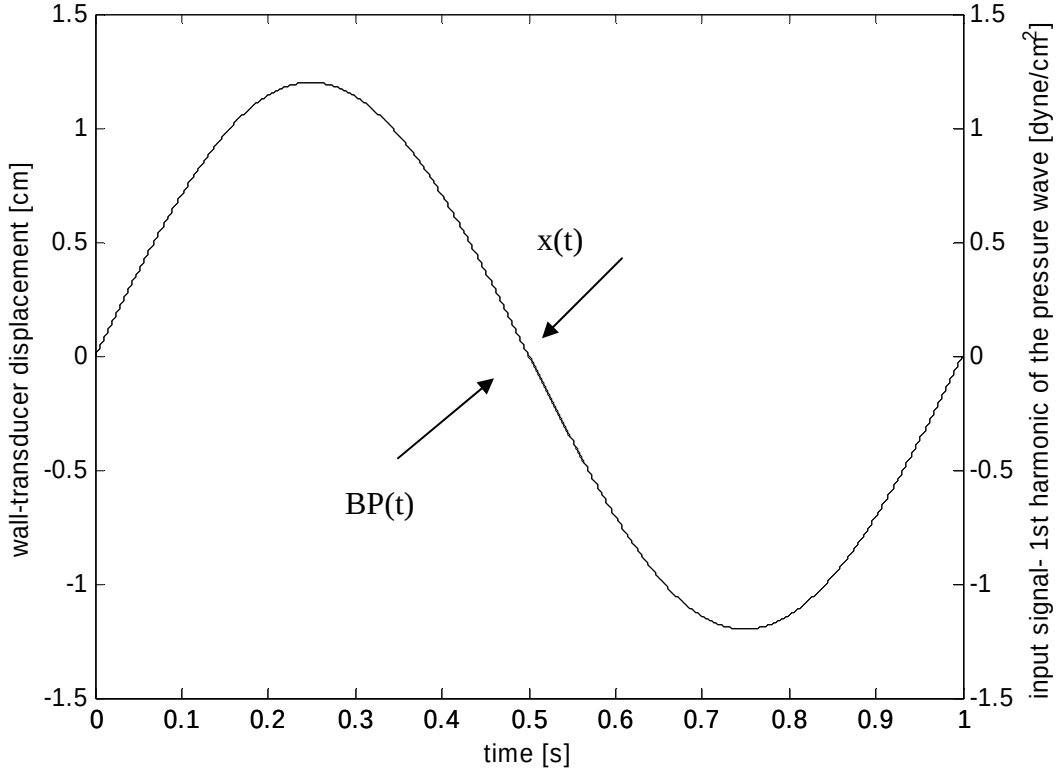

Figure 20. Time response of the wall-transducer system for Etr=10^10

Appendix C Finite element modeling model description

The Finite Element Model definition is given below using ABAQUS input file. The model includes: mesh definition, material definition, boundary conditions and step definition.

```
*Heading
** Job name: young5_600 Model name: Model-1
**
** PARTS
**
*Part, name=Part-1
*End Part
*Part, name=Part-3
*End Part
*Part, name=Part-4
*End Part
**
** ASSEMBLY
**
*Assembly, name=Assembly
**
*Instance, name=Part-1-1, part=Part-1
        0.,       -0.05,        -0.9
*Node
  {Nodes definition}
*Element, type=C3D8R
  {Element definition}
** Region: (Section-1:Picked)
*Elset, elset=_I1, internal, generate
    1,  10440,      1
** Section: Section-1
*Solid Section, elset=_I1, material=tissue
0.001,
*End Instance
**
*Instance, name=Part-3-1, part=Part-3
        0.,       -0.05,        -0.3
*Node
     1,  -5.551115e-17,         0.1,         0.3
*Nset, nset=Part-3-1-RefPt_, internal
1,
*Surface, type=CYLINDER, name=RigidSurface_, internal
START,          0.,        -0.3
 CIRCL,         0.4,         0.1,          0.,         0.1
```

```
 LINE,          0.4,          0.2
*End Instance
**
*Instance, name=Part-4-1, part=Part-4
         0.,        0.25,          0.
         0.,        0.25,          0.,          0.,        1.25,          0.,         90.
*Node
    {Nodes definition}
*Element, type=R3D4
{Element Definition}
*Node
    85,         0.3,          0.,          0.
*Nset, nset=Part-4-1-RefPt_, internal
85,
*Elset, elset=Part-4-1, generate
  1,  65,   1
*End Instance
*Nset, nset=_PickedSet37, internal, instance=Part-1-1
  {}
*Elset, elset=_PickedSet37, internal, instance=Part-1-1
  {}
*Nset, nset=_PickedSet38, internal, instance=Part-1-1
  {}
*Elset, elset=_PickedSet38, internal, instance=Part-1-1
  {}
*Nset, nset=_PickedSet41, internal, instance=Part-3-1
 1,
*Nset, nset=_PickedSet43, internal, instance=Part-3-1
 1,
*Nset, nset=_PickedSet61, internal, instance=Part-1-1
  {}
*Elset, elset=_PickedSet61, internal, instance=Part-1-1
  {}
*Nset, nset=_G64, internal, instance=Part-4-1
  2,  3,  5,  6,  9, 10, 11, 12, 19, 20, 21, 22, 23, 24, 25, 26
 27, 28, 29, 30, 31, 32, 33, 34, 35, 36, 37, 38, 39, 40, 49, 50
 51, 52, 53, 54, 55, 56, 57, 58, 59, 60, 61, 62, 63, 64, 65, 66
 67, 68, 69, 70, 71, 72, 73, 74, 75, 76, 77, 78, 79, 80, 81, 82
 83, 84
*Elset, elset=_G64, internal, instance=Part-4-1, generate
 16,  65,   1
*Nset, nset=_G65, internal, instance=Part-1-1, generate
 10798,  14396,      1
*Elset, elset=_G65, internal, instance=Part-1-1, generate
  6961,  10440,      1
*Nset, nset=_PickedSet71, internal, instance=Part-4-1
```

```
 85,
*Nset, nset=_PickedSet72, internal, instance=Part-4-1
 85,
*Nset, nset=_PickedSet78, internal, instance=Part-4-1
 85,
*Nset, nset=_PickedSet79, internal, instance=Part-1-1
    {}
*Elset, elset=_PickedSet79, internal, instance=Part-1-1
    {}
*Elset, elset=__PickedSurf55_S2, internal, instance=Part-1-1, generate
   1,  3480,     1
*Surface, type=ELEMENT, name=_PickedSurf55, internal
__PickedSurf55_S2, S2
*Elset, elset=__PickedSurf57_S2, internal, instance=Part-1-1, generate
   1,  3480,     1
*Surface, type=ELEMENT, name=_PickedSurf57, internal
__PickedSurf57_S2, S2
*Elset, elset=__PickedSurf59_S1, internal, instance=Part-1-1, generate
  6961,  10440,      1
*Surface, type=ELEMENT, name=_PickedSurf59, internal
__PickedSurf59_S1, S1
*Elset, elset=__PickedSurf67_SPOS, internal, instance=Part-4-1, generate
 16,  65,   1
*Surface, type=ELEMENT, name=_PickedSurf67, internal
__PickedSurf67_SPOS, SPOS
*Elset, elset=__PickedSurf68_S1, internal, instance=Part-1-1, generate
  6961,  10440,      1
*Surface, type=ELEMENT, name=_PickedSurf68, internal
__PickedSurf68_S1, S1
*Rigid Body, ref node=Part-4-1.Part-4-1-RefPt_, elset=Part-4-1.Part-4-1
** Constraint: Constraint-1
*Rigid Body, ref node=_PickedSet41, analytical surface=Part-3-1.RigidSurface_
*End Assembly
**
** MATERIALS
**
*Material, name=tissue
*Density
1.,
*Elastic
 5e+06, 0.499
**
** INTERACTION PROPERTIES
**
*Surface Interaction, name=IntProp-1
1.,
```

```
*Surface Behavior, pressure-overclosure=HARD
**
** BOUNDARY CONDITIONS
**
** Name: BC-1 Type: Displacement/Rotation
*Boundary
_PickedSet37, 3, 3
** Name: BC-2 Type: Displacement/Rotation
*Boundary
_PickedSet38, 4, 4
_PickedSet38, 5, 5
_PickedSet38, 6, 6
** Name: BC-3 Type: Displacement/Rotation
*Boundary
_PickedSet43, 1, 1
_PickedSet43, 2, 2
_PickedSet43, 3, 3
_PickedSet43, 4, 4
_PickedSet43, 5, 5
_PickedSet43, 6, 6
** Name: BC-6 Type: Displacement/Rotation
*Boundary
_PickedSet79, 1, 1
** Name: BC-8 Type: Displacement/Rotation
*Boundary
_PickedSet61, 4, 4
_PickedSet61, 5, 5
_PickedSet61, 6, 6
** Name: BC-9 Type: Displacement/Rotation
*Boundary
_PickedSet71, 1, 1
_PickedSet71, 3, 3
_PickedSet71, 4, 4
_PickedSet71, 5, 5
_PickedSet71, 6, 6
**
** INTERACTIONS
**
** Interaction: Int-2
*Contact Pair, interaction=IntProp-1
_PickedSurf59, Part-3-1.RigidSurface_
** Interaction: Int-3
*Contact Pair, interaction=IntProp-1
_PickedSurf68, _PickedSurf67
** ----------------------------------------------------------------
**
```

```
** STEP: applanation
**
*Step, name=applanation, nlgeom
Applanation by force
*Static
0.01, 0.1, 1e-08, 0.01
**
** LOADS
**
** Name: Load-4   Type: Concentrated force
*Cload
_PickedSet78, 2, -600.
**
** OUTPUT REQUESTS
**
*Restart, write, frequency=1
**
** FIELD OUTPUT: F-Output-1
**
*Output, field, variable=PRESELECT
**
** HISTORY OUTPUT: H-Output-1
**
*Output, history, variable=PRESELECT
*El Print, freq=999999
*Node Print, freq=999999
*End Step
** ----------------------------------------------------------------
**
** STEP: pressurizing up to mean
**
*Step, name="pressurizing up to mean", nlgeom
*Static
0.01, 0.1, 1e-06, 0.01
**
** BOUNDARY CONDITIONS
**
** Name: BC-1 Type: Displacement/Rotation
*Boundary, op=NEW
_PickedSet37, 3, 3
** Name: BC-10 Type: Displacement/Rotation
*Boundary, op=NEW, fixed
_PickedSet72, 1, 1
_PickedSet72, 2, 2
_PickedSet72, 3, 3
_PickedSet72, 4, 4
```

```
_PickedSet72, 5, 5
_PickedSet72, 6, 6
** Name: BC-2 Type: Displacement/Rotation
*Boundary, op=NEW
_PickedSet38, 4, 4
_PickedSet38, 5, 5
_PickedSet38, 6, 6
** Name: BC-3 Type: Displacement/Rotation
*Boundary, op=NEW
_PickedSet43, 1, 1
_PickedSet43, 2, 2
_PickedSet43, 3, 3
_PickedSet43, 4, 4
_PickedSet43, 5, 5
_PickedSet43, 6, 6
** Name: BC-6 Type: Displacement/Rotation
*Boundary, op=NEW
_PickedSet79, 1, 1
** Name: BC-8 Type: Displacement/Rotation
*Boundary, op=NEW
_PickedSet61, 4, 4
_PickedSet61, 5, 5
_PickedSet61, 6, 6
** Name: BC-9 Type: Displacement/Rotation
*Boundary, op=NEW
**
** LOADS
**
** Name: Load-2   Type: Pressure
*Dsload
_PickedSurf55, P, 103974.
** Name: Load-4   Type: Concentrated force
*Cload, op=NEW
**
** OUTPUT REQUESTS
**
*Restart, write, frequency=1
**
** FIELD OUTPUT: F-Output-1
**
*Output, field, variable=PRESELECT
**
** HISTORY OUTPUT: H-Output-1
**
*Output, history, variable=PRESELECT
*End Step
```

```
** ----------------------------------------------------------------
**
** STEP: arterial pulse 1
**
*Step, name="arterial pulse 1", nlgeom
*Static
0.05, 0.05, 5e-07, 0.05
**
** LOADS
**
** Name: Load-2   Type: Pressure
*Dsload, op=NEW
** Name: Load-3   Type: Pressure
*Dsload, op=NEW
_PickedSurf57, P, 103974.
**
** OUTPUT REQUESTS
**
*Restart, write, frequency=1
**
** FIELD OUTPUT: F-Output-1
**
*Output, field, variable=PRESELECT
**
** HISTORY OUTPUT: H-Output-1
**
*Output, history, variable=PRESELECT
*End Step
** ----------------------------------------------------------------
**
** STEP: arterial pulse 2
**
*Step, name="arterial pulse 2", nlgeom
*Static
0.05, 0.05, 5e-07, 0.05
**
** LOADS
**
** Name: Load-3   Type: Pressure
*Dsload
_PickedSurf57, P, 101308.
**
** OUTPUT REQUESTS
**
*Restart, write, frequency=1
**
```

```
** FIELD OUTPUT: F-Output-1
**
*Output, field, variable=PRESELECT
**
** HISTORY OUTPUT: H-Output-1
**
*Output, history, variable=PRESELECT
*End Step
** ----------------------------------------------------------------
**
** STEP: arterial pulse 3
**
*Step, name="arterial pulse 3", nlgeom
*Static
0.05, 0.05, 5e-07, 0.05
**
** LOADS
**
** Name: Load-3   Type: Pressure
*Dsload
_PickedSurf57, P, 99975.
**
** OUTPUT REQUESTS
**
*Restart, write, frequency=1
**
** FIELD OUTPUT: F-Output-1
**
*Output, field, variable=PRESELECT
**
** HISTORY OUTPUT: H-Output-1
**
*Output, history, variable=PRESELECT
*End Step
** ----------------------------------------------------------------
**
** STEP: arterial pulse 4
**
*Step, name="arterial pulse 4", nlgeom
*Static
0.05, 0.05, 5e-07, 0.05
**
** LOADS
**
** Name: Load-3   Type: Pressure
*Dsload
```

```
_PickedSurf57, P, 126635.
**
** OUTPUT REQUESTS
**
*Restart, write, frequency=1
**
** FIELD OUTPUT: F-Output-1
**
*Output, field, variable=PRESELECT
**
** HISTORY OUTPUT: H-Output-1
**
*Output, history, variable=PRESELECT
*End Step
** ----------------------------------------------------------------
**
** STEP: arterial pulse 5
**
*Step, name="arterial pulse 5", nlgeom
*Static
0.05, 0.05, 5e-07, 0.05
**
** LOADS
**
** Name: Load-3   Type: Pressure
*Dsload
_PickedSurf57, P, 135966.
**
** OUTPUT REQUESTS
**
*Restart, write, frequency=1
**
** FIELD OUTPUT: F-Output-1
**
*Output, field, variable=PRESELECT
**
** HISTORY OUTPUT: H-Output-1
**
*Output, history, variable=PRESELECT
*End Step
** ----------------------------------------------------------------
**
** STEP: arterial pulse 6
**
*Step, name="arterial pulse 6", nlgeom
*Static
```

```
0.05, 0.05, 5e-07, 0.05
**
** LOADS
**
** Name: Load-3   Type: Pressure
*Dsload
_PickedSurf57, P, 141298.
**
** OUTPUT REQUESTS
**
*Restart, write, frequency=1
**
** FIELD OUTPUT: F-Output-1
**
*Output, field, variable=PRESELECT
**
** HISTORY OUTPUT: H-Output-1
**
*Output, history, variable=PRESELECT
*End Step
** ----------------------------------------------------------------
**
** STEP: arterial pulse 7
**
*Step, name="arterial pulse 7", nlgeom
*Static
0.05, 0.05, 5e-07, 0.05
**
** LOADS
**
** Name: Load-3   Type: Pressure
*Dsload
_PickedSurf57, P, 159960.
**
** OUTPUT REQUESTS
**
*Restart, write, frequency=1
**
** FIELD OUTPUT: F-Output-1
**
*Output, field, variable=PRESELECT
**
** HISTORY OUTPUT: H-Output-1
**
*Output, history, variable=PRESELECT
*End Step
```

```
** ----------------------------------------------------------------
**
** STEP: arterial pulse 8
**
*Step, name="arterial pulse 8", nlgeom
*Static
0.05, 0.05, 5e-07, 0.05
**
** LOADS
**
** Name: Load-3   Type: Pressure
*Dsload
_PickedSurf57, P, 173290.
**
** OUTPUT REQUESTS
**
*Restart, write, frequency=1
**
** FIELD OUTPUT: F-Output-1
**
*Output, field, variable=PRESELECT
**
** HISTORY OUTPUT: H-Output-1
**
*Output, history, variable=PRESELECT
*End Step
** ----------------------------------------------------------------
**
** STEP: arterial pulse 9
**
*Step, name="arterial pulse 9", nlgeom
*Static
0.05, 0.05, 5e-07, 0.05
**
** LOADS
**
** Name: Load-3   Type: Pressure
*Dsload
_PickedSurf57, P, 170624.
**
** OUTPUT REQUESTS
**
*Restart, write, frequency=1
**
** FIELD OUTPUT: F-Output-1
**
```

```
*Output, field, variable=PRESELECT
**
** HISTORY OUTPUT: H-Output-1
**
*Output, history, variable=PRESELECT
*End Step
** ----------------------------------------------------------------
**
** STEP: arterial pulse 10
**
*Step, name="arterial pulse 10", nlgeom
*Static
0.05, 0.05, 5e-07, 0.05
**
** LOADS
**
** Name: Load-3   Type: Pressure
*Dsload
_PickedSurf57, P, 157294.
**
** OUTPUT REQUESTS
**
*Restart, write, frequency=1
**
** FIELD OUTPUT: F-Output-1
**
*Output, field, variable=PRESELECT
**
** HISTORY OUTPUT: H-Output-1
**
*Output, history, variable=PRESELECT
*End Step
** ----------------------------------------------------------------
**
** STEP: arterial pulse 11
**
*Step, name="arterial pulse 11", nlgeom
*Static
0.05, 0.05, 5e-07, 0.05
**
** LOADS
**
** Name: Load-3   Type: Pressure
*Dsload
_PickedSurf57, P, 149296.
**
```

```
** OUTPUT REQUESTS
**
*Restart, write, frequency=1
**
** FIELD OUTPUT: F-Output-1
**
*Output, field, variable=PRESELECT
**
** HISTORY OUTPUT: H-Output-1
**
*Output, history, variable=PRESELECT
*End Step
** ----------------------------------------------------------------
**
** STEP: arterial pulse 12
**
*Step, name="arterial pulse 12", nlgeom
*Static
0.05, 0.05, 5e-07, 0.05
**
** LOADS
**
** Name: Load-3   Type: Pressure
*Dsload
_PickedSurf57, P, 143964.
**
** OUTPUT REQUESTS
**
*Restart, write, frequency=1
**
** FIELD OUTPUT: F-Output-1
**
*Output, field, variable=PRESELECT
**
** HISTORY OUTPUT: H-Output-1
**
*Output, history, variable=PRESELECT
*End Step
** ----------------------------------------------------------------
**
** STEP: arterial pulse 13
**
*Step, name="arterial pulse 13", nlgeom
*Static
0.05, 0.05, 5e-07, 0.05
**
```

```
** LOADS
**
** Name: Load-3   Type: Pressure
*Dsload
_PickedSurf57, P, 135966.
**
** OUTPUT REQUESTS
**
*Restart, write, frequency=1
**
** FIELD OUTPUT: F-Output-1
**
*Output, field, variable=PRESELECT
**
** HISTORY OUTPUT: H-Output-1
**
*Output, history, variable=PRESELECT
*End Step
** ----------------------------------------------------------------
**
** STEP: arterial pulse 14
**
*Step, name="arterial pulse 14", nlgeom
*Static
0.05, 0.05, 5e-07, 0.05
**
** LOADS
**
** Name: Load-3   Type: Pressure
*Dsload
_PickedSurf57, P, 129301.
**
** OUTPUT REQUESTS
**
*Restart, write, frequency=1
**
** FIELD OUTPUT: F-Output-1
**
*Output, field, variable=PRESELECT
**
** HISTORY OUTPUT: H-Output-1
**
*Output, history, variable=PRESELECT
*End Step
** ----------------------------------------------------------------
**
```

```
** STEP: arterial pulse 15
**
*Step, name="arterial pulse 15", nlgeom
*Static
0.05, 0.05, 5e-07, 0.05
**
** LOADS
**
** Name: Load-3   Type: Pressure
*Dsload
_PickedSurf57, P, 123969.
**
** OUTPUT REQUESTS
**
*Restart, write, frequency=1
**
** FIELD OUTPUT: F-Output-1
**
*Output, field, variable=PRESELECT
**
** HISTORY OUTPUT: H-Output-1
**
*Output, history, variable=PRESELECT
*End Step
** ----------------------------------------------------------------
**
** STEP: arterial pulse 16
**
*Step, name="arterial pulse 16", nlgeom
*Static
0.05, 0.05, 5e-07, 0.05
**
** LOADS
**
** Name: Load-3   Type: Pressure
*Dsload
_PickedSurf57, P, 119970.
**
** OUTPUT REQUESTS
**
*Restart, write, frequency=1
**
** FIELD OUTPUT: F-Output-1
**
*Output, field, variable=PRESELECT
**
```

```
** HISTORY OUTPUT: H-Output-1
**
*Output, history, variable=PRESELECT
*End Step
** ----------------------------------------------------------------
**
** STEP: arterial pulse 17
**
*Step, name="arterial pulse 17", nlgeom
*Static
0.05, 0.05, 5e-07, 0.05
**
** LOADS
**
** Name: Load-3   Type: Pressure
*Dsload
_PickedSurf57, P, 117304.
**
** OUTPUT REQUESTS
**
*Restart, write, frequency=1
**
** FIELD OUTPUT: F-Output-1
**
*Output, field, variable=PRESELECT
**
** HISTORY OUTPUT: H-Output-1
**
*Output, history, variable=PRESELECT
*End Step
** ----------------------------------------------------------------
**
** STEP: arterial pulse 18
**
*Step, name="arterial pulse 18", nlgeom
*Static
0.05, 0.05, 5e-07, 0.05
**
** LOADS
**
** Name: Load-3   Type: Pressure
*Dsload
_PickedSurf57, P, 115971.
**
** OUTPUT REQUESTS
**
```

```
*Restart, write, frequency=1
**
** FIELD OUTPUT: F-Output-1
**
*Output, field, variable=PRESELECT
**
** HISTORY OUTPUT: H-Output-1
**
*Output, history, variable=PRESELECT
*End Step
** ----------------------------------------------------------------
**
** STEP: arterial pulse 19
**
*Step, name="arterial pulse 19", nlgeom
*Static
0.05, 0.05, 5e-07, 0.05
**
** LOADS
**
** Name: Load-3   Type: Pressure
*Dsload
_PickedSurf57, P, 113305.
**
** OUTPUT REQUESTS
**
*Restart, write, frequency=1
**
** FIELD OUTPUT: F-Output-1
**
*Output, field, variable=PRESELECT
**
** HISTORY OUTPUT: H-Output-1
**
*Output, history, variable=PRESELECT
*End Step
** ----------------------------------------------------------------
**
** STEP: arterial pulse 20
**
*Step, name="arterial pulse 20", nlgeom
*Static
0.05, 0.05, 5e-07, 0.05
**
** LOADS
**
```

```
** Name: Load-3   Type: Pressure
*Dsload
_PickedSurf57, P, 106640.
**
** OUTPUT REQUESTS
**
*Restart, write, frequency=1
**
** FIELD OUTPUT: F-Output-1
**
*Output, field, variable=PRESELECT
**
** HISTORY OUTPUT: H-Output-1
**
*Output, history, variable=PRESELECT
*End Step
** ----------------------------------------------------------------
**
** STEP: arterial pulse 21
**
*Step, name="arterial pulse 21", nlgeom
*Static
0.05, 0.05, 5e-07, 0.05
**
** LOADS
**
** Name: Load-3   Type: Pressure
*Dsload
_PickedSurf57, P, 99975.
**
** OUTPUT REQUESTS
**
*Restart, write, frequency=1
**
** FIELD OUTPUT: F-Output-1
**
*Output, field, variable=PRESELECT
**
** HISTORY OUTPUT: H-Output-1
**
*Output, history, variable=PRESELECT
*End Step
```

Appendix D Lumped parameter simulation code

Arterial wall response:
Function definition

```
function xdot=wallresponsektr0(t,x)
% GENERAL
% call syntax: xdot=prtrans(t,x)
%input: t=time
%x=[x(1);x(2);x(3)];
% output: xdot=[;;;]
%defnition of Wall constants
% units: dyne, cm, g,

% GEOMETRY
g=.1;       %gap between the reigid structure and the pin
Spin=.1;    %pin surface
h=.1;       %wall thickness
l=.1;       %width of the pin

% MATERIAL PROPERTIES
global increment Ewall

Mwall=.1;
Kwall=Ewall*(l*h)/g;
Bwall=1200000*(l*h)/g;

%definition of the pressure signal
%BP=sin(x);
xdot=[-2*sin(atan(x(2)./g))*(sqrt(g^2+x(2).^2)-g).*Kwall./Mwall-
2*sin(atan(x(2)./g)).*(1/(2*sqrt(g^2+x(2).^2))).*(2*x(2)).*x(1).*(Bwall/Mwall)+10*13
33*sin(1*2*pi*t)./Mwall;
x(1)];
%atan(g/(x(3)+.0001))
%tspan=[0 10]; x0=[0,0,0];
%[t,x]=ode23('walltrans',tspan,x0);
%displacement=x(:,3);
%plot(t,displacement, t, sin(20*pi*t));figure(2)
%t=0:0.0001:100;plot(abs(fft(displacement)))
```

Solving program

```
%script file to solve wallresponsektr0
global increment Ewall
Number_of_steps=1;
N=2048*2;

 S=linspace(1,257,257);
 S=S';
 S=[];
for increment=0:1:Number_of_steps

 Ewall=1000 + increment*10000;
 tspan=[0 1]; x0=[0,0];
 [t,x]=ode23('wallresponsektr0',tspan,x0);
 displacement=x(:,2);
f = length(displacement)*(1:257)/N;
 Y = fft(displacement,N);
 Pyy = Y.* conj(Y) / N;

 %plot(f,Pyy(1:257)); axis([0 50 -inf inf]);
  title('Frequency content of the arterial wall response. Input frequency-1Hz')
 xlabel('frequency (Hz)')
 %figure(increment+1);
 Pyy(258:length(Pyy),:)=[];Pyy=Pyy./max(Pyy);
S=[S Pyy];
end;
x=1:1:Number_of_steps; y=1:1:256;
%surf(;
%[x,y]=meshgrid(x,y);
mesh(x,y,S(y,x))
figure(2);
plot(t,displacement,t,100*sin(1*2*pi*t))
```

Wall-tonometer system response:

Function definition

```
function xdot=walltransducerresponse(t,x)
% GENERAL
% call syntax: xdot=prtrans(t,x)
%input: t=time
%x=[x(1);x(2);x(3)];
% output: xdot=[;;;]
%defnition of Wall constants
% units: dyne, cm, g,
```

```
% GEOMETRY
g=.1;       %gap between the reigid structure and the pin
Spin=.1;    %pin surface
h=.1;       %wall thickness
l=.1;       %width of the pin

% MATERIAL PROPERTIES
Ewall=1000000;
Etr=10000000000;
Btr=120;

Mwall=.01;
Kwall=Ewall*(l*h)/g;
Bwall=1200000*(l*h)/g;

%definition of the pressure signal
%BP=sin(x);

xdot=[-Etr.*x(2)-Btr.*x(1)-2*sin(atan(x(2)./g))*(sqrt(g^2+x(2).^2)-g).*Kwall./Mwall-
2*sin(atan(x(2)./g)).*(1/(2*sqrt(g^2+x(2).^2))).*(2*x(2)).*x(1).*(Bwall/Mwall)+1.8*1
333*sin(4*2*pi*t)./Mwall;
x(1)];
```

Solving program

```
%script file to solve wallresponsektr0

Number_of_steps=1;
N=2048*1024*2;

 S=linspace(1,257,257);
 S=S';
 S=[];



 tspan=[0 1]; x0=[0,0];
 [t,x]=ode45('walltransducerresponse',tspan,x0);
 displacement=x(:,2);
 f = length(displacement)*(1:257)/N;
 Y = fft(displacement,N);
 Pyy = Y.* conj(Y) /N;

 plot(f,Pyy(1:257)); axis([0 50 -inf inf]);
 title('frequency content of the arterial wall-transducer system response (Input
frequency-1Hz, amplitude 9 mmHg)')
 xlabel('frequency (Hz)')
```

```
 ylabel('normalized wall response')
 figure(2);

 xlabel('time [s]')
title('time response of the arterial wall-transducer system (input signal-1Hz,
amplitude 9 mmHg')
plotyy(t,displacement,t,1333*9*sin(1*t*2*pi))
[AX,H1,H2] = plotyy(t,displacement,t,1333*9*sin(1*t*2*pi),'plot');
set(get(AX(1),'Ylabel'),'String','wall displacement [cm]')
set(get(AX(2),'Ylabel'),'String','input signal- 1st harmonic of the pressure wave
[dyne/cm^2]')
 %figure(increment+1);
 %Pyy(258:length(Pyy),:)=[];Pyy=Pyy./max(Pyy);
%S=[S Pyy];

%figure(2);
%plot(t,displacement,t,100*sin(1*2*pi*t))
```

Appendix E Signal analysis

The signal analysis has been performed using LabVIEW software. The software block diagram is presented below.

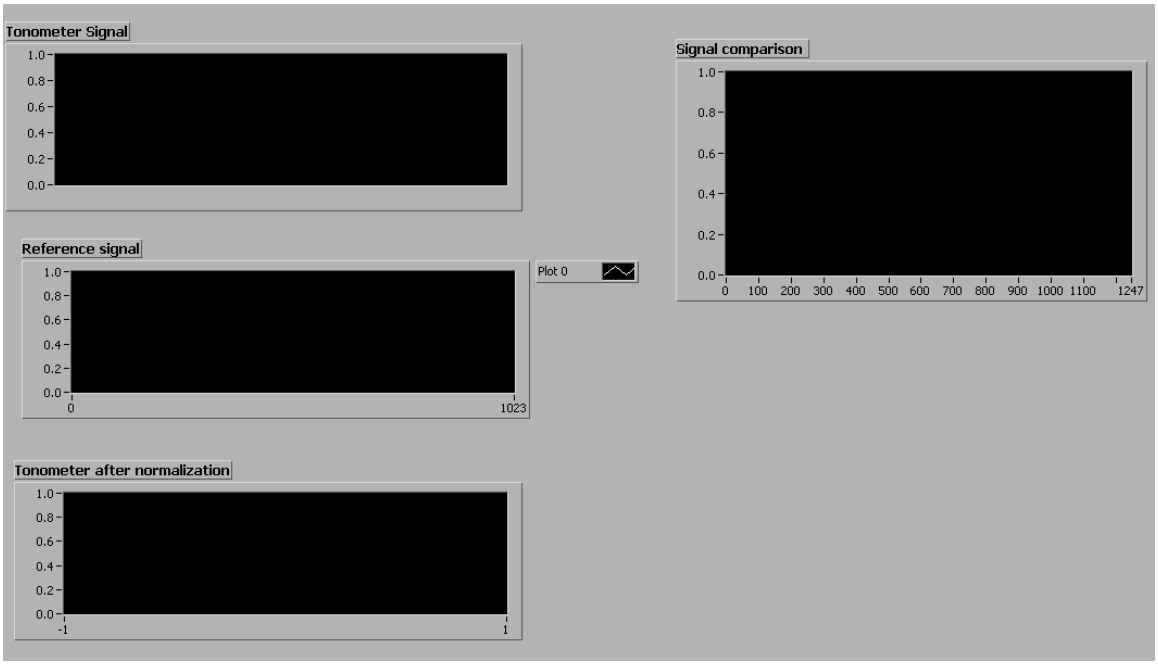

Figure 1. Signal analysis. LabVIEW application front panel

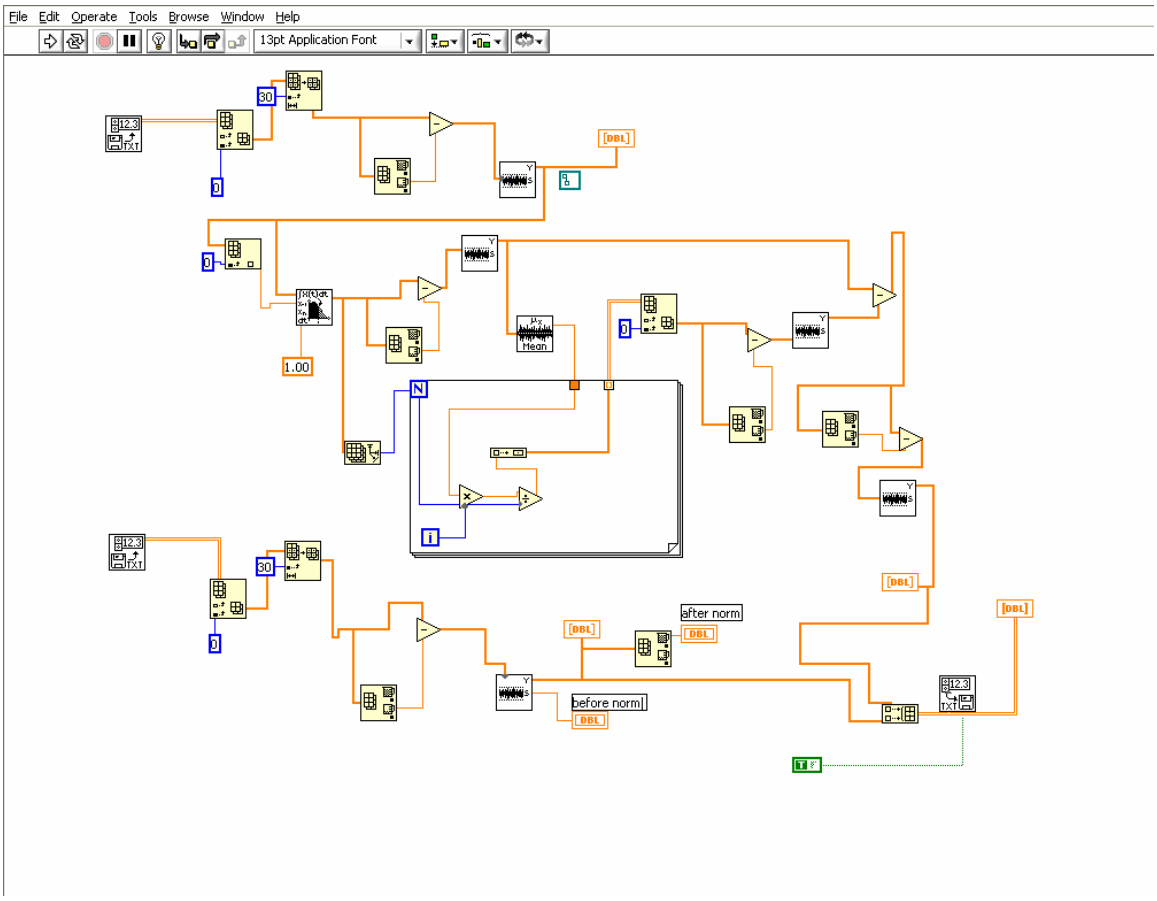

Figure 2. Signal analysis. LabVIEW application back panel

Vita

Marek Swoboda, M.Sc. received his B.S. and M.Sc. degrees in Applied Physics at Silesian Technical University, Poland. From 1993 to 1999 he worked as a Research and Development Engineer at the Institute of Heart Prostheses in Zabrze, Poland, where he was involved in the development of Artificial Heart and Left Ventricle Assist Devices. During this period, he designed and developed several devices including electro-pneumatic actuator for Heart Assist Devices, a prototype of the implantable electro-hydraulic Left Ventricle Assist Device and a polyurethane valve for LVAD. His and his research team's work was awarded by Polonia Business Club – Special Merit Awards, 1998, Warsaw; Poland Polish Ministry of Science and Research Award for Outstanding Research Achievements, 1998, Warsaw, Poland; Japanese Society for Artificial Organs Award for young researchers: 1997, Yokohama, Japan. He received as a member of the research team a Gold Medal at "The London International Fair" for "Electro-hydraulic Implantable Ventricular Assist Device EHIVAD," 1998, London, United Kingdom.

In 1999 he returned to academia, starting his Ph.D. studies at Drexel University to pursue his biomedical education. In 2000 he became a member of joint Thomas Jefferson University and Drexel University research team working on an Implantable Tonometer Project. The development of the Implantable Tonometer provided several research problems, which form the basis of his Ph.D. dissertation.

Mr. Swoboda was awarded a patent in the field of biomechanical Engineering and is a coauthor of several patent applications in Europe and the United States.